UNIVERSIDAD AUTÓNOMA DE NUEVO LEÓN

FACULTAD DE CIENCIAS QUÍMICAS

TESIS

METABOLOMICS-DERIVED INSIGHTS INTO THE METABOLIC REGULATION AND CONTROL OF CENTELLOSIDES IN HAIRY ROOT CULTURES OF *Centella asiática*

PRESENTA

ANTONI GARCIA BAEZA

COMO REQUISITO PARA OBTENER EL GRADO DE

DOCTORADO EN CIENCIAS CON ORIENTACIÓN EN FARMACIA

NOVIEMBRE 2023

UNIVERSIDAD AUTÓNOMA DE NUEVO LEÓN

FACULTY OF CHEMICAL SCIENCES

METABOLOMICS-DERIVED INSIGHTS INTO THE METABOLIC REGULATION AND CONTROL OF CENTELLOSIDES IN HAIRY ROOT CULTURES OF *Centella asiatica*

By

ANTONI GARCIA BAEZA, MSc

As a partial requirement to obtain the Degree of DOCTOR IN SCIENCES with Orientation in Pharmacy

Nov, 2023

The experimental design and development of the present work were performed in the Laboratory of Cell Metabolism, Faculty of Chemical Sciences at the Universidad Autónoma de Nuevo León (Mexico), in the Laboratory of ISOMer UR2160 at the Nantes Université (France), in the Laboratory of Plant biotechnology at the Faculty of Pharmacy at the University of Barcelona (Spain) and in the Laboratory of NMR of the Centro de Nanociencias y Micro y Nanotecnologías at the Instituto Politécnico Nacional (Mexico).

AKNOWLEGMENTS

To the **Faculty of Chemical Sciences of the U.A.N.L.** and to the laboratory **UR2160 ISOMer from the Faculty of Pharmaceutical Science of the Université de Nantes** for the opportunity to pursue the Doctoral studies in cotutelle and the present research.

To the **Consejo Nacional de Ciencia y Tecnología (CONACyT)** for the 109502-support grant provided during this project.

To **Dr. Karla Ramírez Estrada**, Faculty of Chemical Sciences UANL. For the direction and support in the realization of this research project.

To **Prof. Olivier Grovel**, ISOMer UR2160, Faculty of Pharmaceutical and biological Sciences, Nantes Université for the direction and support in the realization of this research project.

To **Dr. Karina-Ethel Petit**, ISOMer UR2160, Faculty of Pharmaceutical and biological Sciences, Nantes Université for the co-direction and the engagement in my professional development.

To both **Doctoral Schools**, Escuela de Posgrado de la Facultad de Ciencias

Químicas de la UANL and the École Doctoral SML at the Université Bretagne-Loire.

To **Dr. Javier Palazón Barandela** and his PhD student **Miguel Ángel Alcalde Alvites**, Laboratori de Fisiologia Vegetal, Facultat de Farmàcia, Universitat de Barcelona for providing the hairy roots and the research stay in his laboratory.

To my tutorial committee in México: **Dr. María del Rayo Camacho Corona**, **Dr. Isaías Balderas Rentería** and **Dr. Eder Ubaldo Arredondo Espinoza**; and in France: **Dr. Séverine Derbre** and **Dr. Mohamed Haddad**. For your observations and suggestions during the tutorial reunions and the seminars, which took part in the shaping of this project.

To the **platform Corsaire-ThalassOMICS Biogenouest**, Université de Nantes, for the UHPLC-MS/MS facilities.

To **Dr. Emmanuel Gentil**, ISOMer UR2160, Faculty of Pharmaceutical and biological Sciences, Nantes Université for the analytical support on the UHPLC-MS/MS analysis and the interpretation of the results.

To **Prof. Samuel Bertrand**, ISOMer UR2160, Faculty of Pharmaceutical and biological Sciences, Nantes Université for his support with data treatment.

To **Dr. Séverine Boisard and the SONAS facilities**, EA 921 SONAS/SFR 4207 QUASAV, Université d'Angers for the UPLC-HRMS/MS analysis.

To the **coordinators of the degree in the UANL**, Dr. Lucía Guadalupe Cantú Cárdenas, Dr. María Elena Cantú Cárdenas, Dr. Omar González Santiago, and Karina Navarro Zapata.

To **Dr. Jesús Alberto Gómez Treviño** and **Dr. Alma Elisabeth Gómez**

Loredo, Facultad de Ciencias Químicas, UANL, for sharing the facilities from their laboratories.

To **Dr. Elvia Martínez Becerra**, Laboratorio de Centro de Nanociencias y Micro y Nanotecnologías, Instituto Politécnico Nacional UNAM for NMR analysis.

To **Dr. Ana Mariel Torres Contreras** for being an excellent colleague and labmate in the Laboratorio de Metabolismo Celular in the UANL. To my friends form the same laboratory, Laura, Kevin, Luis, Nicole, Karla Jr. and Mariela.

To my friends from ISOMer, Université de Nantes, Delphine, Bastien, Olivier, Aurore, Antoine and Simon. Having labmates like you makes the difference in a PhD.

To Manuel Sorroche, Biogenouest, for being an invaluable support for my career development.

To my friends from the Laboratori de Fisiología Vegetal, Universitat de Barcelona, Miguel, Edgar, Ainoa, María and Laia. I had a great time with you.

To my therapist Laura Rojas and to the Dr. Maria Teresa Adell from the Centre de Salud Mental de Nou Barris for the diagnosis and treatment of my depression and anxiety disorder derived from the PhD.

To Alkion Bioinnovations for giving me the opportunity to pursue my professional carreer.

This work is specially dedicated to my mum Gabriela, my dad Antonio, my brother Xavier, my nephews Dídac and Jan, and to Eduardo Cruz.

THESIS APPROVAL

Dra. Karla Ramírez Estrada
Thesis director

Prof. Olivier Grovel
External Thesis director

ABSTRACT

MSc Antoni Garcia Baeza **Grade evaluation date: 10th November 2023**

Universidad Autónoma de Nuevo León
Facultad de Ciencias Química

Nantes Université
UFR des Sciences Pharmaceutiques et Biologiques

Project title: Metabolomics-derived insights into the metabolic regulation and control of centellosides in hairy root cultures of *Centella asiatica*

Number of pages: 226

Candidate for the grade of Doctor in Science with orientation in Pharmacy Study discipline: Pharmacy Purpose and method of study:

Study discipline: Pharmacy and Natural Products Chemistry

Purpose and method of study:

Centella asiatica (L.) Urban is a medicinal perennial herb belonging to the Apiaceae family. The ethnomedical uses by different folk medicines date back to the 16th century until nowadays. Extracts from *C. asiatica* have been reported in scientific studies as a treatment for wound healing, asthma, leprosy, psoriasis, lupus, and used as memory-enhancing, antidepressant, antibacterial, antifungal, antiviral, and anticancer agents. Over the past eight decades, phytochemical research on *C. asiatica* has reported approximately 130 phytochemicals present in this plant including pentacyclic triterpenes, flavonoids, and phenolic compounds among others. However, the search for new molecular entities and their biological activities is still ongoing. The bioactivities of *C. asiatica* have been mainly attributed to its exclusive pentacyclic triterpenoids natural products commonly known as centellosides. This molecular family includes triterpene saponins and sapogenins with pharmacological potential in cancer, diabetes, neurological diseases, liver diseases, wound healing, and infectious diseases. However, the most highlighted bioactivities of

centellosides-like compounds are wound-healing and the enhancement of cognitive performance. Over the past few years, the cosmetic market has shown interest in centellosides. Their demand has been growing and many companies include *C. asiatica* extracts or isolated centellosides products in their portfolio. Mainly, they are found as over the counter products. The chemical complexity of centellosides makes unviable their chemical synthesis. *C. asiatica* plants have become the principal source of these bioactive compounds needed to develop valuable products in the cosmetic and herbalism market. The uncontrolled supply to the market has led to wild stock depletion, especially in India and Madagascar. In the last decades, research has drawn the attention to the development of biotechnological production using *in vitro* tissue cultures of *C. asiatica*. *In vitro* cultures allow the natural production of the metabolites of interest instead of obtaining the metabolites by chemical extraction from the plant. Different and promising results have been reached depending on the type of culture. Among the plethora of *in vitro* systems developed, hairy roots are one of the most suitable systems for biotechnological bioproduction. Hairy roots derive from the *Agrobacterium rhizogenes* infection of plant explants. They are convenient as a production platform due to their high genetic stability, biosynthetic capabilities without the need of external factors, fast biomass production and the possibility to be used for several successive generations. However, *C. asiatica* hairy root lines do not produce basal amounts of centellosides comparable to other *in vitro* systems. Nonetheless, specialised metabolite production is generally low in any kind of culture. Plant specialised metabolism does not usually operate in a constitutive manner. It is a highly specialised and diverse metabolism within the plant kingdom. The complexity of the pathways and the molecules that are formed often require a lot of energy for the plant. In most cases the specialised pathways are silenced, they are activated when the plant is stressed by an external factor. Biotechnological studies have taken advantage of this observation by using external signals to activate specialised metabolism as it occurs in nature. This strategy is called elicitation in scientific terminology and has been crucial for the feasibility of producing specialised metabolites of interest in *in vitro* systems. In the case of *C. asiatica*, the addition of elicitors to the culture media has been shown to be crucial for activating the biosynthesis of centellosides and other specialised metabolites. Through a collaboration with

Dr. Palazon's laboratory (Faculty of Pharmacy, University of Barcelona), it was obtained a hairy roots line from *C. asiatica* plants. Previous studies on this line have demonstrated the overproduction of centellosides under elicitation conditions using two phytoregulators: methyl-jasmonate (MeJA) and coronatine (CORO). However, the choice of the elicitor is empirically, and the plant-derived responsiveness is often unpredictable. The biotechnological system productivity depends on the knowledge of the biosynthesis machinery of the culture. However, elicitation has a duality: it is not only a brute force tool to activate specialised biosynthetic pathways, but also allows the study of the metabolism of the culture. The controlled conditions provided by *in vitro* culture together with the over-activation of specialised metabolism triggered by elicitation, create an optimal biological platform for sample collection and subsequent analysis of the state of their metabolism. Omics sciences enable high-throughput analysis of metabolites, genes and/or proteins involved in metabolism at the time of collection. To date, two metabolomics approaches have dealt with the regulation of MeJA elicited *C. asiatica* plant tissue cultures. These studies revealed the activation of the caffeoylquinic acids (CQAs), pentacyclic triterpenes and flavonoids pathways after MeJA-elicitation. However, these studies published so far, lack from the exploration beyond the centelloside pathway, the influence of time of harvesting, and the role of the elicitation in the primary metabolism. The effects of CORO on the metabolome in *in vitro* systems of *C. asiatica* are not already explored. The mode of action of CORO is at some extend like MeJA, but often shows a higher activation of the specialised metabolism. Therefore, in this work the regulation of primary metabolism of hairy roots cultures of *C. asiatica* treated with MeJA and CORO was explored through a time-series proton Nuclear Magnetic Resonance (^{1}H-NMR) metabolomics approach. The specialised metabolism was also explored with the same samples through an Ultra High Performance Liquid Chromatography-Tandem Mass Spectrometry (UHPLC-MS/MS) and an Ultra Performance Liquid Chromatography-High Resolution Tandem Mass Spectrometry (UPLC-HRMS/MS) metabolomics approach. The variations on the primary and specialised metabolome were detected by comparing control cultures against cultures treated with elicitors 0-16 days after treatment. Multivariate data analysis (MVDA) supported the

biochemical interpretation of the data to get insights into the regulation and control of the metabolism of hairy roots of *C. asiatica*.

Conclusions and Contributions:

The regulation of primary metabolism of hairy roots cultures of *C. asiatica* treated with MeJA and CORO was explored through a time-series ^{1}H-NMR metabolomics approach. MVDA revealed that CORO caused an early and superior reprogramming effect on the primary metabolome compared to MeJA. The comparison of the experimental NMR chemical shifts of specific signals with those reported in similar condition allowed the identification of 40 compounds. The list of detected primary metabolites included carbohydrates, amino acids, nucleosides, and some organic acids. On the other hand, three CQAs belonging to the specialised metabolism were detected. The relative production kinetics for the detected metabolites and their possible links of each treatment was discussed. Both elicitors triggered a significant reduction of carbohydrates, major changes on amino acids production and a significant over-production of CQAs compared to control conditions. In MeJA-treated samples, CQAs were initially produced at day 8 and remained constant throughout the 16 days of culture. On the other hand, CORO elicited the production of these compounds from day 4 until the end of the experiment. Overall, both elicitors demonstrated having a reprogramming effect in the primary metabolism through the specialised. However, CORO proved a stronger effect since primary sources of carbon and amino acids were consumed to the differential and earlier production of CQAs. These results are crucial for the application of metabolic engineering strategies in biotechnological production platforms of hairy roots of *C. asiatica*.

The investigations in the responses of the specialised metabolism after elicitation were developed through both UHPLC-MS/MS targeted and untargeted metabolomics approaches. Prior to analysis, the UHPLC-MS/MS method was optimised for the correct separation, ionisation and mass fragmentation of the principal compounds expected to be found in the extracts. The optimisation also permitted the characterisation of the chromatographic and mass spectrometry

features of the standard compounds. Then, this knowledge facilitated the targeted analysis-derived data interpretation. The UHPLC-MS/MS targeted metabolomics analysis was employed to semi-quantitatively compare the production of the annotated ions in the different treatments and days of harvesting. Accordingly, a total of 12 *m/z* ions were tentatively annotated including asiatic acid, madecassic acid, madecassoside, asiaticoside and 7 CQAs. The evaluation of base peak intensity chromatograms showed differences in the presence/absence of some peaks and differences in peak intensities across the different samples and through the time of harvesting. In general, MeJA and CORO had a positive effect in the accumulation of both the CQAs and centellosides detected. CORO was able to significatively enhance the production of centellosides at days 8 and 16 after elicitation compared to MeJA. The production of CQAs under CORO conditions was only statistically different from the rest of the groups after 12 days of elicitation. In contrast to the targeted approach, the untargeted one allowed the global comparison of the metabolome at the quantitative and qualitative level of the extracts under the different conditions and times of harvesting. This approach was especially important as a hypothesis generator about the regulation of the specialised metabolism. The Principal Component Analysis and the Hierarchical Cluster Analysis revealed a strong and rapid reprogramming effect of CORO on the metabolome starting after 4 days of elicitation. Moreover, they showed the strength of the two elicitors and their usefulness as possible regulators of metabolism towards the enhancement and/or activation of the specialised metabolism. The UHPLC-MS/MS-derived data did not allow further *de novo* metabolite annotation. Therefore, Molecular Networks were constructed with the UPLC-HRMS/MS-derived data with the aim of visualising the structural relationships between the detected ions based on their MS/MS spectra. Molecular Networks facilitated the dereplication of ions of interest or, at least, their classification within a family of compounds. The ions of interest were those that contributed variability to the supervised statistical models used to explore the differences between treatments and collection times. OPLS-DA and correlation analyses revealed that CORO and MeJA were able to down-regulate the oleanane branch of the centellosides, while simultaneously enhancing the ursane pathway (from which the most biologically active centellosides are derived). These two pathways are the last branching point in the centelloside

pathway. The same analysis also suggested that the production of chalcones could be inhibited by CORO at some extend. Some of the putatively annotated ions of interest were described so far in *C. asiatica*. This work presents the first a time-series metabolomic analysis for the study of the regulation of both primary and specialised metabolism of hairy roots of *C. asiatica*. It may well contribute to understand the metabolism of hairy roots of *C. asiatica* after the elicitation of MeJA and CORO and how the metabolism can be controllable.

RESUMEN

MSc Antoni Garcia Baeza **Fecha de graduación: 10 de noviembre del 2023**

Universidad Autónoma de Nuevo León
Facultad de Ciencias Químicas

Nantes Université
UFR des Sciences Pharmaceutiques et Biologiques

Título del proyecto: Estudio metabolómicode la regulación metabólica y el control de la producción de centellósidos de hairy roots de *Centella asiatica*

Número de páginas: 226

Candidato a obtener el grado de Doctor en Ciencias con Orientación en Farmacia

Área de estudio: Farmacia y Qímica de Productos Naturales

Propósito y Método de estudio:

Centella asiatica (L.) Urban es una planta medicinal perenne perteneciente a la familia Apiaceae. Es reconocida por sus usos etnomédicos por parte de diferentes medicinas populares desde el siglo XVI hasta nuestros días. Estudios científicos han reportado que *C. asiatica* puede ser útil para el tratamiento de cicatrización de heridas, tratamiento contra el asma, la lepra, la psoriasis, el lupus, como agente potenciador de la memoria, antidepresivo, antibacteriano, antifúngico, antiviral y anticanceroso. En las últimas ocho décadas, la investigación fitoquímica sobre *C. asiatica* ha ireportado 130 fitoquímicos presentes en esta planta, incluyendo triterpenos pentacíclicos, flavonoides y compuestos fenólicos, entre otros. Sin embargo, la búsqueda de nuevas entidades moleculares y sus actividades biológicas sigue en marcha. Las bioactividades son atribuidas principalmente a los triterpenoides pentacíclicos exclusivos de esta planta. Estas moléculas son comúnmente conocidas como centellósidos. Esta familia molecular incluye saponinas y sapogeninas triterpénicas con potencial farmacológico contra el cáncer, diabetes, enfermedades neurológicas, enfermedades hepáticas, cicatrización de heridas y enfermedades

infecciosas. No obstante, las bioactividades más destacadas de los centellósidos son la regeneración de heridas en la piel y la potenciación de la actividad congnitiva. En los últimos años el mercado de la cosmética ha mostrado mucho interés por los centellósidos. Su demanda ha ido en aumento y muchas empresas incluyen en su cartera productos que contienen extractos de la planta o centellósidos aislados. Principalmente, estos productos son de venta libre. La complejidad química de los centellósidos hace inviable su obtención por síntesis química. Por ello, las plantas de *C. asiatica* se han convertido en la principal fuente de estos compuestos bioactivos necesarios para desarrollar productos dentro del mercado de la cosmética y la herboristería. El suministro incontrolado de la planta ha provocado el agotamiento de las existencias silvestres, especialmente en India y Madagascar. En las últimas décadas, la investigación científica ha puesto especial atención al desarrollo de plataformas de producción biotecnológicas basadas en cultivos *in vitro* de *C. asiatica*. Los cultivos *in vitro* permiten la producción natural de los metabolitos de interés de una forma más sostenible que la obtención de los metabolitos por extracción química de la planta. A lo largo de la historia reciente, se han alcanzado diferentes y prometedores resultados dependiendo del tipo de cultivo de tejidos. Entre ellos, las raíces pilosas (en inglés: hairy roots) son uno de los sistemas preferidos para llevar a cabo una producción biotecnológica. Derivan de la infección de *Agrobacterium rhizogenes* en explantos de plantas. Destacan como plataforma de producción debido a su alta estabilidad genética, su capacidad biosintética de metabolitos especializados sin necesidad de señales activadoras externas, su rápida producción de biomasa y la posibilidad de ser utilizadas durante varias generaciones sucesivas. Sin embargo, las líneas de raíces pilosas de *C. asiatica* no producen cantidades de centellósidos de forma basal equiparables a otros sistemas *in vitro*. Aun así, la producción de metabolitos secundarios suele ser baja en cualquier tipo de cultivo. El metabolismo secundario de plantas no suele operar de forma constitutiva. Es un metabolismo altamente especializado y diverso dentro del reino vegetal. La complejidad de las vías y de las moléculas que se forman suelen requerir de mucha energía para la planta. En la mayoría de los casos las vías secundarias están silenciadas. Se activan únicamente cuando la planta sufre estrés a causa de un factor externo. Los estudios en biotecnología han tomado partido de este

fenómeno a través del uso de señales artificiales que activan el metabolismo secundario tal y como ocurre en la naturaleza. Esta estrategia recibe el nombre de elicitación en el argot científico y ha sido crucial para lograr la factibilidad de la producción biotecnológica de metabolitos secundarios. En el caso de *C. asiatica*, se ha demostrado que la adición de elicitores en los medios de cultivo es crucial para activar la biosíntesis de centellósidos y otros metabolitos secundarios. A través de una colaboración con el laboratorio del Dr. Palazón (Facultad de Farmacia, Universidad de Barcelona), se obtuvo una línea de raíces pilosas derivada de *C. asiatica*. Han demostrado la sobreproducción de centellósidos en condiciones de elicitación utilizando los fitorreguladores metil-jasmonato (MeJA) y coronatina (CORO). Sin embargo, la elección del elicitor suele ser empírica y la capacidad de respuesta de la planta es a menudo imprevisible. La productividad del sistema biotecnológico depende del conocimiento de la maquinaria de biosíntesis del cultivo. No obstante, la elicitación presenta una dualidad: no es solo una herramienta de fuerza bruta para activar rutas biosintéticas secundarias, sino que también permite estudiar el metabolismo del cultivo. Las condiciones controladas que proporcionan el cultivo *in vitro* (cultivo axénico, control en la composición del medio de cultivo, ambiente, etc.) junto con la sobre activación del metabolismo secundario provocada con elicitación crean una plataforma biológica óptima para la recolección de muestras y el posterior análisis del estado de su metabolismo. Las ciencias ómicas permiten el análisis de alto rendimiento de los metabolitos, los genes y/o las proteínas que participan en el metabolismo en el momento de la recolección. Hasta la fecha, solo dos enfoques metabolómicos han explorado la regulación del metabolismo en cultivos de células en suspensión de *C. asiatica* elicitados con MeJA. Estos estudios revelaron la activación de las vías de los ácidos cafeoilquínicos (ACQs), los triterpenos pentacíclicos (centellósidos) y de los flavonoides después de la elicitación con MeJA. Sin embargo, estos estudios publicados hasta ahora carecen de la exploración más allá de estas vías, de la influencia del tiempo de cultivo y del papel de la elicitación en el metabolismo primario. El modo de acción de CORO es en cierta medida similar al de MeJA, pero a menudo muestra una mayor activación del metabolismo secundario. Los efectos de CORO en el metaboloma en sistemas *in vitro* de *C. asiatica* no han sido todavía explorados. Por lo tanto, en este trabajo se explora la regulación del

metabolismo primario y secundario de cultivos en suspensión de raíces pilosas de *C. asiatica* tratados con MeJA y CORO a través de un enfoque metabolómico a lo largo del tiempo. El metabolismo primario se analizó mediante Resonancia Magnética Nuclear de Protón (^{1}H-NMR, por sus siglas en inglés), mientras que el metabolismo secundario se analizó usando las mismas muestras mediante un enfoque metabolómico de Cromatografía Líquida de Ultra Alta Resolución acoplada a Espectrometría de Masas en tándem (UHPLC-MS/MS, por sus siglas en inglés) y Cromatografía Líquida de Ultra Resolución acoplada a Espectrometría de Masas de Alta Resolución en tándem (UPLC-HRMS/MS, por sus siglas en inglés). Las variaciones en el metabolismo primario y secundario a causa de la elicitación y del tiempo de recolección se detectaron comparando los cultivos no elicitados (muestras control) con los cultivos tratados con elicitores a los 0, 4, 8, 12 y 16 días después del tratamiento. El análisis de datos multivariante apoyó la interpretación bioquímica de los datos para obtener información sobre la regulación y el control del metabolismo de las raíces pilosas de *C. asiatica*.

Conclusiones y Contribuciones:

La regulación del metabolismo primario de los cultivos en suspensión de raíces pilosas de *C. asiatica* tratados con MeJA y CORO se exploró mediante un enfoque metabolómico de RMN ^{1}H en serie temporal. El análisis de datos multivariante reveló que la CORO causó un efecto de reprogramación en el metaboloma primario superior y más temprano en comparación con el MeJA. La comparación de los desplazamientos químicos experimentales de RMN de señales específicas con los reportados en condiciones similares permitió la identificación de 40 compuestos. La lista de metabolitos primarios detectados incluyó carbohidratos, aminoácidos, nucleósidos y algunos ácidos orgánicos. Por otra parte, se detectaron tres isómeros de ACQs que pertenecen al metabolismo secundario. Se discutió la cinética de producción relativa de los metabolitos detectados y las posibles vías interconectadas por cada tratamiento. Ambos elicitores provocaron, en comparación con los cultivos control, una reducción significativa de carbohidratos, cambios importantes en la producción de aminoácidos y una sobreproducción significativa de ACQs. De forma particular, en las muestras tratadas con MeJA los ACQs se produjeron

inicialmente al día 8 después de la elicitación y se mantuvieron constantes hasta el final del experimento. Por otro lado, CORO provocó la producción de estos compuestos desde el día 4 hasta el final del experimento. En general, ambos elicitores demostraron tener un efecto de reprogramación en el metabolismo primario hacia el secundario. Sin embargo, CORO demostró un efecto más fuerte ya que las fuentes primarias de carbono y aminoácidos fueron consumidas para, posiblemente, la producción diferencial y más temprana de ACQs. Estos resultados son cruciales para la aplicación de estrategias de ingeniería metabólica en plataformas de producción biotecnológica de raíces pilosas de *C. asiatica*.

Las respuestas del metabolismo secundario a la elicitación se exploraron mediante un enfoque de metabolómica dirigida y no dirigida mediante UHPLC-MS/MS. En primer lugar, se optimizó el método de UHPLC-MS/MS para la correcta, ionización y fragmentación de los principales compuestos que se esperaba encontrar en los extractos. Además, se estudiaron las características cromatográficas y espectrométricas de diversos estándares para facilitar su identificación en las muestras. En el enfoque dirigido se anotaron tentativamente un total de 12 iones *m/z*, incluyendo el ácido asiático, el ácido madecásico, el madecasósido, el asiaticósido, 7 ACQs y la sucrosa. La evaluación de los picos base mostró diferencias en la presencia/ausencia de algunos picos y diferencias en sus intensidades entre las distintas muestras y entre los distintos tiempos de recolección. En general, MeJA y CORO tuvieron un efecto positivo en la acumulación tanto de los AQCs como de los centellósidos detectados. CORO fue capaz de aumentar significativamente la producción de centellósidos en los días 8 y 16 después de la elicitación en comparación con MeJA. La producción de AQCs bajo condiciones CORO sólo fue estadísticamente diferente del resto de los grupos después de 12 de elicitación. A diferencia del enfoque dirigido, el no dirigido permitió la comparación global del metaboloma a nivel semi-cuantitativo y cualitativo de los extractos bajo las diferentes condiciones y tiempos. Este enfoque fue especialmente importante como una herramienta generadora de hipótesis sobre la regulación del metabolismo secundario. El análisis de componentes principales y el análisis jerárquico de conglomerados revelaron un fuerte y rápido efecto de reprogramación de CORO en el metaboloma a partir de los 4 días de elicitación. Además, mostraron la fuerza de los dos elicitores

y su utilidad como posibles reguladores del metabolismo hacia la potenciación y/o activación del metabolismo secundario. Los datos del UHPLC-MS/MS de baja resolución no permitieron la anotación de más moléculas. Por lo tanto, se construyeron Redes Moleculares con datos derivados de UPLC-HRMS/MS con el objetivo de visualizar la relación estructural de los iones detectados en base a sus espectros MS/MS. Las Redes Moleculares facilitaron la dereplicación de los iones de interés o, al menos, su clasificación dentro de una familia de compuestos. Además, se anotaron putativamente nuevos compuestos nunca descritos hasta ahora en *C. asiatica*. Los iones de interés fueron aquellos que resultaron aportar variabilidad a los modelos estadísticos empleados para conocer las diferencias entre los tratamientos y los tiempos de recolección. Los análisis de OPLD-DA y de correlación revelaron que CORO y MeJA podrían regular a la baja la rama oleana de los centellósidos, mientras, al mismo tiempo, potenciarían la vía ursana (de la cual derivan los centellósidos con mayor actividad biológica). Estas dos vías representan un importante punto de ramificación en la ruta biosintética de los centellósidos. El mismo análisis también sugirió que producción chalconas podría ser inhibida por CORO. Este trabajo presenta el primer análisis metabolómico de series temporales para el estudio de la regulación del metabolismo primario y secundario de las raíces pilosas de *C. asiatica*. El conocimiento generado puede contribuir a entender el funcionamiento del metabolismo de las raíces pilosas de *C. asiatica* después de ser elicitadas con MeJA y CORO. Cómo el metabolismo puede ser controlable y flexible al mismo tiempo.

RÉSUMÉ

MSc Antoni Garcia Baeza **Date de la soutenance : le 10 novembre du 2023**

Universidad Autónoma de Nuevo León
Facultad de Ciencias Química

Nantes Université
UFR des Sciences Pharmaceutiques et Biologiques

Titre du projet : Etude métabolomique de la régulation métabolique et du contrôle de production des centellosides par des cultures de hairy roots de *Centella asiatic*a

Nombre de pages : 226

Candidate au grade de Docteur en Science avec Orientation en Pharmacie

Discipline d'étude : Pharmacie et Chimie des Produits Natureles

Objectif et méthode d'étude :

Centella asiatica (L.) Urban est une herbe médicinale pérenne appartenant à la famille des Apiaceae. Les utilisations ethnomédicales par différentes médecines populaires remontent au 16ème siècle jusqu'à nos jours. Des extraits de *C. asiatica* ont été rapportés dans des études scientifiques comme traitement de la cicatrisation des plaies, de l'asthme, de la lèpre, du psoriasis, du lupus, et utilisés comme agent améliorant la mémoire, antidépresseur, antibactérien, antifongique, antiviral et anticancéreux. Au cours des huit dernières décennies, la recherche phytochimique sur *C. asiatica* a rapporté environ 130 substances phytochimiques présentes dans cette plante, y compris des triterpènes pentacycliques, des flavonoïdes et des composés phénoliques, entre autres. Cependant, la recherche de nouvelles entités moléculaires et de leurs activités biologiques est toujours en cours. Les bioactivités de *C. asiatica* ont été principalement attribuées à ses produits naturels triterpéniques pentacycliques exclusifs, communément appelés centellosides. Cette famille moléculaire comprend des saponines et des sapogénines

triterpéniques ayant un potentiel pharmacologique dans le cancer, le diabète, les maladies neurologiques, les maladies du foie, la cicatrisation des plaies et les maladies infectieuses. Toutefois, les bioactivités les plus remarquables des composés de type centellosides sont la cicatrisation des plaies et l'amélioration des performances cognitives. Au cours des dernières années, le marché des cosmétiques a montré un intérêt pour les centellosides. Leur demande a augmenté et de nombreuses entreprises incluent des extraits de *C. asiatica* ou des produits centellosides isolés dans leur portefeuille. On les trouve principalement sous forme de produits en vente libre (OTC). La complexité chimique des centellosides rend leur synthèse chimique non viable. Par conséquent, les plantes *C. asiatica* sont devenues la principale source de ces composés bioactifs nécessaires au développement de produits de valeur sur le marché des cosmétiques et de l'herboristerie. L'approvisionnement incontrôlé du marché a conduit à l'épuisement des stocks sauvages, notamment en Inde et à Madagascar. Au cours des dernières décennies, la recherche a attiré l'attention sur le développement d'une usine de production biotechnologique utilisant des cultures tissulaires *in vitro* de *C. asiatica*. Les cultures *in vitro* permettent la production naturelle des métabolites d'intérêt d'une manière plus durable que l'obtention des métabolites par extraction chimique de la plante puisqu'elles sont indépendantes du sol cultivable. Des résultats différents et prometteurs ont été obtenus en fonction du type de culture. Parmi la pléthore de systèmes *in vitro* développés, les « hairy roots « (littéralement, les racines chevelues, mais nous garderons le terme anglais par la suite) sont l'un des systèmes les plus adaptés à la bioproduction biotechnologique. Les hairy roots sont issues de l'infection d'explants végétaux par *Agrobacterium rhizogenes*. Elles conviennent comme plateforme de production en raison de leur grande stabilité génétique, de leurs capacités de biosynthèse sans besoin de facteurs externes, de leur production rapide de biomasse et de la possibilité d'être utilisées pour plusieurs générations successives. Cependant, les lignées de hairy roots de *C. asiatica* ne produisent pas de quantités basales de centellosides comparables à celles d'autres systèmes *in vitro.* Néanmoins, la production de métabolites secondaires est généralement faible dans tout type de culture. Le métabolisme secondaire des plantes ne fonctionne généralement pas de manière constitutive. Il s'agit d'un métabolisme hautement spécialisé et diversifié au sein

du règne végétal. La complexité des voies et les molécules qui sont formées nécessitent souvent beaucoup d'énergie pour la plante. Dans la plupart des cas, les voies secondaires sont réduites au silence. Elles ne sont activées que lorsque la plante est stressée par un facteur externe. Les études biotechnologiques ont tiré parti de cette observation en utilisant des signaux artificiels pour activer le métabolisme secondaire tel qu'il se produit dans la nature. Cette stratégie, appelée élicitation dans la terminologie scientifique, a été cruciale pour la faisabilité de la production de métabolites secondaires d'intérêt dans des systèmes *in vitro.* Dans le cas de *C. asiatica*, l'ajout d'éliciteurs aux milieux de culture s'est avéré crucial pour activer la biosynthèse des centellosides et d'autres métabolites secondaires. En ce qui concerne *C. asiatica*, il a été clairement démontré que l'ajout d'éliciteurs dans les milieux de culture est crucial pour stimuler la production de centellosides et d'autres métabolites secondaires. Grâce à une collaboration avec le laboratoire du Dr. Palazon-Barandela (Faculté de pharmacie, Université de Barcelone), une lignée de hairy roots a pu être obtenue à partir de plantes de *C. asiatica*. Des études précédentes sur cette lignée ont démontré la surproduction de centellosides dans des conditions d'élicitation utilisant deux phytorégulateurs : le méthyl-jasmonate (MeJA) et la coronatine (CORO). Cependant, le choix de l'éliciteur est empirique, et la réponse de la plante est souvent imprévisible. La productivité du système biotechnologique dépend de la connaissance du mécanisme de biosynthèse de la culture. Cependant, l'élicitation présente une dualité : elle n'est pas seulement un outil de force brute pour activer les voies de biosynthèse secondaires, mais elle permet également d'étudier le métabolisme de la culture. Les conditions contrôlées offertes par la culture *in vitro* (culture axénique, contrôle de la composition du milieu de culture, de l'environnement, etc.) ainsi que la suractivation du métabolisme secondaire déclenchée par l'élicitation créent une plateforme biologique optimale pour le prélèvement d'échantillons et l'analyse ultérieure de l'état de leur métabolisme. Les sciences omiques permettent une analyse à haut débit des métabolites, des gènes et/ou des protéines impliqués dans le métabolisme au moment du prélèvement. À ce jour, deux approches métabolomiques ont traité de la régulation des cultures de tissus végétaux de *C. asiatica* élicités par le MeJA. Ces études ont révélé l'activation des voies des acides caféoylquiniques (ACQs), des triterpènes pentacycliques et des flavonoïdes après l'élicitation du

MeJA. Cependant, ces études publiées jusqu'à présent ne vont pas au-delà de l'exploration de la voie des centellosides, l'influence du moment de la récolte et le rôle de l'élicitation dans le métabolisme primaire ont été écartés. Le mode d'action de CORO est dans une certaine mesure similaire à celui de MeJA, mais il présente souvent une activation plus importante du métabolisme secondaire. Les effets du CORO sur le métabolome dans les systèmes *in vitro* de *C. asiatica* n'ont pas encore été explorés. Par conséquent, dans ce travail, la régulation du métabolisme primaire des cultures de de hairy roots de *C. asiatica* traitées avec du méthyl-jasmonate (MeJA) et de la coronatine (CORO) est explorée par une approche métabolomique de la RMN des protons (RMN 1H) en série temporelle. Le métabolisme secondaire a également été exploré avec les mêmes échantillons par une approche métabolomique UHPLC-MS/MS et UPLC-HRMS/MS. Les variations du métabolome primaire et secondaire ont été détectées en comparant des cultures témoins à des cultures traitées avec des éliciteurs 0-16 jours après le traitement. Des modèles statistiques d'analyse de données multivariées (MVDA) ont soutenu l'interprétation biochimique des données afin de mieux comprendre la régulation et le contrôle du métabolisme des hairy roots de *C. asiatica*.

Conclusions et Contributions :

La régulation du métabolisme primaire des cultures de de hairy roots de *C. asiatica* traitées avec du méthyl-jasmonate (MeJA) et de la coronatine (CORO) a été explorée par une approche métabolomique RMN 1H en série temporelle. Des modèles statistiques d'analyse de données multivariées (MVDA) ont révélé que CORO provoquait un effet de reprogrammation précoce et supérieur sur le métabolome primaire par rapport au MeJA. La comparaison des déplacements chimiques expérimentaux par RMN de signaux spécifiques avec ceux rapportés dans des conditions similaires a permis l'identification de 40 composés. La liste des métabolites primaires détectés comprenait des glucides, des acides aminés, des nucléosides et certains acides organiques. De plus, trois ACQs appartenant au métabolisme secondaire ont été détectés. La cinétique de production relative des métabolites détectés et leurs liens possibles avec chaque traitement ont été discutés. Les deux éliciteurs ont déclenché une réduction significative des

glucides par rapport au contrôle, des changements majeurs sur la production d'acides aminés par rapport au contrôle et une surproduction significative d'ACQs par rapport aux conditions de contrôle. Dans les échantillons traités au MeJA, les ACQ ont été initialement produits au jour 8 et sont restés constants pendant les 16 jours de culture. D'autre part, le CORO a provoqué la production de ces composés du jour 4 jusqu'à la fin de l'expérience. Dans l'ensemble, les deux éliciteurs ont démontré avoir un effet de reprogrammation dans le métabolisme primaire à travers le secondaire. En outre, CORO a démontré un effet plus fort puisque les sources primaires de carbone et d'acides aminés ont été consommées pour la production différentielle et plus précoce de ACQs. Ces résultats sont cruciaux pour l'application de stratégies d'ingénierie métabolique dans les plateformes de production biotechnologique de hairy roots de *C. asiatica*.

D'autres recherches sur les réponses du métabolisme secondaire après élicitation ont été développées par une approche métabolomique à la fois par UHPLC-MS/MS basse résolution et UPLC-HRMS/MS en utilisant les mêmes extraits méthanoliques. Cette étude a impliqué l'analyse par UHPLC-MS/MS des composés standard censés se trouver dans les échantillons de hairy roots de *C. asiatica*. Ainsi, cette connaissance a facilité le criblage ciblé de ces composés en extrayant leurs chromatogrammes d'ions et leur annotation appropriée dans l'analyse ultérieure. Elles ont également permis d'optimiser la méthode UHPLC-MS/MS pour la séparation correcte des principaux composés que l'on s'attend à trouver dans les extraits méthanoliques des racines poilues. L'analyse ciblée par UHPLC-MS/MS a été utilisée pour comparer quantitativement le profil des métabolites des différents traitements et jours de récolte des hairy roots de *C. asiatica*. En conséquence, un total de 12 ions m/z ont été provisoirement annotés, dont l'acide asiatique, l'acide madécassique, le madécassoside, l'AD et 7 acides caféoylquiniques. L'évaluation des chromatogrammes d'intensité des pics de base a montré des différences dans la présence/absence de certains pics et des différences dans l'intensité des pics entre les différents échantillons et selon le moment de la récolte. En général, MeJA et CORO ont eu un effet positif sur l'accumulation des ACQ et des centellosides détectés. La CORO a pu augmenter de manière significative la production de centellosides aux jours 8 et 16 après l'élicitation par rapport au MeJA. La production d'ACQ dans les conditions CORO n'était statistiquement différente de celle des

autres groupes qu'après 12 jours d'élicitation. Contrairement à l'approche ciblée, l'approche non ciblée a permis la comparaison globale du métabolome au niveau quantitatif et qualitatif des extraits dans les différentes conditions et moments de récolte. Cette approche était particulièrement importante en tant que générateur d'hypothèses sur la régulation du métabolisme secondaire. L'analyse en composantes principales et l'analyse en clusters hiérarchiques (HCA) ont révélé un effet de reprogrammation fort et rapide de CORO sur le métabolome à partir de 4 jours d'élicitation. En outre, elles ont montré la puissance des deux éliciteurs et leur utilité en tant que régulateurs possibles du métabolisme en vue de l'amélioration et/ou de l'activation du métabolisme secondaire. Les données obtenues par UHPLC-MS/MS n'ont pas permis une annotation plus poussée des métabolites. Par conséquent, des réseaux moléculaires (RM) ont été construits à partir des données obtenues par UPLC-HRMS/MS dans le but de visualiser la relation structurelle des ions détectés sur la base de leurs spectres MS/MS. Les RM ont facilité la déréplication des ions d'intérêt ou, au moins, leur classification dans une famille de composés. De nouveaux composés jamais décrits jusqu'à présent chez *C. asiatica* ont été annotés de manière putative. Les ions d'intérêt étaient ceux qui se sont avérés contribuer à la variabilité des modèles statistiques utilisés pour les différences entre les traitements et les temps de collecte. Les analyses OPLD-DA et de corrélation ont révélé que CORO et MeJA étaient capables de réguler à la baisse la branche oléane des centellosides, tout en renforçant simultanément la voie de l'ursane (dont sont dérivés les centellosides les plus actifs sur le plan biologique). Ces deux voies représentent une branche importante de la voie de biosynthèse des centellosides. La même analyse a également suggéré que les flavonoïdes de *C. asiatica* pourraient être régulés par les deux éliciteurs dans une certaine mesure. Ce travail présente la première analyse métabolomique en série temporelle pour l'étude de la régulation du métabolisme primaire et secondaire des hairy roots de *C. asiatica*. Elle pourrait contribuer à la compréhension du métabolisme des hairy roots de *C. asiatica* après l'élicitation de MeJA et CORO et à la manière dont le métabolisme peut être contrôlé.

TABLE OF CONTENTS

TABLE INDEX

FIGURE INDEX

LIST OF ABBREVIATIONS

AA	Asiatic Acid
AD	AsiaticosiDe
ANOVA	ANalysis Of Variance
AP	Aerial Part
BPI	Base Peak Intensity
CaCYS	*C. asiatica* CYcloartenol Synthase
CaDDS	*C. asiatica* DammareneDiol Synthase
CaFPS	*C. asiatica* Farnesyl Pyrophosphate Synthase
CaHMGR	*C. asiatica* 3-Hydroxy-3-MethylGlutaryl-CoA Reductase
CaSQS	*C. asiatica* Squalene Synthase
cDNA	Complementary DNA
CIR	Cosmetic Ingredient Review
CNS	Central Nervous System
COI1	COronatine Insensitive1
CORO	Coronatine
COSY	homonuclear COrrelation SpectroscopY
CQA	CaffeoylQuinic Acid
CYP450	CYtochrome P450 monooxygenase
D_2O	Deuterium Oxide
DDA	Data Dependent Analysis
DMAPP	DiMethylAllyl PyroPhosphate
DNP	Dictionary of Natural Products
DS	3-Deoxy-d-arabino-heptulosonate-7-phosphate Synthase
DW	Dry Weight
EDTA	EthyleneDiamine-Tetraacetic Acid
EMA	European Medicines Agency
EPM	Elevated Plus-Maze
ESI	ElectroSpray Ionisation
FA	Formic Acid
FDA	Food and Drug Administration
FPP	Farnesyl Diphosphate
FPS	Farnesyl Pyrophosphate Synthase
FQA	FeruloylQuinic Acid
FW	Fresh Weight
GABA	γ-AminoButyric Acid
GABA-T	GABA Transaminase
GAD	Glutamic Acid Decarboxylase
GC-MS	Gas Chromatography Mass Spectrometry
Gln	Glutamine
GNPS	Global Natural Product Social Molecular Networking
GGPP	Geranyl-Geranyl PyroPhosphate

GPP	Geranyl PyroPhosphate
GT	Glucosyl-Transferase
HCA	Hierarchical Clustering Analysis
HCl	Hydrochloric acid
HMBC	Heteronuclear Multiple Bond Correlation
HPLC	High Performance Liquid Chromatography
HR	Hairy Roots
HSQC	Heteronuclear Single Quantum Correlations
INEGI	Mexican National Institute of Statistics and Geography
IPP	Isopentenyl PyrophosPhate
IT	Ion Trap
IUPAC	International Union of Pure and Applied Chemistry
JA	Jasmonates
JA-Ile	7-iso-Jasmonoyl-*L*-Isoleucine
LC-MS	Liquid Chromatography Mass Spectrometry
LV	LeaVes
m/z	mass to charge ratio
MA	Madecassic Acid
MD	MadecassosiDe
MeJA	Methyl-JAsmonate
MN	Molecular Network
Mr	Relative Molecular mass
mRNA	messenger RiboNucleic Acid
MS	Mass Spectrometry
MS/MS	tandem Mass Spectrometry
MVA	MeVAlonate
MVDA	Multivariate Data Statistical Analysis
NaN_3	Sodium azide
$NaNO_3$	Sodium nitrate
NMR	Nuclear Magnetic Resonance
NR	Not Reported
OPLS-DA	Orthogonal Projections to Latent Structures Discriminant Analysis
OSC	OxidoSqualene Cyclase
OSE	OxidoSqualene Epoxidase
OTC	Over The Counter
p-CoQA	ρ-CoumaroylQuinic-Acid
PAL	Phenylalanine Ammonia-Lyase
PC	Principal Component
PCA	Principal Component Analysis
PDA	PhotoDiode Array
Q-TOF	Quadrupole Time-Of-Flight
Ri	Root induction
RNA-Seq	RNA-Sequencing
rpm	Revolutions per minute
Rt	Retention time

SPS	Sucrose-Phosphate-Synthase
SQS	SQualene Synthase
TIC	Total Ion Chromatogram
TSP	3-(TrimethylSilyl)-1-Propanesulfonic acid sodium salt
UGT	UDP-GlucosylTransferase
UHPLC-HRMS/MS	Ultra High Performance Liquid Chromatography-High Resolution Tandem Mass Spectrometry
v/v	volume/volume
VIP	Variable Importance in Projection
WP	Whole Plant
XIC	Base peak traces
α/β**AS**	α/β Amyrin Synthase
δ	Chemical Shift

CHAPTER 1

1. BACKGROUND

1.1. *Centella asiatica* as Medicinal Plant

C. asiatica (Fig. 1.1) has been utilised as a medicinal herb since prehistoric times dating back to the 16th century. Many healing cultures in the globe consider *C. asiatica* as an important medicinal plant. Japanese and African traditional medicine and the Indian Ayurvedic medical system use the plant for various medical purposes. Usually, the extracts are applied topically in the form of creams or ointments, or made into powder drugs or infusions (1,2). The principal therapeutic effects include enhancement of wound healing, treatment of asthma, leprosy, psoriasis, lupus, and used as memory-enhancing, antidepressant, antibacterial, antifungal, antiviral, and anticancer agent.

Figure 1. *Centella asiatica*: (A), (B) and (C) habit, and (D) stolons. (Figures were obtained from https://commons.wikimedia.org; licensed under the Creative Commons Attribution-Share Alike 4.0)

Nowadays, *C. asiatica* is an important medicinal herb for commercial products. Specially, they are found as over the counter (OTC) medicines in the cosmetic and herbalism market in semisolid forms or pills. Its extensive commercial applications in cosmetics and health supplements are attributed to its ability to nourish skin, to reduce pigmentation, fine lines, and dark circles, to maintain venous circulation and cognitive functioning, to improve blood circulation, to decrease inflammation, among others. The formulations containing the plant have been reported as skin lotion, organic shampoo, hair oil, hair gel,

hair conditioner, skin cream, skin toner, mask pack, cleansing balm, skin moisturizer, facial serum, vitamin, dietary and nutritional supplements, cognitive booster, buffet serum, and many more (3). Many companies manage products including *C. asiatica* extracts or ingredients based on this plant especially in Asia (4) but also in Europe (5,6). In India it was placed as the third most important medicinal herb (7). Examples of commercial products are CenteroxTM (Indena, Italy), CentevitaTM (Indena), Centellino (Sabinsa Corp, USA), Revitalift CitaCrème (L'Òreal, France), Ciclaplast (L'Òreal, France), and Centella Reversa (Vytrus Biotech, Spain) (6). However, *C. asiatica* is also found in herbal medicines and nutraceuticals as anxiolytic (8). The European Pharmacopeia include monographs about the preparation of *C. asiatica* herbal products (8,9).

1.1.1. Centellosides as Natural Products

C. asiatica has received much attention due to its broad range of therapeutic applications which are mainly associated to its exclusive specialised metabolites (formely known as secondary metabolites) commonly known as centellosides. This term includes the pentacyclic saponins and their remaining part without the sugar moiety, known as aglycone or sapogenin. Centellosides account on average for up to 8% of the dry mass of the herb (10). Among the plethora of centellosides, research have focused mainly in asiatic acid (AA) and madecassic acid (MA) and their saponins asiaticoside (AD) and madecassoside (MD) (Figure 2). These centellosides are the most active constituents among the family.

Scientist have done many efforts in exploiting the medical applications of both the plant centellosides-enriched extracts and isolated centellosides. The principal reported biological effects of these molecules include wound healing (8,11–15), protective effects to neurological injury (16,17,26–31,18–25), improvement of memory, physical performance and anti-depressant (25,32,41–47,33–40), anti-cancer (48–50), anti-inflammatory activity (7,51–54), and metabolic syndrome (55,56) (Figure 3). The literature evidences the interest in their isolation and massive production for industrial purposes.

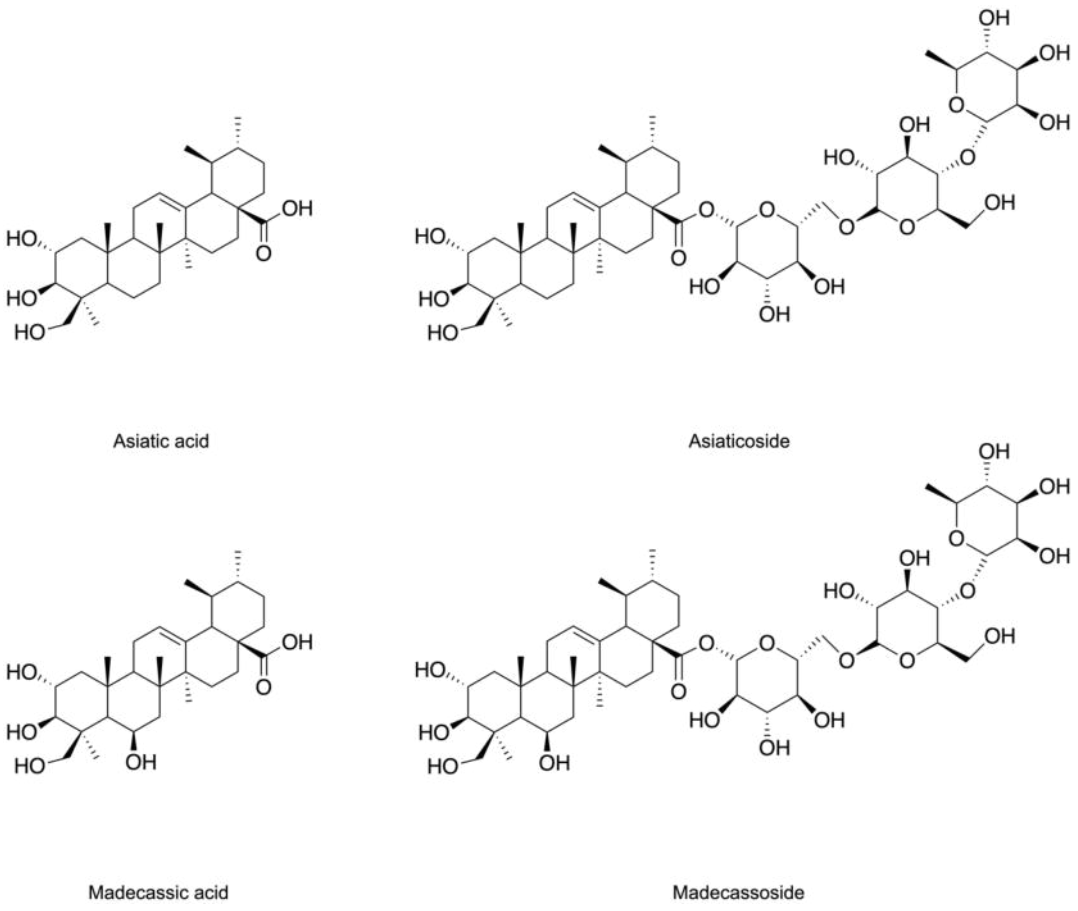

Figure 2. Chemical structure of the four principal centellosides

As above-mentioned*, C. asiatica*-derived products are mainly sold as OTC. These types of medicines are under less strict regulation framework compared to prescribed medicines. However, its toxicity and pharmacology are well-described (57,58). A report of Cosmetic Ingredient Review (CIR) expert panel (2015) (59) confirmed the safety of different extracts of *C. asiatica*. It was based on data from oral administration in human studies and *in vitro* human cell cultures. The assessment report on *C. asiatica* by European Medicines Agency (2022) (60) concluded that the tolerability of oral *C. asiatica* preparations has generally been good and no known adverse events from pharmacovigilance data exist. However, the FDA has not approved any centelloside as a drug. Probably because there is an ambiguity in the underlying mechanism of action. The proposed mode of action is mainly by the (i) inhibition of enzymes in a non-specific manner based on hydrophobic interaction within the hydrophobic domain of enzymes and (ii) the influence in the membrane fluidity. However, many efforts have been done in order to elucidate the mechanism of action and the pharmacological aspects of centellosides (61).

One of the most promising applications of centellosides are their activities as anxiolytics and antidepressants. Centellosides seem to avoid the typical secondary effects from classic medicinal therapies of anxiety-like disorders (25). The principal outcomes regarding this are described in the following sections.

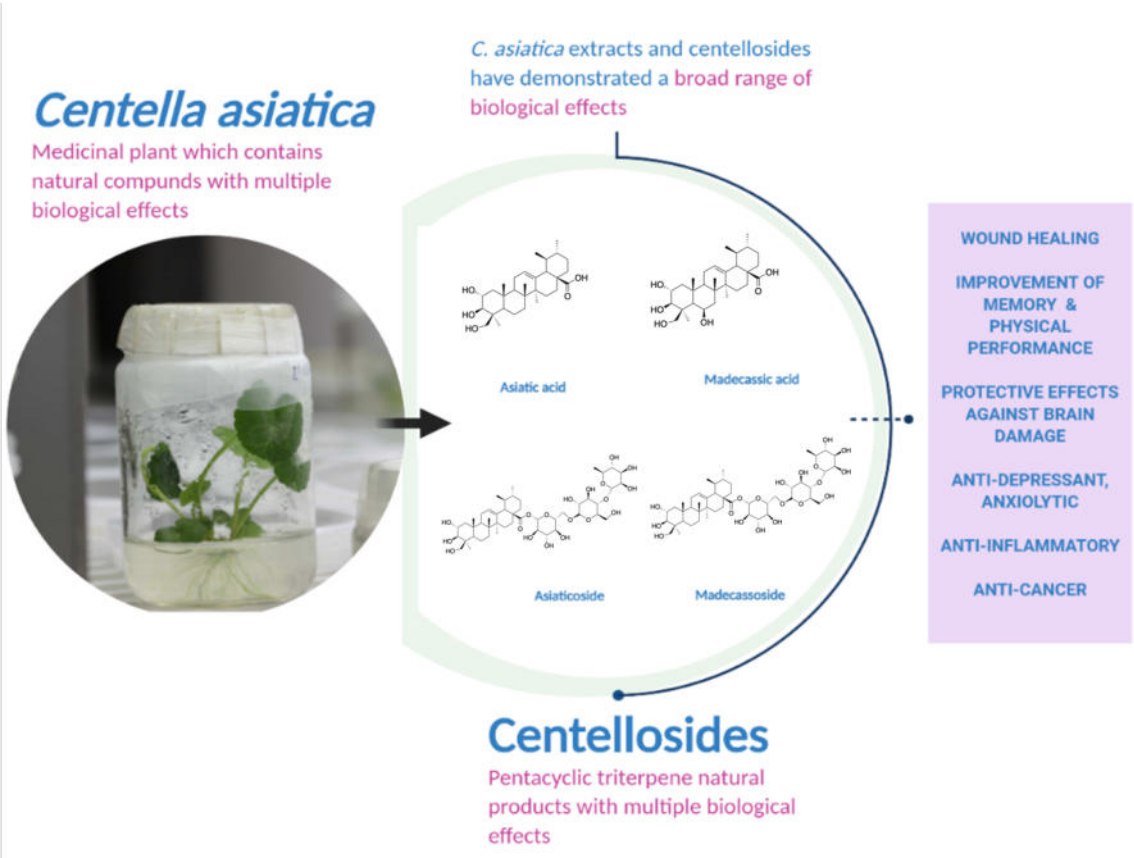

Figure 3. *C. asiatica* grown in *in vitro* conditions (left). Centellosides and their principal biological effects (right)

1.1.2. *C. asiatica* and centellosides as anxiolytics

Anxiety is a mental disorder characterised for uncertainness and fear about the future leading to a nervous mood. The intensity among patients is highly variable since anxiety occurs due to personal traumas or stress situations. It is usually accompanied by cognitive, somatic, and behavioural manifestations (62). Due to the high prevalence of anxiety, it has become as common mental problems for the population. The symptoms and forms of anxiety are highly variable, and, in many cases, it derives in fatal consequences as suicide. Moreover, the duration

also differs among patients (from months to years). About 4–6% of the global population suffer from various forms of anxiety disorders with such symptoms as high blood pressure, elevated heart rate, sweating, fatigue, unpleasant feeling, tension, irritability, and restlessness. In Mexico, the prevalence of anxiety is over 4.2 million people. In addition, the Mexican National Institute of Statistics and Geography (INEGI) showed that deaths related to mental and behavioural disorders increased by 33% between 2008 and 2014 (63). Suicidal thoughts are the fatal consequence of anxiety, and it is listed as one of the most important factor risk of suicide (64,65).

Treatment of anxiety must be dealt accurately by a therapist who evaluates whether psychotherapy should combine pharmacotherapy. Despite the availability of numerous classes of drugs for the treatment of anxiety and depression, the full remission of disease symptom has remained elusive. Current treatment of anxiety consists in the administration of benzodiazepines, barbiturics, selective serotonin reuptake inhibitors or selective serotonin norepinephrine reuptake inhibitors, among others. Clinical use of these drugs is limited by their characteristic side effects and poor tolerability profile. The mode of action overall is to enhance monoaminergic and γ-aminobutyric acid-ergic (GABAergic) function. It is achieved inhibiting the enzyme responsible for the breakdown of monoamines (norepinephrine, serotonin, and dopamine) or γ-aminobutyric acid (GABA). Thus, the reuptake of monoamines is blocked. This causes an increase in their concentration at the synaptic cleft. The secondary effects are sometimes severe and affect the regular daytime of patients: addiction or sedative effects resulting in drowsiness or fatigue (66,67).

Studies have demonstrated that many phytochemicals such as saponins, alkaloids, polyphenols, triterpenoids, essential oils, fatty acids and flavonoids possess anxiolytic and antidepressant-like effects (68). However, during 1981–2019 only 10 new drugs with anxiolytic activity and 28 with antidepressant activity were developed. These were mainly synthetic drugs. Among them, there was only 1 anxiolytic drug derived from a pharmacophore found in nature (69). This evidences the need for further research on anxiolytic natural products. Currently, all the anxiolytic medicines based on plant natural products are plant-based medicines found as OTCs (68). For example, the European Medicines Agency (EMA) includes *Hypericum perforatum*, *Melissa officinalis, Valeriana officinalis,* among others in the list of herbal medicines for the treatment of mental stress and anxiety (70).

Centellosides have shown to have similar neuroactive and neuroprotective effects to the entire plant extract in many of the same experimental contexts. For instance, both AA and AD have shown to have anxiolytic properties in rat models (35,47) without exhibiting sedative effects (47). Table 1 summarizes the description and the principal outcomes of the available studies regarding the anxiolytic effect of both centellosides and extracts of *C. asiatica*.

Table 1. Results of human clinical trials and mice *in vivo* studies to assess the anxiolytic effect of *C. asiatica* and centellosides

Type of extract or Compound	Plant part	Model	Analysis	Dosage	Controls	Result	Ref.
Human clinical trials							
Non-standardised *Centella* extract	WP	40 healthy participants	Measurements of acoustic startle response (ASR), mood self-rating scale, heart rate, and blood pressure	12 g dissolved in 300 mL grape juice	Placebo	Significantly reduced the amplitude of the startle response both 30- and 60-min following treatment	(71)
Powder of dried plant	LV	60 Patients aged 65 years and above	Sense of well being	500 mg twice a day for 6 months	NR	A significant improvement in the sense of well-being was observed in most of the patients	(39)
70% hydro-ethanolic extract of *Centella asiatica*	WP	33 individuals from the age of 18 to 60	Hamilton's Brief Psychiatric Rating Scale	500 mg capsules for 60 days	NR	All the scale scores improved after 60 days, with no side effects	(72)
Mice model							
Aqueous extract	WP	Wistar rats	EPM	20 mL/kg body weight for 2 months	Tap water	Decrease of anxiety in offspring of alcoholic mothers.	(46)
Standardised ethanolic extract	NP	Male Laca mice	EPM	150 and 300 mg/kg for 8 days	L-NAME and L-Arginine dissolved in normal saline.	Significant attenuation of anxiety like behaviour.	(42)
AA	NR	55 male Sprague Dawley rats	EPM	30 mg/kg	Midazolam	AA alone at the 30 mg/kg dose is not statistically significant	(35)
Methanolic extract (not less than 80% and the ratio between MD and AD should be 1.5±0.5)	NR	Adult male ICR mice (non-stressed)	EPM, Dark–light box test and Open-field test	30, 100 or 300 mg/kg (twice a day for 10 days)	Diazepam (1 or 2 mg/kg)	There was an anxiolytic effect (except for the 30mg/kg dose) and a lack of effect on locomotor activity.	(41)
Methanolic extract ((not less than 80% and the ratio between MD and AD should be 1.5±0.5)	NR	Adult male ICR mice (stressed)	EPM	10, 30 or 100 mg/kg (twice a day for 10 days)	Diazepam (2 or 10 mg/kg)	Repeated administration of Eca 233 during stress exposure produced anxiolytic effects in EPM.	(41)
AD and MD	NR	Adult male ICR mice (stressed)	EPM	10 mg/kg and 16 mg/kg respectively	0.5% carboxymethyl cellulose 10mL/kg	At the dose approximately equal to their respective contents in Eca 233 (30 mg/kg) showed a significant anxiolytic effect	(41)
Two Commercial *C. asiatica* products	WP	Male Sprague–Dawley rats	EPM	200 mg/kg or 500 mg/kg body wt.	Water (vehicle)	A pronounced anxiolytic effect with both commercial products.	(47)
Hexane, ethyl acetate and methanol extracts	AP	Male Sprague–Dawley rats	EPM	212 mg/kg body wt., 111 mg/kg body wt. And 3047 mg/kg body wt. Respectively	Not reported	Presence of anxiolytic principles in the ethyl acetate and methanol extracts	(47)
AD	NR	Male Sprague–Dawley rats	EPM, Open field, Social interaction, Locomotor activity and Vogel test	1 and 3 mg/ kg body wt for all tests except for the opened field test with dosage of 3, 5 and 10 mg/kg body wt.	NP	Anxiolytic activity	(47)

AP = aerial parts, EPM = Elevated Plus Maze, LV = leaves, NR = not reported, WP = whole plant

1.1.2.1. Centellosides mechanism of action in anxiety

The mechanism of action of *C. asiatica* could be related with an overproduction of γ-aminobutyric acid (GABA) in the brain (Figure 4). GABA is the principal inhibitory neurotransmitter in the central nervous system (CNS). Its low concentration leads to different disorders including anxiety. It is hypothesised that to achieve an increase of GABA it is necessary either to stimulate glutamic acid decarboxylase (GAD) or inhibit GABA-transaminase (GABA-T) (67,73). Accordingly, low concentrations of aqueous extract of *C. asiatica* increased GAD activity by more than 50%, and ethanolic extract showed moderate inhibitory potential of GABA-T (45,74,75). The effect that the extracts exerted on both enzymes supports this GABAergic hypothesis. Recently, it was shown that a standardised extract of *C. asiatica* increased the excitatory responses of neurons that releases GABA in the amygdala. The extract suppressed the output signals of the amygdala that activates the alert feeling that characterizes anxiety (44). It was proposed that this extract could have a similar mode of action as diazepam; by binding the GABA-type A receptor ($GABA_A$) enhancing its permeability (43), and reducing the level of corticosterone in blood (36). Corticosterone participates in the molecular mechanism involved in anxiety by activating receptors in the hypothalamus that lead to a secretion of other hormones related in the fight-or-flight response (73). The corticosterone hypothesis was also proposed in a depression study using mice (76).

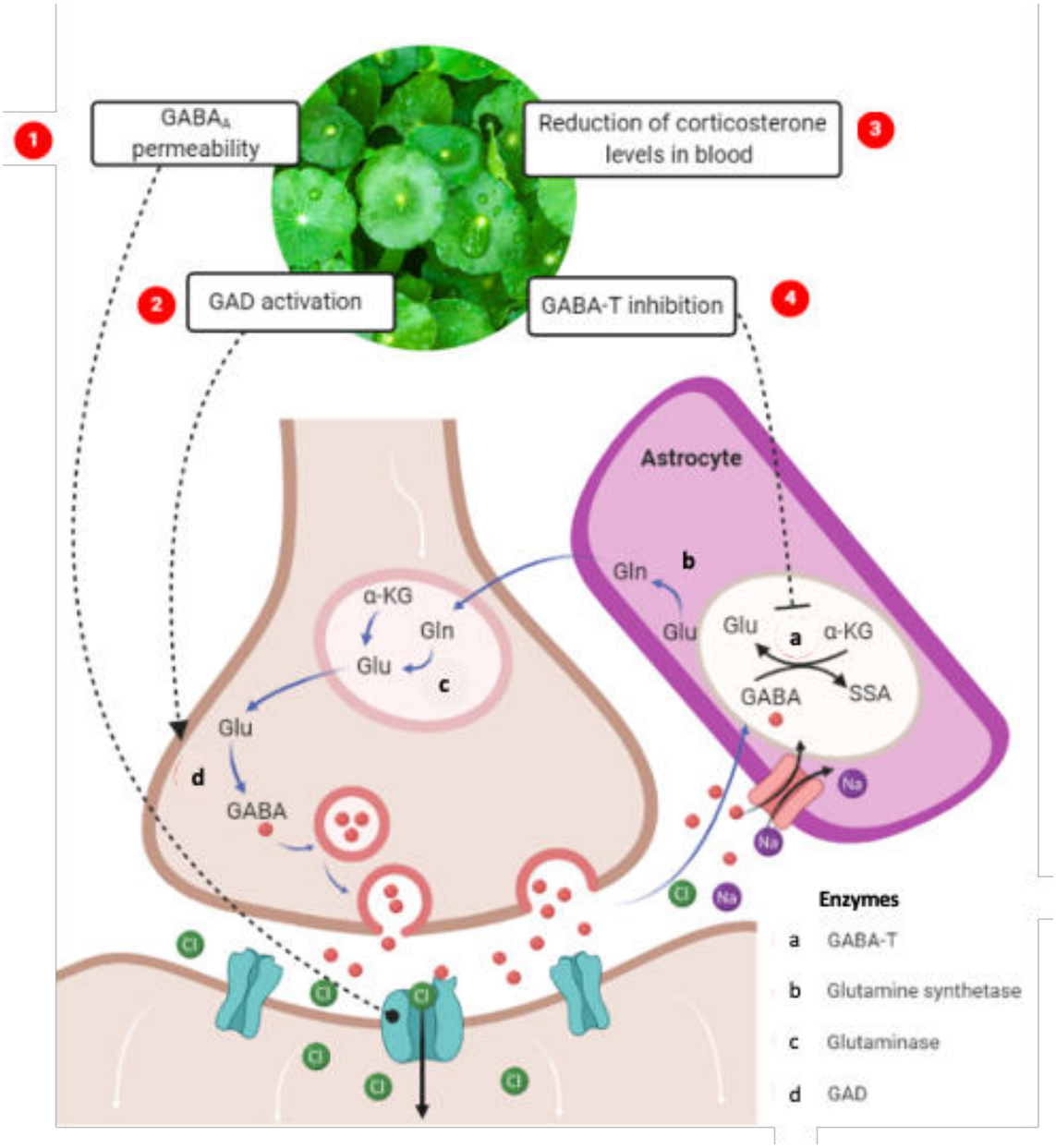

Figure 4. Different proposed mechanism of action of *C. asiatica* as anxiolytic. (1) GABA is translocated into synaptic vesicles, from where it is released into the synaptic cleft. Here, GABA acts on synaptic GABA$_A$ activating the influx of chloride ions to the post-synaptic neuron. The influx provokes the hyperpolarization and the subsequent inhibitory effect. Centellosides are believed to enhance the permeability of GABA$_A$. (4) The presynaptic terminal of a GABAergic neuron takes up glutamine (Gln) released from neighbouring astrocytes. It is proposed that GABA is not consumed in astrocytes because a putative inhibition of GABA-T because of centellosides. (2) Glutamine is then metabolised into GABA through glutaminase and GAD. This last enzyme could be overactivated by centellosides. (3) Centellosides could reduce levels of corticosterone in blood.

1.2. Phytochemistry of *C. asiatica*

In this section, major families found in *C. asiatica* of compounds are briefly described. In addition, Table 2 shows the plethora of reported specialised metabolites in *C. asiatica* so far (pentacyclic triterpenes and saponins are not included in the table). Phytochemical variability has been observed among the wild populations *C. asiatica*; macronutrients, micronutrients, phenolics, including flavonoids, anthocyanins, fatty acids, and sterols. The plant phytochemical composition also varies due to seasonal variations, the cultivation and harvesting procedures, light conditions, and post-harvesting treatments. This underlines the potential challenges involved in the study of *C. asiatica* plant extracts and phytochemical profiles (77).

1.2.1. Pentacyclic triterpenes

Pentacyclic triterpenoids and saponins are not exclusive in *C. asiatica*. They are widely distributed in the plant kingdom. In the biological point of view, their role has been traditionally classified as specialised metabolites (78). They are generally considered defences against pathogens or herbivores (79). As most defence compounds in plants, the endogenous production, accumulation, and distribution is induced in response to abiotic and biotic stresses. The pentacyclic triterpenes levels increase in response to endogenous phytohormones. The signalling culminates in activating transcription factors and defence-related genes

(78–80).

Pentacyclic triterpenes are referred as this due to the structure of hydrocarbon of five rings with no heteroatoms, and an alcohol functional group. They are formed from six isoprene units ($C_{30}H_{48}$). Numerous pentacyclic triterpenes have been described so far in the plant kingdom. There is a vast diversification of genes related to this pathway among plant species. However, the first step in the triterpene route seems to be ubiquitous in nature (56). The molecule 2,3-oxidosqualene is the branch point between sterols and triterpenes. This molecule is the last acyclic triterpene since it suffers a cyclization to produce sterol or triterpene products. This cyclization is the most complex enzymatic reaction in terpene biosynthesis pathway. The cyclization process into pentacyclic triterpenes involves: (i) folding of 2,3-oxidosqualene into a chair-chair-chair conformation, (ii) protonation of the epoxide, (iii) cyclization and rearrangement of carbocation species, and (iv) termination by deprotonation to a final terpene product. Variations in carbocation cyclization and rearrangement steps (step (iii)) contribute to the pentacyclic triterpene scaffold diversity. The end formed triterpenes can be classified depending on the C=C double bond positions and the number of rearrangements of steps occurring before them. The cyclization and the rearrangement are enzymatic steps carried out by oxidosqualene cyclases (OSCs) (Figure 5). Plants usually contain a couple of OSCs isoforms and their occurrence among species is diverse. The capacity of the OSC to reach a certain rearrangement varies. Then, triterpene end products differ among plant species in quantity and form (81,82).

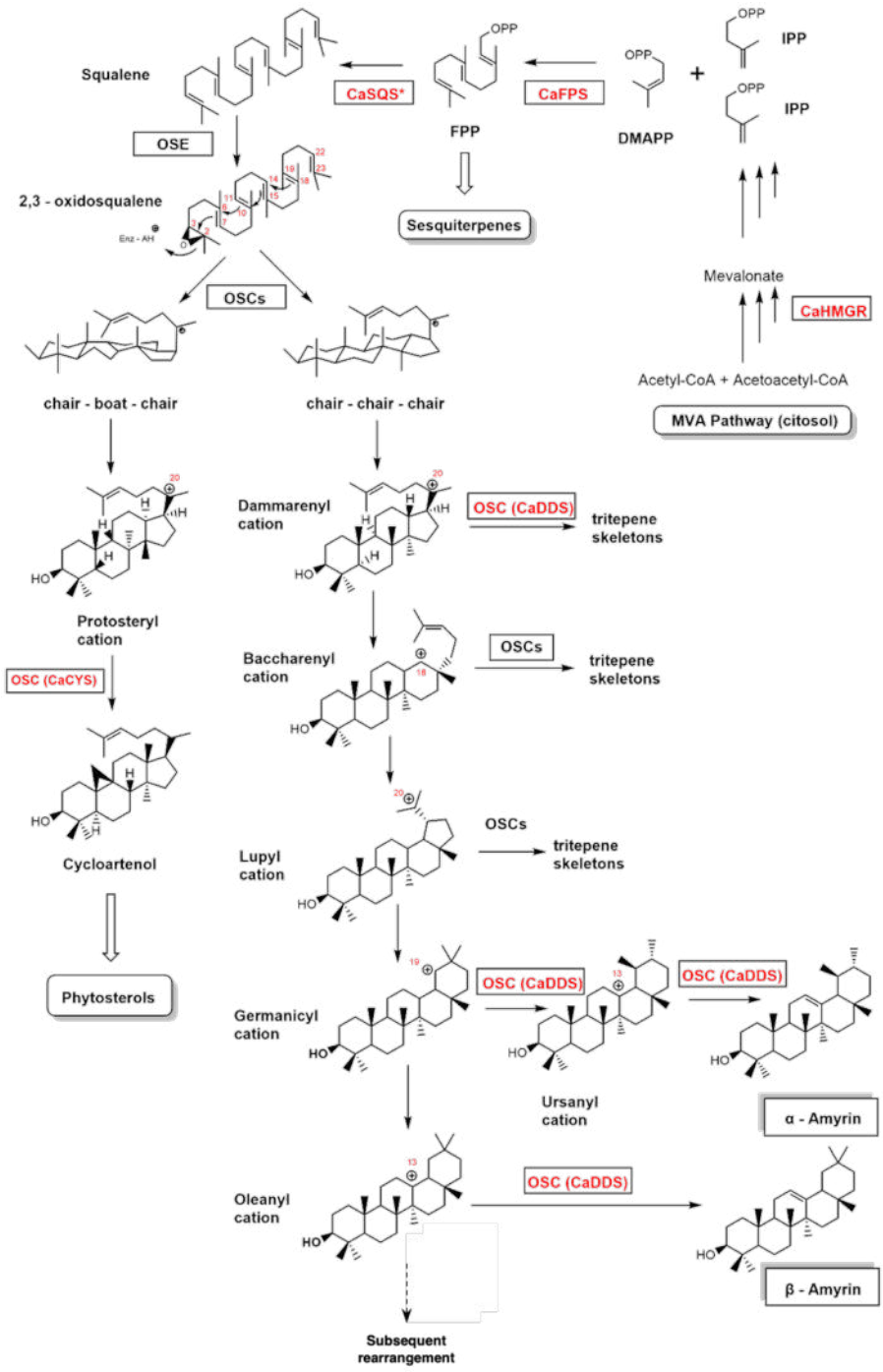

Figure 5. Main steps in the biosynthesis of both α–amyrin and β-amyrin. MVA = mevalonate, IPP = isopentenyl diphosphate, DMAPP = dimethylallyl diphosphate, FPP = Farnesyl diphosphate. Enzymes and their GenBank accession Number: CaHMRG = 3-Hydroxy-3-methylglutaryl-CoA reductase (KJ939450.2) (83), CaFPS = Farnesyl diphosphate synthase (AY787627) (84), CaSQS = Squalene synthase (AY787628) (85), OSE = Squalene epoxidase (unpublished), OSC = Oxidosqualene cyclase, CaCYS = (86), Cycloartenol synthase, CaDDS = Multifunctional oxidosqualene cyclase (dammareiol, α/β-amyrin synthase) (AY520818) (87).

1.2.1.1. Centellosides

Centellosides are pentacyclic triterpenes saponins and sapogenins that derive from the triterpene end products α-amyrin and β-amyrin. In *C. asiatica*, the multifunctional OSC called α/β amyrin synthase (α/β AS) is capable to arrange the usanyl and oleanalyl carbocations forming α-amyrin and β-amyrin, respectively (88). Among the OSCs that have been functionally characterised in the plant kingdom, it is rare to find a OSCs capable of producing α-amyrin more favourably than β-amyrin (89). The two amyrins are structural isomers since the ursane-like structure of α-amyrin harbours a methyl substitution pattern on C-19 and C-20, and the oleanane structure of β-amyrin has a double methylation in C-20. Therefore, centellosides are divided into two subfamilies depending on the precursor: the ursane and oleanane family. Both α-amyrin and β -amyrin further undergo various enzymatic modifications such as oxidation, hydroxylation, and glycosylation by different groups of cytochrome P450 monooxygenase (CYP450) and glycosyl-transferases (GTs) (Fig. 6) (10). Figures 7 and 8 show the putative steps in the centellosides pathway (adapted from (90)). AD, MD, AA, and MA are, so far, the last products discovered in the ursane branch. They are the most accumulated centellosides in *C. asiatica*. Moreover, the biological activities of *C. asiatica* are mainly attributed to these four centellosides. Literature dealing with *C. asiatica* and centellosides is mainly focus on these four centellosides, indeed. Regarding their structures, AA is 2*α*,3*β*,23-trihydroxy-urs-12-ene-28-oic-acid, MA is 6*β*-hydroxy-AA, AD is the ester of AA with two molecules of glucose and one

molecule of rhamnose attached as *O*-2-*L*-rhamhnopyranosyl(1→4)-*β*-*D*-glucopyranosyl(1→6)-*β*-glucopyranosyl, MD is an ester of MA with the same described oligosaccharide. The glycosylation occurs in the C-28 in both cases (Figure 2) (91). In contrast, the oleanane series have not been studied as extended as ursane series (92).

Over 40 triterpenoid compounds of *C. asiatica* derived either from the ursane and oleanane structural subtypes have been reported. Azerad (2016) comprehensively listed these compounds, based on their ring substitution, the hydroxylation positions, the double bond(s) position(s), and the structure of the glycosyl moiety, with their usual and canonical denominations.

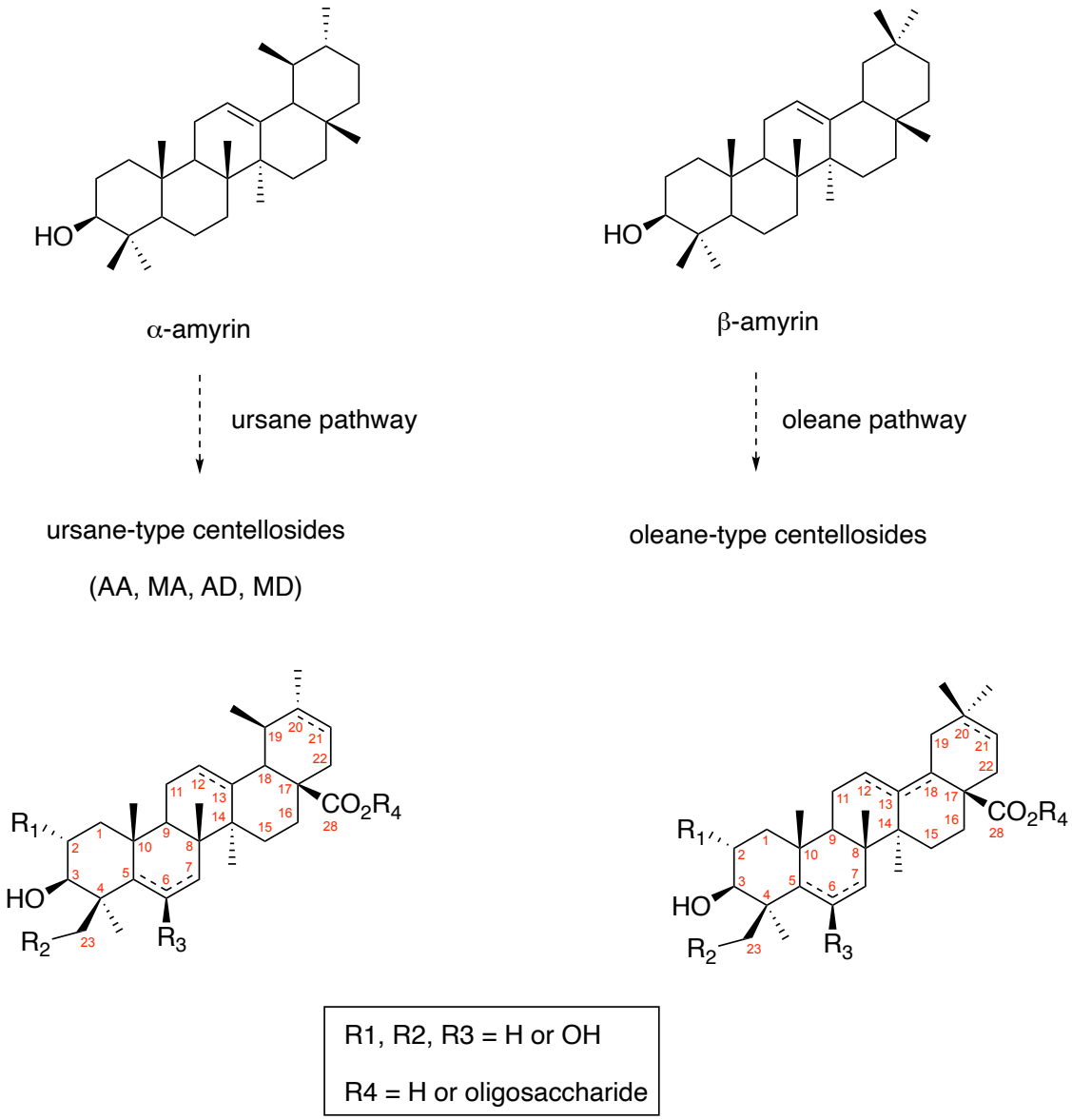

Figure 6. Structures of the pentacyclic triterpenes end products precursors of the two branches of the centellosides pathway: α-amyrin for the ursane branch, and β-amyrin for the oleanane branch (above). Substitution patterns of the centellosides of the ursane family (left) and the oleanane family (right). Centellosides can occur in the ursane (C-19, C-20 - methyl) or oleanane (C20 - dimethyl) types with double bonds occurring at C12-C13, C13-C18 or C20-C21, and possible substitutions (R1, R2, R3 = H or OH and R4 = H or oligosaccharide) (below).

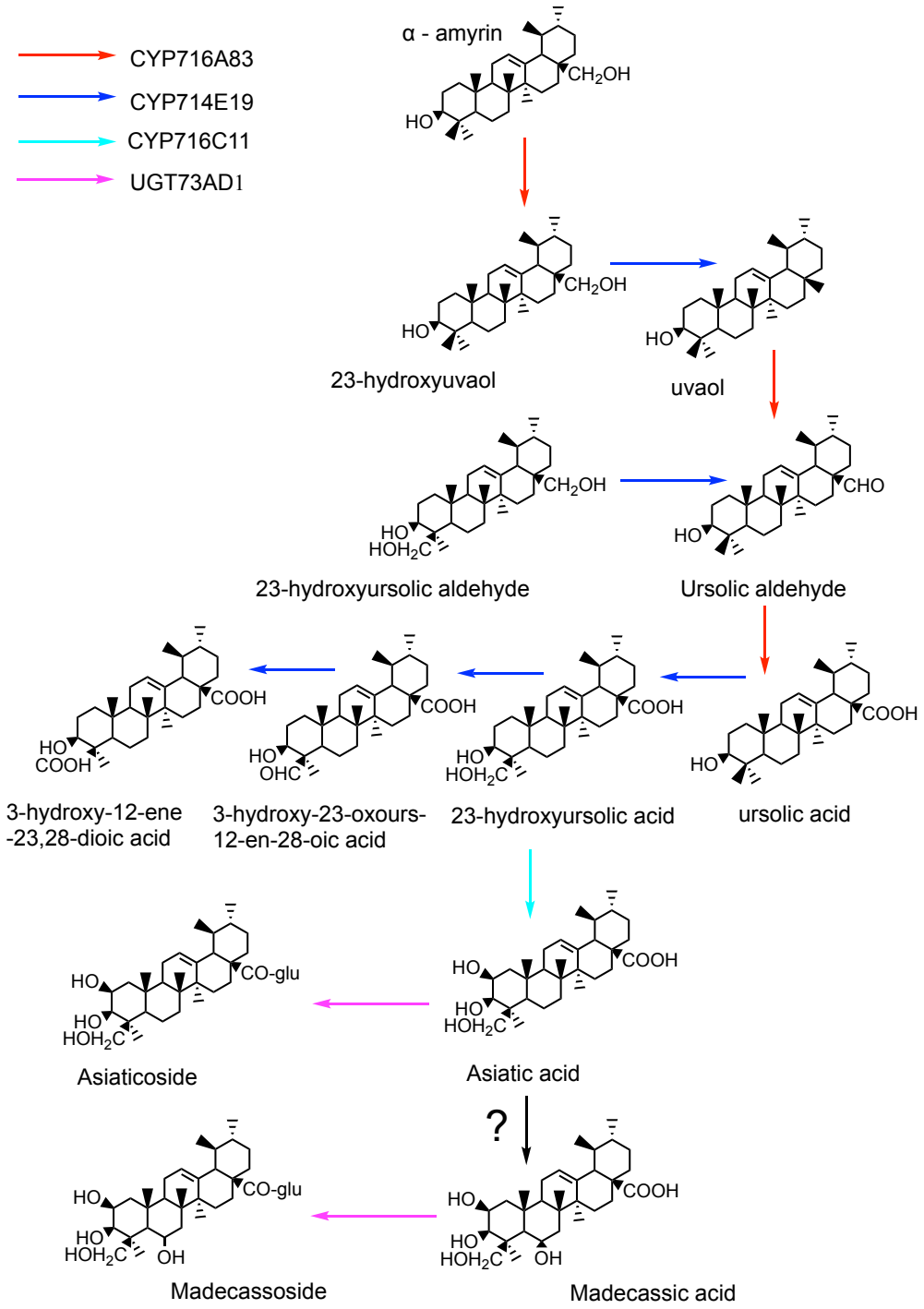

Figure 7. A summarised scheme of biosynthesis of ursane-like centellosides (oxidations and glycosylations). (Figure adapted from (90)). Enzymes and their GenBank accession Number: CYP716A83 = Cytochrome P450-dependent C28 monooxygenase oxidizing (KF004519) (125), CYP714E19 = Cytochrome P450-dependent C23 monooxygenase oxidizing (KT004520.1) (125), CYP716C11 = Cytochrome P450-dependent C2α monooxygenase oxidizing (KU878852) (93), UGT73AD1 = Triterpenoid carboxylic acid: UDP-glucose 28-O-glucosyltransferase (KP195716.1) (159)), ? = unknwon enzyme.

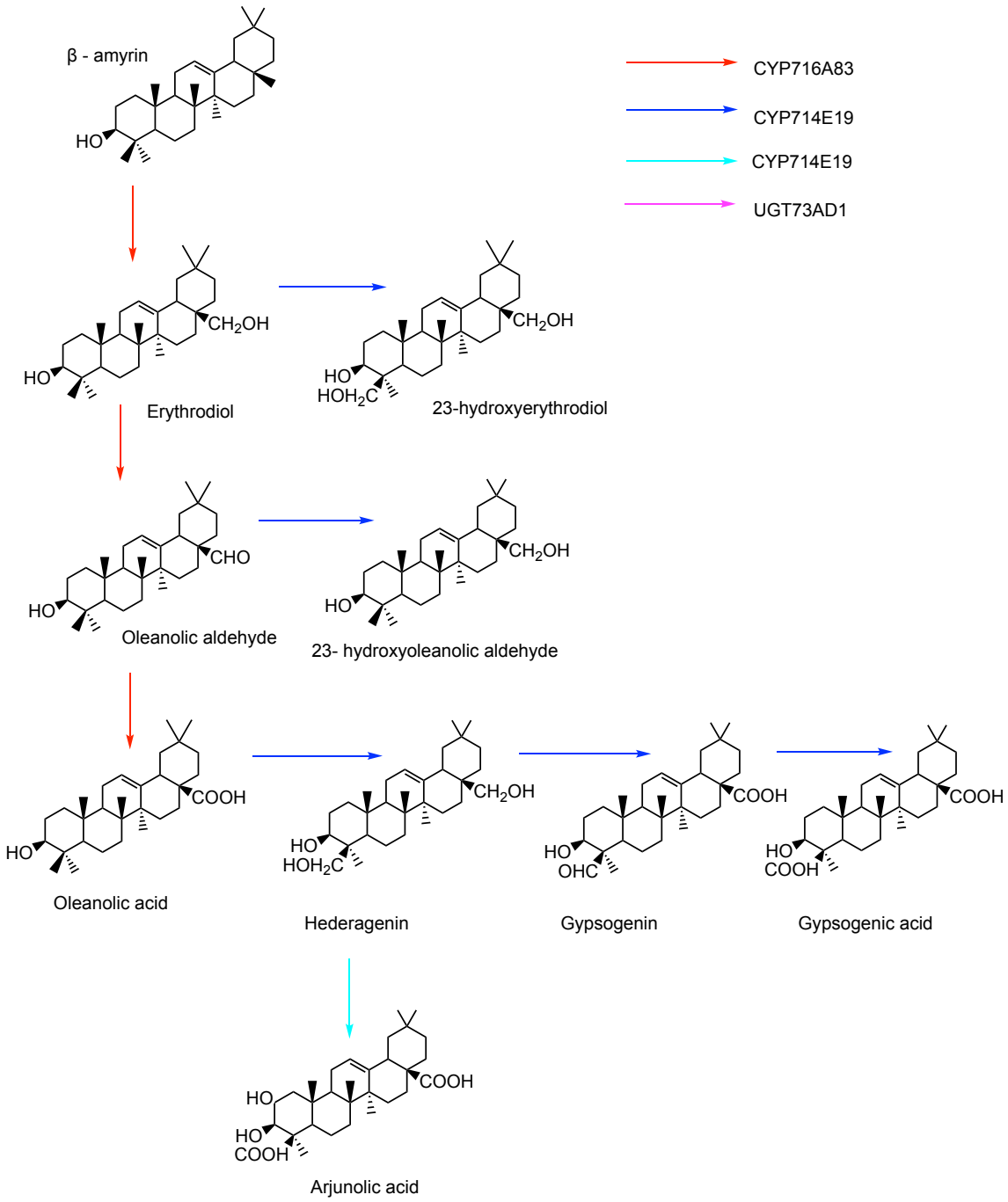

Figure 8. A summarised scheme of biosynthesis of oleanane-like centellosides (oxidations and glycosylations). (Figure adapted from (90)). Enzymes and their GenBank accession Number: CYP716A83 = Cytochrome P450-dependent C28 monooxygenase oxidizing (KF004519) (125), CYP714E19 = Cytochrome P450-dependent C23 monooxygenase oxidizing (KT004520.1) (125), CYP716C11 = Cytochrome P450-dependent C2α monooxygenase oxidizing (KU878852) (93), UGT73AD1 = Triterpenoid carboxylic acid: UDP-glucose 28-O-glucosyltransferase (KP195716.1) (159)), ? = unknwon enzyme.

1.2.2. Caffeoylquinic acids (CQAs)

C. asiatica possess considerably quantities of caffeoylquinic acids (CQAs) and di-CQAs. The anti-inflammatory and the positive effect neurodegenerative diseases could also bo attributed to CQAs (25). CQAs consist of caffeic acid esterified to quinic acid. Many plants produce caffeoylquinic acid and esterification occurs at positions 3, 4 and 5 of the quinic acid moieties (94,95). *C. asiatica* possess an unusual chemical modification leading to irbic acid. It is a CQA-derivative with a malonyl group attached to its quinic acid moiety. Irbic acid has shown *in vitro* anticollagenase and radical scavenging activity (96–98). Other hidroxycinnates such as *ρ*-coumaric or ferulic acid can form also quinic acid-estirified compounds: *ρ*-coumaroylquinic-acid (*ρ*-CoQA) and, feruloylquinic acid (FQA) (Figure 9).

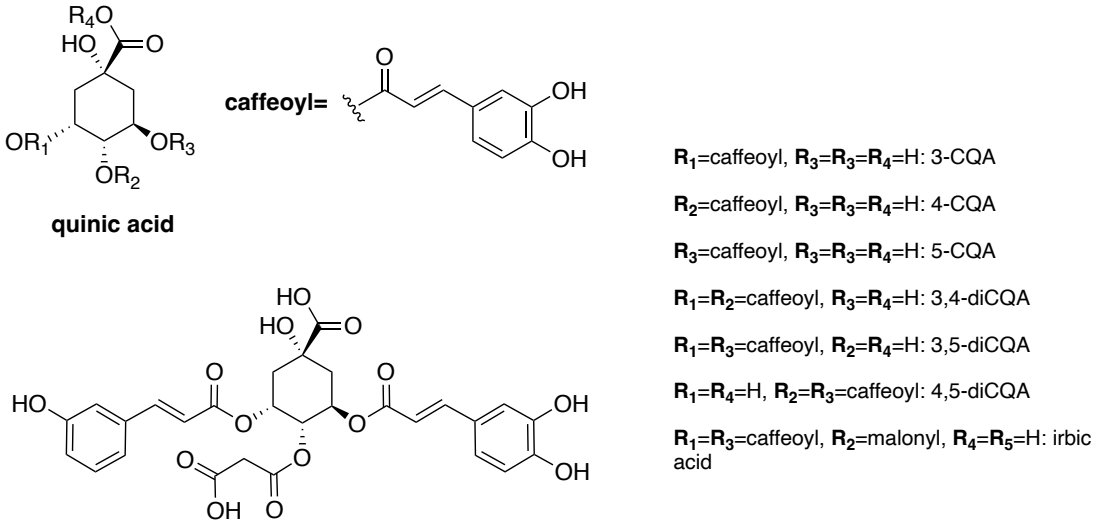

Figure 9. Composition of CQAs and di-CQAs found in *C. asiatica*

1.2.2. Other phytochemicals

Most of the described therapeutical activities of *C. asiatica* are mediated by centellosides. However, *C. asiatica* contains other metabolites such as phenolic compounds, including flavonoids, fatty acids, and sterols. The biological activities of most of these molecules found in *C. asiatica* remains unexplored.

Flavonoids found in *C. asiatica* such as kaempferol, quercetin (Figure 10) and related glycosides have demonstrate antioxidant properties in human foreskin fibroblasts (99).

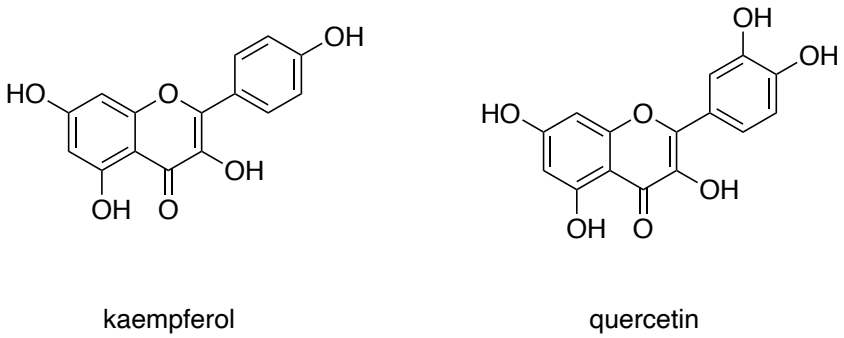

Figure 10. Flavonoids kaempferol and quercetin

Essential oil from the aerial parts of *C. asiatica* contains high levels of sesquiterpenes (C15) and monoterpenoids (C10), including α-humulene, β-caryophyllene, bicyclogermacrene, germacrene-D, and myrcene as the major constituents. Essential oil extracts showed antibacterial activities (100). Other

compounds have been characterised as oxygenated sesquiterpenes (e.g., humulene epoxide, caryophyllene oxide), oxygenated monoterpenes (e.g., menthone, α-terpineol) and a sulfide sesquiterpenoid (mintsulfide).

Table 2. Specialised metabolites found in *C. asiatica*

Chemical constituent	Ref.
Phenolics	
Anthocyanin-3'-*O*-β-*D*-glucoside	(101)
Baicalein-5,6,7-trimethyl ether	(101)
1-caffeoyl-β-*D*-glucose	(102)
Caffeoylquinate / scopolin	(102)
3-*O*-β-*D*-*p*-coumaroylglucoside	(102)
1,3-dicaffeoylquinate	(102)
Dihydroconiferyl alcohol glucoside	(102)
Feruloylhexose	(103)
Feruloylserotonin	(102)
Flavonol-3-*O*-*D*-xylosylglucoside	(101)
3-hydroxy-9-apo-δ-caroten-9-one	(101)
Methyl 3,4-dicaffeoylquinate	(102)
4'-*O*-methylisoflavone	(101)
4-methylumbelliferone glucuronide	(101)
O-sinapoylglucarolactone	(102)
4,5,6,7-tetramethoxyflavone	(102)
trans-5-FQA	(103)
Ubiquinol	(101)
Flavonoids	
Albafuran A	(102)
Castillicetin	(104)
Castilliferol	(104)
Dehydrocycloguanandin	(101)
(2S)-7,4'-dihydroxy-8-geranylflavanone	(102)
7,4'-dihydroxy-8-methylflavan	(101)
Euchrenone	(102)
Glyinflanin H	(102)
Isomer of quercetin-rutinoside	(105)
Kaempferol	(105–107)
Kaempferol 3-*O*-glucoside-7-*O*-rhamnoside	(105)
Kaempferol 3-*O*-rhamnoside	(105)
Kaempferol-3-*O*-glucoside	(105)
Kaempferol-3-*O*-glucuronide	(105,107)
Kievitone	(101)
Kinocoumarin	(102)
Luteolin 7-glucoside-4'-(*Z*-2-methyl-2-butenoate	(102)

4'-*O*-methylbavachalcone	(102)
2'-*O*-methylphaseollinisoflavan	(102)
Mirificin	(102)
Quercetin	(105,107)
Quercetin	(105)
Quercetin-3-(6''-p-hydroxybenzoylgalactoside)	(102)
Quercetin-3-*O*-β-*D*-glucuronide	(105)
Quercetin tetramethyl (5,7,3',4') ether	(102)
Quercetin-3-*O*-glucuronide	(105)
Quercetin-3-diglucoside	(105)
Quercetin-3-*O*-glucoside	(103,105)
Quercetin-3-*O*-rhamnoside	(105)
Quercetin-7-glucuronide	(103)
Quercetin-*O*-pentosyl-hexoside	(105)
Quercetin-rutinoside	(103,105)
Quercetin-rutinoside analogue with an additional pentose moiety	(105)
5,6,7,8-tetramethoxy-3',4'-methylenedioxy isoflavone	(102)
2'',4'',6''-triacetylglycitin	(102)
Wighteone	(102)
CQAs	
trans-3-CQA	(103)
cis-5-CQA	(103)
trans-5-CQA	(103)
3-caffeoyl-, 5-FQA	(103)
3-caffeoyl-, 5-FQA	(103)
Chlorogenic acid	(1,29,101,105,107,108)
Crytochlorogenic acid	(1,29)
(mono-*cis*) 3,4-di-CQA	(103)
3,5-*O*-dicaffeoyl-4-*O*-malonylquinic acid	(1,103,105,108)
(di-*trans*) 3,4-diCQA	(1,103,107)
(di-t*rans*) 3,5-diCQA	(1,103,105,108)
1,3-diCQA	(29)
1,4-diCQA	(1)
1,5-diCQA	(29,105,107)
4,5-diCQA	(107)
Isochlorogenic acid A	(29)
Isochlorogenic acid C	(29)
Neochlorogenic acid	(1,29)
Triferulic acid	(108)
Phytohormones	
2,6-diamino-7-hydroxy-azelaic acid	(102)
Gibberellin 2-*O*-β-*D*-glucoside	(101)
11-hydroxy-9,10-dihydrojasmonic acid 11-β-*D*-glucoside	(102)
Jasmonic acid	(102)
Methyl epijasmonate	(102)
Fatty acids	
Ascorbic acid 2,6-dihexadecanoate	(102)
Chaulmoogric acid	(102)
Lauric acid	(102)
Oleic acid	(102)

Oleomide	(102)
Palmitic acid	(102)
Stearic acid	(102)
Tridecanoic acid	(102)
Tridecanoic acid	(102)
Polyacetylenes (organic polymers)	
Acetoxycentellynol	(109)
Monoterpenes	
Bicycloelemene	(100)
Bornyl acetate	(100)
Camphene	(100)
β-caryophyllene	(110)
π-cymene	(100)
β-elemene	(100)
χ-elemene	(100)
trans-farnesene	(2)
Geranyl formate	(101)
Limonene	(100)
Linalool	(100)
Menthone	(100)
Methyl carvacrol	(100)
Methyl thymol	(100)
Myrcene	(100)
3-nonen-2-one	(100)
α-phellandrene	(100)
α-pinene	(100)
β-pinene	(100)
Pinene	(2)
Pulegone	(100)
Terpinen-4-ol	(100)
α-terpinene	(100)
χ-terpinene	(100)
Terpinolene	(100)
α-thujene	(100)
Sesquiterpenes	
Abscinate	(102)
Aristolochene	(102)
allo-aromadendrene	(100)
Aromadendrene	(100)
Bicyclogermacrene	(100)
δ-cadinene	(100)
Caryophyllene	(2)
Caryophyllene oxide	(100)
Cedrenol	(102)
χ-curcumene	(100)
Deoxy-capsidiol	(102)
Elemene/bicycloelemene	(2)
Epicedrol	(102)
Ermacrene D	(2)
Farnesane	(102)

Farnesol	(102)
Germacrene A	(100)
Germacrene B	(2)
Germacrene B	(100)
Germacrene D	(100)
Glutinosone	(101)
Hexahydrofarnesol	(102)
α-humulene	(100)
Humulene epoxide	(100)
9'-hydroxyabscisate	(102)
3-hydroxylubimin	(102)
15-hydroxysolavetivone	(102)
Isopauthenol	(100)
Mintsulfide	(100)
Neophytadiene	(100)
Phytuberin	(102)
Rishitin	(101)
cis-sesqui sabinene hydrate	(102)
Solavetivone	(102)
Spauthulenol	(100)
Viridiflorol	(100)
Sterols	
Demethylsqualene	(102)
Methylsqualene	(102)
Squalene	(102)
Squalene	(102)
Stigmast-5-en-3-ol	(102)
Stigmasterol	(2)
Other terpenoids	
Pheophytin a	(101)
Solanesol	(102)

1.3. Production of Centellosides

1.3.1. Status of centellosides production

There are reasons why there is an urgent need for an alternative production model of centellosides. *C. asiatica*-derived medicines are exclusively found as OTCs. This type of medicines are under a less strict regulation framework compared to prescription medicines (111). In Europe, only four countries encompass the regulation *C. asiatica*-based products (5). This forgiveness in quality assurance together with overexploitation due to the enormous market demand has caused a wild stock depletion in some countries. Moreover, *C. asiatica* stands usually in marshy and swampy ditches and ponds. Those habitats are problematic for industrial supply due to the presence of unaccepted levels of heavy metals, microbial loads, awful waste, and other hazardous chemicals. Then, its harvesting can cause the failure in the quality assurance to industrialize the extraction of centellosides in phytopharmaceutical companies (112). Regarding the ecology of this plant, it presents high chemodiversity variance among their populations (92). Medicinal plants are usually chemo-variable since their bioactive molecules are mainly specialised metabolites. This type of molecules have a great variability among populations since they are related to adaptation to the environment (113). This variations also comprise the quality control in the exploitation of a medicinal plant (111). In fact, the level of total triterpenes can vary between 1 - 8% among populations (114). Moreover, the

distribution of *C. asiatica* is restricted to the wetlands of tropical and subtropical areas and is characterised by slow growth in natural environments (115).

The extraction of centellosides is mainly through chemical extraction directly from the plant. To develop large number of plants and a suitable production of centelloside-enriched extracts or their purification, alternative systems should be used. Plant biotechnology production platforms can cope the enlisted limitations compared the classical harvesting methods. In the las two decades, many efforts have been done to establish plant *in vitro* cultures of *C. asiatica* and to achieve suitable biotechnological production of centellosides.

1.3.2. Biological production of centellosides

Plant *in vitro* culture is a versatile and important tool in both basic and applied research, in addition to commercial applications. It consists in the *in vitro* culture of plant cells, tissues, and organs under specific physical and chemical conditions. Totipotency of plant cells is the crucial feature that has led to the development of plant biotechnology. Cell totipotency is defined as the genetic potential of a cell to generate a whole multicellular organism. It permits the clonal propagation of plants *in vitro*. This is one of such alternative method for multiplying genetically identical copies of individual plant through asexual reproduction (116).

Plant *in vitro* culture includes both differentiated cultures (the whole plant, shoots, or roots) or dedifferentiated cultures (e.g., calluses or protoplasts). These tissues can be placed into liquid media to perform either batch or continuous

bioproduction of natural compounds endogenous produced by the plants. These platforms are commonly named Plant Biofactories (117).

Plant biotechnology can cope the enlisted limitations compared the classical centellosides production. They are soil independent and reduced the need for high water supplies. Then, *C. asiatica in vitro* cultures can be repeatedly passed in a controlled environment. Moreover, cells can be stored in cryopreservation. These features make plant *in vitro* cultures an eco-friendly biotechnology. In terms of production, plant biotechnology opens a broad framework to feat and to investigate how to manipulate the cultures to optimize the production of centellosides. Regarding the quality, these platforms are free of pesticides, heavy metals, and other poor environmental conditions that can affect field cultivation (118).

1.3.2.1. *C. asiatica in vitro* cultures

The production of a specific metabolite in plant *in vitro* culture depends on system productivity. When first established a plant *in vitro* culture, and before culture optimization, the yield is relatively low (119). This have been observed in *C. asiatica*. Leaves of *ex vitro C. asiatica* plants accumulate more centellosides than any other *in vitro* culture. Some transcript profiling work has revealed that centellosides-related enzymes are preferentially expressed in leaves (120,121). Therefore, higher levels in the leaf cyto-differentiation of the culture favours the centelloside accumulation. For instance, calluses or hairy root (HR) cultures do

no produce comparable centellosides to those levels found in the aerial plants (122–126). The obvious differentiated genotype of HR into a non-leafy tissue is likely to be the reason. However, the control of the parameters affecting the environment in plant *in vitro* cultures allows the manipulation of the production.

1.3.2.2. Elicitation as a tool to improve the production in Plant Biofactories

Most of the compounds with therapeutical application in plants are specialised metabolites. The synthesis of plant specialised metabolites is far from cheap for the plant. Most of the structures of the metabolites are complex and their biosynthetic pathways require high energy and the expression of specific enzymes. For this reason, the function of these metabolites must overcome the costs. Overall, the principal functions of this metabolism seem to be related to the fact that plants are sessile organisms, but they must ensure their surveillance. The principal functions of this metabolism are then related to stress scenarios: defence responses of both abiotic and biotic stress, communication with pollinators and herbivores (seed dispersers), plant-plant interactions, and avoidance of auto-toxicity (127).

Plant biotechnology takes advantage of this natural feature by mimicking the stress signals that lead to the activation of the specialised metabolism. This biotechnological approach is known as elicitation. Elicitors are synthetic and natural signals (chemical and physical) that induce similar responses in plants as induced the abiotic and biotic stresses described above (128). This approach has

been one of the most effective strategies to increase the productivity of bioactive specialised metabolites in plant *in vitro* cultures. It leads to specialised metabolite concentration improvement in, most cases, a short period of time (119,129). Many elicitors have been described and they can be classified as Figure 11 shows (130).

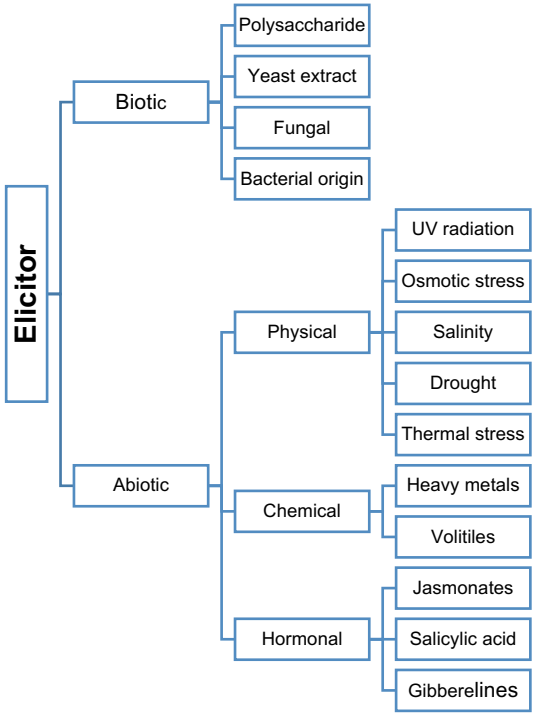

Figure 11. Classification of elicitors

1.3.2.2.1. Elicitation strategies in *C. asiatica in vitro* cultures

Many studies dealings with the elicitation of *C. asiatica in vitro* cultures for the overproduction of centellosides have been described so far. Different results

have been achieved depending on the elicitor and/or type of culture (6,131). The use of methyl-jasmonate (MeJA) is the most outstanding elicitation strategy in *C. asiatica*. MeJA belongs to the family of jasmonates (JAs) that are plant-specific signalling molecules. In nature, the biosynthesis of JAs is induced mainly by the activation of local and systemic defence response to biotic stresses (i.e., pathogen infection and herbivory attack). While the initial activation of JAs biosynthesis remains unclear (132), the JAs downstream effects have been studied. The signal cascade mediated by JAs culminate in the expression of specialised pathways-related genes to respond to the stress-like scenarios. Most of the JAs-responsible genes are repressed by JAZ repressor proteins in basal conditions. After JAs overproduction, they are converted into the active form 7-iso-jasmonoyl-L-isoleucine (JA-Ile). The last binds the CORONATINE INSENSITIVE1 (COI1) F-box protein receptor. It works as an E3 ubiquitin ligase: it targets the JAZ repressor proteins for its degradation. Thus, multiple transcription factors are repressed, which turns in the activation of JA-Ile-dependent transcriptional reprogramming. Then, the basal cell state switch into the cell stress-responsive scenario (133,134). In elicitation studies, the activation of the JAs signalling is achieved by the exogenous application of MeJA. MeJA is a methyl ester of jasmonic acid ubiquitously found in plants and able to activate JAs signalling pathways. The use of MeJA as elicitor is unquestionably preferred in elicitation studies more than JAs. The literature does not clarify this preference. However, MeJA seems to be more effective than JAs in the matter of elicitation (135).

The biological function of centellosides is as plant defence molecules. They

are considered phytoanticipins able to combat pathogenic infection. Due to the defence role of centellosides, they are likely to be up-regulated by MeJA. When exogenously applied to plant cell cultures of a variety of species, MeJA (100–200 μM) positively stimulates the workflow of specialised biosynthetic pathways, leading to an increased production of diverse specialised metabolites, including terpenoids, flavonoids, alkaloids and phenylpropanoids (129). MeJA causes the metabolic reprogramming of some specialised metabolic pathways, in particular the terpenoid pathway (8,59,64,65). Actually, exogenous MeJA treatment on *C. asiatica* callus resulted in the up-regulation of genes involved in this pathway, which subsequently activate the biosynthesis of centellosides (101,102,137–139). In several other studies, exogenous treatment of MeJA showed to be effective for enhanced synthesis of centellosides in HR (136,140–142). Recently, the exogenous application of another elicitor, coronatine (CORO) in cultures and HRs of *C. asiatica*, showed the most powerful effect in the enhancement of centellosides so far (138). CORO is a phytotoxin produced by several pathovars of *Pseudomonas syringae.* CORO is a structural analogue of JA-Ile. Then, it has a similar mode of action of MeJA. However, CORO has special interest since provokes higher production effects than MeJA in less concentration. The main hypothesis is that CORO is more stable then MeJA. (129).

1.3.3. *C. asiatica* HR as production platforms of centellosides

Among the biotechnological production platforms, HRs have many

advantages: high growth capacity, hormone independent growth, and genetic stability (143,144). Many examples of HR cultures for the biotechnological production of plant specialised metabolites can be found in the literature. Moreover, companies such as Green2chem (Belgium) and Naturex (France) use HR as biofactories (145).

HR cultures are obtained by infection of plant material with the soil pathogenic bacteria *Agrobacterium rhizogenes*. In nature, it infects the host plant resulting in a biotrophic pathogenesis. This ability is due to the possession of a root induction (Ri) plasmid. The plasmid directs the infected plant cells to synthesize molecules for its own metabolism as well as the abnormal growth of roots. Specifically, *Agrobacterium* transfers a section of the Ri plasmid, called T-DNA, that is randomly inserted into the genome of host plant cells. The T-DNA contains the *rol* genes responsible for the development of the characteristic phenotype displayed by HRs (Figure 12). In *in vitro* conditions, roots appear in the plant material at points of bacterial infection. Roots are excised and cultured separately without requiring the addition of plant growth regulators to maintain their state. Roots are cultivated in solid medium supplemented with antibiotics to eliminate the agrobacteria. Finally, roots can be transferred to liquid medium to generate a high quantity of biomass (146,147). The *rol* genes can induce the biosynthesis of a variety of specialised metabolites. Although the mechanism is not yet clear, it makes HR a self-sufficient system to induce specialised metabolites biosynthesis without any special induction signal or metabolic engineering strategy. For instance, the *A. rhizogenes*-mediated transformation in the medicinal plant *Codonopsis lanceolata* and *Bacopa monnieri* resulted in

higher production of their own triterpene saponins (148). However, in *C. asiatica* this self-induction has not been observed, and strategies such as elicitation are required to induce the production of centellosides.

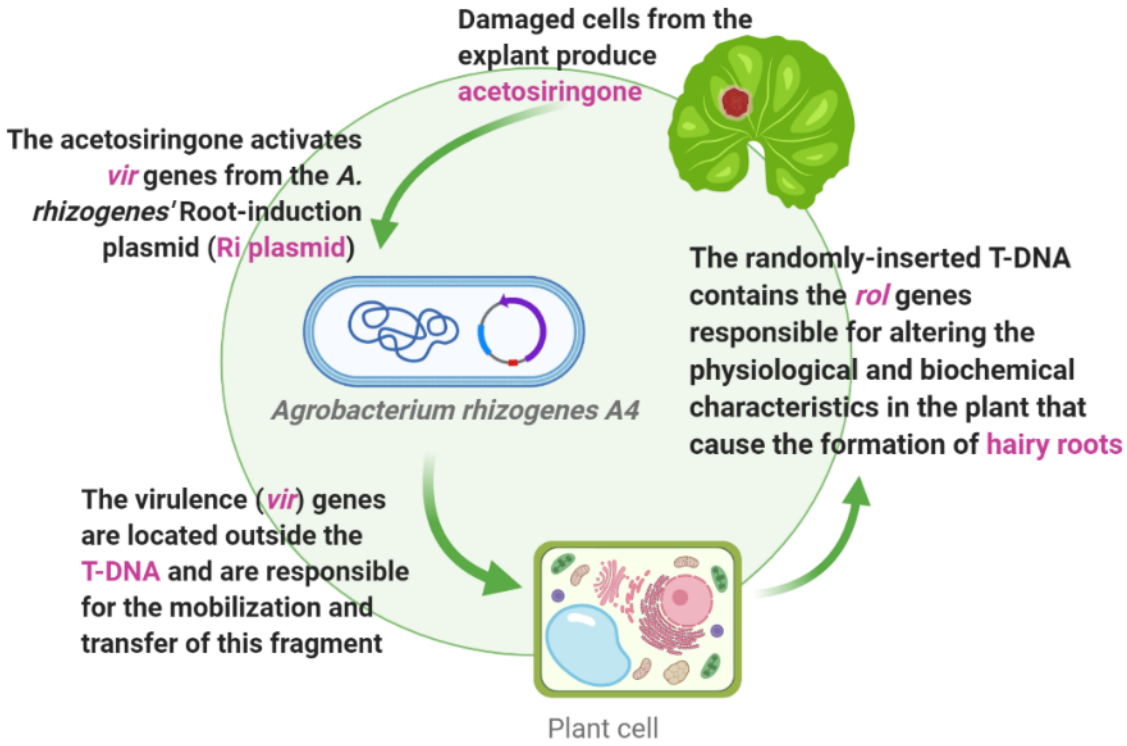

Figure 12. Formation of HR mediated by *A. rhizogenes* infection.

Table 3 summarizes the achievements in the production of centellosides with HRs. The first report regarding the transformation into *C. asiatica* HR using *A. rhizogenes* R1601 showed a production about 90% lower compared to other platforms (122). Unlike other plant-derived HRs, it seems that *rol* genes in *C. asiatica* HR do not promote the expression of genes related to the production of centellosides. The strains R1000 (149,150), ATCC 43057 (151) and KCCM

11,879 (152) showed a low production of centellosides under MeJA elicitation. An interesting outcome was achieved with *A. rhizogenes* strain ATCC 15834 since the transformed HR produced 172% more centellosides that calli culture (153). This article does not clarify the quantity in magnitude of the produced centellosides (e.g., the calli culture may well have produced in micrograms and the increase could represent a very low quantity). However, no more research has been done using this strain.

Unfortunately, the production of centellosides in HRs were not comparable to leaves in wild plants or whole-plant *in vitro* cultures. However, the interest into the creation of production platforms of HR of *C. asiatica* is still ongoing due to its advantages. Recently, the Plant Physiology Research Group of the Faculty of Pharmacy at the University of Barcelona obtained a centellosides-productive HR line of *C. asiatica*. The elicitation with MeJA 100 μM and CORO 1 μM demonstrated to increase the production of total centellosides in HR cultures. In fact, they obtained the highest production with HRs so far (154). The latter study was crucial to validate the use of HR as bioproduction platforms of centellosides. However, it was limited to bioproduction with the use of elicitors. The regulation underlying the overactivation of the centelloside pathway under elicitation remains unexplored.

Table 3. Production of centellosides using HR of *C. asiatica* and elicitation

A. rhizogenes **strain**	**Elicitor**	**Production**	**Day of max. production after elicitation**	**Ref**
R1601	No elicitation	0.26 mg/g DW	NR	(122)
R1000	0.1 mM MeJa	7.12 mg/g DW	NR	(140)
	100 µM MeJa	MD: 0.17% DW AD: 0.38% DW	21 28	(136)
	300 ppm squelene	AD: 4.07 mg/g DW	NR	(150)
ATCC 15834	No elicitation	172% of centellosides compared to untransformed calli	NR	(153)
ATCC 43057	50 µM MeJa	25.87 µg/mg AD	21	(151)
KCCM 11,879	400 µM MeJa	60 mg/g total centellosides content	NR	(152)
A4	100 µM SA	MD: 40 mg/g DW AD: 7 mg/g DW AA: 0 mg/g DW MA: 0 mg/g DW	14 8 h - -	(154)
	100 µM MeJa	MD 40 mg/g DW AD: 1.5 mg/g DW AA: 0.5 mg/g DW MA: 0.1 mg/g DW	14 7 7 7	(154)
	1 µM CORO	MD:135 mg/g DW AD: 1 mg/g DW AA: 7 mg/g DW MA: 5 mg/g DW	14 7 7 7	(154)
	100 µM MeJa + 1 µM CORO	MD:140 mg/g DW AD: 3 mg/g DW AA: 8 mg/g DW MA: 7 mg/g DW	14 7 7 7	(154)

SA = Salicylic acid, AD = Asiaticoside, MD = Madecassoside, AA = Asiatic acid, MA = Madecassic acid, DW = Dry weight, HR = Hairy roots, NR = Not Reported.

1.3.4. Rational approaches in biotechnological production

The success in biotechnological production of plant specialised metabolites requires the optimisation of the system, either by empirical or rational methods. The investigations about the optimization of a plant production system have been mainly through empirical approaches: the analysis of inputs in a culture system (i.e., the optimization of media culture, scaling-up processes, try an error-elicitation approaches, selection of a line, etc.) and the subsequent evaluation of the output effects in the culture. However, the responses of a culture are unpredictable. In contrast, rational approaches are directed to understand the genetic and biochemical machinery governing biosynthetic pathways of specialised metabolism: identification of genes, enzymes, and pathways potentially involved. Overall, rational approaches aim in better understanding the specialised metabolite pathways. Thus, gaining knowledge in making cultures more predictable and controllable. Far for being easy, the study of the biochemistry of the specialised metabolism must deal with the complexity of the networks governing the pathways, the variability of specialised metabolites among plant families and the complex genomes of plant. The omics approaches together with high-throughput technologies can face the study of the regulation of the specialised metabolism. There has been a trend in applying transcriptomics (RNA-Seq, cDNA libraries), metabolomics and proteomics to better understand how specialised metabolism work in plants: transduction signals, storage, transport, rate-limiting steps, protein structures and metabolic profiles. The

integration of the omics sciences is becoming crucial for gaining the knowledge to further create system biology approaches to engineer rational strategies to make the production more predictable: metabolic engineering, genetic modification or the exogenous application of a specific elicitors or precursor (155,156). In conclusion, the improvement of specialised compound production depends on knowledge of the complex biosynthetic pathways.

1.3.5. Elicitation as tool for rational studies

Elicitation has a dual role in plant biotechnology. It is not only a brute force tool to activate specialised biosynthetic pathways, but also allows the study of the metabolism of the culture. Elicitation allows the awakening of the latent state of specialised metabolism. Otherwise, it would be not impossible to study it under basal conditions. The controlled conditions provided by *in vitro* culture together with the over-activation of specialised metabolism triggered by elicitation, provides a biological platform under controlled conditions to observe the stress response in terms of gene expression, proteins and metabolites from specialised metabolism biosynthesis (157). Thus, data derived from an elicitor treatment infers in the discovery of metabolites, pathways and controlling limiting steps (119,158,159).

1.4. Metabolomics Studies in *C. asiatica*

There are two metabolomics studies performed in *C. asiatica* cell cultures in the literature. The first study was carried out by James, *et al*. (2013) and comprised the identification and quantification of metabolites by High Performance Liquid Chromatography-Tandem Mass Spectrometry (HPLC-MS/MS) after elicitation with MeJA. Elicitation accumulated centellosides at the end of the 3-days-time-course experiment, especially MD and AD. Moreover, they identified 29 metabolites that were significantly altered in MeJA-treated cultures. The list of these metabolites indicated that somehow flavonoid pathway decreased while terpenoid pathway increased (160). In 2015, Tugizimana *et al*. performed a similar metabolomic study but only 24 h after the treatment. They analyse the samples by both HPLC-MS/MS and Gas Chromatography Mass Spectrometry (GC-MS). They observed that MeJA decreased flavonoids while increased pentacyclic triterpenoids and sesquiterpenoids. In addition, some cinnamic acids, some fatty acids and some sesquiterpenoids increased. Overall, this study indicated that the changes in the metabolome are associated with an inducible defensive function in response to elicitation by MeJA (102). These studies indicated a compensatory decrease in one pathway when another one is activated. These are clear examples about how metabolism of centellosides is highly flexible and controllable with elicitation (Figure 13).

Therefore, there is strong evidence that elicitation, particularly MeJA, activates the centellosides metabolism. However, other pathways are likely to be activated since MeJA is one the most promiscuous elicitor: exogenous application

into plant *in vitro* cultures usually stimulates diverse specialised pathways such as flavonoids, terpenoids, alkaloids and phenylpropanoids (129). Moreover, the variable time is crucial to obtain a more realistic state of the centelloside metabolism. Which it is not always comprised in the experimental designs.

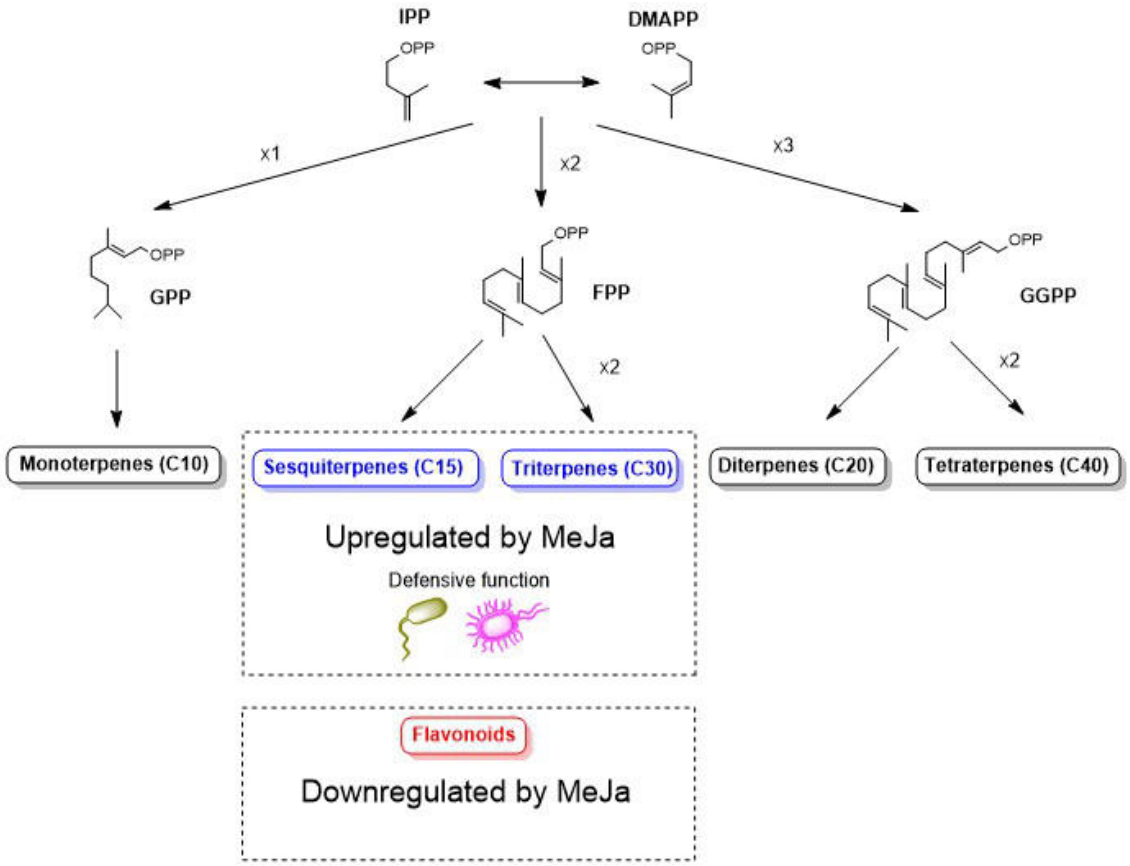

Figure 13. Summary of general terpenoid pathways. MeJa stimulates the *C. asiatica* sesqui- and triterpenoid pathway (blue) while down-regulates flavonoids (red). DMAPP: Dimethylallyl diphosphate ; IPP: Isopentenyl diphosphate; GPP: Geranyl diphosphate; FPP: Farnesyl diphosphate; GGPP: Geranyl-geranyl diphosphate.

CHAPTER 2

2. HYPOTHESIS, SCIENTIFIC CONTRIBUTION, AND OBJECTIVES

2.1. Hypothesis

The untargeted and targeted time-scaled Proton Nuclear Meganetic Resonance (^{1}H-NMR) and Ultra High Performance Liquid Chromatography-Tandem Mass Spectrometry (UHPLC-MS/MS) metabolomic study of MeJA- and CORO-elicited and non-elicited *C. asiatica* HR cultures will reveal regulation and control patterns of its metabolism.

2.2. Scientific Contribution

This study will provide:

i) New knowledge about the time-dependent metabolism regulation in *C. asiatica* HR

ii) The better understanding of the centelloside metabolism in *C. asiatica* HR.

2.3. Objectives

2.3.1. General objective

To get insights into the regulation of the metabolism of HR of *C. asiatica* after elicitation of MeJA and CORO through both ^{1}H-NMR and UHPLC-MS/MS untargeted and targeted metabolomics approach.

2.3.2. Specific objectives

1. To explore the primary metabolism of HR of *C. asiatica* under MeJA and CORO elicitation with a particular focus on its time dependency using a ^{1}H-NMR targeted and untargeted metabolomics approach.

2. To perform an UHPLC-MS/MS untargeted time-scaled metabolomics study on MeJA- and CORO-elicited *C. asiatica* HR to compare the specialised metabolism changes through the time with the aid of Multivariate Data Analysis (MVDA).

3. To further explore the specialised metabolism using Molecular Networks (MN) constructed with data derived from Ultra High Performance Liquid Chromatography-High Resolution Tandem Mass Spectrometry (UHPLC-HRMS/MS).

CHAPTER 3

3. MATERIALS AND METHODS

^{1}H-NMR, UHPLC-MS/MS and UHPLC-HRMS/MS have their own particularities. However, plant metabolomics usually follows the same procedure: (i) sample collection/harvesting; performance of the experimental design and biological sample collection, (ii) data acquisition; performance of the analytical method, (iii) data processing and (iv) data analysis; statistical tools-aided MVDA. The workflow is summarised in Figure 14 and also described in the present section.

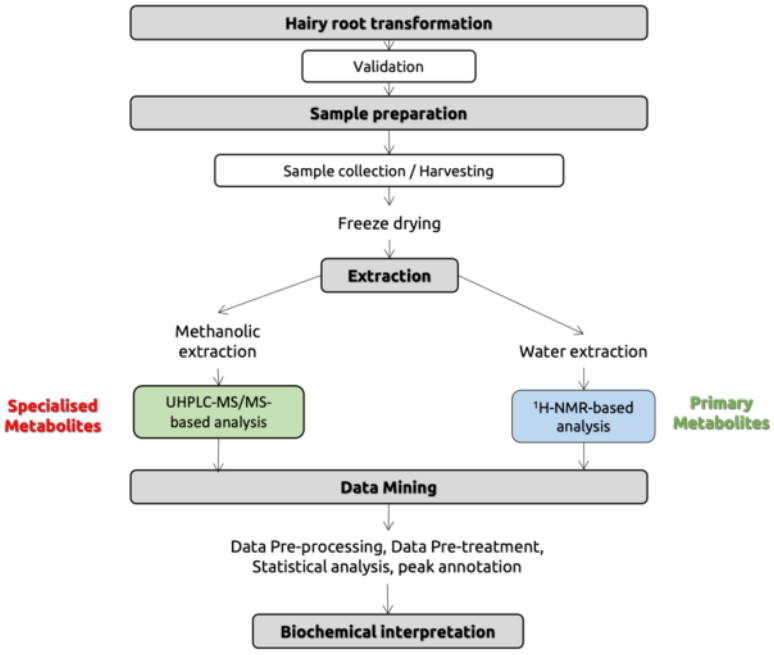

Figure 14. Workflow for plant metabolomic approach

3.1. Sample Collection / Harvesting

3.1.1. HR obtention

The HR line was obtained at Dr. Palazon Lab at the Faculty of Pharmacy at the University of Barcelona as follows: *C. asiatica in vitro* plants were grown *in vitro* in solid MS medium (Murashige & Skoog 4.4 g/L, sucrose 30 g/L and phytagel 2.7 g/L) (161), at 25 ºC and 16 h light/ 8 h darkness. Leaves explants from *in vitro* plants of *C. asiatica* were infected underside with *A. rhizogenes* strain A4 and placed into MS solid medium in darkness at 25 ºC. After 2 days, explants were subcultured into solid MS medium + cefotaxime 500 mg/L to remove *A. rhizogenes*. Adventitious roots were cut and placed individually in solid MS + cefotaxime 500 mg/L medium for 1-2 months. After the removing of the bacteria, HRs were maintained and grown in solid hormone-free MS medium including vitamins. We used MS and vitamins mix 4.4 g/L (Duchefa Biochemie, Haarlem, The Netherlands), supplemented with sucrose 30 g/L, gelrite 2.7 g/L and adjusted to pH 5.8 before autoclaving. The culture conditions were darkness at 25ºC and the hairy roots were sub-cultured every 4 weeks to obtain enough biomass to establish the liquid culture for the elicitation experiments.

3.1.2. Elicitation experiment and sample collection

To obtain the HR liquid culture, under aseptic conditions in a laminar flow

cabinet, hairy roots were washed with liquid hormone-free MS medium including vitamins (MS medium and vitamins mix 4.4 g/L, supplemented with sucrose 30 g/L, pH 5.8) to remove the gelling agent attached to the roots. Then, the roots were dried by laying them on sterile absorbent paper for a few seconds and after were transferred into flasks until reaching 1 g of fresh material. Next, 20 mL of liquid MS hormone-free medium (previously described above) was poured into the flasks to obtain a final number of 90 flasks of HRs liquid cultures. The HR cultures were incubated for two weeks in a rotary shaker (115 rpm) in darkness at 25ºC. After this time, the complete set of cultures were sub-cultured in flasks with new MS liquid medium. At this point, 30 flasks were treated adding 100 µM MeJA (> 95 %) (Sigma-Aldrich, Madrid, Spain) to the fresh MS media, 30 cultures with 1 µM CORO (> 95 %) Sigma-Aldrich, Madrid, Spain), and 30 cultures were not treated as control samples, then incubated in the same conditions as before. For sampling, 6 flasks of each treatment were collected at 0, 4, 8, 12 and 16 d after the treatment. The obtained roots were placed for a few seconds on sterile absorbent paper to remove the culture media, afterwards freeze- dried and pulverized with a mortar and pestle.

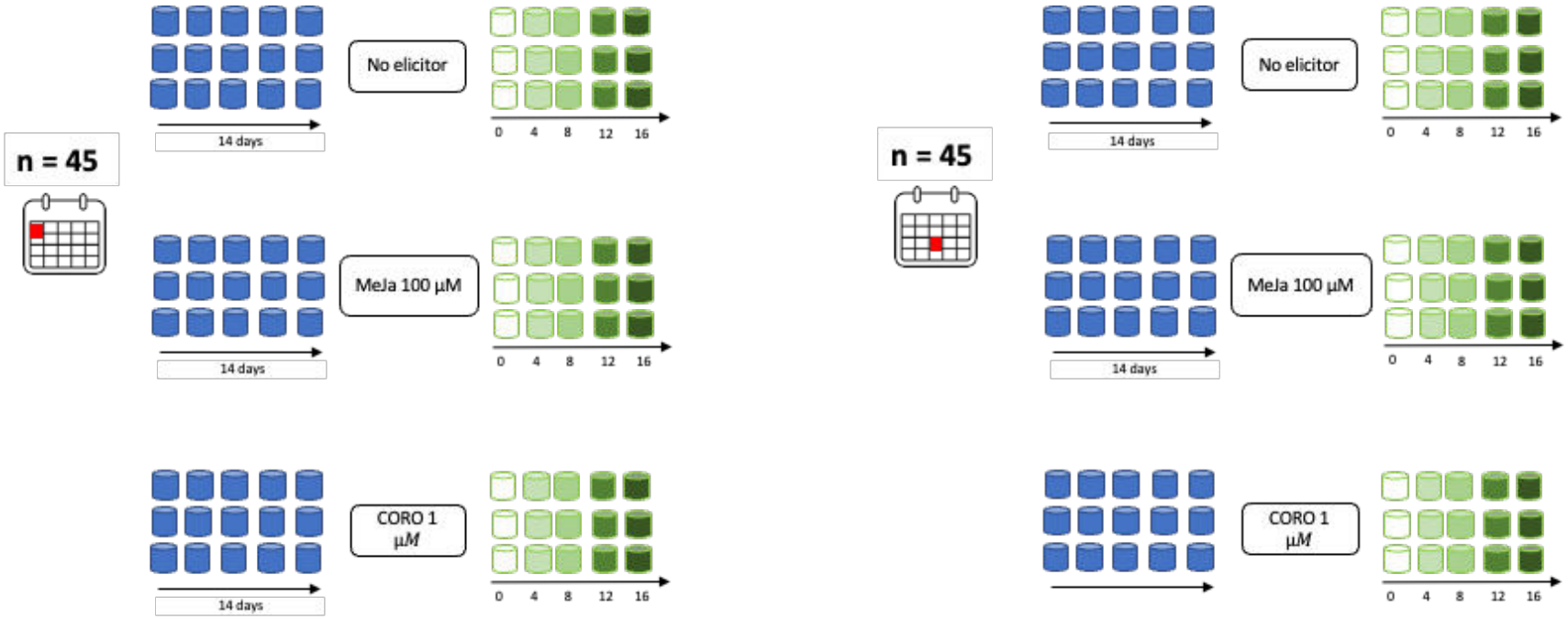

Figure 15. Experimental design for elicitation and sample harvesting

3.2. ^{1}H-NMR Metabolomics

3.2.1. Chemicals

The solvent used for the sample preparation was deuterium oxide (D_2O, D 99.9 at.%) (Cambridge Isotope Laboratories, Inc.). The internal standard for the ^{1}H-NMR analysis was 3-(trimethylsilyl)-1-propanesulfonic acid sodium salt (Sigma-Aldrich Co.; TSP, 97%). EDTA (ethylenediamine-tetraacetic acid) and sodium azide (NaN_3) (Merck™) were also added to samples. Sodium hydroxide (NaOH) and Hydrochloric acid (HCl) (Sigma-Aldrich Co.) were employed to adjust pH.

3.2.2. Sample preparation

Extracts for the ^{1}H-NMR analysis resulted from mixing 30 mg of dry HRs powder (of each of the 90 cultures; MeJA- and CORO-elicited and control) with 100 µL of a solution of 7 mM 3-(trimethylsilyl)-1- propanesulfonic acid sodium salt (Sigma-Aldrich, St. Louis, MO ; TSP, ≥97%) as internal standard, 2 mM sodium azide (NaN_3, ≥99.5%) (Sigma-Aldrich, St. Louis, MO, USA) and 10 mM ethylenediamine- tetraacetic acid (EDTA) (Sigma-Aldrich, St. Louis, MO, USA) in deuterium oxide (D_2O, 99.9 atom % D) (Cambridge Isotope Laboratories Inc., Tewksbury, MA, USA). The resulted solutions were adjusted at pH 6.0 ± 0.05 and sonicated for 15 min to obtain the samples. Prior data acquisition, the solutions

were treated as described in previous protocols (162).

3.2.3. ^{1}H-NMR experiments

The equipment for NMR experiments was a Bruker 750 MHz spectrometer (Bruker Biospin, Rheinstetten, Germany) equipped with a 5 mm TXI cryoprobe. All the aqueous extracts from the HR's dry material were measured at 298.1 ± 0.1 K, without rotation and with 4 dummy scans prior to 64 scans. Acquisition parameters were set as follows: FID size = 64 K, spectral width = 19.9967 ppm, receiver gain = 1, acquisition time = 2.18 s, relaxation delay = 10 s, and FID resolution = 0.45 Hz. Data acquisition was achieved by NOESY presaturation pulse sequence (Bruker 1D noesypr1d) with water suppression via irradiation of the water frequency during the recycle and mixing time delays (162). To corroborate the signal assignments, we performed ^{13}C NMR spectroscopy, and the following 2D analysis: homonuclear correlation spectroscopy (2D ^{1}H-^{1}H COSY), heteronuclear multiple bond correlation (2D ^{1}H-^{13}C HMBC) and heteronuclear single quantum correlations (2D ^{1}H-^{13}C HSQC) (Figure A.1) (163).

3.2.4. Metabolite profiling

The ^{1}H-NMR spectra were automatically phased, calibrated to the internal standard (TSP) signal at 0.0 ppm and baseline-corrected using the MestReNova software (164–171). After this processing, Chenomx NMR

Suite version 8.3 (Chenomx, Edmonton, Canada) processed the ^{1}H-NMR spectra with the “Processing module” for the baseline correction, line broadening, phase correction, shim correction, the calibration of the spectra to the signal of TSP and the setting of pH = 6.0; the “Profiler module” permitted the determination of the relative abundance (in nM) of the detected metabolites. Chenomx works by fitting signals from its *in-house* spectral data base to the appropriate signals within the experimental spectra. After the experimental signal has been fit the concentration is given. The software automatically adjusts the reference database to acquisition conditions (pH, NMR field strength, spectra line width) (172). Metabolite identification was corroborated consulting literature as previously described (163,173). The statistical analysis of the relative quantity of identified metabolites was performed using GraphPad Prism (version 9.0.0 for Windows, GraphPad Software, San Diego, California USA). Two-way analysis of the variance (ANOVA), followed by Tukey’s multiple comparison test was performed for the statistical analysis of the relative metabolites production between different treatments at the same day of harvesting. Significantly difference between groups was determined with a p-value ≤ 0.05. All analyses were calculated using six biological replicates of each day of harvesting for each treatment, and were presented in the graphics as means ± SEM.

3.2.5. Bucketing for untargeted metabolomics analysis

This data processing was performed by MestReNova software version

14.0 (MestReC, Santiago de Compostela, Spain).The NMR spectra was divided into a series of buckets each one of 0.04 ppm. The resulted NMR data was digitalized into a matrix with numeric values corresponding to the peak areas of each bucket. These values were introduced into a text file (.csv) for further statistical analysis described in the next section.

3.2.6. MVDA

The text file (.csv) derived from the previous bucketing process containing the data from all the 90 samples (six replicates of each day of harvesting for treatment) was used for the MVDA. The unsupervised principal component analysis (PCA) and the supervised orthogonal projections to latent structures discriminant analysis (OPLS-DA) were used to show the relationship of the observed variables (peak areas of the buckets) between the experimental treatments at different times of harvesting and their repetitions. Both analyses were applied on a Pareto-scaling data matrix normalized by its sum using the software SIMCA version 13.0.3 (Umetrics, Kinnelon, NJ, USA). The quality of the models was described by the Rx2 and Q2 values. Variable Influence in the Projection (VIP) scores were provided by SIMCA software and further used to build a Venn Diagram showing the metabolites influencing the OPLS-DA model at different times of harvesting by both treatments. MetaboAnalyst 4.0 was used to perform the hierarchical clustering model and the heatmap visualization of the quantified metabolites between the treatments, days of harvesting and its

repetitions (following the Euclidian method). All the statistical analysis here described were generated on a Pareto-scaling data matrix and data was normalized by its sum.

3.3. UHPLC-MS/MS Metabolomics

3.3.1. Methanolic extraction

Extraction consisted in adding 10 mL of methanol:H_2O (9:1) (Fisher, Barcelona, Spain) in 0.5 g of freeze-dried material . The solutions were submitted to sonication for 1 h at room temperature. Next, solutions were centrifugated at 20,000 rpm for 10 min. The supernatants were separated, and the previous step was repeated on the harvested solid pellet. The pool of supernatants was evaporated at 38 °C for approximately 24 h.

3.2.2. Tandem mass spectrometry analysis of standards compounds

Electrospray Ionisation-Mass spectrometry (ESI-MS) analyses were carried out using a LTQ XL™ Electrospray Ionization (ESI) Ion Trap (IT) mass spectrometer (Thermo Fisher Scientific, Bremen, Germany). All spectra acquisitions were done using LTQ Xcalibur 4.3. software (Thermo Fisher Scientific). Authentic compounds (gallic acid, 3-CQA, caffeic acid, coumaric acid, ferulic acid, quercentin, madecassoside, asiaticoside, kaempferol, madecassic acid and asiatic acid) were all purchased by Sigma-Aldrich and kindly provided by Dr. Javier Palazon-Barandela (Faculty of Pharmacy, Universitat de Barcelona). Methanolic solutions of standard (0.1 mg/mL) were infused directly into the LTQ XL™ ESI probe with a 250 mL micrometrically automated syringe (Hamilton,

Massy, France) at a flow rate of 3 µL/min. The positive and negative ionization ESI conditions were as follows: source voltage 4 kV; sheath gas and auxiliary gas flow rates 35 and 10 (N_2, arbitrary units), respectively; capillary voltage and temperature 10 V and 200 ºC, respectively; acquisition mass range mass to charge ratio (*m/z*) 100 – 1500.

3.2.3. UHPLC-ESI-Low Resolution-MS/MS analysis

UHPLC-MS/MS analyses of the extracts were carried out on an Ultra High Performance Liquid Chromatography (UHPLC) Vanquis LTQ XL™ (Thermo Fisher Scientific), equipped with a photodiode array (PDA) detector and hyphenated to a LTQ XL™ ESI mass spectrometer type IT. Chromatographic separation of the extracts was achieved using an analytical Reverse Phase C18 Kinetex UHPLC column (100 mm × 2.1 mm, 2.6 µm; Phenomenex), thermostatted at 60 °C. A gradient elution at a flow rate of 0.3 mL/min consisted of a binary solvent with eluent A (consisting of water contaning 0.1% formic acid, Biosolve Chimie, Dieuze, France) and eluent B (consisting of acetonitrile containing 0.1% formic acid, Biosolve Chimie, Dieuze, France). Sample volumes of 1 µL were injected. The initial chromatographic conditions were 3 % B at a flow rate of 0.3 mL/min and were kept constant for 1 min. Then, a gradient was introduced to change the chromatographic conditions to 55 % of B for 15 min. A second gradient was applied to 90 % B at 15 min until 16 min. The condions were kept constant at 90 % B from 16 min to 21 min. Thereafter, the column was

returned to initial conditions at 21 min for equilibration for 4 min. The injection volume was 1 µL and all analyses were performed alternatively in the positive and negative ionization mode. The ESI parameters were as follows: source voltage 4 kV; sheath and auxiliary gas flow rates 65 and 10 (N_2) (arbitrary units), respectively; capillary voltage and temperature 10 V and 200 ºC, respectively; acquisition mass range *m/z* 150 to 1500. MS/MS spectra acquisitions were carried out with a collision energy of 35%, collision gas 50%, q (frequency) 0.250 (45.0 Hz). and an isolation width of the precursor ion of 2 u. A data-dependent scan program was used in the UHPLC-MS/MS analyses so that the two most abundant ions in each scan were selected and subjected to MS/MS analysis. Daughter ions were measured in the range *m/z* 100 to 1500 with 30 ms accumulation, an execution trigger set at 1×10^6. The obtained raw mass spectral data was processed using the Xcalibur 4.3. software (Thermo Fisher Scientific).

3.2.4. UHPLC-ESI-Low Resolution-MS/MS data pre-processing

The UHPLC-ESI-negative mode-MS/MS (UHPLC-(-)ESI-MS/MS) generated a file with the raw data that was converted to *.mzXML file by using MsConverter (version 3 – ProteoWizard) (174). This software automatically detects the chromatographic peaks; process known as *automated peak peaking*. The *.mzXML files were processed using the MZmine 2.3 on-line software. In this software, the analyst makes decisions at this stage avoiding false positives meanwhile not losing peaks. This processing allows the removal of background

noise; chromatogram aligment; and the recution of the redundant information (adducts, istopoes, etc.). The processing results in the obtention of a peak peaking list (175). The parameters set are presented in Table 4.

Table 4. Parameters used for the peak peaking of the UHPLC-(-)ESI-MS/MS data in MZmine 2.3

Stage	Algorithm	Parameter	Set value
Mass detection for MS	Centroid	Noise Level	700
Chromatogram building	ADAP builder	Minimum intensity of the highest data	500
		m/z tolerance	0.6
Chromatogram deconvolution	Wavelets (ADAP)	Minimum acceptable peak height	500
		Range of acceptable peak duration	0.01 to 2.5 min
		Coefficient/area threshold	500
		Signal to Noise threshold	100
		Rt wavelets range	0.01 to 2.5
Deisotoping	Isotopic peak grouper	*m/z* tolerance	0.6
		Retention time tolerance	1
		Maximum charge	3
		Representative isotope	Lowest *m/z*
Alignment	Join aligner	*m/z* tolerance	0.6
		Retention time tolerance	0.1
Gap-filling		*m/z* tolerance	0.6
		Retention time tolerance	0.1
Adduct identification			When 2 adducts referred to the same molecular mass at the same retention time, only the deprotonated adducts were kept in the list

The resulting high-throughput data was within a multidimensional matrix. This matrix consisted of variables representing each characteristic ion or feature (*m/z*, Retention time (Rt)) with the respective relative intensity abundance (which served as a quantitative representation of concentration) in every biological sample of the experimental design. The data matrix was then exported to statistical modelling-software (176,177).

3.2.5. Targeted feature detection

Targeted metabolomics analyses were performed on the resulting peak peaking list derived from the UHPLC-Low Resolution-MS/MS analysis thought the module *targeted feature detection* integrated in MZmine 2.3. The analysis constited in the identification of ions by comparision with authetinc standards or with the spectral data in the literature, and the obtention of their area under the peak. Authetinc compounds (3-CQA, AA, MA, AD, MD) were all purchased by Sigma Aldrich and kindly delivered by Dr. Javier-Palazaon (Facultat de Farmacia, Universitat de Barcelona). The rest of ions were identified comparing their mass spectra with the literature. The parameters set for the alignment of the chromatograms for each targeted ion are in Table 5. The parametrization was set individually for each ion since their chromatographic and mass spectrometric features differed. The statistical analysis for the differences in the relative abundance of each targeted ion between days and treatments was performed through two-way Analysis of Variance (ANOVA) and Tuckey multiple comparison

analysis performed with the software Prism v8.2.1.

Table 5. Parameters set for each targeted ion in the *targeted feature detection* module

Targeted ion	Intensity tolerance	Noise level	*m/z* tolerance	Rt tolerance (min)
(1) sucrose	1.0	500	1.0	0.5
(2) 3-CQA	1.0	0	1.0	3.0
(3) 4-CQA	1.0	500	1.0	1.0
(4) di-CQA isomer 1	1.0	0	2.0	4.0
(5) di-CQA isomer 2	1.0	0	2.0	5.0
(6) di-CQA isomer 3	1.0	0	1.0	0.1
(7) irbic acid	1.0	0	2.0	6.0
(8) 3- caffeoyl, 5-feruloylquinic acid	1.0	500	2.0	0.4
(9) MD	1.0	0	2.0	0.4
(10) AD	1.0	0	2.0	0.4
(11) MA	1.0	800	2.0	0.4
(12) AA	1.0	800	2.0	0.4

AD = Asiaticoside, MD = Madecassoside, AA = Asiatic acid and MA = Madecassic acid

3.2.6. MVDA

The data matrix derived from the UHPLC-(-)ESI-MS/MS was submitted to MVDA using the statistical online tool MetaboAnalyst 5.0. Chemometric analyses consisted in PCA, OPLS-DA and HCA (Euclidian clustering method) on the Pareto-scaled matrix and sum-normalised. VIP scores were provided by OPLS-DA.

3.2.7. UPLC-High Resolution-MS/MS experimental conditions

All experiments were conducted on an AcquityUPLC system (Waters,

Manchester, UK) using an analytical Kinetex RP-C18 UHPLC column (100 mm × 2.1 mm, 2.6 µm; Phenomenex), thermostatted at 60°C. A gradient elution consisting of a binary solvent with eluent A (water containing 0.1% formic acid, Biosolve Chimie, Dieuze, France) and eluent B (acetonitrile containing 0.1% formic acid, Biosolve Chimie, Dieuze, France) was used at a flow rate of 0.3 mL/min. Sample volumes of 1 µL were injected. The chromatographic conditions were the same as described in subsection 3.3.3.

Mass chromatograms and spectra were recorded on a WatersXevo®G2-XS Quadrupole Time-of-Flight (QTOF) mass spectrometer (Waters, Manchester, UK) using negative electrospray ionization. Source parameters were as follows: capillary and cone were set to 0.50 and 40 kV respectively. Desolvation gas flow was 1000 L/h at 36°C, and cone gas was set to 100 L/h. Source temperature was 120°C and data were collected in continuum mode at 0.5 scan/s. Instrument calibration was conducted using a leucine-enkephalin solution at a flow rate of 5 µL/min (calibration points: 554.26202 for negative mode). All LC-MS/MS data were acquired in Data Dependent Analysis (DDA) mode. The mass analyser mass range was set to 100 - 1100 Da for full scan mode (scan time: 0.5/s). The MS/MS mode was automatically activated once the Total Ion Current (TIC) exceeded 20,000 intensity/s but remained in MS mode when TIC was below these thresholds. Collision energy ramps of 20 to 25 V for low-mass, and 65 to 85 V for high-mass analytes were employed.

3.2.7.1. Molecular Networking

The methodology for the MN construction involved the creation of a peak list including the MS data on the peaked ions (*m/z*, Rt and peak area) associated with their MS/MS data. For the peak peaking, the UPLC-HR-MS/MS ESI (-) mode raw data files were converted to *.mzXML files by using MsConverter (version 3 – ProteoWizard) (174). The data structure obtained after conversion was set in centroid mode. The *.mzXML files were processed using the MZmine 2.3 software. The setting parameters were used as follows:

Table 6. Parameters used for the peak peaking of the UPLC-(-)ESI-HRMS/ME data in MZmine 2.3

Stage	Algorithm	Parameter	Set value
Mass detection for MS	Centroid	Noise Level	2000000
Mass detection for MS/MS	Centroid	Noise Level	0
Chromatogram building	ADAP builder	Minimum intensity of the highest data	20000
		m/z tolerance	0.02 – 20 (ppm)
Chromatogram deconvolution	Wavelets (ADAP)	Minimum acceptable peak height	15000
		Range of acceptable peak duration	0.01 – 1.00 min
		Coefficient/area threshold	20
		Signal to Noise threshold	110
		Rt wavelets range	0.01 – 0.2
		Retention time range for MS2 scan pairing	0.2 (min)
		m/z range for MS2 scan pairing	0.01 (Da)
Deisotoping	Isotopic peak grouper	*m/z* tolerance	0.2 – 20 (ppm)
		Retention time tolerance	0.05
		Maximum charge	3
		Representative isotope	Lowest *m/z*
Peak list filtration for keeping only MS/MS scans			
Alignment	Join aligner	*m/z* tolerance	0.2 – 20 (ppm)
		Retention time tolerance	0.05
Gap-filling		*m/z* tolerance	0.02 – 20 (ppm)
		Retention time tolerance	0.05
Duplicate peak filter		*m/z* tolerance	0.02 – 20 (ppm)
		Retention time tolerance	0.05
Adduct identification			When 2 adducts referred to the same molecular mass at the same retention time, only the deprotonated adducts were kept in the list

The peak list was exported both as a *.mgf file for GNPS and as a *.csv file (178,179). The *.mgf file was subjected to the online workflow of the Global Natural Products Social molecular networking platform (https://gnps.ucsd.edu). The molecular network was generated using the module “Feature-Based Molecular Netwrok” which integrates all the MS data (*m/z* of the parent ion and Rt) then distinguishing isobaric compounds (of the same *m/z*). It also integrates the sub-peak area of the ions allowing to compare the relative abundances in the different fractions settings, in addition to the MS/MS fragmentation data (180). The data was filtered by removing all MS/MS fragment ions within +/- 17 Da of the precursor *m/z*. MS/MS spectra were window filtered by choosing only the top 6 fragment ions in the +/- 50 Da window throughout the spectrum. The precursor ion mass tolerance was set to 0.01 Da and the MS/MS fragment ion tolerance to 0.01 Da. A molecular network was then created where edges were filtered to have a cosine score above 0.5 and minimum 2 matched peaks. Further, edges between two nodes were kept in the network if and only if each of the nodes appeared in each other respective top 10000 most similar nodes. Finally, the maximum size of a molecular family was set to 10000, and the lowest scoring edges were removed from molecular families until the molecular family size was below this threshold. The analogue search mode was used by searching against MS/MS spectra with a maximum difference of 100.0 in the precursor ion value. The library spectra were filtered in the same manner as the input data. All matches kept between network spectra and library spectra were required to have a score above 0.5 and at least 6 matched peaks. The dereplicator was used to annotate MS/MS spectra (181). The molecular networks were visualised using Cytoscape software

(182).

3.2.7.2. Metabolite annotation

For the features of interest, different adducts and fragments were identified to detect the deprotonated molecular ion. The exact mass of the molecule was calculated, and the most likely crude molecular formula was selected. Subsequently, Dictionary of Natural Products (DNP 22.2 Copyright © 2014) was searched to propose a putative annotation. Other ions were directly dereplicated by the Global Natural Product Social Molecular Networking (GNPS) DEREPLICATOR module. To increase the level of confidence in the annotation, the mass spectra of the dereplicated molecules were compared with spectral data published in the literature. Xcalibur solutions software provided by ThermoFisher allowed the identification of fragments.

3.4. Disposal waste

The disposal of the waste was done according to the regulation of the Environment and Safety department of the Facultad de Ciencias Químicas from the Universidad Autónoma de Nuevo León. The disposal waste generated in the UHPLC-MS/MS and UPLC-MS/MS analyses was according to the Environment and Safety department of the Université de Nantes. The disposal waste generated in the NMR analysis was according to the Coordinación Politécnica para la Sustentabilidad (Comisión Institucional de Residuos) from the Instituto Politécnico Nacional. The disposal of the waste generated during the HR obtention was according to the Pla de Gestió de Residus de La Facultat De Farmàcia from the Universitat de Barcelona.

CHAPTER 4

4. RESULTS AND DISCUSSION

4.1. ^{1}H-NMR-based Metabolomic Approach on Hairy Roots Cultures of *Centella asiatica* Treated with Methyl Jasmonate and Coronatine

A few studies have explored the role of primary metabolism in the biochemistry of plant tissue cultures. Both primary and specialised metabolism comprise the metabolome and do not operate in isolation but are part of extensive networks. There is a lack of information of the primary metabolism and its cross-linking with centellosides and CQAs in tissue cultures of *C. asiatica*. Primary metabolism is the central source of carbon of the whole metabolism. Then, after elicitation, the primary metabolism is probably affected (183). Studies on MeJA-elicited HR of *C. asiatica* have demonstrated their potential as productive platforms of centellosides (150–152,184). Recently, it was obtained a HR line of *C. asiatica* able to produce the maximum quantity of centellosides to date using 1 µM of CORO (154). Even though these important outcomes, there is limited information about the implications of MeJA and CORO on the primary metabolism status. To further interrogate this, it was performed a time-series ^{1}H-NMR-based metabolomic approach in MeJA and CORO-elicited HR cultures of *C. asiatica*. The use of ^{1}H-NMR for plant metabolomics studies is well stablished for the determination of diverse primary metabolites (sugars, lipids, amino acids, and organic acids) (185). NMR has undeniable advantages concerning the non-

destruction nor invasion of the sample, the simplicity in sample preparation, the reliability, and the reproducibility since sample does not get in contact with an ionisation source. The direct analysis of the sample without the use of previous separation permits the covering of the wide array of compounds. The solvents are the only limitation for the range of compounds present in the samples. Plants contain hundreds of metabolites and the signals of the protons in NMR deliver complex but reliable snapshot of the sample content. The complexity and signal-overlapping spectra of NMR metabolomics analysis difficult the structural elucidation of molecules. However, it does not represent a concern when the scope of the analysis is targeted to primary metabolites. Primary metabolites are central compounds for essential processes (i.e., development) and their concentrations are regularly superior to specialised metabolites. Some of the characteristic signals of certain primary metabolites have been well-validated. Nowadays, several databases and cheminformatics tools include those signals, and the identification of central primary metabolites is relatively simple. The spectra complexity does not limit neither the performing of untargeted metabolomics studies. The analysis of equal-size buckets of the spectra are sufficient for untargeted comparative studies. The major strength of NMR for targeted metabolomics is the relative quantification of signals proportional to the standard signal. Among the advantages, the principal drawback of NMR is the lower sensitivity compared to other analytical platforms. However, as mentioned, it does not exhibit difficulties for the identification of primary compounds in plant samples (186–188). The NMR metabolomic-derived qualitative and MVDA here described provides a detailed and comprehensive metabolic state under

elicitation. The time-series experimental design allowed the obtention of time-dependent data showing the course of the metabolism through time. Then, contributing to the understanding of the responsiveness of HR of *C. asiatica* to MeJA and CORO and how functional metabolism can be both highly flexible and controllable.

4.1.1. Growth kinetics of HRs

The induction of HRs is mediated by the plant pathogen *Agrobacterium rhizogenes* in co-culture with a plant explant. In controlled conditions, the infection results in the random integration of the *Agrobacterium* Ri plasmid into the plant genome while eliminating the bacteria from the plant culture. The plasmid confers the phenotypic characteristics of HRs. As a random insertion, each transformed root appearing from the explant becomes phenotypically unique (147). Therefore, it is assumed that biomass production of HRs may vary among lines from the same species (189). Moreover, the type of elicitor and the time exposure may affect the biomass production of the culture (157). As biotic elicitors and plant-signalling molecules, MeJA and CORO modulate the metabolism and, in most cases, the biomass production of HR cultures (190). Therefore, the growth kinetics of HR cultures were recorded after the addition of the elicitors (Table 7). Dry Weight (DW) kinetics did not show significative differences between groups. Previous studies have reported that 1 µM CORO treatment inhibited the growth of the cell cultures (138) and in HR cultures of *C. asiatica* (154). However, in *Taxus*

media cell cultures the same cell line presented different behaviour in presence of 1 μM CORO, suggesting the growth depends not only of the cell line and elicitor but also culture conditions (159,191). Interestingly, an evident change in the colour of the cultures was observed according to both time-course and elicitation. As shown in Figure 16, HRs turned progressively browner along the time. However, in elicitated samples the browning was more evident, especially in CORO-treated samples. The exposure to elicitation provokes stress into tissue (129). Moreover, the progressive consumption of essential nutrients is likely to activate stress signals. It is described that in the browning process, phenolic compounds are oxidised into brown pigments. The biological function of the pigments is defensive since they can act as protective agents for phytopathogens (192). Therefore, in both elicited and late-cultured samples, phenolic compounds can be produced and oxidating in response to the stress signalling of the plant tissue.

Table 7. Effect of the elicitation in the time course of growth measured as g DW/L of HRs of *C. asiatica* in a culture period of 16 days after the elicitation.

Days after elicitation	Control	MeJA	Coro
d0	14.35 a ± 1.21	14.90 a ± 0.77	14.68 a ± 1.21
d4	21.80 a ± 3.21	22.32 a ± 0.73	24.60 b ± 1.91
d8	25.80 a ± 1.74	28.32 a ± 2.77	27.06 a ± 3.21
d12	24.15 a ± 3.02	25.09 a ± 1.32	26.19 a ± 1.00
d16	21.28 a ± 0.62	22.63 a ± 1.59	23.64 a ± 0.91

Each value is the average of 6 biological replicates ± SEM. One-way ANOVA was performed for each harvesting day. For a given day, points sharing the same letter are not significantly different at 95% confidence.

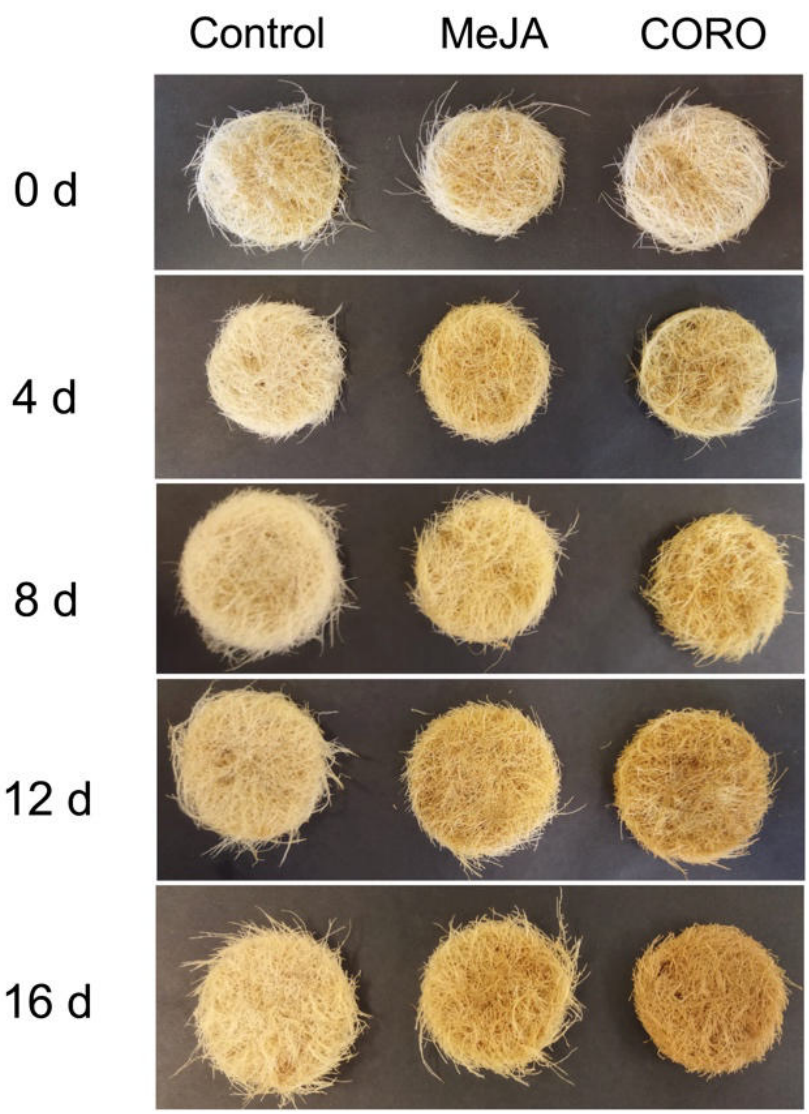

Figure 16. Fresh material of HRs of *C. asiatica* obtained after 0, 4, 8, 12 or 16 days after elicitation with no elicitor, MeJA or CORO

4.1.2. ^{1}H-NMR spectra

Aqueous extracts of HR cultures of *C. asiatica* were analysed by ^{1}H-NMR. Full NMR spectra (δH 0–10 ppm) of control and elicited HR at 0, 4, 8, 12 and 16

days after treatment are presented (Figure 17). NMR spectra showed quantitative and qualitative variations according to the treatment and cultivation time. Visual inspection of NMR spectra revealed a reduction of signals in the carbohydrate region (δH 3.0–5.5 ppm) along the cultivation time. Treatment with both elicitors decreased the intensity of the signals on this region after 8 days of elicitation. The intensity of the signals from the aliphatic regions (δH 1.0–3.0 ppm) were especially decreased 4 d after the elicitation with CORO and by the end of the experiment in MeJA-treated cultures. In this region it is common to find non-aromatic aminoacids and organic acids. Interestingly, differential signal intensities in the aromatic region (δH 6.0–8.0 ppm) were revealed. The spectra of elicitor-treated cultures showed a significant increase in the intensity of signals on the aromatic region through time. MeJA increased the intensities of the signals in this region from day 8 until the end of the experiment (Figure 17). CORO triggered a higher accumulation of aromatic signals than MeJA, at 8 and 12 days after treatment (Figure 17). On the other hand, control groups presented poor intensities of these signals during all the experiment. The increase of the aromatic signals is likely to be related with the production of phenolic compounds. Previous studies reported that exogenous addition of MeJA to cell suspension cultures of *C. asiatica* affects metabolism and changes the profile of phenolic (aromatic) compounds, especially CQAs, which were detected by UHPLC-MS/MS (160). Mendoza *et al*. (2019) observed similar ^{1}H-NMR full spectra in MeJA-elicited cell suspension cultures of *Thevetia peruviana*. They detected a similar change in the carbohydrate and aromatic signal intensities in response to the elicitor.

The reduction of the signal intensity on the carbohydrates and the aliphatic

region presented an inversely behaviour to the aromatic signals in the extracts of treated roots. This can be due to the reprograming of the cell metabolism in response to the elicitor; the primary metabolism circulates to the specialised to give carbon backbones to synthetize specialised metabolites (193). According to the spectra visualization, phenolic compounds could be produced to the detriment of carbohydrates, amino acids, and aliphatic compounds (194).

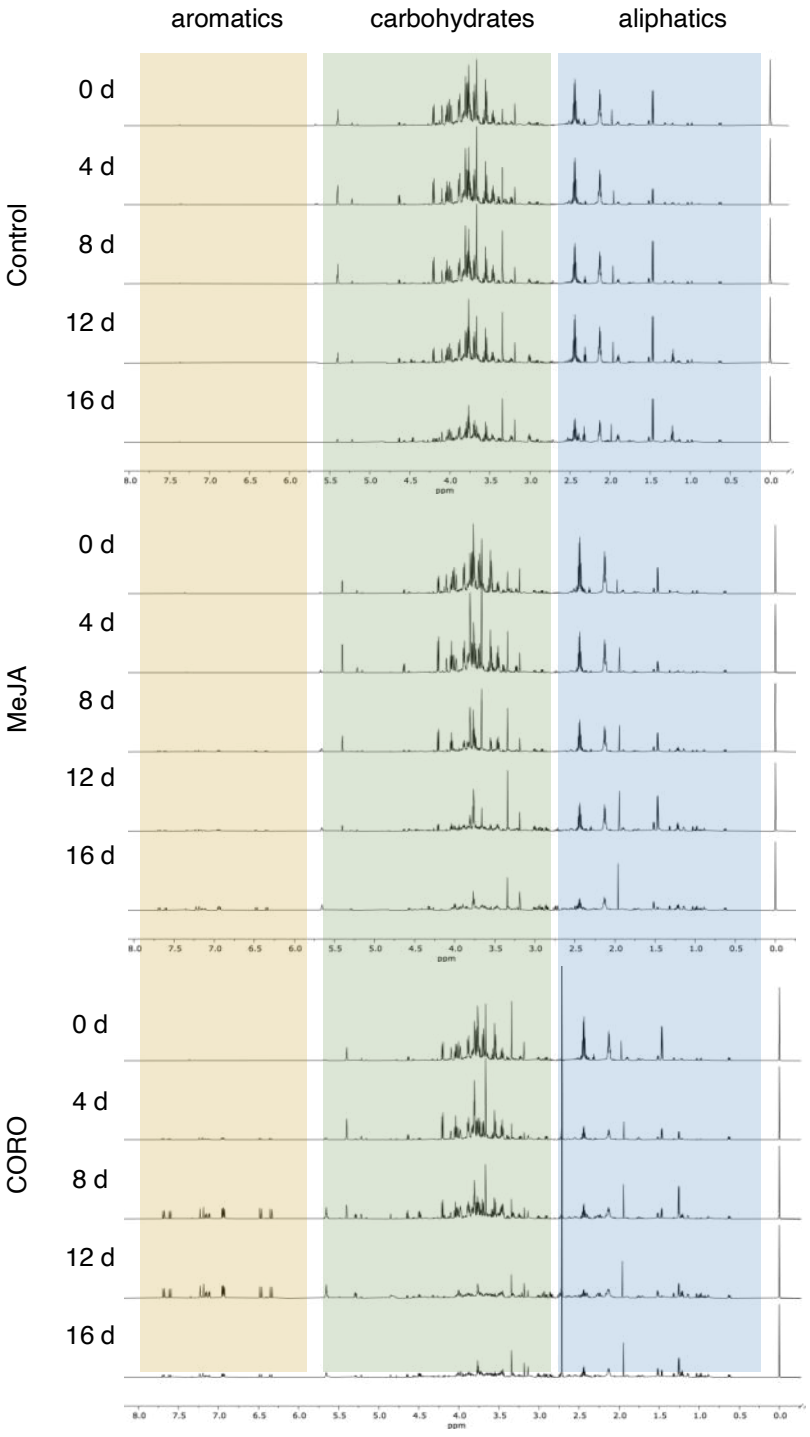

Figure 17. Overlay of stacked ^{1}H NMR spectra (750 MHz, 298.1 ± 0.1 K, 99.9% D2O, (NaNO3, pH 6.0 ± 0.05)) of intracellular extracts of HRs of *C. asiatica* harvested at 0, 4, 8, 12 and 16 days after elicitation with no elicitor (control), MeJA and CORO. TSP (at pH 6) was used as an internal standard at 0.000 ppm. Regions of common signals are highlighted in different colours.

4.1.3. Untargeted metabolomics approach

To better assess the effect of the treatment in the metabolome-derived signals and their dynamic course, the relative peak areas were analysed using an untargeted metabolomic approach. The following statistical analysis was focused on the variables "elicitor" (Control, MeJA or CORO) and "time" (0, 4, 8, 12 and 16 days after elicitation). This allowed us to explore either the effect of the elicitation in the metabolome-derived signals and their dynamic course.

Firstly, PCA was performed with the bucketing-derived data for the 90 samples (30 from each treatment) (Figure 18). A concomitant effect of time and treatment influenced in the separation of samples: the first principal component (PC1) distinctly discriminated among days of harvesting within each elicitation group, and the PC2 among treatments. The PCA showed a drift from samples of each treatment collected at day 0 to day 16. Samples followed a trajectory from right to left along the PC1 (arrows in Figure 18). This behaviour has been reported for other metabolomics kinetic studies and underlies the ordinal structural characteristics in the data (195). This highlighted the sequential apparition and disappearance of compounds in the extracts along the time-course. Additionally, the treatment provided a different separation between samples within each trajectory. In MeJA and CORO treatments, day 0 and day 4 samples were more separated that in control treatment. This indicated a drastic reprograming effect in the metabolism starting at day 4 after elicitation. On the contrary, samples from day 12 and 16 were scarcely separated in all the samples. This suggested a

possible depletion of the metabolism activity after 16 days.

Regarding the effect of the elicitor (mainly explained by the PC2), we observed an obvious separation of the CORO treatment from the rest of the groups, suggesting a higher metabolomic response to this treatment. Moderate discrimination between MeJA and Control groups was observed. CORO is a toxin produced by *Pseudomonas syringae*. It acts as an agonist of isoleucine-conjugated form of jasmonic acid (JA-Ile). This form is the naturally active end-product of MeJA. Thus, CORO achieves the activation of the specialised metabolism without the need of previous transformation to achieve an active form. Moreover, it has been observed that CORO promotes a higher interaction with the downstream transcription factors related to the activation of the specialised metabolism (129).

In summary, untargeted metabolomics analysis showed; (i) a putative dominance of CORO as metabolism reprogramming elicitor, (ii) earlier effects on the metabolism than MeJA and no elicitation and (iii) the effect of the time in the metabolism reprograming. To the best of our knowledge, this is the first untargeted metabolomic study that explores the primary metabolism of an elicited *C. asiatica in vitro* culture.

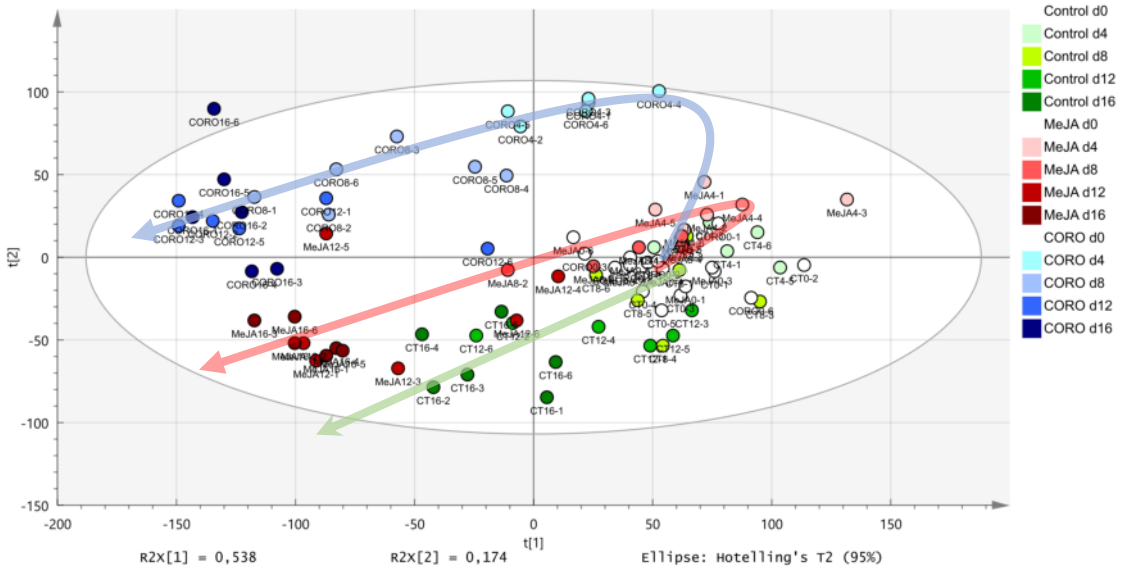

Figure 18. Principal component analysis (PCA) profiles (Pareto scaling data matrix) including all aqueous extracts of HRs of *C. asiatica* non elicitated (control), elicitated with MeJA (b) or CORO (c). Every sample is a result of 6 replicates per day. Data is based on the bucketing process obtained from 1H NMR spectra (750 Hz).

4.1.4. Compound identification

The comparison of the experimental NMR chemical shifts of specific signals with those reported in similar condition in Chenomx and in other NMR plant metabolomics-based studies (D_2O, 1:1 v/v, pH 6.0) (164,170,171,196), allowed the identification of 40 compounds (Table 8). Some compounds were differentially identified according to the sample treatment (day of collection and elicitor). Plant crude extracts present an analytical challenge. They contain molecules with a wide range of polarities and difference in their concentration (197). The complex mixture of compounds of the HRs provided spectra with superimposed signals. Those compounds whose signals were coupled are not

susceptible to be identified. Different solvents and/or extraction methods should be considered for further asses the metabolite profiling of HRs of *C. asiatica*. However, we were able to identify a wide range of primary metabolites, including sugars, amino acids, nucleosides, and some organic acids.

Table 8. Chemical shift (δ in ppm) of metabolites detected in ^{1}H-NMR spectra (D_2O, 1:1 v/v, pH 6.0) of HRs cultures of *C. asiatica*.

Metabolite	Chemical shift (δ in ppm) multiplicity and *J* coupling (Hz)
Sugars	
Fructose	4.01 (dd, *J*=12.7, 1.3 Hz)
Galactose	4.57 (d, *J*=1.9 Hz)
Glucose (α, β form)	3.23 (dd, *J*=9.4, 8.0 Hz)
Myo-inositol	3. 27 (t, *J*=9.4 Hz)
Sucrose	4.21 (d, *J*=8.8 Hz)
Amino acids	
Alanine	1.47 (d, *J*=7.37 Hz)
Asparagine	2.94 (dd, *J*=16.9, 4.2 Hz)
Aspartate	2.81(dd, *J*=17.5, 3.7 Hz)
4-Aminobutyrate	2.30 (t, *J*=7.6 Hz)
Glutamine	2.11 (m), 2.14 (m)
Histidine	8.51 (m)
Isoleucine	0.93 (t, *J*=7.4 Hz), 1.00 (d, *J*=7.0 Hz)
Leucine	0.94 (d, *J*=6.2 Hz), 0.95 (d, *J*=6.2 Hz)
Phenylalanine	7.32 (d, *J*=7.5), 7.37 (m), 7.42 (t, *J*=7.5 Hz)
Pyroglutamate	2.07(m), 2.48 (m)
Threonine	1.32 (d, *J*=6.6 Hz)
Tryptophan	7.53 (d, *J*=8.30 Hz)
Tyrosine	7.18 (d, *J*=7.18 Hz)
Valine	0.98 (d, *J*=7.0 Hz), 1.03 (d, *J*=7.0 Hz)
Organic acids	
Acetate	1.93 (s)
Citrate	2.61 (d, *J*=15.6 Hz), 2.72 (d, *J*=15.6 Hz)
Formate	8.44 (s)
Fumarate	6.52 (s)
Lactate	1.32 (d, *J*=6.6 Hz)
Malate	2.40 (dd, *J*=15.5, 9.9 Hz)
Pyruvate	2.36 (s)
Succinate	2.48 (s)
Malonate	3.16 (s)
Alcohols	
Ethanol	1.17 (t, *J*=7.1 Hz)
Methanol	3.35 (s)
Nucleosides	
Adenosine	6.06 (d, *J*=6.2 Hz), 8.2 (s), 8.3 (s)
Cytidine	7.85 (d, *J*=7.2 Hz)
Guanosine	5.93 (d, *J*=5.7), 7.99 (s)
Uridine	7.86 (d, *J*=8.1 Hz)
Phenolic compounds	
3-O-Caffeoylquinic acid	6.36 (d, *J*=15.93 Hz)
4-O-Caffeoylquinic acid	6.44 (d, *J*=15.93 Hz)
5-O-Caffeoylquinic acid	6.41 (d, *J*=15.93 Hz)
Ferulate	6.37 (d)
Other compounds	
Choline	3.19 (s)
NAD+	9.45 (s)

Despite the apparent lower concentration in the samples and the complexity of the spectra, we were able to detect specialised metabolites, we found three isomers of caffeoylquinic acids (CQAs), also known as chlorogenic acids (3-O-CQA, 4-O-CQA; 5-O-CQA); and ferulic acid. UHPLC-MS/MS-derived metabolite profiling studies in *C. asiatica ex vivo* plants and cell suspension cultures showed the endogenous production of diverse CQA-like compounds in basal conditions. Most of these compounds belonged to structural isomers of O-CQAs and O-feruloylquinic acids (103). The same authors also revealed the capacity of MeJA to promote the overproduction of certain CQAs (160,198). Interestingly, the literature has demonstrated the therapeutical application of these compounds due to their antimalarial, antioxidant, antineoplastic, cytotoxic, anti-mutagenic, antiviral, hemostatic, leukopoietic activity (160).

Flavonoids previously reported in *C. asiatica* plants and cell cultures such quercetin-derived compounds (160,198), were not detected. Possibly due to (i) their low concentration in HR suspensions, (ii) the poor solubility of certain compounds in the aqueous extract or (iii) the limitation of the databased here used.

As aforementioned, *C. asiatica* is well known to produce centellosides. Literature clearly supports the interest of the academia for investigating effective biotechnological production of these molecules. Nevertheless, no centellosides or other metabolites participating in the centelloside pathway were here detected. Centellosides-like compounds are mid- or non-polar compounds. Therefore, the water extraction performed for the present experiment probably were not able to extract them. Although we were not able to detect flavonoids nor centellosides,

we were capable to find out the earlier precursors of the pathways related to these metabolites, we discussed later this finding.

4.1.5. Quantitation of metabolites using NMR spectra

Chenomx NMR Suite v.8.3 software was used for the relative quantification to TSP (0.7 mM) of all metabolites previously identified. Chenomx works by fitting signals from its *in-house* spectral data base to the appropriate signals within the experimental spectra. After the experimental signal has been fit, the concentration is given. The software automatically adjusts the reference database to acquisition conditions (pH, NMR field strength, spectra line width) (172).

Relative quantity of primary compounds is presented in Figure 19-22. Notably, treatment of HR suspensions of *C. asiatica* with CORO produced major differences in kinetics production when compared to control in most of the analysed metabolites. MeJA showed similar production patterns to CORO, but in a slighter manner.

4.1.5.1. Carbohydrates

As observed in Figure 19, the pool of carbohydrates (sucrose, fructose, and glucose) decreased gradually in control conditions. This behaviour has been previously observed in ^{1}H-NMR metabolomics analysis of *Papaver somniferum* (199), *Thevetia peruviana* cell cultures (200) and in HR cultures of *Rhazya stricta*

(201). Moreover, they observed that MeJA caused a higher consumption of carbohydrates. This suggests the need of carbohydrates in the respiratory metabolism for the development and growth of the HRs, especially after elicitation. Here, both elicitors triggered a significant reduction of carbohydrates compared to control. This depletion during elicitation was notably from day 8 after elicitation. Studies in *Arabidopsis thaliana* have demonstrated the regulatory role of MeJA in the carbohydrate metabolism in an enzymatic level. After MeJA elicitation, enzymes related to the catabolism of carbohydrates, Krebs cycle and different specialised pathways were up regulated; including those involved in the phenolic pathway. Thus, it is suggested that the catabolism of carbohydrates become essential after elicitation not only for getting energy for the specialised metabolites biosynthesis, but also for the formation of carbon skeletons needed as precursors for these pathways (201,202).

4.1.5.2. Organic acids: Intermediates from the Krebs cycle

Organics acids play a central role in the primary metabolism. Igamberdiev and Eprintsev (2016) reviewed the role of organic acids in the carbon balance of plants. Organic acids are produced because of no-completed oxidation. They represent a supply of carbon for the Krebs cycle and/or other pathways when the redox balance in the cells increases (i.e., under elicitation stress conditions). In the present work, levels of some Krebs cycle intermediaries (fumarate, malate, and citrate) gradually increased during the experiment in all groups. However,

they were not differentially produced/consumed between groups. Liu *et al*. (2019) observed in metabolomics studies in HRs of *Salvia miltiorrhiza* that elicitation with MeJA increased levels of malate, fumarate, citrate, and succinate. They suggested that the principal carbon source of the Krebs cycle is the catabolism of carbohydrates. Thus, the decrease in the carbohydrate pool could be dominated by the Krebs cycle as it is further described (Figure 19).

Interestingly, CORO was able to induce 100-fold more concentration of succinate than in the other groups. Succinate can be formed either from the catabolism of carbohydrates or by the non-protein amino acid 4-aminobutyric acid (4-GABA). 4-GABA is one of the linking points between amino acids and the Krebs cycle. It is synthetised from glutamine (203) and plays a central role in the balance carbon/nitrogen in plants. In this work, CORO reduced both concentration of glutamine and 4-GABA. It has been observed that ,under biotic stress, 4-GABA acts as a carbon supply for the Krebs cycle through its transformation into succinate (204). Succinate can either recirculate through the Krebs cycle or deriving electrons to the respiratory chain. The accumulation of succinate has been observed under reduction of the mitochondria activity and hypoxia in stress conditions (205).

The treatment with CORO also induced the accumulation of malonate while it was undetectable in the other treatments (Figure 19). Malonate accumulation is toxic for plants since it inhibits succinate dehydrogenase. It is a key enzyme in the movement of organics acids towards the Krebs cycle (205). The malonate accumulation here observed could explain the accumulation of succinate after addition of CORO. The biosynthesis of malonate derives from acetyl-CoA.

Malonate is a precursor of lipids and polyketides in plants, which are also specialised metabolites (206). However, these metabolites were not detected in the present work, due to its non-polar nature. Additionally, the metabolism of malonate implies the decarboxylation of this last molecule forming acetate (205). This organic acid was differently produced in elicitation treatments compared to the control during the experiment. For further studies, it should be recommended exploring in detail the effect of CORO in all the specific metabolites of the Krebs cycle.

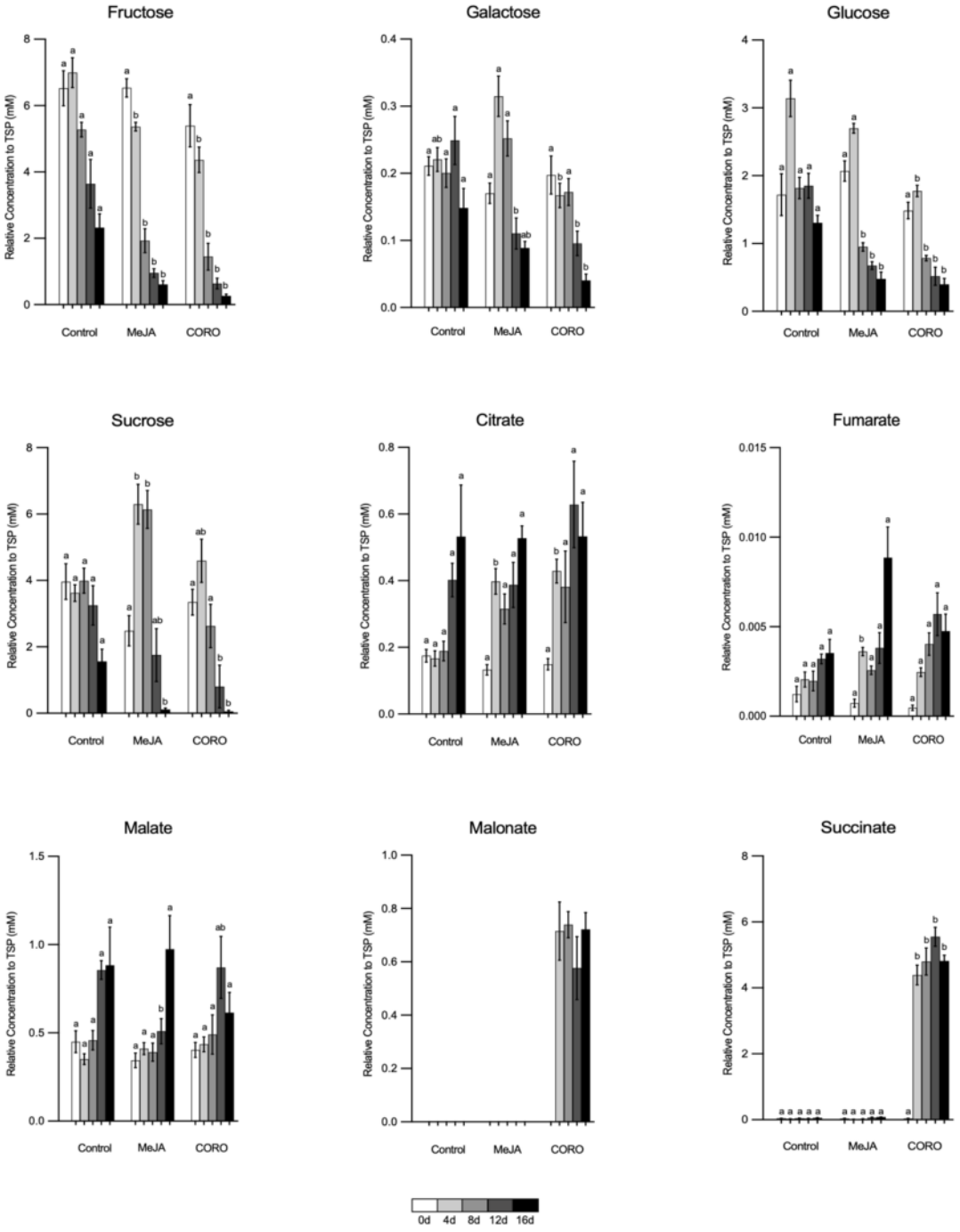

Figure 19. Relative quantity of identified carbohydrates and organic acids by NMR in aqueous extracts of control and elicited HR cultures of *C. asiatica* at different harvesting times after addition of MeJA or CORO. Quantitative data was calculated using six biological replicates and it is presented as means ± SEM. Two-way ANOVA was performed for each harvesting day. Then, for a given day, columns sharing the same letter are not significantly different at 95% confidence. Quantification was performed using the software Chenomx NMR Suite v. 8.5 with TSP as the internal standard.

4.1.5.3. Amino acids

MeJA and CORO-treated cultures caused major changes on amino acids production compared to the control. Both elicitors negatively affected the production of alanine, glutamine, and arginine. On the other hand, isoleucine, tryptophan, asparagine, and proline were enhanced (Figure 20). However, the superiority of CORO in triggering more drastic changes was observed. The concentration of most of the amino acids (i.e., leucine, valine, alanine, threonine, lysine, glutamine, asparagine, aspartate, arginine, histidine, phenylalanine, tyrosine, and tryptophan) were reduced at early stages (4 and 8 days after elicitation) in the elicited groups; specially in CORO-elicited samples (Figure 20-21). This behaviour suggests a higher demand of nitrogen in response to CORO. This demand could be in response to the expression of proteins related to the specialised metabolism. Glutamine is the most abundant amino acid in plants and one of the major amino group donor in the biosynthesis of amino acids (207). Studies in rice roots suggested that glutamine regulates the expression of transcription factors participating in stress response (208). In our study, glutamine was one of the most abundant metabolites present in the extract in all the groups. Its concentration levels were gradually decreased in all groups during the experiment. However, the reduction was significatively higher in MeJA groups and even more in those treated with CORO (maybe for the consumption to synthetize 4-GABA as mentioned before). Asparagine shares with glutamine its function as nitrogen carrier. It is believed that under pathogenic infection in plants asparagine

is overproduced. It seems to be crucial in the exportation of nitrogen from damaged tissues limiting the nitrogen uptake from pathogens (209). Interestingly, this scenario has been observed in *Pseudomonas syringae*-infected (natural CORO producer) tomato leaves. Levels of asparagine increased significatively at days 12 and 16 in the elicited samples later than other amino acids. Nevertheless, other studies found that the exogenous application of glutamine can act as a negative feedback for the biosynthesis of glutamine and asparagine (208). Another amino acid playing a key role in the storage and recycling of nitrogen is arginine. Catabolism of arginine in the mitochondria produces the sequential production of glutamine, α-ketoglutarate, NADH+ and free ammonia. Therefore, the end products of arginine degradation represent a supply of precursors for anabolic/recycling pathways; glutamine is a supply for the reassimilation of nitrogen, α-ketoglutarate for the Krebs cycle and NADH+ for the respiratory production of ATP. The catabolism of arginine seems to be coordinated with the consumption of sugars (210). This could explain the significative progressive reduction of arginine in both treatments compared to the control.

It is extendedly observed that proline is a nonenzymatic antioxidating and ROS scavenger. This amino acid protects the cell membrane and the structure of macromolecules (211). Studies in HRs of soybean showed that the addition of MeJA is associated with an enhancement of proline. Presumably, proline accumulation could ameliorate the oxidative stress observed in the HRs after elicitation with MeJA (212). It is consistent with the results here presented since proline was significatively higher in elicitated samples than in control (Figure 20).

Several studies have reported the role of GABA in biotic stress and its

production after the accumulation of jasmonates. The biological role of GABA in ameliorate the stress could be its inhibitory effect in the nervous systems of insects or its ability for activate several antioxidant enzymes (204). However, as shown in Figure 20, levels of 4-GABA were significatively reduced in elicitation groups compared to control. As mentioned before, succinate can be synthetised from 4-GABA, therefore its depletion can be related to succinate accumulation. This could be a response of a putative reactive oxygen species (ROS) increment in elicited cultures.

As we mention before, centellosides are one of the most valuable specialised metabolites in *C. asiatica*. Unfortunately, not centellosides-like molecules were identified in the present ^{1}H-NMR spectra. Centellosides-like molecules are pentacyclic triterpenes. The primary building block for the formation of triterpenes is acetyl-CoA. The amino acids valine and isoleucine are precursors of the biosynthesis of CoA and pyruvate from carbohydrates catabolism. As we mention before we observed a depletion in carbohydrates biosynthesis in the elicited cultures. Additionally, levels of valine and isoleucine were significative decreased at day 4 and 8 but enhanced at days 12 and 16. This was also observed in MeJA-elicited HRs of *Salvia miltiorrhiza* (213). This metabolism behaviour could suggest an improvement of centellosides levels. Different extraction methods are required to detect centellosides-like molecules.

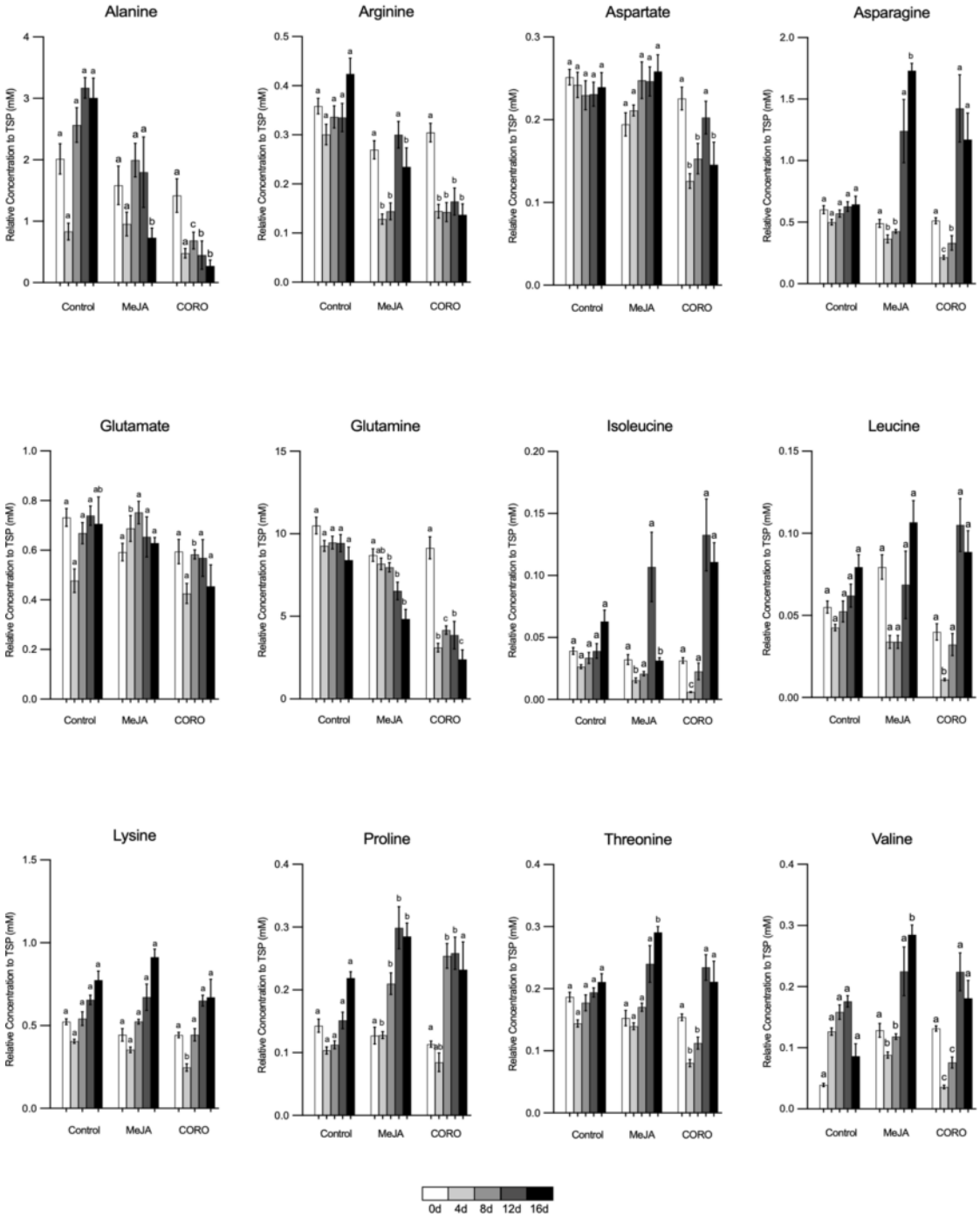

Figure 20. Relative quantity of identified amino acids by NMR in aqueous extracts of control and elicited HR cultures of *C. asiatica* at different harvesting times after addition of MeJA or CORO. Quantitative data was calculated using six biological replicates and it is presented as means ± SEM. Two-way ANOVA was performed for each harvesting day. Then, for a given day, columns sharing the same letter are not significantly different at 95% confidence. Quantification was performed using the software Chenomx NMR Suite v. 8.5 with TSP as the internal standard.

4.1.5.4. Phenolic compounds

Characteristic signals in the aromatic region led to the identification of three structural isomers of CQAs; 3-O-CQA, 4-O-CQA, 5-O-CQA; and ferulic acid. As shown in Figure 21, Elicitation caused the significant over-production of these compounds compared to control conditions. In MeJA-treated samples, phenolic compounds were initially produced at day 8 and remained constant throughout the 16 days of culture. On the other hand, CORO elicited the production of these compounds from day 4 until the end of the experiment. After 8 days of elicitation, their concentration was 10-fold increased. At day 12 remained stable and decreased slightly at the end of the experiment. During all the experiment, levels of total CQAs in CORO-elicited samples were significatively higher compared to MeJA. In control samples the concentration of these four phenolic compounds was almost undetectable. Therefore, CORO can be considered the best elicitor for *de novo* biosynthesis of phenolic compounds in HR cultures of *C. asiatica*. The increased production of detected phenolic compounds evidenced a strong reprogramming effect of CORO on the primary metabolism towards the specialised. Some studies demonstrated that CORO causes a stronger activation of the specialised metabolism than MeJA (214–216). The shikimate pathway is the upstream biosynthetic process involved in the production of most of phenolic compounds including CQAs. Even though no shikimate pathway intermediates were detected, some events could suggest its activation. Firstly, early steps of the shikimate pathway are linked to carbohydrate metabolism. The consumption of

carbohydrates in elicited cultures (specially in CORO) has already been mentioned. Secondly, phenylalanine is one of the main intermediates in the synthesis of CQAs. Its levels were sharply reduced at early stages after CORO elicitation, but not in MeJA treatment. Few studies have explored the regulation of CORO on the expression of enzymes in the specialised metabolism. In *Cephalotaxus mannii* cell suspension cultures, transcripts of enzymes involved in the biosynthesis of phenolic compounds were up-regulated after CORO elicitation: 3-deoxy-d-arabino-heptulosonate-7-phosphate synthase (DS) from the shikimic acid pathway, phenylalanine ammonia-lyase (PAL), and caffeoyl-CoA O-methyltransferases (217). In addition, it was reported that the expression of PAL was enhanced by coronatine in suspension cell cultures of *Vitis vinifera* (166). The amino acids tyrosine and tryptophan are also biosynthesised in the shikimate pathway. The intermediate chorismate (not identified in this project) can be converted into either tyrosine, tryptophan, or phenylalanine (218). In the present work, the concentrations of tyrosine and tryptophan were significatively reduced at days 4 and 8 after CORO elicitation (Figure 21). Thus, these two amino acids apparently did not create a bottleneck towards the biosynthesis of CQAs. Overall, it is recommended exploring the gene expression of shikimate pathway in HRs of *C. asiatica*. This exploration could deliver strategies for improving the production of valuable phenolic compounds of *C. asiatica*.

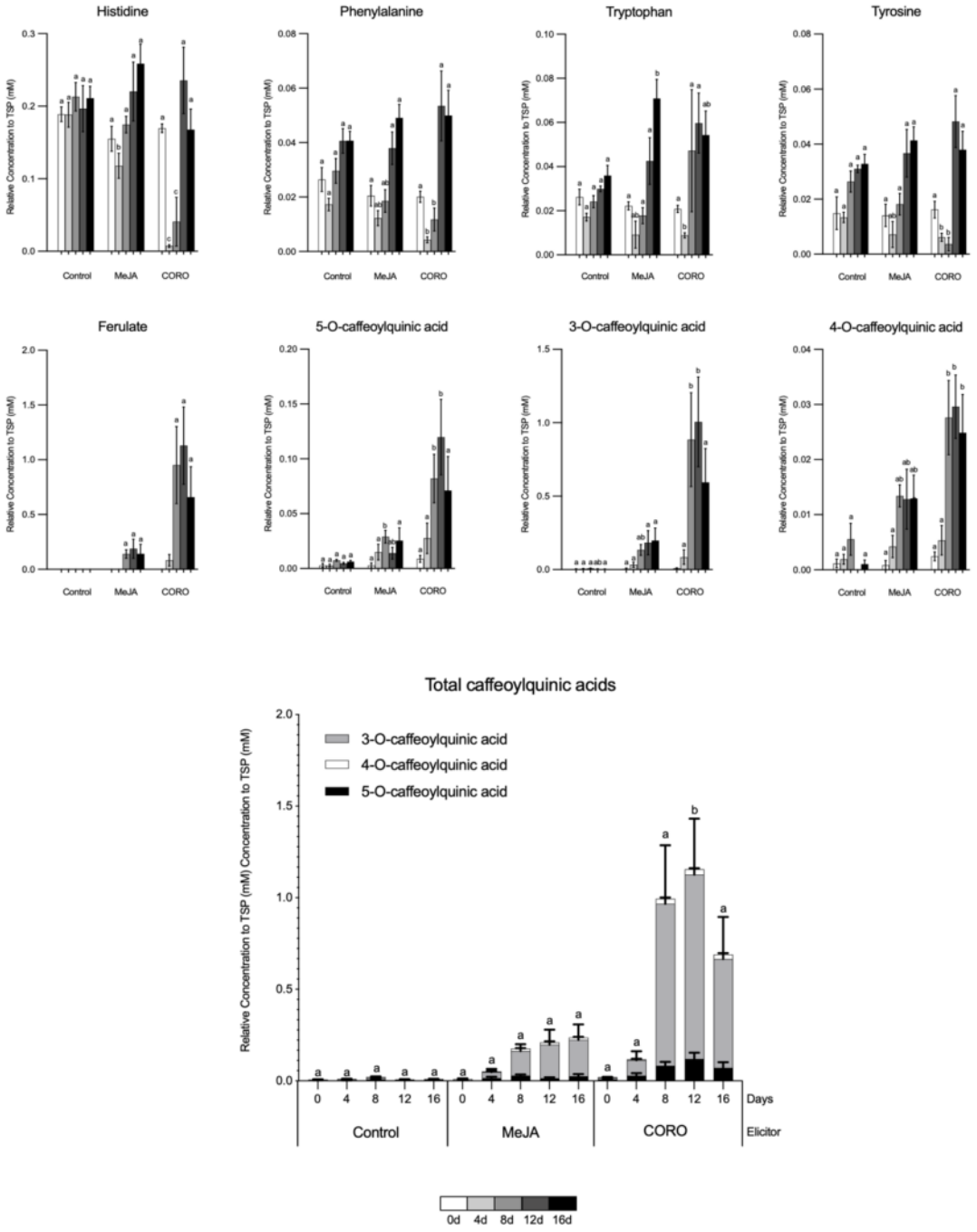

Figure 21. Relative quantity of identified phenolic compounds and some amino acids by NMR in aqueous extracts of control and elicited HR cultures of *C. asiatica* at different harvesting times after addition of MeJA or CORO. Quantitative data was calculated using six biological replicates and it is presented as means ± SEM. Two-way ANOVA was performed for each harvesting day. Then, for a given day, columns sharing the same letter are not significantly different at 95% confidence. Quantification was performed using the software Chenomx NMR Suite v. 8.5 with TSP as the internal standard.

4.1.5.5. Other compounds

Purine nucleosides uridine and guanosine and the pyrimidine nucleoside cytidine were detected in all samples. Nucleosides are the direct precursor of the biosynthesis of nucleic acids. These metabolites do not only participate in the biosynthesis of macromolecules, but also serve as an ultimate source of energy for the synthesis of both primary and specialised metabolites (219). Their production showed a decrease under elicitation, especially at day 4 after both elicitations and at the end of the experiment (Figure 22). Time-course metabolomics studies in barley by Yuan *et al*. (2018) suggested that the demand of nucleosides at early stages could be related to the biosynthesis of proteins. While at late time points, the catabolism of nucleosides could be redirected to the obtention of ultimate energy due to starvation of the culture (220). In this work we observed a decrease in the early stages of the culture, suggesting a demand in protein synthesis, which could be related to the need of enzymes for the specialised metabolism.

Choline was significatively decreased in elicited cultures (Figure 22). Choline is generally present in form of phospholipid forming phosphocholine. Phospholipids play several roles in plant cells, especially in the cell membrane: membrane trafficking and signal transduction. However, Gao *et al*. (2020) found that choline and choline-derivate sphingolipids are also implicated in plant hypersensitive response. Choline and its derivatives regulate in some extend the regulation of signal transduction, programmed cell death, vesicular trafficking,

autophagy, and alternative splicing in response to stress. The authors observed that *Arabidopsis* plants deficient of an enzyme implicated in the biosynthesis of choline exhibited susceptibility to the pathogen *P. syringae*. As mentioned, this pathogen is a natural producer of CORO (207). This could explain the significative reduction of choline concentration in CORO-elicited samples. Choline could be consumed to diminish the hypersensitive response in response to CORO.

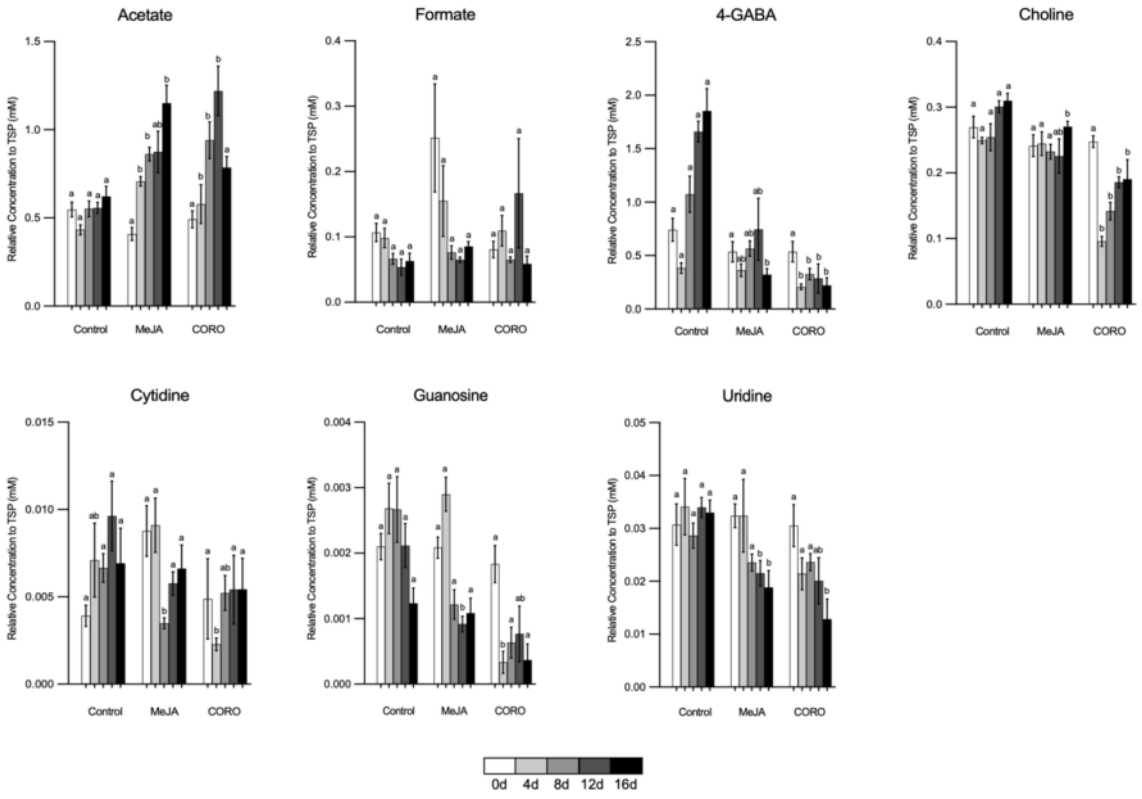

Figure 22. Relative quantity of different identified metabolites by NMR in aqueous extracts of control and elicited HR cultures of *C. asiatica* at different harvesting times after addition of MeJA or CORO. Quantitative data was calculated using six biological replicates and it is presented as means ± SEM. Two-way ANOVA was performed for each harvesting day. Then, for a given day, columns sharing the same letter are not significantly different at 95% confidence. Quantification was performed using the software Chenomx NMR Suite v. 8.5 with TSP as the internal standard.

According to the data obtained and discussed previously, day 12 after elicitation presented the main differences between the groups. Therefore, the impact of the elicitors on the metabolism at day 12 after elicitation is simplified in a metabolic map with the identified metabolites spotlighted (Figure 23).

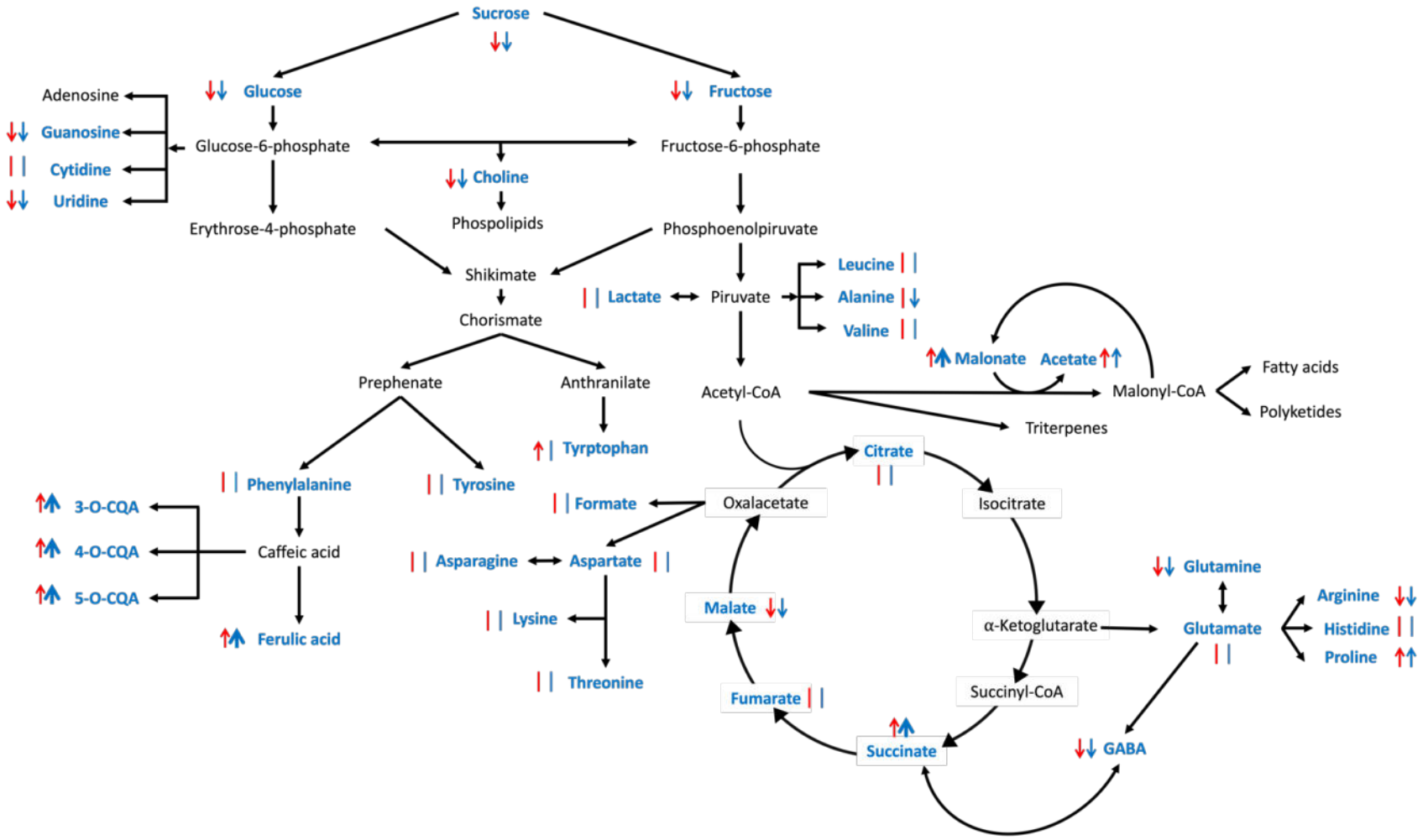

Figure 23. Simplified metabolic network representing the influence of MeJA and CORO in the HR cultures of *C. asiatica* 12 days after elicitation. Compounds identified in the ^{1}H-NMR analysis are shown in blue, while those undetected are shown in black. Symbols associated with each metabolite show the significant changes with comparison with control conditions at $p < 0.05$: (↑) overproduced, (↓) downproduced, (|) no differences. Colour red describes MeJA, while colour blue CORO.

4.1.6. MVDA of quantification

After detailed quantitative analysis of the targeted metabolites, targeted MVDA was performed using the data matrix containing the relative concentration to TSP in mM of the identified metabolites.

Targeted data was sorted by Hierarchical Clustering Analysis (HCA) in a heatmap visualization (Figure 24). It allowed the identification of links between the production of groups of metabolites. Clusters were divided into cluster (a) and cluster (b). They were further subdivided into two minor clusters for each one: (a1), (a2), (b1) and (b2). Qualitatively, cluster (a1) corresponded mainly to carbohydrates and nucleosides; cluster (a2) to some aliphatic amino acids; cluster (b1) to phenolic compounds, succinate, and malonate; and cluster (b2) to aromatic amino acids, other aliphatic amino acids and the rest of Krebs Cycle by-products. The hierarchical clustering showed a link between the overproduction of phenolic compounds belonging to cluster (b1) and those phenolic amino acids from cluster (b2). Therefore, it shows the relation between the phenolic amino acids as precursors of phenolic compounds. Regarding cluster (a), in MeJA treated samples the metabolites from cluster (a1) showed higher production than in CORO-elicited cultures. This suggested again a slighter boosting effect of MeJA in the specialised metabolism when compared to CORO. For control samples, while clusters (b1-2) were practically suppressed in terms of production, clusters (a1-2) were maintained productive along the time. Clusters (a1-2) corresponded to primary sources of carbon (e.g., aliphatic amino acids and pool

of carbohydrates). Therefore, in control samples these sources were less redirected to downstream processes.

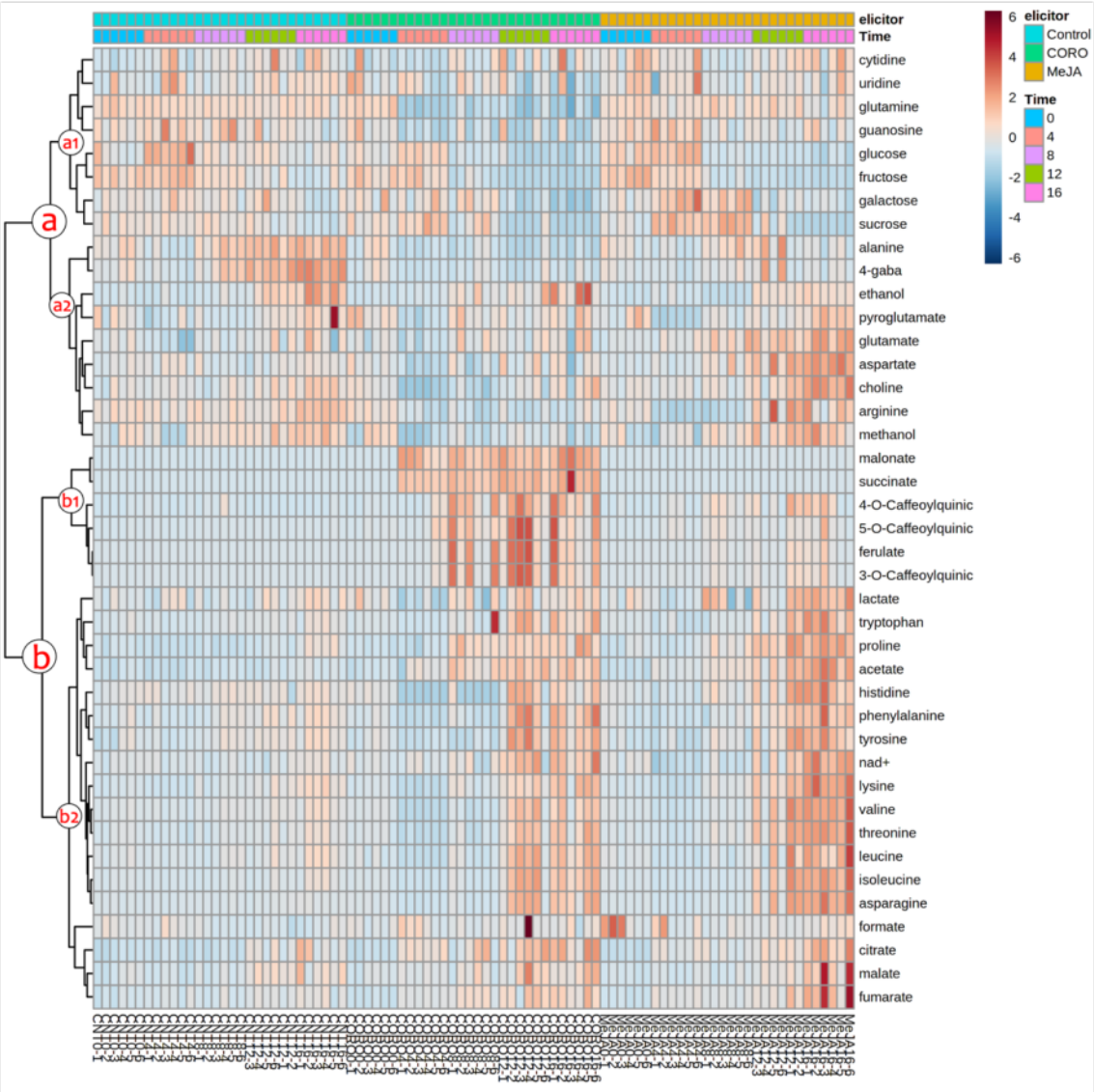

Figure 24. Hierarchical clustering of quantitative data of identified metabolites in ^{1}H NMR spectra (750 Hz) in response to different elicitation treatments (control, MeJA and CORO) after 0, 4, 8, 12 and 16 after elicitation of HR cultures of *C. asiatica*. Metabolites were divided into two major clusters (a) and (b) and further subdivided into two minor clusters for each one: (a1), (a2), (b1) and (b2) to facilitate the interpretation.

OPLS-DA (R2X cum 0.77 and R2Y cum 0.936, Q2 cum 0.818; CV-ANOVA (p-value = 1.51×10^{-5})) was further applied to assign the characteristic compounds of interest in terms of variability. It is a supervised classification model that differs from PCA by the addition of grouping variables that indicate in which class the samples belong. This method allows the identification of the metabolite(s) responsible for the discrimination between groups (221). The OPLS-DA models were processed for each cultivation time showing a clear separation of the three treatments. Thus, confirming the influence of elicitation in the production kinetics of those metabolites included in the model (Figure 25). Variables of OPLS-DA were analysed thorough their value of VIP parameters. The corresponding VIP scores (Table 9) indicated the most influencing metabolites (either up or downproduced) in the dispersion of the samples in the OPLS-DA plots (VIP > 1). VIP scores were analysed in a Venn diagram to better asses the distribution of shared and common VIPs at different time points (Figure 26). As shown, a few metabolites influenced the model constitutively: glutamate, proline, and acetate in MeJA treatment; and glutamine, succinate, malonate, glucose, and arginine in elicitation with CORO. In the case of MeJA, glutamate and proline were down-regulated along all the experiment. These two amino acids are related to nitrogen supply to different biosynthetic pathway. This suggests the elicitation-derived effect in the repartitioning of nitrogen to, possibly, specialised pathways. Similarly, in CORO elicitation other two nitrogen carrier (glutamine and arginine) influenced the model constitutively. Glucose also influenced the model along all the experiment. Glucose (and the rest of the sugar here detected) represents the primary source of energy. Then, it should be considered for

continuous production platforms to replace the media of the culture after 12 days of elicitation in order to maintain the stability and production of the culture. In general, more metabolites were found to be time specific in the MeJA treatment compared to CORO. It suggests a faster reprograming effect of CORO than MeJA in the metabolism.

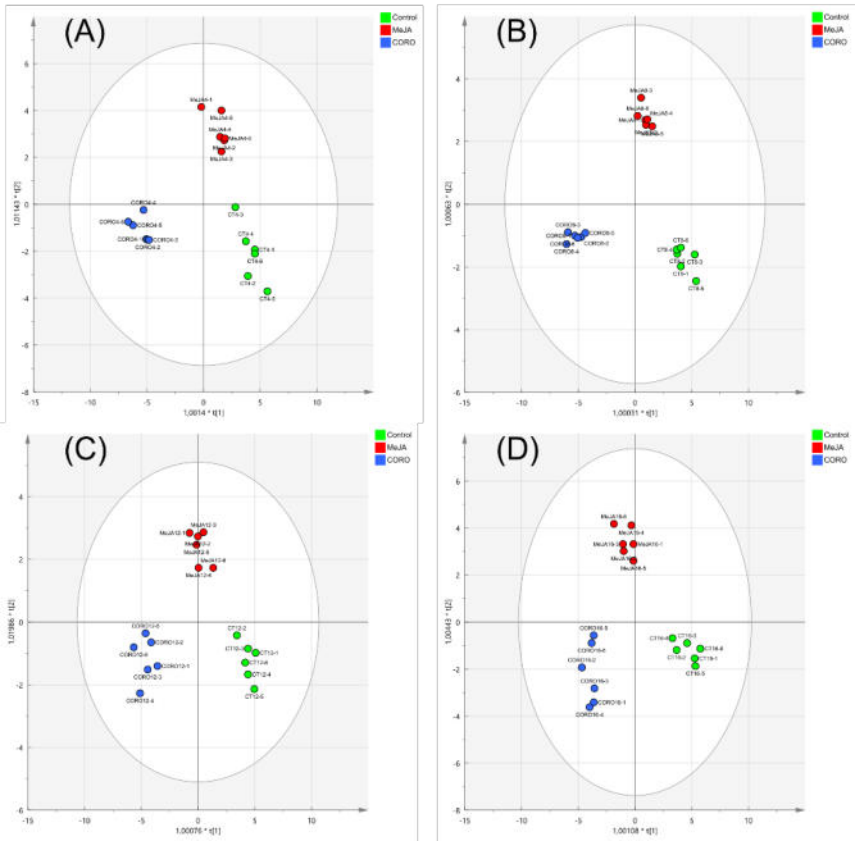

Figure 25. Score plot of OPLS-DA analyses of the quantitative data at different days of harvesting: (a) day 4, (b) day 8, day 12 (c) and day 16 (d). Samples are labelled according to their treatment: control (blue), MeJA (red), CORO (yellow).

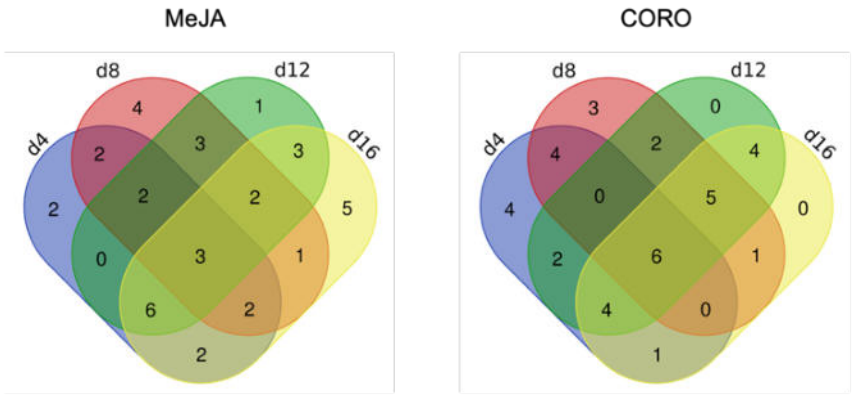

Figure 26. Venn diagrams of the VIPs obtained from the OPLS-DA (R2X cum 0.77 and R2Y cum 0.936, Q2 cum 0.818; CV-ANOVA (p-value = 1.51×10^{-5})) analyses of the quantitative data at different days of harvesting (day 4 - 16) after elicitation with MeJA (left) and CORO (right).

Table 9. Variable importance in the projection (VIP) values (next to each name of molecule) for predictive components in OPLS-DA data modelling at each harvesting day (day 4, 8, 12 and 16) for each treatment (MeJA or CORO).

MeJA							
d4		d8		d12		d16	
leucine	1.5301	acetate	1.6247	proline	1.5287	lysine	1.3150
arginine	1.5095	fructose	1.6030	glucose	1.5012	nad+	1.3149
acetate	1.4674	glucose	1.5170	acetate	1.3588	threonine	1.3114
asparagine	1.4344	sucrose	1.5131	fructose	1.3515	4-gaba	1.3045
isoleucine	1.4186	arginine	1.4943	succinate	1.3186	asparagine	1.2945
citrate	1.4067	proline	1.4057	threonine	1.3055	valine	1.2893
sucrose	1.3923	5-cqa	1.3530	aspartate	1.2940	aspartate	1.2836
valine	1.3905	ethanol	1.3336	asparagine	1.2164	isoleucine	1.2810
lysine	1.3771	citrate	1.3210	isoleucine	1.2002	alanine	1.2550
nad+	1.3610	galactose	1.3158	lysine	1.1889	acetate	1.2404
fructose	1.3283	glutamate	1.2771	valine	1.1513	proline	1.2298
glutamate	1.2307	cytidine	1.2337	formate	1.1507	choline	1.2226
histidine	1.2011	ferulate	1.2205	galactose	1.1494	succinate	1.1978
fumarate	1.1967	4-cqa	1.2041	4-cqa	1.1152	lactate	1.1972
glutamine	1.1572	3-cqa	1.1987	glutamate	1.0921	sucrose	1.1912
succinate	1.1136	fumarate	1.0772	tryptophan	1.0557	tryptophan	1.1514
proline	1.0886	guanosine	1.0178	5-cqa	1.0410	histidine	1.0866
pyroglutamate	1.0761	4-gaba	1.0084	ferulate	1.0320	leucine	1.0743
galactose	1.0745	aspartate	1.0035	3-cqa	1.0282	glucose	1.0339
				nad+	1.0277	glutamate	1.0245
						phenylalanine	1.0171
						tyrosine	1.0069
						fumarate	1.0047
						formate	1.0018
CORO							
d4		d8		d12		d16	
glutamine	1.4083	succinate	1.4927	succinate	1.4245	alanine	1.4545
succinate	1.3983	malonate	1.4781	acetate	1.4077	4-gaba	1.4428
leucine	1.3924	proline	1.4287	alanine	1.3829	malonate	1.4210
valine	1.3803	glutamine	1.4053	malonate	1.3766	arginine	1.3772
choline	1.3782	fructose	1.3900	4-gaba	1.3735	acetate	1.3457
isoleucine	1.3724	alanine	1.3294	proline	1.3700	sucrose	1.3231
asparagine	1.3655	methanol	1.3262	glutamine	1.2821	glutamine	1.3002
histidine	1.3576	acetate	1.2986	glucose	1.2527	methanol	1.2822
citrate	1.3405	glucose	1.2972	fructose	1.2009	succinate	1.2804
lysine	1.3187	arginine	1.2960	4-cqa	1.1619	isoleucine	1.2799
threonine	1.2422	tyrosine	1.2863	galactose	1.1524	glucose	1.2159
malonate	1.2299	fumarate	1.1888	arginine	1.1263	asparagine	1.2090
aspartate	1.2295	valine	1.1887	methanol	1.1192	fructose	1.1778
guanosine	1.1883	4-gaba	1.1859	isoleucine	1.0911	galactose	1.1736
phenylalanine	1.1728	histidine	1.1801	asparagine	1.0671	4-cqa	1.1736
arginine	1.1102	5-cqa	1.1434	leucine	1.0433	nad+	1.1089
malate	1.0960	4-cqa	1.1167	threonine	1.0421	leucine	1.0791
sucrose	1.0647	guanosine	1.0844	nad+	1.0389	tryptophan	1.0718
glucose	1.0475	pyroglutamate	1.0552	sucrose	1.0245	3-cqa	1.0461
tryptophan	1.0140	choline	1.0100	3-cqa	1.0209	fumarate	1.0140
				citrate	1.0199		
				5-cqa	1.0088		

4.2. UHPLC-MS/MS-based Targeted and Untargeted Metabolomic Approach for investigation of Treatment with Methyl Jasmonate and Coronatine on HR Cultures of *Centella asiatica*: Specialised Metabolome.

The ^{1}H-NMR metabolomics analysis previously described yielded detailed information on the identification and molar concentration of primary metabolites. However, it is not the preferable analytical platform to develop specialised metabolism metabolomics approaches mainly because NMR spectroscopy suffers from low sensitivity. Indeed, specialised metabolites are often found in lower abundance than the primary and their concentrations are mainly influenced by exogenous signals since they are non-essential for the plant development. The specialization and diversification of plant specialised metabolites is also often translated into complex chemical structures. Then, the chemical identification of NMR-analysed specialised metabolites is complex as a result of overlapped signals (222). Therefore, other analytical techniques are more convenient for specialised metabolism metabolomics studies of plant extracts. As previous reports have indicated that *C. asiatica* plant biosynthesize various specialised metabolites belonging to the classes pentacyclic triterpenoids, caffeoylquinic acids (CQAs) and flavonoids, we engaged a complementary strategy to observe the effects of elicitors on these compounds.

UHPLC-MS/MS-based metabolomics analysis have proven to be the most relevant for the global coverage of specialised metabolites in plant metabolomics studies. Modern UHPLC techniques offer high resolution in separation of the sample components based on the analyte interaction between the mobile and

stationary phase under high pressure and using low granulometry. Also coupling UHPLC to MS/MS provides a stable detection of metabolites through atmospheric ionisation processes like ESI or Atmospheric Pressure Chemical Ionization (APCI). ESI is the preferred ionisation mode in metabolomics studies since it produces a large number of ions for most organic compounds such as specialised metabolites (223). Also, MS is the key platform for compound identification which is an essential step in a metabolomics workflow. High Resolution MS allows the deduction of the molecular formula of detected compounds, and MS/MS spectral data provides a fragmentation pattern which is often compound specific. Then, each molecule detected can be characterised by a peak with specific data consisting of its Rt, *m/z* value, abundancy and MS/MS fragmentation spectrum associated. These unique identities or features can be collected from raw LC-MS-data using some processing softwares such as MzMine 2. This software identifies *m/z* signals above a noise-level threshold returning features with the relative abundance according to its peak area/height. The listing of unique ions (named features) is crucial for the subsequent MVDA and for the differentiation of isobaric compounds according to their Retention Time (Rt).

The attempt to “put a name” on each detected ion is called the “dereplication” process. Dereplication is based on the spectral information of the features and its comparison with the ones of either standard compounds or spectral databases. Then, the success of dereplication is directly dependant on the completion of databases. It is noteworthy that dereplication is not synonym of identification, mainly because MS data do not give information about stereochemistry nor positional isomery. The dereplication process is not strictly needed for untargeted

metabolomic studies, but it completes the biochemical interpretation of the data. Many natural products spectral MS/MS databases from different biological sources are currently available. Nevertheless, LC-MS platforms have disadvantages specially by the means of its reproducibility and that there is an enormous heterogeneity in the LC-MS workflows, parameter settings and data formats (186,223,224).

Targeted metabolomics is restricted to the analysis of pre-defined metabolites from specific pathways or from the same family. The success of the targeted metabolomics approach lies in the prior knowledge of the spectral characteristics of the molecules expected to be found. The use of standard compounds allows reliable identification by comparison. When standards are not available, spectral information provided by other studies under similar conditions helped the identification. In this case, however, with a lower level of confidence. While untargeted metabolomics is a hypothesis-generator approach, targeted metabolomics is a hypothesis-driven approach (224). In this case, the hypothesis is the positive effect of MeJA and CORO elicitation on the production of centellosides and CQAs through their production monitoring in a targeted metabolomics time-course experimental design.

In another way, UHPLC-MS/MS-based untargeted metabolomics becomes essential to further explore the effects of MeJA and CORO on the global specialised metabolism of HR of *C. asiatica* to pinpoint the main metabolites and pathways, other than centellosides, which can be influenced by such elicitations. In this work, it has been remarked the crucial role of the study of the metabolism for future fine-tunning of metabolic engineering studies. A few studies have

explored the dynamics of specialised metabolism changes caused by MeJA elicitation in *C. asiatica* tissue cultures. It is suggested that it involves alterations in some pathways, with an increase in triterpenoids, centellosides and CQAs levels (102,103,160). However, the MeJA signalling pathway is connected to others, thus constituting a complex regulatory network (102). The genes up-regulated by MeJA include those involved in jasmonate biosynthesis. Consequently, specialised metabolism and other stress-like physiological manifestations can also be activated. Recently, it has been observed that elicitation with CORO triggers a considerable higher production of triterpenoids than MeJA in *C. asiatica* cell suspension cultures (138). Moreover, one study have demonstrated the positive effect of 100 µM of MeJA and 1 µM of CORO on the production of centellosides and expression of genes involved in the centelloside pathway in the same line of HR used in this study (154). However, these previous studies have been centered on the 4 main molecules in the centellosides family which is much larger.

To fulfil these objectives, two different metabolomics studies have been performed on the HR samples: a targeted one focused on centellosides and phenolics, and an untargeted one for broader insgihts on the global metabolome changes. Furthermore, a Molecular Networking (MN) approach using High Resolution MS has been done to give an overview of the pathways, chemical classes involved in the response to elicitors, together with the investigation of centellosides analogs. Before these analyses, a development of an UHPLC-MS/MS method has been necessary to ensure an optimal detection of centellosides and other *C. asiatica* typical compounds.

4.2.1. Development of UHPLC-MS/MS detection of centellosides and phenolic acids characteristic of *C. asiatica*

4.2.1.1. MS detection optimisation of standards compounds: full MS and MS/MS fragmentation spectra.

This investigation involved the mass spectral analysis of the standard compounds supposed to be found in the *C. asiatica* HR samples. With the aim to both optimise their ionisation in the ESI source of the mass spectrometer and to verify the obtention of good quality MS/MS spectra for determining their fragmentation pattern and to obtain an *in-house* database. This study made the subsequent identification of ions from the samples straightforward. Commercial standard compounds were kindly delivered by Dr. Palazon from the Faculty of Pharmacy of the University of Barcelona. Table 10 lists the compounds and their monoisotopic mass. ESI mass spectrometry conditions were set using the automatic tune procedure of the instrument. The Multi-stage Mass Spectrometry (MS^n) analysis of full scan mass spectra in both ESI modes either in the isolated standards or the mixture solutions confirmed the (i) nature of these substances and (ii) the possibility of observing them in the following analysis of the *C. asiatica* HRs samples.

Table 10. List of available standard compound and their monoisotopic mass

	Compounds	Monoisotopic mass (g/mol)
1	Gallic acid	170.0215
2	Chlorogenic acid	354.0951
3	Caffeic acid	180.0422
4	Coumaric acid	164.0473
5	Ferulic acid	194.0579
6	Quercentin	302.0426
7	Madecassoside	974.5086
8	Asiaticoside	958.5137
9	Kaempferol	286.0477
10	Madecassic acid	504.3451
11	Asiatic acid	488.3501

4.2.1.1.1. Aglycones (AA and MA)

Full scan mass spectral in the (-)ESI mode analyses for AA and MA showed the deprotonated ions $[M-H]^-$ at *m/z* 487 for AA and *m/z* 503 for MA (Figure 27), both accompanied by their formic acid adduct and a $[2M-H]^-$ cluster. The full scan (+)ESI mode displayed prominent sodium adducts of the nature $[M+Na]^+$ in both parent standards at *m/z* 511 for AA and *m/z* 527 for MA (Figure 28). Here also other ionic adducts were observed such as the $[2M+Na]^+$ cluster. The protonated molecule could not be observed even if the mobile phase was acidified.

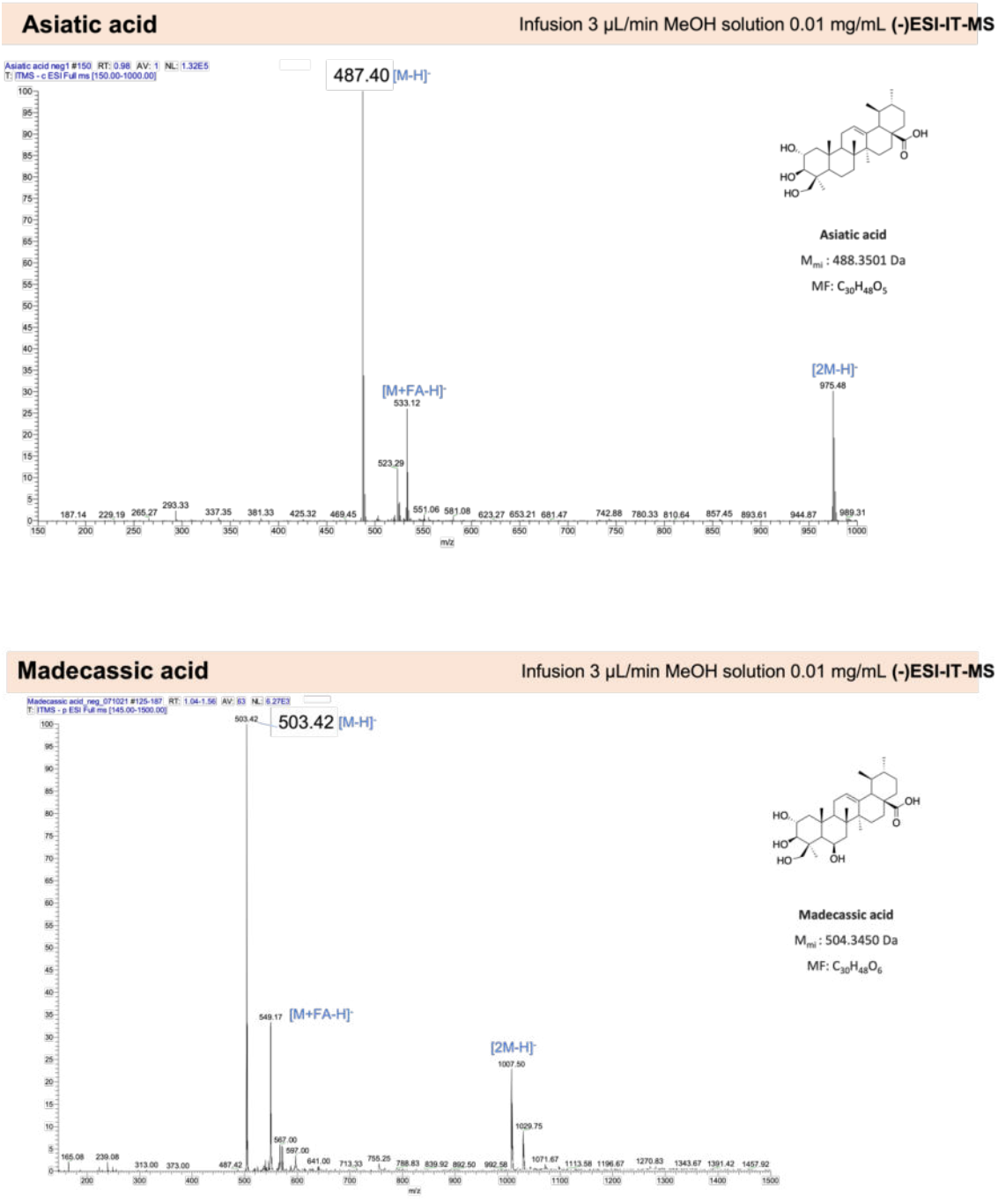

Figure 27. Full MS spectra in (-)ESI of AA (above) and MA (below)

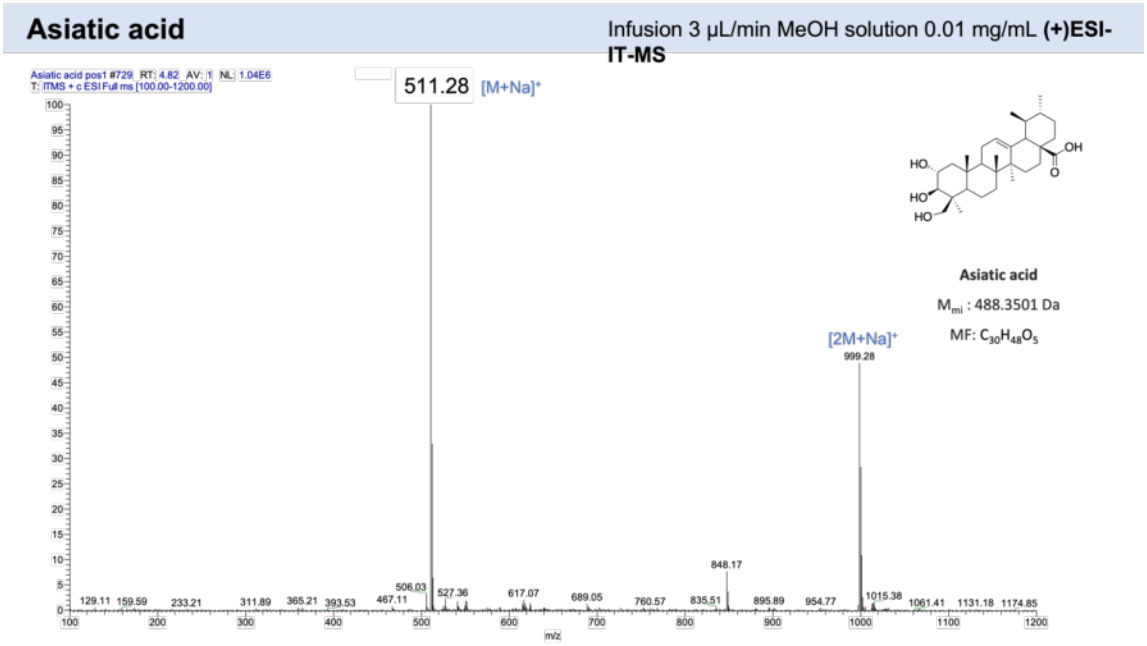

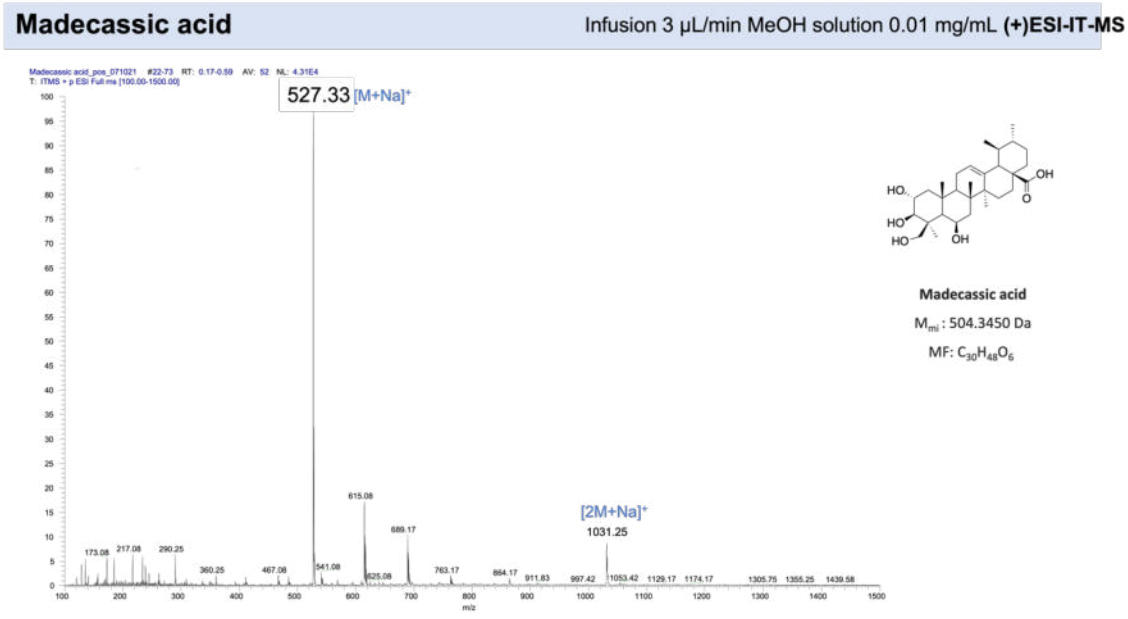

Figure 28. Full MS spectra in (+)ESI of AA (above) and MA (below)

Both aglycones were dissolved together in a single solution to observe their response in the mass spectrometer as part of a mixture. The infusion of the mix solution containing both standards at 10 µg/mL, resulted in the same ions as those obtained when compounds were analysed separately in both ESI modes (Figure 29). However, in fullscan mass spectra, MA gave the most abundant ions in both ESI modes.

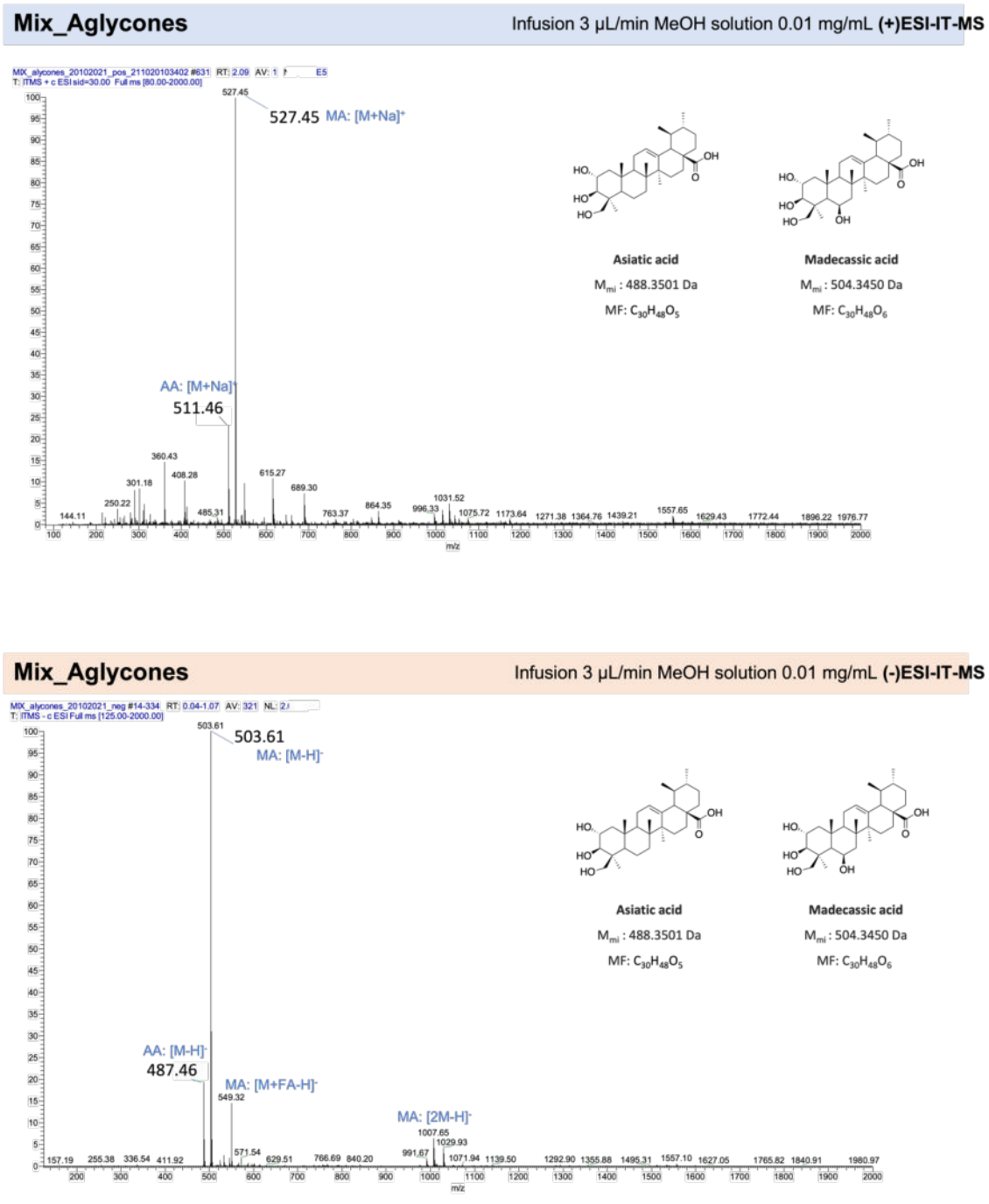

Figure 29. Full MS spectra of the mix solution of aglycones in (+)ESI (above) and (-)ESI (below)

MS/MS analyses of the molecular ions of both compounds in the (+)ESI (Figure 30) and in the (-)ESI mode (Figure 31), showed losses in accordance with those described by Xia *et al*. (2015) for the (-)ESI mode (225) and by Du *et al*. (2004) for (+)ESI-mode (226) and by Shen *et al*. (2009) for both ESI modes (227). It can be observed that the (+)ESI mode does not give informative spectra with only the loss of the acidic moiety, which was observed, contrary to those obtained in the (-)ESI mode. In this way, dereplication of these aglycones would be facilitated in these last analytical conditions.

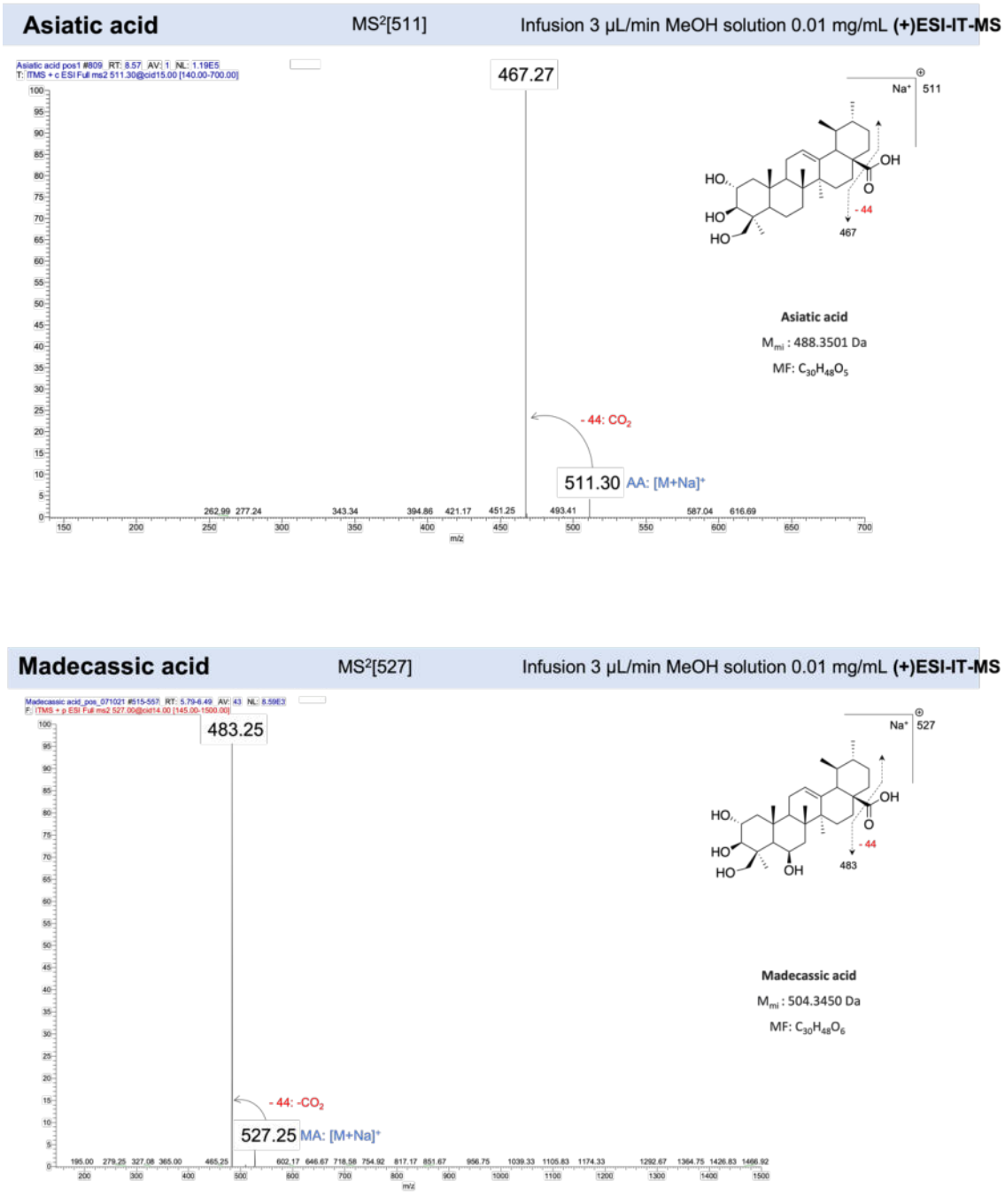

Figure 30. MS/MS spectra in (+)ESI of the fragment ion at *m/z* 511 for AA (above) and *m/z* 527 for MA (below)

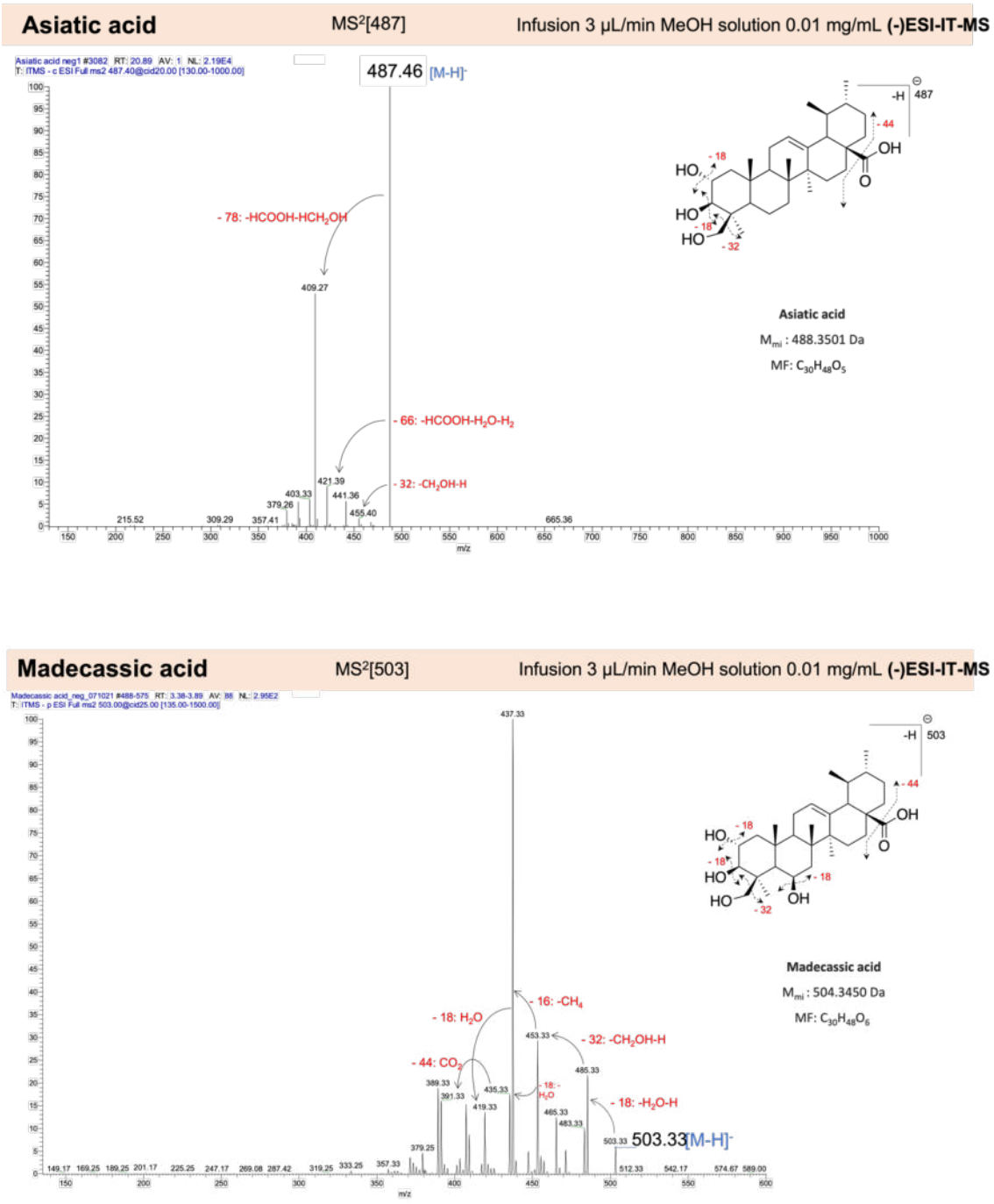

Figure 31. MS/MS spectra in (-)ESI of the molecular ion at *m/z* 487 for AA (above) and *m/z* 503 for MA (below)

Surprisingly, while the MS^n analysis was difficult with the individual compound solutions, in the mix solution it was possible to obtain in some cases MS^n spectra of the most prominent molecular ions and fragments. For example, in the case of MS^4 analysis of the deprotonated molecular ion $[M–H]^-$ of AA [487→409→379] (Figure 32). These results were also in accordance with those described by Xia *et al*. (2015) and by Du *et al*. (2004).

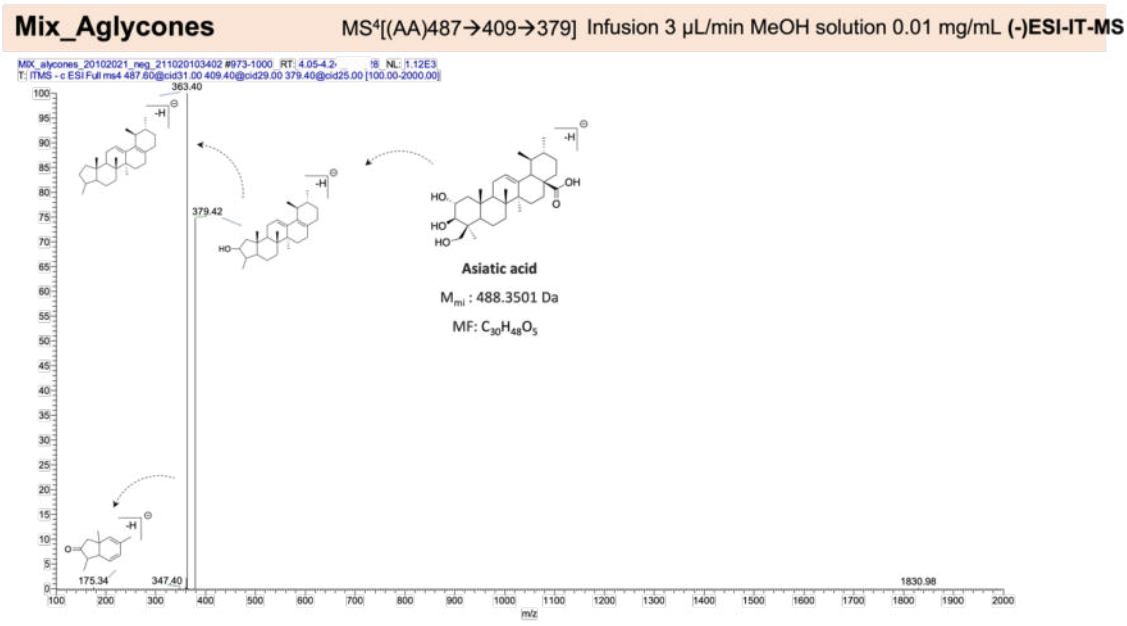

Figure 32. MS^4 spectrum in (-)ESI of the fragment ion at *m/z* 487→409→379 of the mix solution of aglycones

4.2.1.1.2. Saponins (AD and MD)

The mass spectra in full scan in the (-)ESI mode analyses for AD and MD showed as main peak the deprotonated molecular ions $[M-H]^-$ at *m/z* 957 for AD and *m/z* 973 for MD (Figure 33). The spectra also showed peaks corresponding

the two parts of the saponins in both compounds: in the analysis of AD, ions at *m/z* 487 and *m/z* 469 might corresponded to the [aglycone-H]$^-$ and the [trisaccharide unit-H]$^-$ respectively; regarding MD, the ions at *m/z* 506 and *m/z* 469 might correspond to the [aglycone+2H]$^-$ and the [trisaccharide unit-H]$^-$ respectively. This repeated observation indicates that the ion at *m/z* 469 could correspond to [trisaccharide unit-H]$^-$ in both cases. These observations are the reflect of the lability of the osidic bond during the ionisation process in the ESI probe. The infusion of the mix solution containing both standards at 10 µg/mL resulted in the same molecular ions in the (-)ESI mode as those obtained when infused isolated (Figure 34). However, in this case, [AD–H]$^-$ was the most abundant ion.

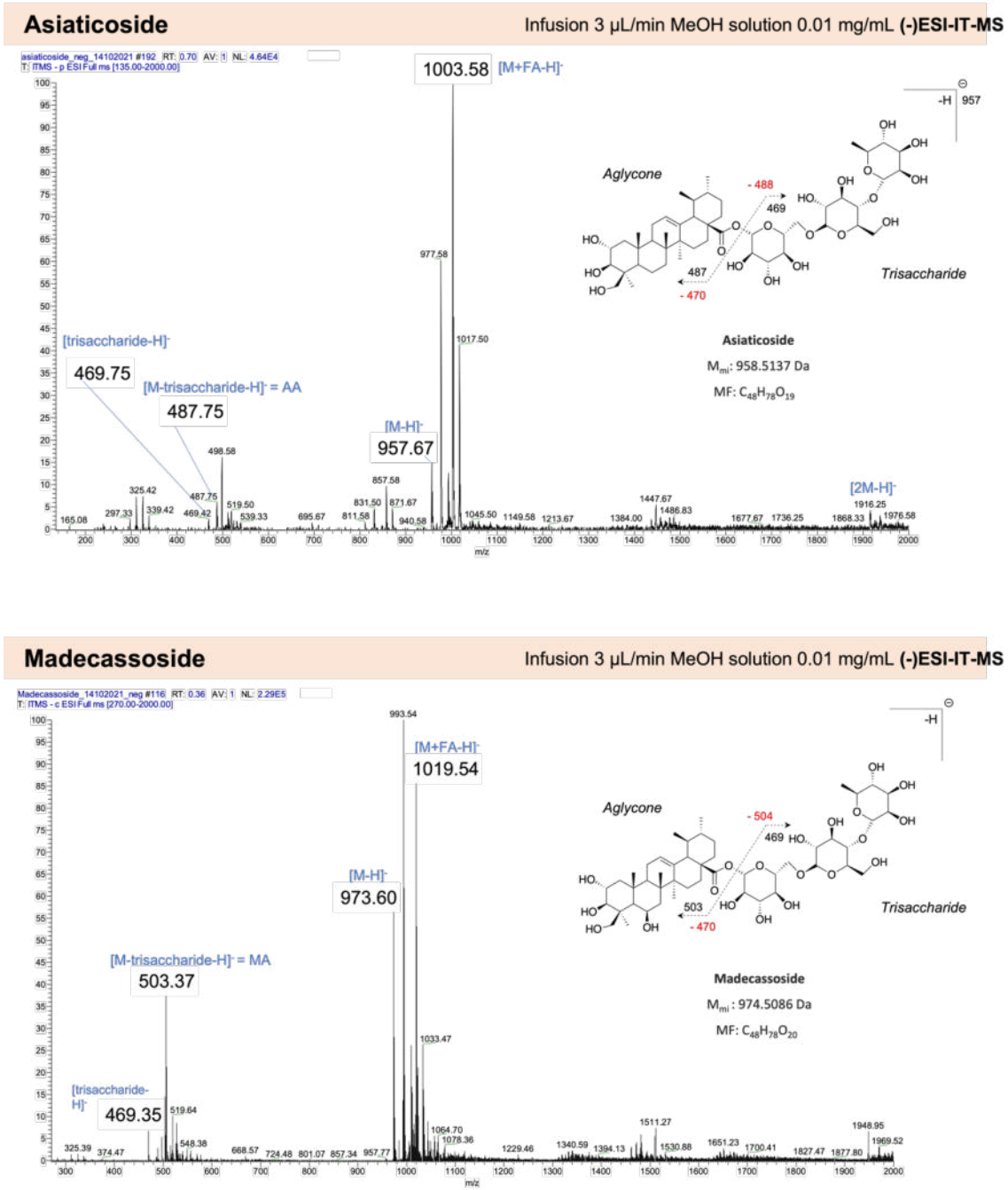

Figure 33. MS spectra in (-)ESI of AD (above), MD (below)

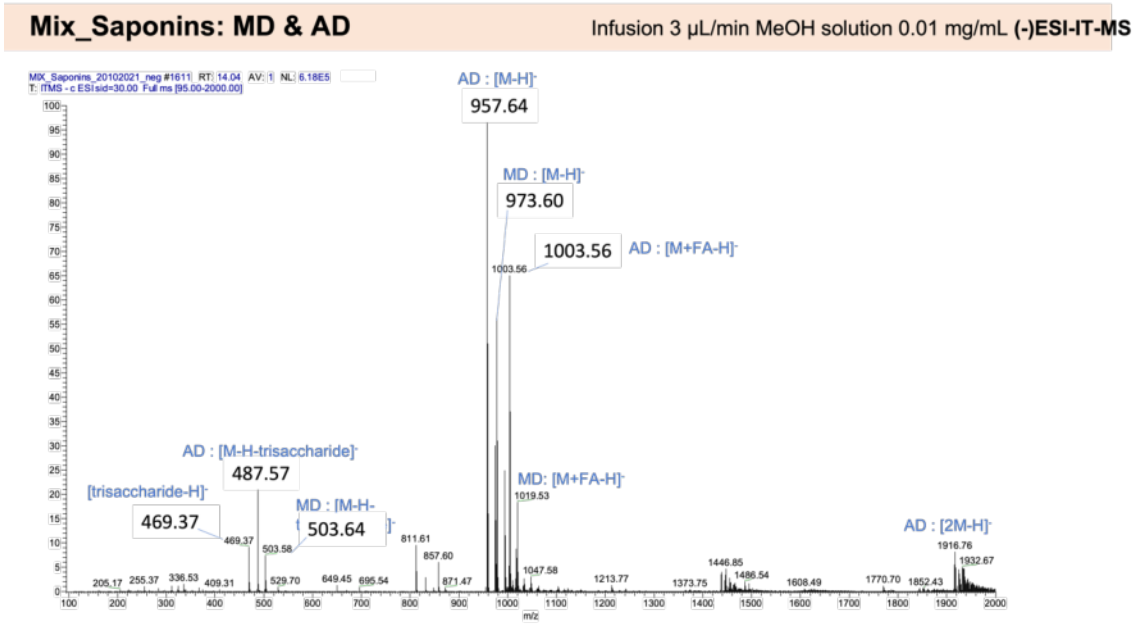

Figure 34. MS spectra in (-)ESI of mix solution of saponins

MS/MS analysis in the (-)ESI mode of the molecular ions $[M-H]^-$ in both AD (at *m/z* 957) and MD (at *m/z* 973) revealed: (1) the same base peak at *m/z* 469 and (2) the products ions at *m/z* 487 for AD and *m/z* 503 for MD putatively corresponding to the deprotonated aglycone moiety (Figure 35). The ion at *m/z 469* could be interpreted as $[\text{trisaccharide unit-H}]^-$ (as described in the interpretation of the (-)ESI mode full scan). Du *et al*. (2004) described this ion as $[\text{trisaccharide unit-H}]^-$ while Shen *et al*. (2009) as the respective ionised aglycone with some losses (227). The product ions from MS^3 analysis of MD at *m/z* 973→469 seemed to belong to the fragmentation of the trisaccharide unit into a monosaccharide (Figure 36). Unfortunately, the MS^3 analysis of the ion at *m/z* 469 could be only obtained for MD analysis since for AD analysis the abundance of this ion was too low. On the other hand, the putative aglycone ion for each

compound was submitted to MS/MS fragmentation: at *m/z* 487 for AD and *m/z* 503 for MD (Figure 37). The spectra revealed a similar fragmentation pattern that observed in the MS/MS analysis of the aglycones when infused directly. Therefore, the fragment ion at *m/z* 469 could be putatively assigned as the [trisaccharide-H]- for both compounds and the ions at *m/z* 487 and *m/z* 503 as the deprotonated aglycone moiety for AD and MD respectively.

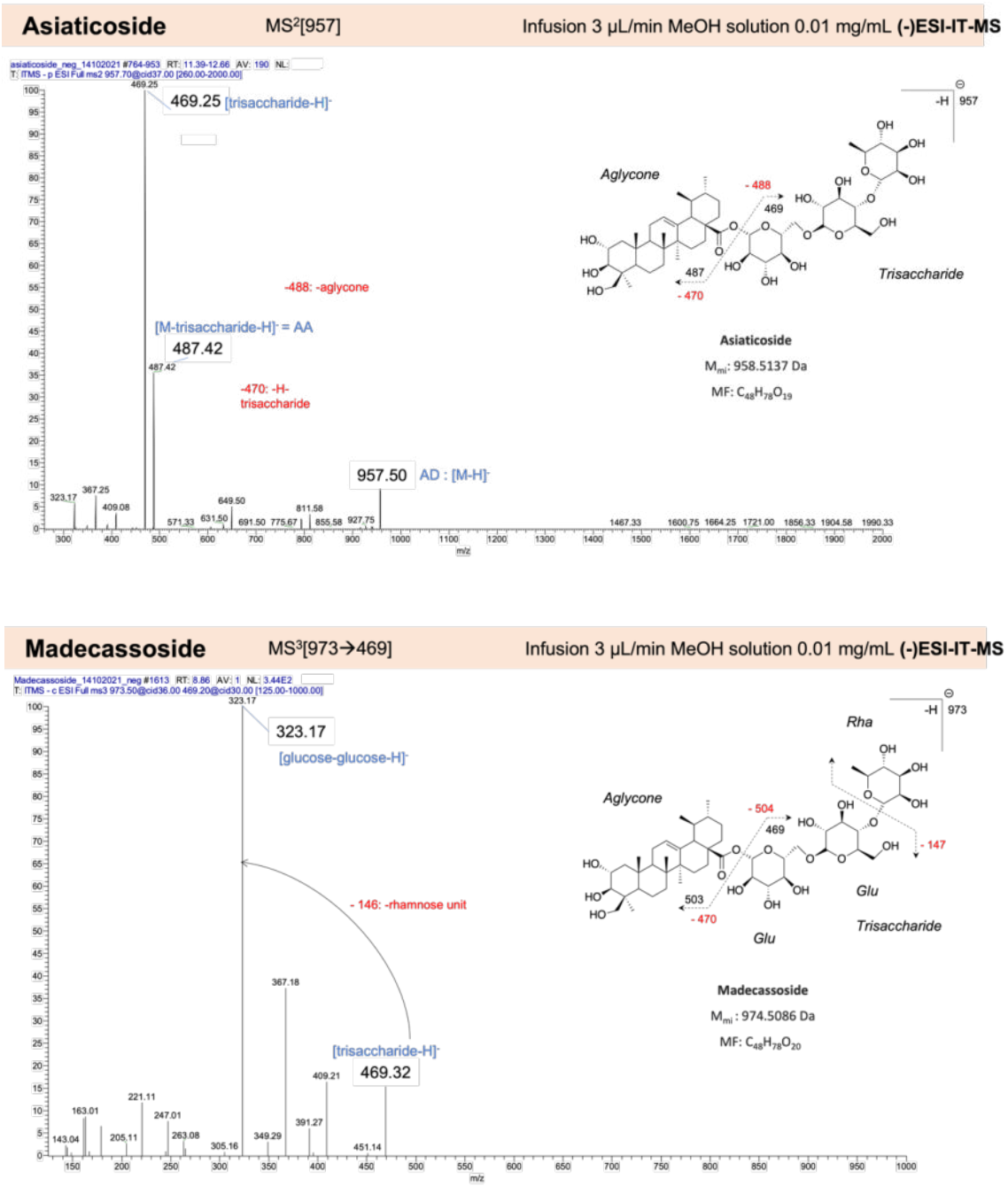

Figure 35. MS/MS spectra in (-)ESI of the molecular ion at *m/z* 957 *m/z* for AD (above) and *m/z* 973 *m/z* for MD (below)

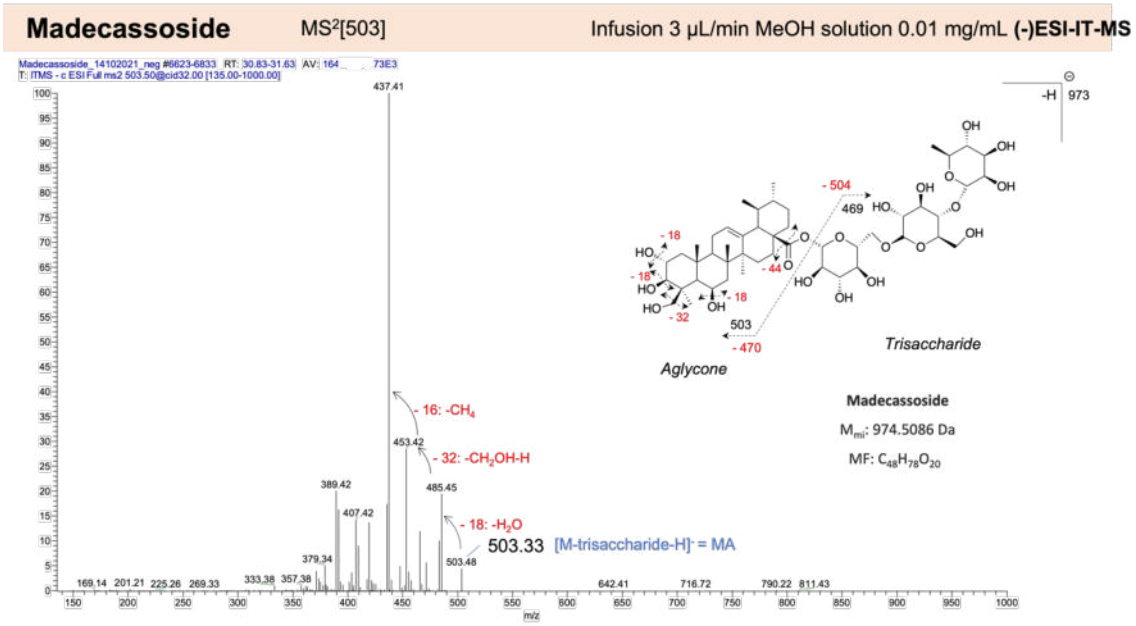

Figure 36. MS^3 spectrum in (-)ESI of the fragment ion at m/z 973→469 for MD.

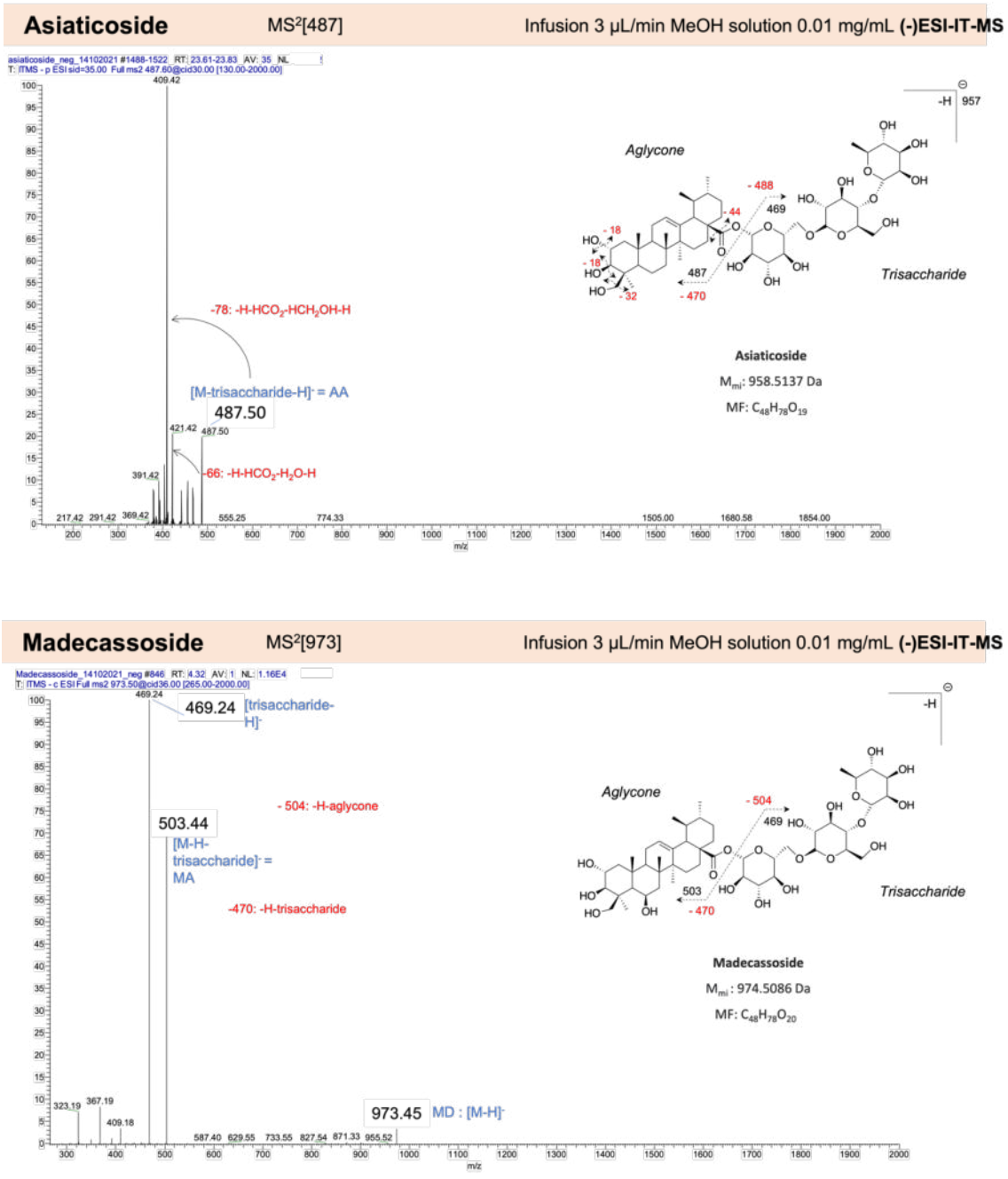

Figure 37. MS/MS spectra in (-)ESI of the fragment ion at *m/z* 487 for AD (above) and *m/z* 503 for MD (below)

The MS-full scan analysis in (+)ESI mode displayed prominent sodium cationised molecular ions of the nature $[M+Na]^+$ in both parent standards: at *m/z* 981 for AD and *m/z* 997 for MD (Figure 38). This observation was in accordance with Shen *et al*. (2009) and Du *et al*. (2004). The infusion of the mix solution containing both standards at 10 µg/mL resulted in the same molecular ions as those obtained when infused isolated (Figure 39). However, AD gave the most abundant ion.

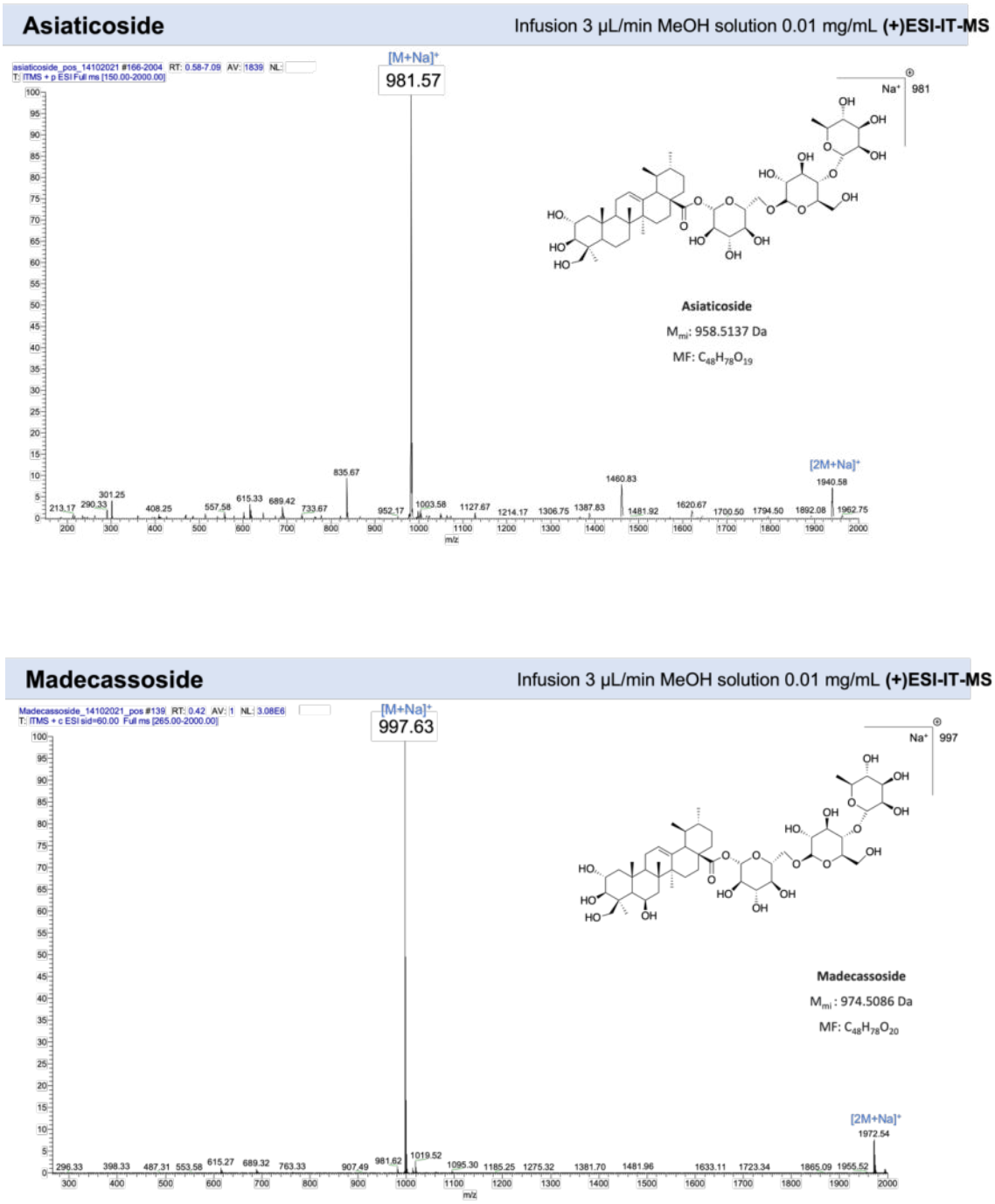

Figure 38. MS spectra in (+)ESI of AD (above), MD (below)

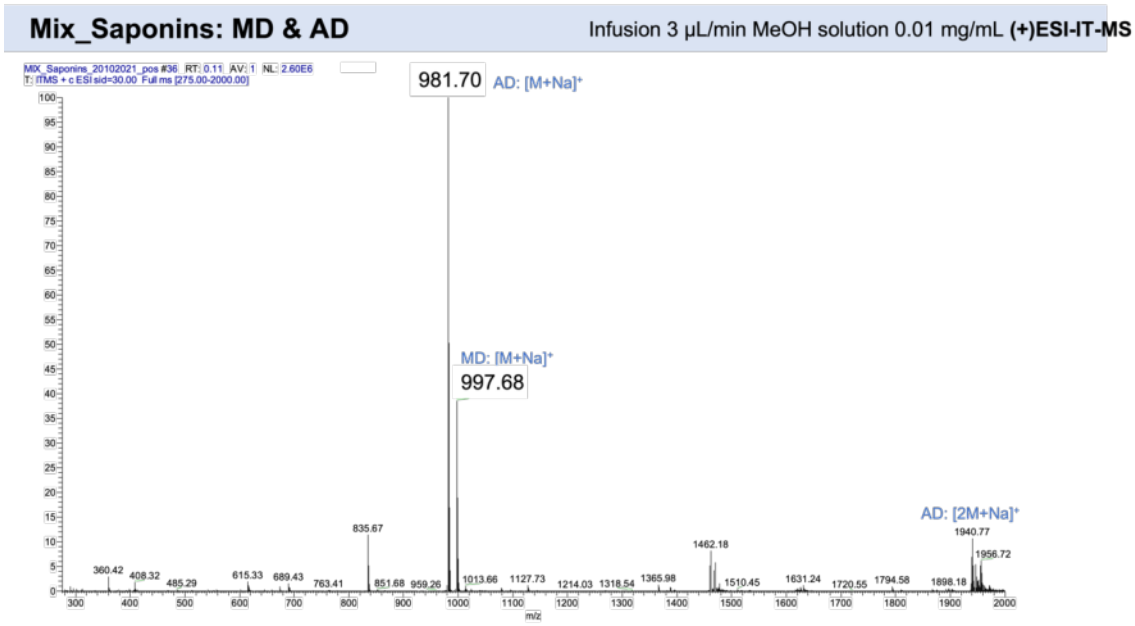

Figure 39. MS spectra in (+)ESI of (mix solution of saponins)

MS/MS analysis of the molecular ions in the positive mode in both AD and MD analysis (Figure 40) revealed the same base peak at *m/z* 493. This ion could be interpreted [trisaccharide unit+Na]$^+$ for both AD and MD. Du *et al*. (2004) described this ion as [trisaccharide unit+Na]$^+$(226). However, Shen *et al*. (2009) described this observation as the respective ionised aglycone. It was also possible to observe as minor peaks the corresponding [aglycone+Na]+ for AD (at *m/z* 511) and for MD (at *m/z* 527).

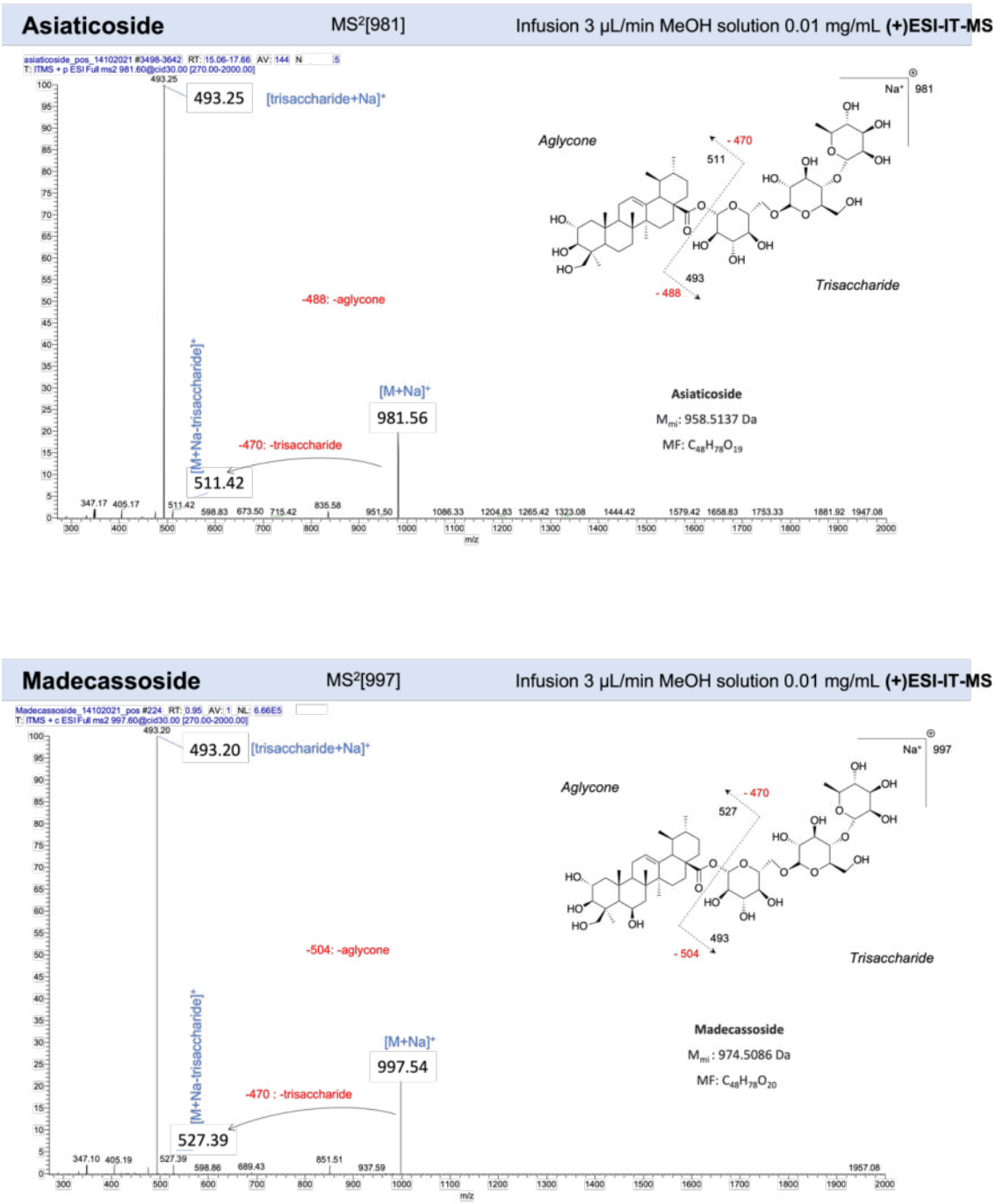

Figure 40. MS/MS spectra in (+)ESI of the fragment ion at *m/z* 981 m/z for AD (above) and *m/z* 997 for MD (below)

The subsequent MS^3 analysis on the ion at *m/z* 493 for both AD and MD revealed close similarities in the spectra (Figure 41). Moreover, next MS^n of the base peak ion in both standards starting from the ion at *m/z* 493 revealed also high similarities in the spectra. The fragmentation pattern did not match with that obtained from the infusion of the aglycones (see point 1 above). Then, the interpretation of the possible losses in these mass spectra suggested that the fragmentation of the ion at *m/z* 493 corresponded to the sugar moiety of the saponins.

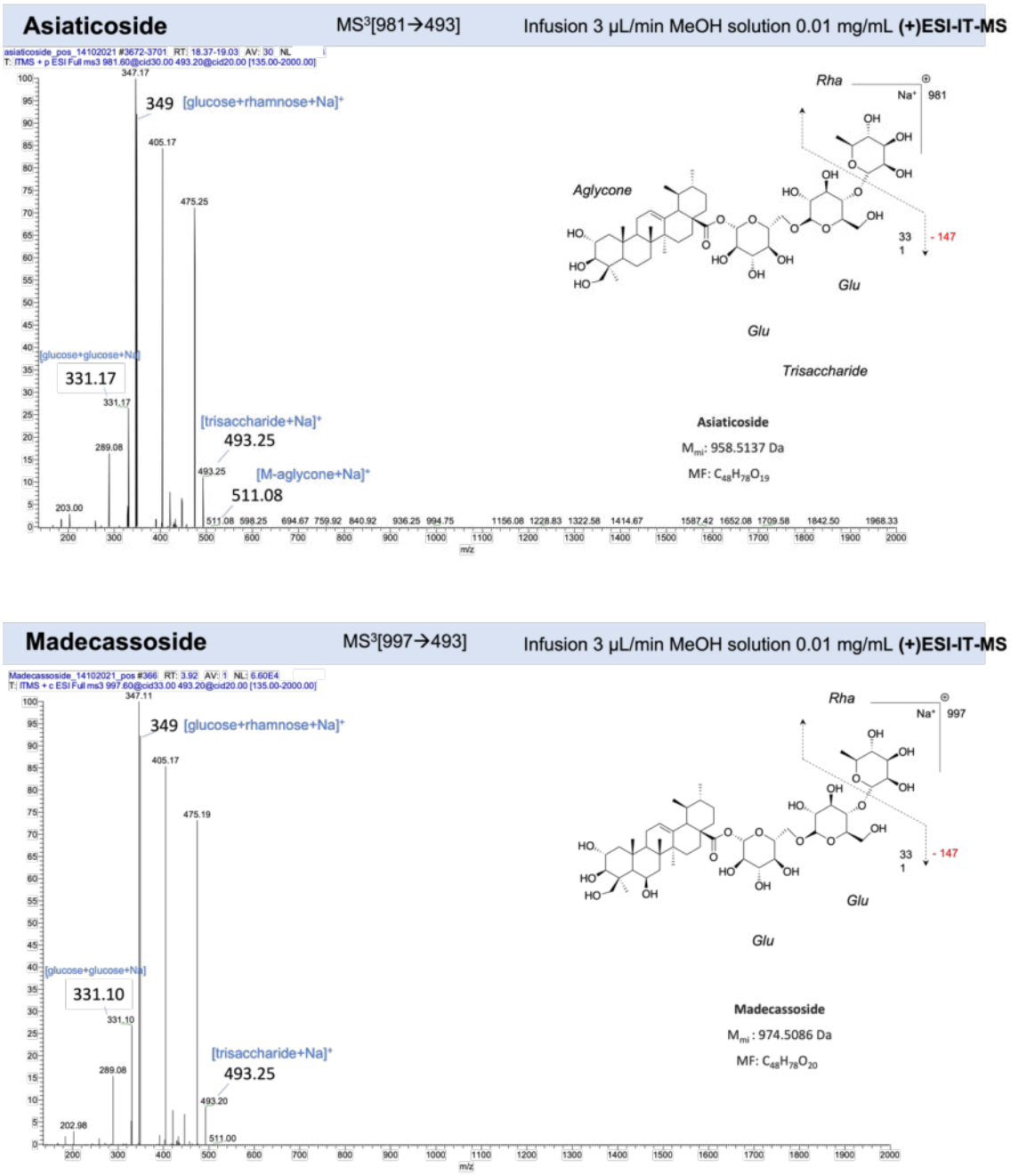

Figure 41. MS3 spectra in (+)ESI of the fragment ion at m/z 981→493 for AD (above) and m/z 997→493 for MD (below)

4.2.1.1.3. Phenolic acids

The mix solution containing phenols-like compounds was prepared mixing chlorogenic acid, ferulic acid, gallic acid, coumaric acid, cinnamic acid and caffeic acid at 10 µg/mL. In the fullscan spectrum of the (+)ESI mode (Figure 42) it was not possible to observe all the six sodium-ionised parent ions $[M+Na]^+$nor their protonated molecule, which is consistent with their carboxylic acid nature. The base peak at *m/z* 377 could correspond to the sodium adduct of chlorogenic acid. Low signals at *m/z* 217 and *m/z* 203 could correspond to the $[M+Na]^+$ ions for ferulic acid and caffeic acid respectively. For the rest of compounds, it was not possible to assign their parent ions (gallic acid, coumaric acid and cinnamic acid).

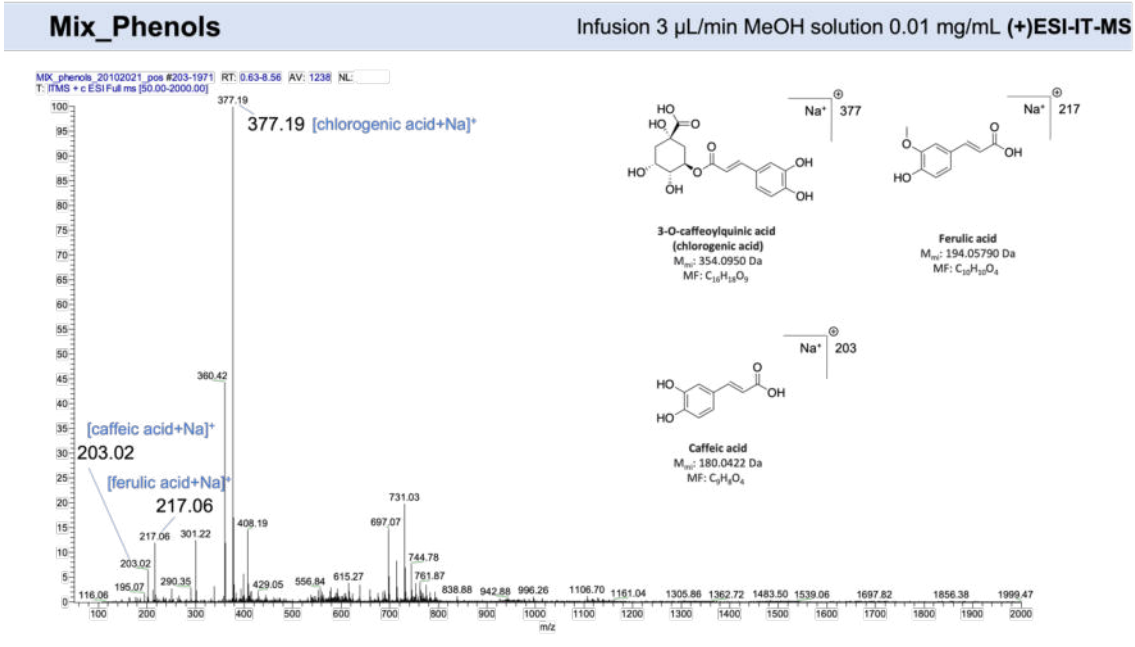

Figure 42. MS spectrum in (+)ESI of the mix solution of phenols

On the other hand, all the putative $[M-H]^-$ parent ions seemed to appear in the fullscan spectrum obtained in the (-)ESI mode (Figure 43). According to the literature the assignment of the signals was the following: at *m/z* 353 for chlorogenic acid (228,229), *m/z* 193 for ferulic acid (229), *m/z* 179 for caffeic acid (229,230), *m/z* 169 for gallic acid (228,231), *m/z* 163 for coumaric acid (228,230,232) and *m/z* 147 for cinnamic acid (231).

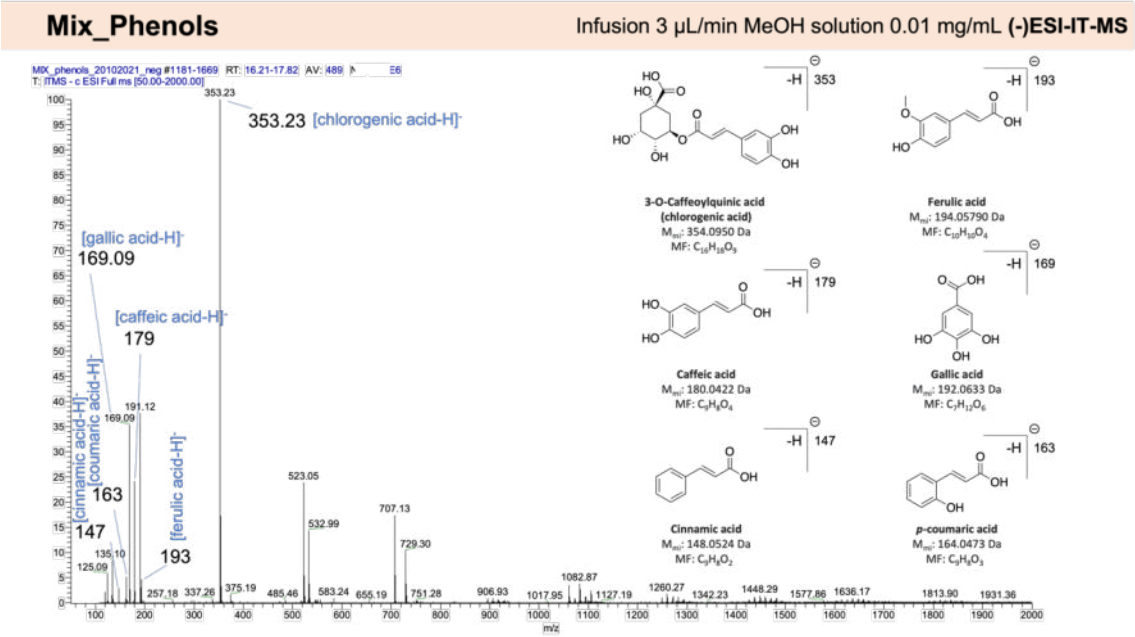

Figure 43. MS spectrum in (-)ESI of the mix solution of phenols

In both modes, it was only possible to perform MS/MS fragmentation on the parent ion corresponding to chlorogenic acid. This analysis showed the possible fragmentation into two clear ions might corresponding to either the ionised caffeic acid moiety or the ionised quinic acid moiety.

4.2.1.1.4. Flavonoids

The MS behaviour of kaempferol and quercetin was analysed by the infusion of a solution containing both compounds at 10 µg/mL.

Spectral analysis of the fullscan (+)ESI mode (Figure 44) displayed mainly some background noise, indicating their poor ionisation under this condition. However, it was possible to observe the sodium adduct at *m/z* 325 and *m/z* 309 corresponding to quercetin and kaempferol respectively as described in the literature (232–234).

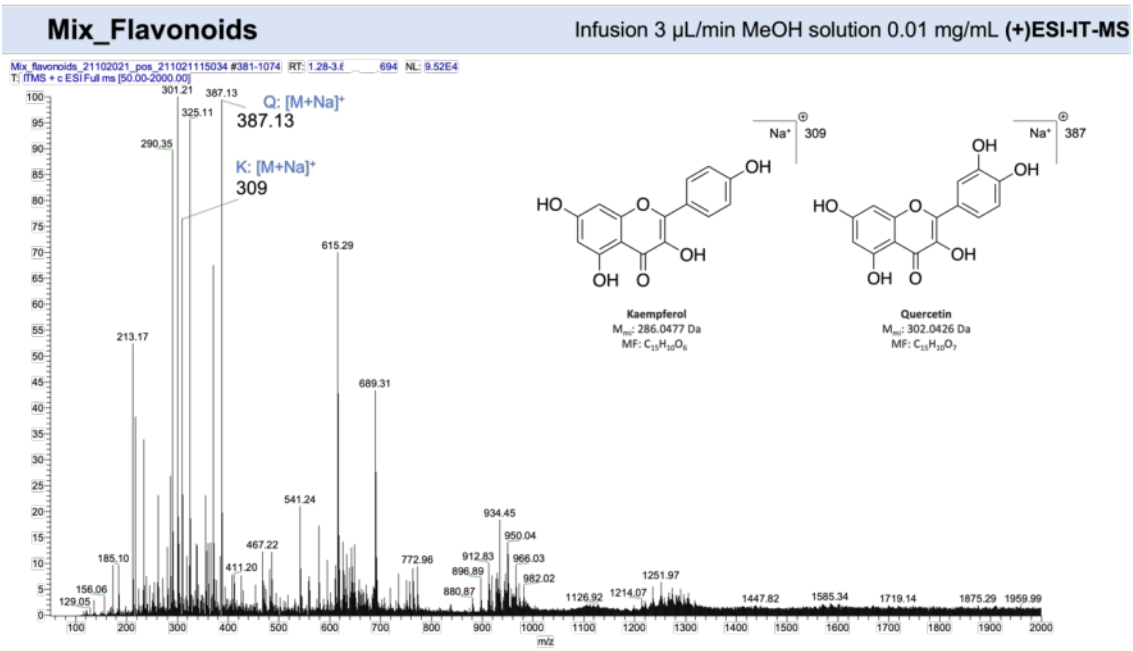

Figure 44. MS spectrum in (+)ESI of the mix solution of flavonoids. K: kaempferol, Q: quercetin.

In the (-)ESI mode (Figure 45), the fullscan spectrum was cleaner than in the positive mode, which was consistent with their weak acidic character. The two

most abundant peaks clearly seemed to correspond to the deprotonated ions of the parent compounds: at *m/z* 301 for quercetin and *m/z* 285 for kaempferol. The assignment was concordant with the literature (228,232,235).

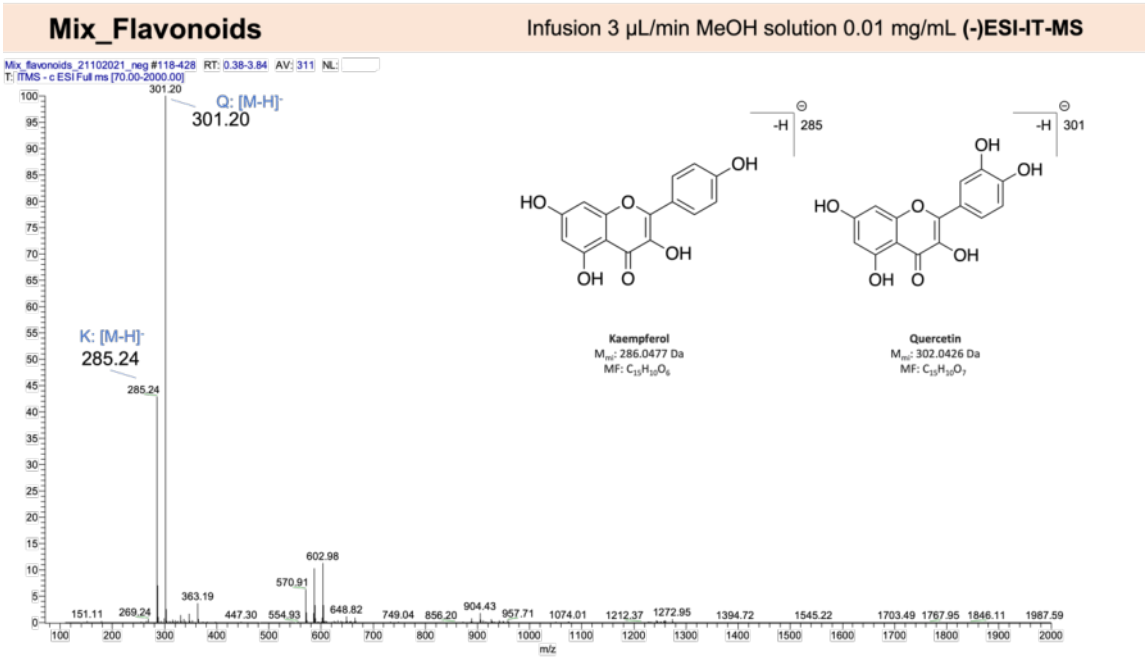

Figure 45. MS spectrum in (-)ESI of the mix solution of flavonoids. K: kaempferol, Q: quercetin.

4.2.1.2. Optimization of the UHPLC-MS/MS method for the simultaneous analysis of standard compounds

The separation of polar compounds in methanolic extracts of cell cultures of *C. asiatica* thorugh UHPLC-MS/MS was described by Ncube *et al*. (2017). However, the method is not adapted to methanolic extracts of HR of *C. asiatica*. Therefore, with aim to separate all the compounds and to detect them correctly in

the complex matrices of *C. asiatica* HR, the analyticial method was optimised. The initial parameters for the UHPLC-MS/MS analysis were set as described in Ncube *et al*. (2017). The chromatogram obtained (Figure 46) showed a poor separation between the standard compounds with most of them being co-eluted. Then an optimization of the UHPLC-MS/MS method for achieving a better separation was mandatory for the future metabolomics studies. The UHPLC-MS/MS optimised method (final optimised parameters are described in section 3.3.4) was established using a mix of all the available standards compounds available, following an injection of each individual compound (Table 10). The resulting chromatogram using the pool of standard compounds showed an enhanced resolution of the peaks with an – if not ideal – acceptable separation (Figure 47). Standards were identified according to their *m/z* ratio and their Rt compared when standards were previously injected isolated. Figure 48 shows the base peak extracted ion chromatogram (XIC) of each standard. The ESI source produced mostly molecular ion species in the form of single or multiple adducts such as $[M-H]^-$ or $[M+Formic\ acid-H]^-$ ($[M+FA-H]^-$) (since formic acid was used as proton donor in the mobile phase in order to enhance the ionisation of basic compounds in the (+)ESI mode, and to enhance the shape of the chromatographic peaks) for the negative mode, and $[M+H]^+$ or $[M+Na]^+$ for the positive mode. Dimerization of ions also occurred as observed in direct infusion. At this point, it was considered to seek the adducts that were preferably formed (i.e. reproducibilty and signal intensity) for each standard compounds in order to determine which would be considered for quantitative analysis in the targeted metabolomics studies. Table 11 shows the analysis of the *m/z* base peaks for

their identification in ESI (-) mode and Table 12 for the ESI (+) mode. The intensity was overall superior in the negative mode compared to the positive for all compounds. Therefore, the following UHPLC-MS/MS sample analyses were performed entirely in the ESI (-) mode. There was a prevalence of the $[M+FA-H]^-$ adduct species, especially for centellosides. However, these adducts species often makes the interpretation of the MS/MS spectra more difficult. The collision energy in the mass spectrometer removes the formic acid from the ion but does not further fragment the remaining deprotonated molecular ion $[M-H]^-$ in most cases. To illustrate, Figure B.10 shows the MS/MS spectrum of the parent ion at *m/z* 1019 which corresponds to the $[M+FA-H]^-$ molecular ion of madecassoside. The spectrum only showed the deprotonated ion of madecassoside with no further fragmentation.

The optimised method was then tested using a sample corresponding to the addition of CORO after 12 days of elicitation (Figure 49). The chromatogram showed a separation between saponins and their aglycones. Therefore, the optimization was concluded. Final analysis including all the samples described in the experimental design is described in the following sections.

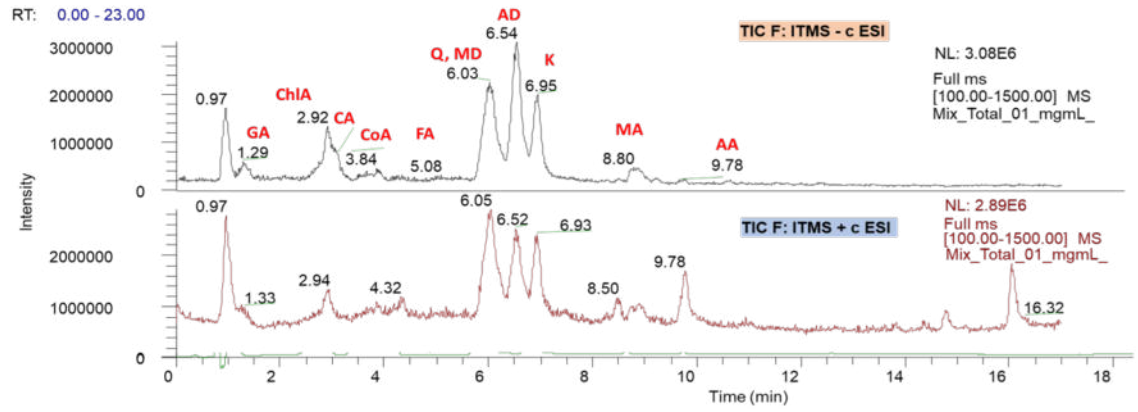

Fig 46. Chromatograms full scan (TIC) UHPLC-MS of the standard mix in both ESI modes. GA = Gallic Acid; ChlA = Chlorogenic Acid; CA = Caffeic Acid; CoA = Coumaric Acid; FA = Ferulic Acid; Q = Quercetin; MD = MadecassosiDe; AD = AsiaticosiDe; K = Kaempferol; MA = Madecassic Acid; AA = Asiatic Acid. Parameters set following the methods described in Ncube *et al*. (2017). (TIC = Total Ion Chromatogram)

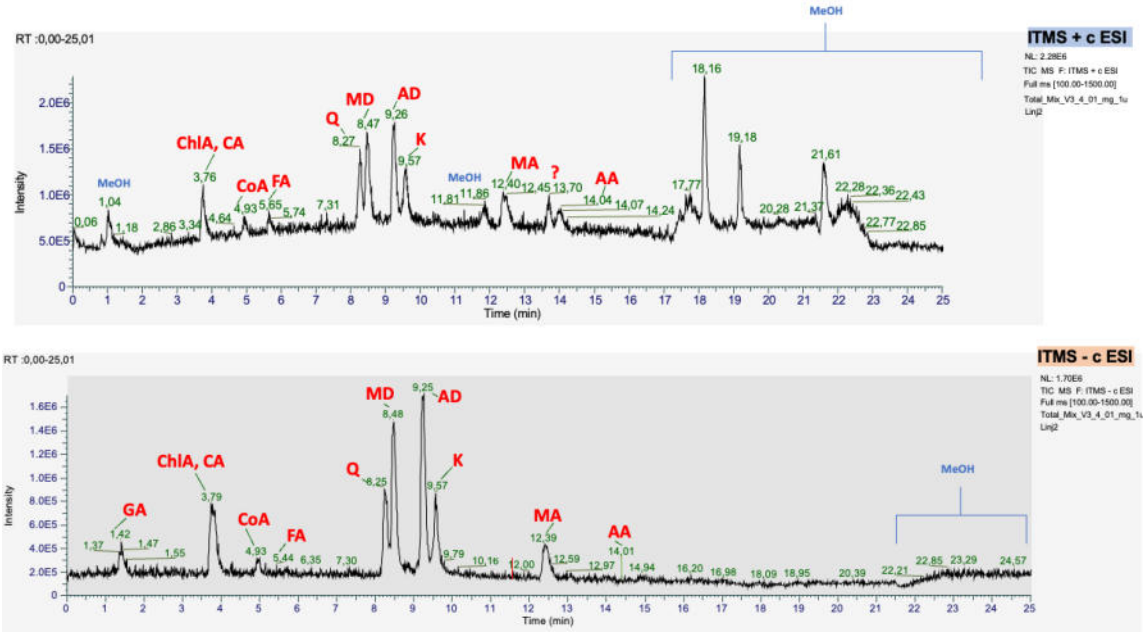

Fig 47. Chromatograms full scan (TIC) UHPLC-MS of the standard mix in both ESI modes after the optimization (described in section 4.3.2). GA = Gallic acid; ChlA = Chlorogenic acid; CA = Caffeic Acid; CoA = Coumaric acid; FA = Ferulic acid; Q = Quercetin; MD = Madecassoside; AD = Asiaticoside; K = Kaempferol; MA = Madecassic acid; AA = Asiatic acid. (TIC = Total Ion Chromatogram)

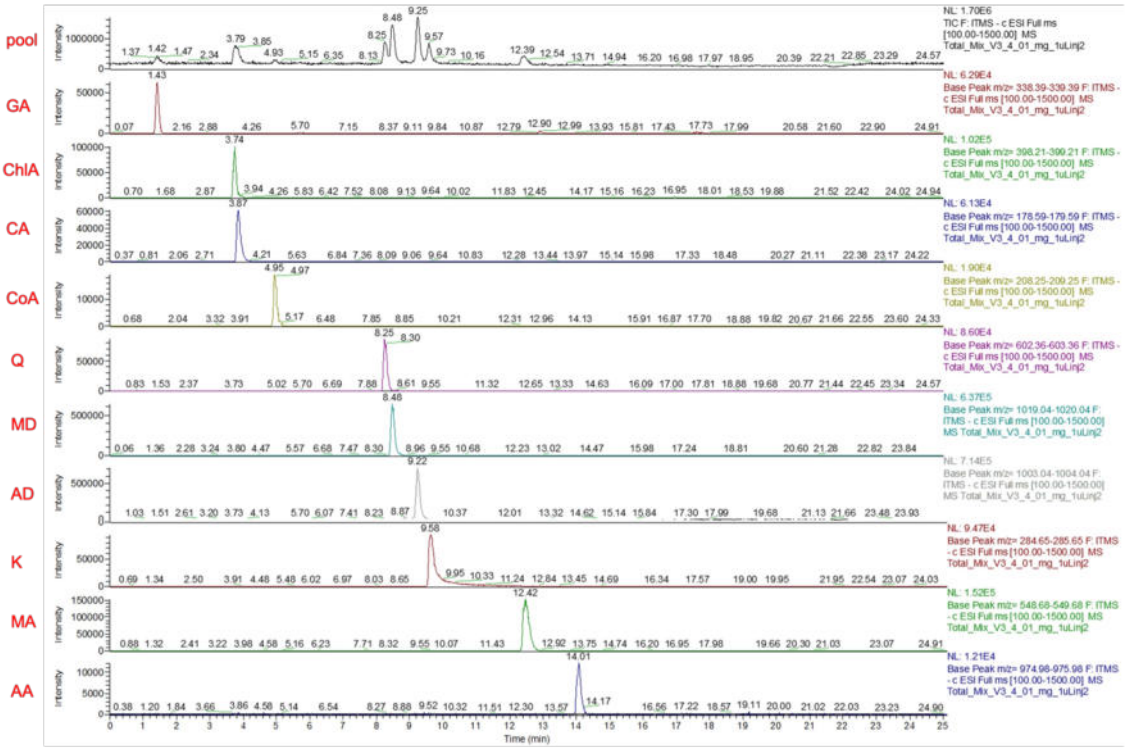

Fig 48. (a): chromatogram Full scan (TIC) of the pooled standard compounds in (-)ESI; (b): trace XIC (*m/z* 338.39-339.39) of gallic acid (GA); (c): trace XIC (*m/z* 398.21-399.21) of chlorogenic acid (ChlA); (d): trace XIC (*m/z* 178.59-179.59) of caffeic acid (CA); (e): trace XIC (*m/z* 208.25-209.05) of coumaric acid (CoA); (f): trace XIC (*m/z* 602.36-603.36) of quercetin (Q); (g): trace XIC (*m/z* 1019.04-1020.04) of MD; (h): trace XIC (*m/z* 1003.04-1004.04) of AD; (i): trace XIC (*m/z* 284.65-285.65) of kaempferol (K); (j): trace XIC (*m/z* 548.68-549.68) of MA; (k): trace XIC (*m/z* 974.98-975.98) of AA. (TIC = Total Ion Chromatogram)

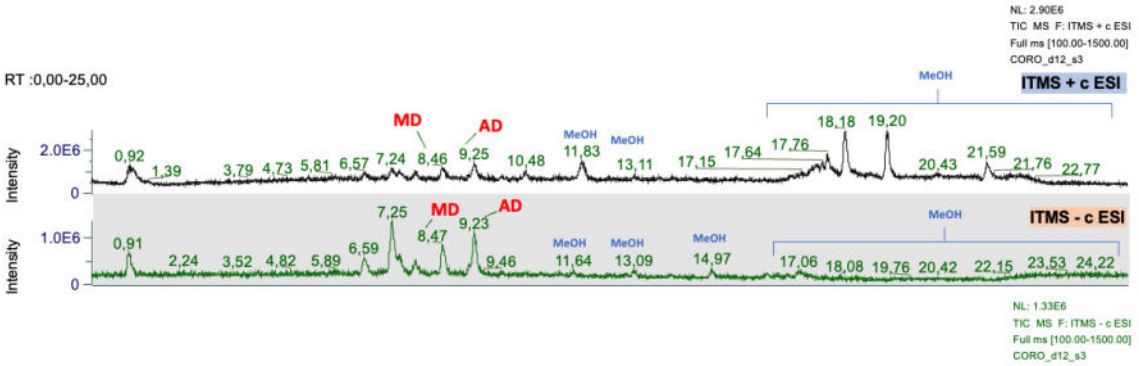

Fig 49. UHPLC-MS fullscan (TIC) mass chromatograms of the methanolic extract of the sample CORO harvested at day 12 (replicate 3). MD = MadecassosiDe; AD = AsiaticosiDe.

At the end of this study, all data obtained for the standard compounds were collected and assembled, which allowed to build a small database of *C. asiatica* characteristic compounds. This base would be of interest for their identification in complex mixtures during both targeted and untargeted analyses. Data are resumed in Table 11-12.

Table 11. UHPLC-MS analysis of pooled standards in (-)ESI

				Detected adduct								
				$[M-H]^-$			$[M+FA-H]^-$			$[2M-H]^-$		
Standard compound	**MF**	**M_{mi} (Da)**	**Rt (min)**	**theor. *m/z***	**obs. *m/z***	**s.i.**	**theor. *m/z***	**obs. *m/z***	**s.i.**	**theor. *m/z***	**obs. *m/z***	**s.i.**
gallic acid	$C_7H_6O_5$	170.0215	1.42	169.01	169.06	1.20E+05	215.02	214.78	7000	339.04	338.89	6.29E+04
chlorogenic acid	$C_{16}H_{18}O_9$	354.0951	3.74	353.09	353.19	3.00E+04	399.09	398.71	1.02E+05	707.18	707.09	2.00E+04
caffeic acid	$C_9H_8O_4$	180.0423	3.85	179.03	179.09	6.13E+04	225.04	224.71	2.10E+04	359.08	358.92	4.50E+04
coumaric acid	$C_9H_8O_3$	164.0473	4.93	163.04	163.08	5.00E+03	209.05	208.75	1.90E+04	327.09	326.74	1.50E+03
ferulic acid	$C_{10}H_{10}O_4$	194.0579	5.65	193.05	0	-	239.06	0	-	387.11	0	-
quercetin	$C_{15}H_{14}O_9$	302.0427	8.27	301.04	301.16	4.50E+04	347.04	346.53	4.00E+03	603.08	602.86	8.60E+04
MD	$C_{48}H_{78}O_{20}$	974.5086	8.47	973.50	0	-	1019.51	1019.54	6.37E+05	1948.01	1947.63	2.40E+03
AD	$C_{48}H_{78}O_{19}$	958.5137	9.25	957.51	0	-	1003.51	1003.54	7.14E+05	1916.02	1916.51	5.00E+03
kaempferol	$C_{21}H_{20}O_{11}$	286.0477	9.57	285.04	285.15	9.47E+04	331.05	330.53	3.00E+04	571.09	570.71	1.40E+03
MA	$C_{30}H_{48}O_6$	504.3451	12.39	503.34	503.56	1.00E+03	549.34	549.18	1.52E+05	1007.68	1007.49	2.00E+04
AA	$C_{30}H_{48}O_5$	488.3502	14.01	487.34	487.86	4.00E+02	533.35	533.22	3.50E+03	975.69	975.48	1.21E+04

MF: Molecular Formula; M_{mi}: Monoisotopic mass; Rt: Retention time; theor.: theorical; obs.; observed; s.i.: Signal intensity at 0.1 mg/mL

Table 12. UHPLC-MS analysis of pooled standards in (+)ESI

				Detected adduct								
				$[M+H]^+$			$[M+Na]^+$			$[2M + H]^+$		
Standard compound	**MF**	**M.m. (Da)**	**Rt (min)**	**theor. *m/z***	**obs. *m/z***	**s.i.**	**theor. *m/z***	**obs. *m/z***	**s.i.**	**theor. *m/z***	**obs. *m/z***	**s.i.**
gallic acid	$C_7H_6O_5$	170.0215	1.42	171.03	0	-	193.01	0	-	341.05	0	-
chlorogenic acid	$C_{16}H_{18}O_9$	354.0951	3.74	355.10	355.04	6.15E+04	377.08	377.15	9.00E+03	709.20	0	-
caffeic acid	$C_9H_8O_4$	180.0423	3.85	181.05	181.03	3.00E+03	203.03	0	-	361.09	361.68	2.50E+03
coumaric acid	$C_9H_8O_3$	164.0473	4.93	165.05	165.06	5.00E+03	187.04	0	-	0.00	0	7.00E+03
ferulic acid	$C_{10}H_{10}O_4$	194.0579	5.65	195.07	195.03	1.00E+04	217.05	0	-	389.12	0	-
quercetin	$C_{15}H_{14}O_9$	302.0427	8.27	303.05	303.08	3.23E+05	325.03	325.53	4.00E+03	320.08	0	-
MD	$C_{48}H_{78}O_{20}$	974.5086	8.47	975.52	974.88	1.30E+05	997.50	997.57	1.20E+04	992.54	992.32	1.70E+04
AD	$C_{48}H_{78}O_{19}$	958.5137	9.25	959.52	959.13	1.60E+05	981.50	981.58	9.72E+03	976.55	976.31	1.60E+04
kaempferol	$C_{21}H_{20}O_{11}$	286.0477	9.57	287.06	287.05	1.80E+05	309.04	0	-	304.08	0	-
MA	$C_{30}H_{48}O_6$	504.3451	12.39	505.35	504.91	5.79E+04	527.33	527.6	3.00E+03	1009.70	0	-
AA	$C_{36}H_{54}O_8$	488.3502	14.01	489.36	488.96	4.43E+04	511.34	0	3.50E+03	977.71	977.27	3.00E+03

MF: Molecular Formula; M.m.: Monoisotopic mass; Rt: Retention time; theor.: theorical; obs.; observed; s.i.: Signal intensity at 0,1 mg/mL

4.2.2. UHPLC-MS/MS targeted metabolomics study of HR extracts treated with MeJA and CORO over time

The objective of the targeted-metabolomics approach was to investigate the level of production variations induced by the elicitors compared to the control, for the compounds of interest. These were the one for which we had developed the optimisation of detection, but the first analyses of HR extracts shown some easily detectable peaks (major) for which we tentatively did the annotation. These compounds were then included in the targeted approach.

The targeting process was achieved using the targeted feature detection offered by MzMine 2.3. After compound identification, the extracted ion chromatograms of the identified compounds were obtained and employed to quantitatively compare the metabolite profile of the different treatments and days of harvestings. Although both positive and negative ESI modes of ionisation were performed, characterisation of the metabolites was only carried out using the latter because of; (1) better ionisation of phenolic acids in negative mode and (2) better signal-to-noise levels of the targeted ions, as described in the previous chapter.

Then, the pipeline followed for this targeted approach initially included the quantification of the 12 standard compounds. However, many other significant peaks were observed in the chromatograms of the various samples. It was then decided to perform a manual dereplication of as many peaks as possible on the basis of the list of metabolites likely to be present in *C. asiatica* (see Table 2). The targeted study was then be conducted on a “targeted ions” list including both standard and annotated compounds.

4.2.2.1. Metabolite annotation

The tentative annotation of the metabolites was carried out by comparing the fragmentation patterns of main peaks obtained from negative mode data with data from the literature. Chromatographic and MS/MS data were also compared to those of the standard compounds in order to confirm chemical classes.

Then, one sugar and 7 caffeoylquinic acids and their analogues or derivatives were putatively annotated in this first study. More minor peaks could be observed in later harvested samples and in elicited samples in comparison to earlier time-points and control cultures. Moreover, the chromatograms indicated the possible coelution of some metabolites. This indicated the richness of the extracts and the possibility to further exploit the dereplication of more compounds. However, the methodology employed for this analysis was limited by the use of Low Resolution-MS/MS. The low-resolution mass spectrometry gave non-accurate *m/z* which difficulted the dereplication of compounds whose no spectral data was available. In future chapters, the dereplication of more molecules will be described by the means of data obtained with an UPLC-HRMS/MS approach.

Rq : note that we will indicate the monoisotopic mass of the compounds putatively dereplicated even if the analysis was conduced by low resolution MS; but they will be of interest for the following chapters.

4.2.2.1.1. Sucrose

Among the peaks of interest, one was constitutively detected in all the samples at Rt 0.94 min. Its MS spectrum showed a major deprotonated ion $[M-H]^-$ at *m/z* 341. The MS/MS spectrum exhibited a fragment ion $[M-162-H]^-$ at *m/z* 179 corresponding to a neutral loss of a glucose moiety. By comparison to the literature (236) and regarding its early Rt indicating a high hydrophilicity, this ion, named **targeted ion 1,** was putatively annotated as sucrose $C_{12}H_{22}O_{11}$ (monoisotopic mass 342.1162) (Figure B.2).

4.2.2.1.2. CQAs and derivatives

With regards to the characterization of CQAs and their derivatives by comparison of their fragmentation pattern with published data on *C asiatica* (102,237), 7 further CQAs could be annotated. Among them, isomers of the same compounds were detected since they shared the same observed mass; on one hand, two compounds exhibited the deprotonated ion $[M-H]^-$ at *m/z* 353 and, on the other hand, two others at *m/z* 515. The global scheme for LC-MS^n identification of positional isomers of CQAs have been described (238). Regarding the *regio*- and geometrical isomers of 5-monoacyl CQAs, it has been demonstrated that on reverse phase columns the *cis*-isomers elutes after their *trans*-isomers, whereas, for 3- or 4-monoacyl CQAs the *trans*-isomers elute before the *cis*. In the MS/MS analyses of CQAs, the presence of a main fragment

ion at *m/z* 191 [quinic acid-H]$^-$ is characteristic of a 5-CQA explained by the neutral loss of a caffeoyl moiety. Whereas an ion at *m/z* 179 [caffeic acid-H-H_2O]$^-$ is indicative of a 3-CQA. In general, the presence of a peak at *m/z* 173 is indicative of 4-acyl position. Using these fragmentation pattern rules, the following CQAs (targeted ion 2 and 3) were characterised. **Targeted ion 2** at 6.42 min showed a precursor ion at *m/z* 353.09 [M-H]$^-$. The MS spectrum exhibited the presence of a product ion at *m/z* 191.05 [M-H-162]$^-$ due to loss of a caffeoyl moiety, *m/z* 179 [caffeic acid-H]$^-$, and *m/z* 135 [caffeic acid-CO_2]$^-$ (Figure B.3). Thus, the molecule was annotated as 3-CQA (chlorogenic acid) with a monoisotopic mass of 354.0950 Da ($C_{16}H_{18}O_9$).

Targeted ions 3 Rt at 7.4 produced a precursor ion at *m/z* 395.07 [M+FA-H]$^-$. The MS spectrum exhibited the presence of a precursor ion at *m/z* 233 [M+FA-H-162]$^-$ due to the loss of a caffeoyl moiety as well as *m/z* 135 [caffeic acid-CO_2]$^-$ (Figure B.4). The fragment ion at *m/z* 223 [caffeic acid+FA-H]$^-$ was here present but represented less than the half of the intensity of *m/z* 233. According to the cited literature for the hierarchal scheme for LC-MS^n identification of CQAs (238) and based on its chromatographic elution this ion was tentatively annotated as 5-CQA, with a monoisotopic mass of 354.0950 Da ($C_{16}H_{18}O_9$).

Targeted ions 4, 5 and 6, found at Rts 6.45, 7.19 and 7.85 min respectively, putatively corresponded to *di*-CQAs. Ions 4 (Figure B.5) and 6 (Figure B.6) were both observed with a molecular ion [M-H]$^-$ at *m/z* 515 and the ion 5 (Figure B.7) with a molecular ion [M+FA-H]$^-$ at *m/z* 557 although the [M-H]$^-$ could also be observed. MS spectra of these three compounds obtained by fragmentation of their respective precursor ion at *m/z* 515.12 [M-H]$^-$ led to the

observation of product ions at *m/z* 353 $[M-H-162]^-$ due to the loss of a caffeoyl moiety, and at *m/z* 179 [caffeic acid-H]$^-$. A similar neutral loss of 162 u was observed from the FA adduct of ion 5 ($[M+FA-H-162]^-$ at *m/z* 395). Ion 4 also showed a fragment ion at *m/z* 191 $[M-H-324]^-$ due to the loss of the second caffeoyl moiety. Then, as these three detected compounds showed a similar fragmentation pattern,therefore, it was not possible to assign their acyl position . Thus, these biomarkers were tentatively annotated as di-CQAs positional isomers with a monoisotopic mass of 516.1267 Da ($C_{25}H_{24}O_{12}$).

Targeted ion 7 observed at Rt 7.25 min exhibited a main ion $[M-H]^-$ at *m/z* 601. The MS/MS spectrum of this ion showed fragments ions at *m/z* 557, 515, 439, 417, and 395 (Figure B.8). This fragmentation was consistent with the literature (239) for its annotation as irbic acid (3,5-O-dicaffeoyl-4-O-malonylquinic acid) with a monoisotopic mass of 602.1271 ($C_{28}H_{26}O_{15}$). This molecule was first described by Antognoni *et al*. 2011 (108) from *C. asiatica*, which is to date the only species known to produced it.

Targeted ion 8 at 7.75 min showed a major ion at *m/z* 529 $[M-H]^-$, and MS/MS generated product ions at *m/z* 353 [M-ferulic acid-H_2O]$^-$ and *m/z* 367 [M-caffeic acid-H_2O]$^-$. (Figure B.9). The product ions at *m/z* 179 and 191 are characteristic for a 3-CQA and the presence of a peak at 191 is also characteristic for a 5-acyl position for FQAs as well (the 3-acyl position of FQAs is represented by a peak at m/z 193) (238). Thus, the molecule was tentatively annotated as 3-caffeoyl, 5-feruloylquinic acid with a monoisotopic mass of 530.1424 Da ($C_{26}H_{26}O_{12}$).

Table 13. Characterization of the tentatively annotated metabolites present in methanolic extracts from *C. asiatica* HRs detected by UHPLC-MS/MS

T. ion	Rt (min)	Detected ions		Fragment ions (*m/z*)	Targeted ion (*m/z*) for quantification	Molecular Formula	Annotation	Ref.
		(*m/z*)	adduct type					
1	0.91	341.11	$[M-H]^-$	178.9; 112.9; 161; 142.9; 118.9; 130.9; 148,8	341.11	$C_{12}H_{22}O_{11}$	sucrose	(240)
2	6.5	353.09	$[M-H]^-$	191; 179; 173; 161; 135	353.09	$C_{16}H_{18}O_9$	3-CQA	(102,237,241)
3	7.2	353.10	$[M-H]^-$	173; 179; 155; 135	353.15	$C_{16}H_{18}O_9$	4-CQA	(102,237,241)
4	6.5	515.15	$[M-H]^-$	353; 335; 191; 173	515.15	$C_{25}H_{24}O_{12}$	di-CQA isomer 1	(102,237,241)
5	7.2	515.17	$[M-H]^-$	353; 335; 179; 173	515.17	$C_{25}H_{24}O_{12}$	di-CQA isomer 2	(102,237,241)
6	7.8	515.15	$[M-H]^-$	353; 335; 179; 173	515.15	$C_{25}H_{24}O_{12}$	di-CQA isomer 3	(102,237,241)
7	7.2	601.09	$[M-H]^-$	557; 515; 439; 417; 395	601.09	$C_{28}H_{26}O_{15}$	3,5-O-di-Caffeoyl-4-O-malonylquinic acid isomer a	(102,237,241)
8	7.75	529.24	$[M-H]^-$	367; 353; 191	529.24	$C_{26}H_{26}O_{12}$	3- caffeoyl-5-feruloylquinic acid	(221)
9	8.5	1019.31	$[M+FA-H]^-$	973	1019.31	$C_{48}H_{78}O_{20}$	MD	std
10	8.87	1003.44	$[M+FA-H]^-$	957	1003.44	$C_{48}H_{78}O_{19}$	AD	std
11	12.5	503.41	$[M-H]^-$	437; 483; 391; 419	503.41	$C_{30}H_{48}O_6$	MA	std
12	14	487.38	$[M-H]^-$	409; 421; 403	487.38	$C_{30}H_{48}O_7$	AA	std

T. ion: targeted ion; Std: standard

4.2.2.2. General observations of the chromatograms

A first visual evaluation of base peak intensity (BPI) MS chromatograms (Figure 50) showed differences in the presence/absence of some peaks among the samples, but also differences in the intensities of some other peaks across the different conditions and times of harvesting. It is noteworthy that most of the major extracted metabolites appeared to be in the mid Rt region (6.0 – 10.0 min) of the chromatograms. It indicated that the *C. asiatica* methanolic plant extracts contained several polar to mid polar compounds in addition to the four most frequently reported centellosides that are relatively apolar. Looking at the zones were the standard and targeted compounds elute (Table 13), it appeared that they were observed to be ubiquitously present in all the extracts but with different intensities depending on the elicitor and the day of harvesting (peaks highlighted in Figure 50). Overall, elicitor-treated samples had enhanced peak intensities for the 12 targeted ions. This enhancement was especially evident from day 8 after elicitation onwards. Between the two elicitors, CORO-treated samples showed higher peak intensities compared to those treated with MeJA. It is interesting to note that, even though their low intensity, CQAs compounds (targeted ions 2-8) were immediately identifiable in the control chromatograms, as well as in the treated ones, showing the consistency of their production. On the contrary, peaks corresponding to centellosides (targeted ions 8-12) where not easily observed in control samples suggesting the dependency of the centelloside pathway to be triggered by stress factors here represented by elicitation.

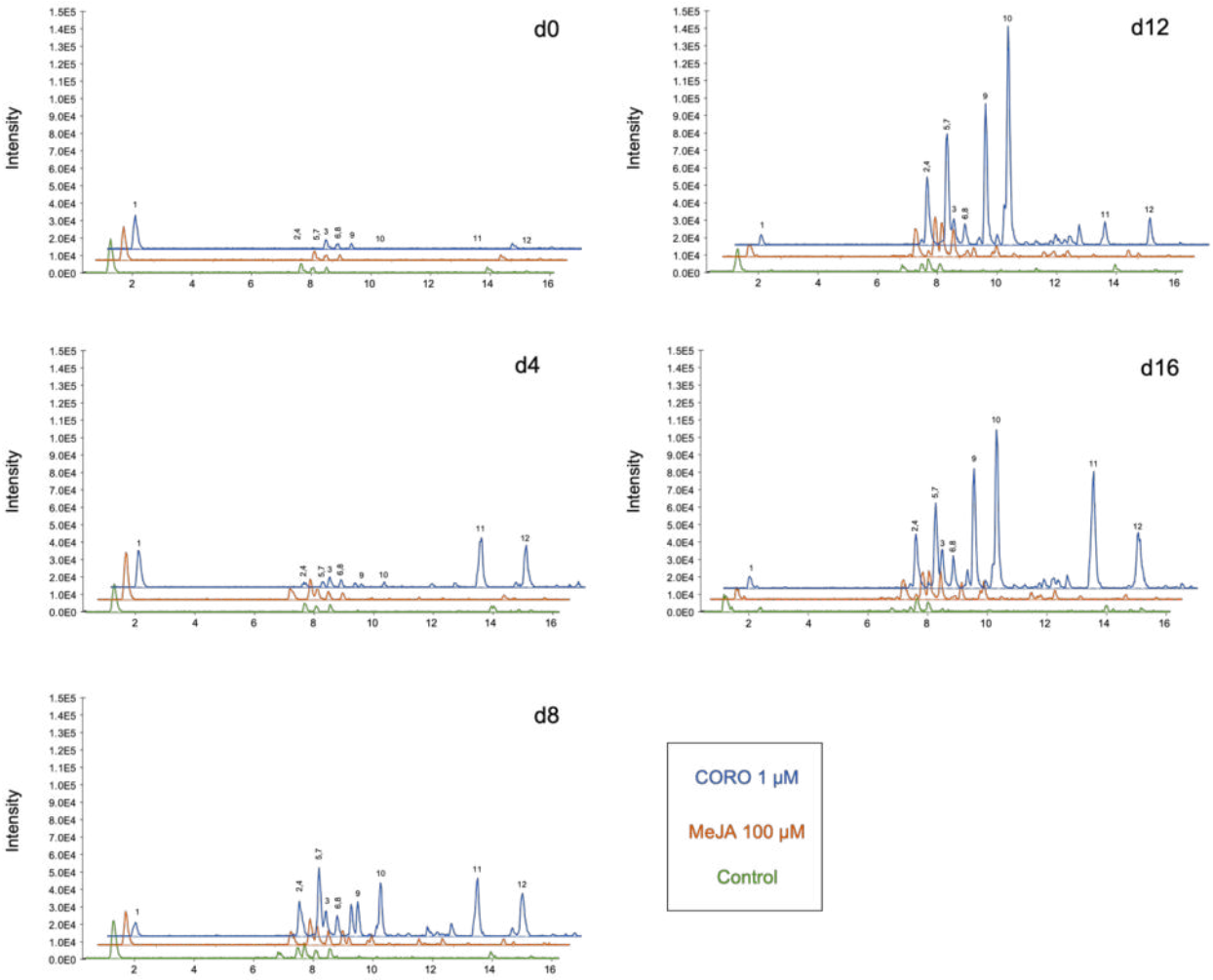

Figure 50. Comparison of the ESI (-) mode BPI chromatograms from the methanolic extracts treated with Control, MeJA and CORO and harvested 0, 4, 8, 12, and days after elicitation. Numbers correspond to the peaks of the 12 targeted ions, namely: 1) sucrose, 2) 3-CQA, 3) 5-CQA, 4) di-CQA isomer, 5) di-CQA isomer, 6) di-CQA isomer, 7) irbic acid, 8) 5-FQA, 9) MD, 10) AD, 11) MA, and 12) AA.

4.2.2.3. Targeted feature detection: relative production kinetics

Quantification of the peak areas of the targeted ions was then performed using MZmine 2 through its internal tool “targeted feature detection”. The area under the curve of the peaks represents the relative abundance of the selected ions that serves the comparison of the relative production between ions. However, unlike quantification with calibration curves, this kind of targeted metabolomics analysis only allows the comparison of the effect of treatments in the relative production (and presence/absence) for each targeted ions independantly. In this case, the peaks belonging to the 12 detected ions were submitted to targeted feature detection. Their relative production kinetics of each of the 12 targeted ions was then presented in bar plots. Each of the plot shows the production after the treatment along all the days of harvesting. Results are shown in Figures 51-52.

The relative abundance of sucrose (Figure 51) followed a similar behaviour to that obtained in the analysis by ^{1}H-NMR described and discussed previously. The levels of sucrose in the control samples showed a gradual increase up from day 0 to day 8 and decreased at day 12. As observed in the ^{1}H-NMR analysis, levels of sucrose were higher at days 4 and 8 after the elicitation of MeJA compared to the control samples. This result suggests that MeJA could upregulate the accumulation of sucrose. The role of MeJA in regulating sucrose metabolism has not been yet explored neither in *C. asiatica* plants nor in HRs so far. Indeed, there is not much information regarding the effect of MeJA in the metabolism of carbohydrates in other plants. Two studies investigated the effect

of exogenous addition of MeJA in the post-harvesting sugar-metabolism state of tomato fruits (242,243). These studies found that the enzyme Sucrose-Phosphate-Synthase (SPS) was up-regulated after the addition of MeJA, while two invertases responsible of the degradation of sucrose into monosaccharides were down-regulated. This is consistent to what was observed here for the first part of the experience but does ot explain the drastic fall of sucrose content from day 12. Regarding the effect of CORO, such a significant depletion of the abundance of sucrose was observed after 8 days until the end of the experiment. As extendedly discussed in the NMR analysis, sucrose represents a carbon source for the specialised metabolism, which suggests that it would be over-activated. CQAs were produced constitutively by the HRs in basal conditions. However, MeJA and CORO had a positive effect in the accumulation of both 3-CQA and 5-CQA from day 8 after elicitation until day 16 (Figure 51). Day 12 after elicitation with CORO was the only statistically different day from MeJA. This same behaviour was observed for the 3 isomers of di-caffeoylquinic acids and for irbic acid (Figure 51). For all these CQAs and di-CQAs except 2, their amout was found lower at the last day of the experiment, which could be the reflect of a metabolization through oxidation. Studies on cell suspension cultures have already demonstrated that CQAs production is enhanced by MeJA at 100 μM (102). Moreover, the global phenolic content and the identification of specific CQAs have been already studied in different tissues of *C. asiatica* (1,96,239,244). However, this is the first study regarding the kinetics production of CQAs in *C. asiatica* and the positive effect on CORO in their production.

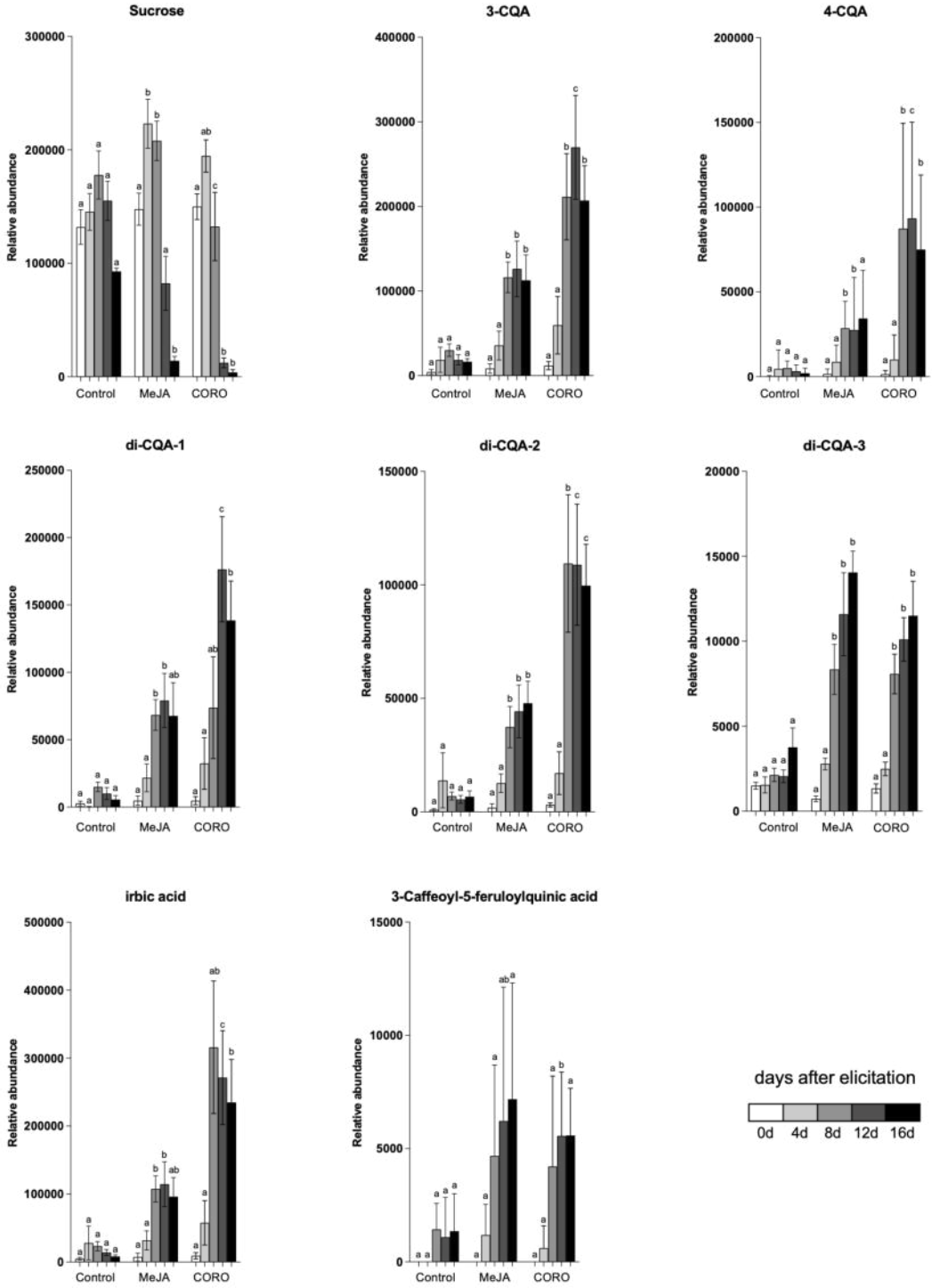

Figure 51. Relative abundance of annotated ions from methanolic extracts of HRs of *C. asiatica* analysed by UHPLC-MS/MS different harvesting times after addition of no elicitor, MeJA or CORO. Quantitative data was calculated using six biological replicates and it is presented as means ± SEM. Two-way ANOVA was performed for each harvesting day. Then, for a given day, columns sharing the same letter are not significantly different at 95% confidence. Quantification was performed using the software MzMine 2.

Concerning centellosides, CORO and MeJA demonstrated their elicitation effect for all the compounds here detected (Figure 52). However, the multiple comparison of the ANOVA of relative abundance of the 4 centellosides revealed a higher effect of CORO only on the production of the two sapogenins (AA and MA) at day 8 (Figure 52). This positive effect of CORO and MeJA has been recently observed in a similar experimental design using the same HRs line as used here (154): in this study, not only the production of centellosides was enhanced by CORO 1 μM but also the expression of mRNAs encoding different enzymes participating in the centelloside pathway. The last steps of the biosynthesis of the 4 most important centellosides were proposed by Kim *et al*. (2017) (see chapter 1.2.1.1 and Figure 7 and 8). This elicitation-based rational study employed MeJA to discover those genes participating in the centelloside pathway, mainly cytochrome P450 oxidases (CYPs). Our results confirm the sequence of these last biosynthetic steps, which can be deduced from Figure 53 showing the superimposition of the production curves for the 4 centellosides here detected. Levels of saponins were nearly undetectable after 4 days of both elicitations, while sapogenins abundance increased from day 0 to 4. After 8 days of elicitation, both saponins sharply increased but at the same time abundances of the sapogenins were depleted.

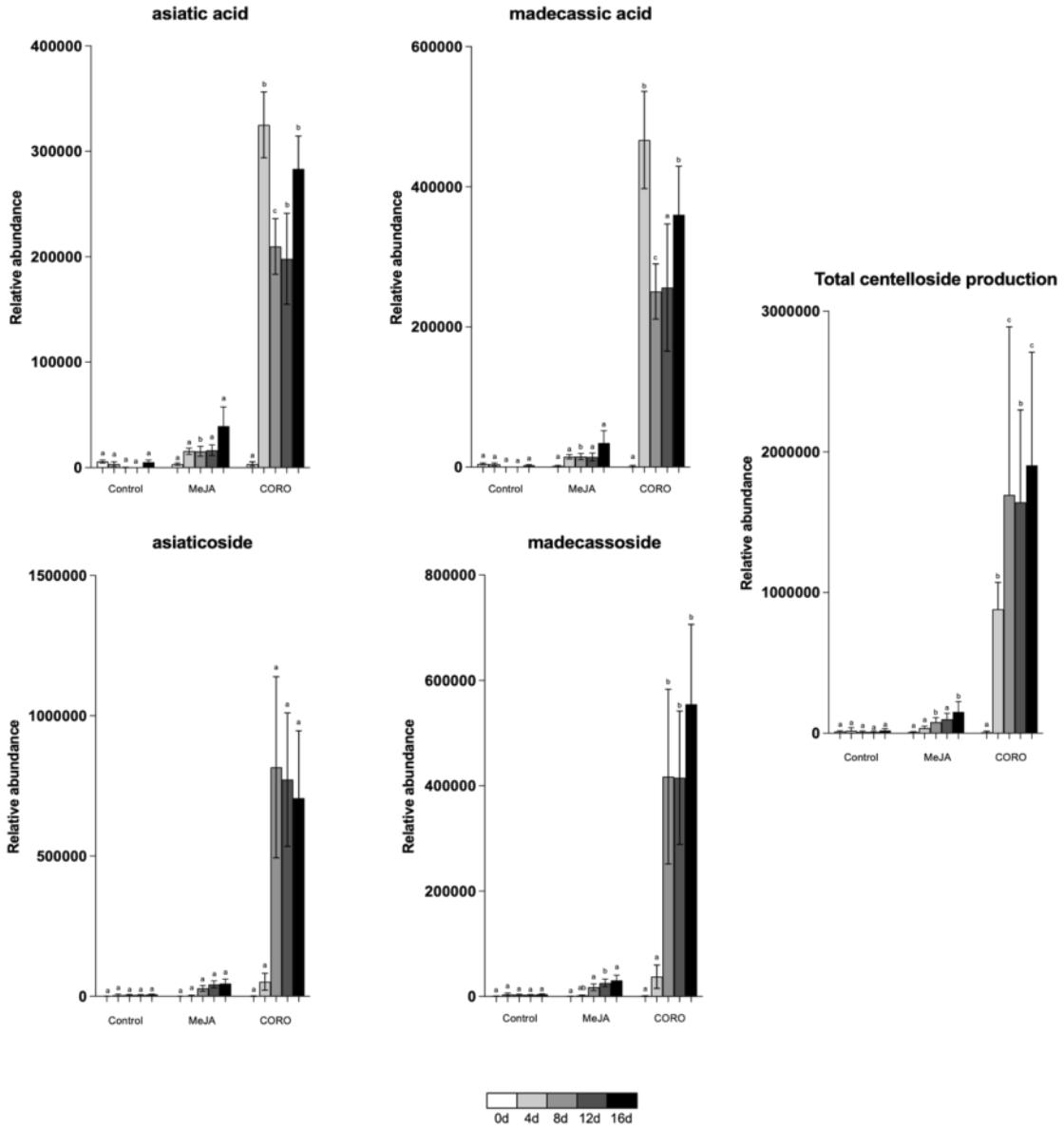

Figure 52. Relative abundance of annotated ions from methanolic extracts of HRs of *C. asiatica* analysed by UHPLC-MS/MS different harvesting times after addition of no elicitor, MeJA or CORO. Quantitative data was calculated using six biological replicates and it is presented as means ± SEM. Two-way ANOVA was performed for each harvesting day. Then, for a given day, columns sharing the same letter are not significantly different at 95% confidence. Quantification was performed using the software MzMine 2.

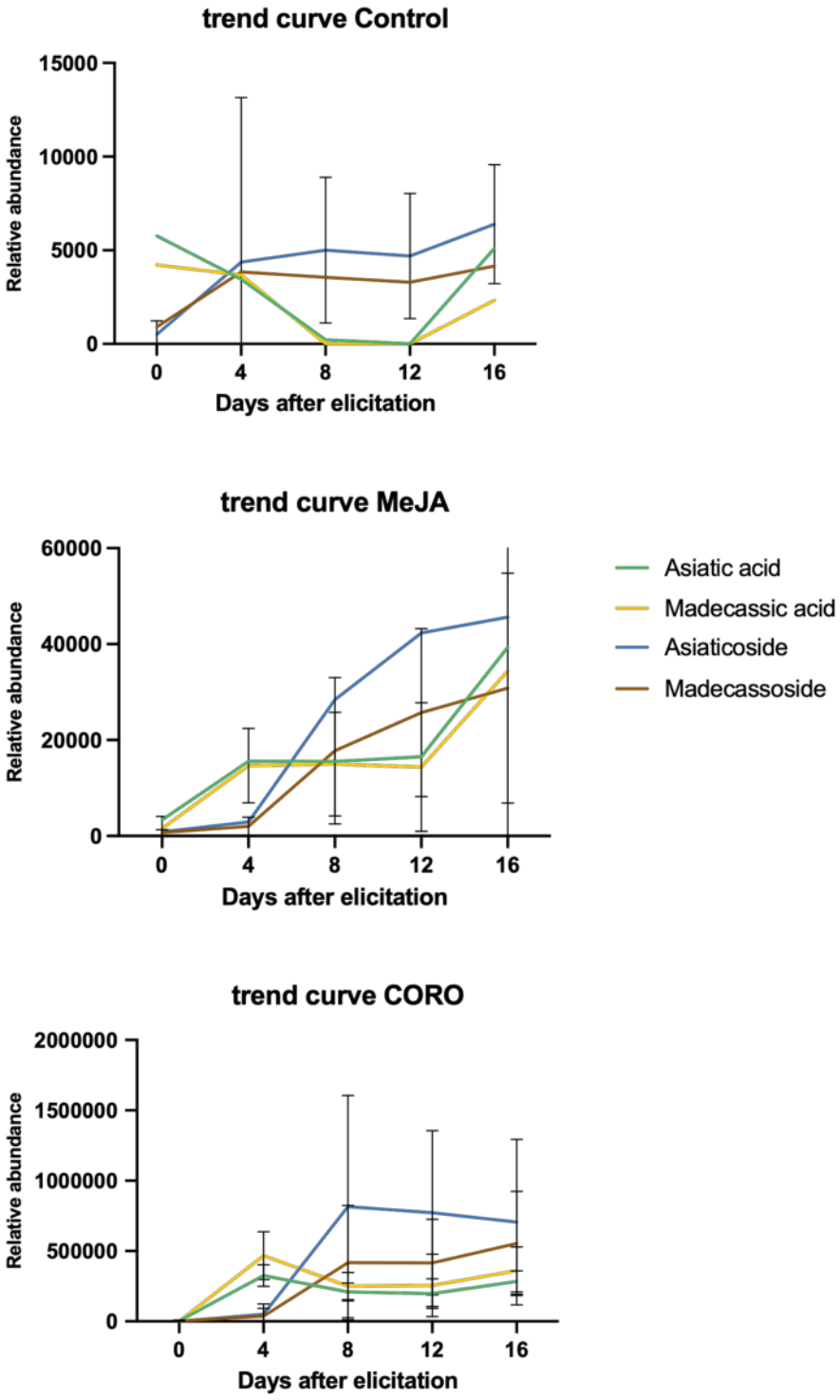

Figure 53. Superimposition of production curves of AA, MA, AD, MD

To conclude, both elicitors acted as enhancers of the specialised metabolism from the beginning of their addition in the culture medium, as shown on the two followed pathways, phenolics and triterpenes, to the detriment of the accumulation of sugars. This confirms the NMR study and give further results to get more insights into the metabolic regulation of CORO and MeJA in the specialised metabolism.

4.2.3. UHPLC-MS/MS untargeted metabolomics approach

Having few standards and annotated metabolites in our database, the previous results are partial: we therefore wanted to have a more global view of the effect of elicitors on the whole expressed metabolome. For this purpose, a non-targeted analysis was performed considering all the features detected thanks to the data processing performed with MZmine2.

An unsupervised comparison of the chemical profiles was performed by PCA on the Pareto-scaled data matrix (Figure 54a). The first three principal components explained a combined 74.3% of the variance in the data model (with 42.7% of the variance explained by PC1, 19.5% explained by PC2 and 12.1% explained by PC3). The time-course effect was mainly explained by the PC1. However, this effect was lighter than the effect of the elicitation mainly represented by the PC2. The score plots highlighted a clear separation between the CORO samples and the others. It could indicate differences in specialised metabolite activation/production after the elicitation with CORO. Interestingly, samples

harvested after 4 days of CORO addition were separated from the rest of all the samples in the model, including the other CORO-treated samples. This suggested a strong and rapid reprogramming effect of CORO on the metabolome after 4 days of its addition. Those samples harvested at days 8, 12 and 16 were not obviously separated, forming a compact group. MeJA-elicited samples were separated from control samples from day 4, but in a lower extent than CORO ones. They nevertheless form a very distinct group from the CORO one. Samples corresponding to 4, 8, 12 and 16 days after elicitation with MeJA were nearly clustered.

Analysis of the loading plot (Figure 54b) permitted the extraction of features of importance responsible for the construction of the PCA model. Interestingly, the significant ions corresponded to the previously detected targeted ions 1-12. In particular, sucrose was correlated with day 0 samples, which is consistent with the previous targeted analysis. Similarly, the 4 main features representative of the CORO samples were the 4 centellosides MA, AA, MD and AD, indicating that this elicitor acts mainly on this pathway, MeJA much less. It can also be seen that the sapogenins were representative of the CORO samples at day 4, while the saponins were significantly discriminated for longer durations. Conversely, phenolic compounds seemed to be impacted in the same way by both treatments MeJA and CORO. Previous studies defined that the biomarkers of MeJA-elicited *C. asiatica* cell cultures and plants were mainly centellosides and caffeoylquinic acids (245). We confirmed these results in this first study on HRs, but we completed them with the fact that CORO acts more specifically on the triterpene pathway. Two additional not previously reported and undefined features at *m/z*

471 and Rt 7.4 and 7.8 also affected the separation between the groups. These compounds seemed to be specifically present in the late MeJA samples.

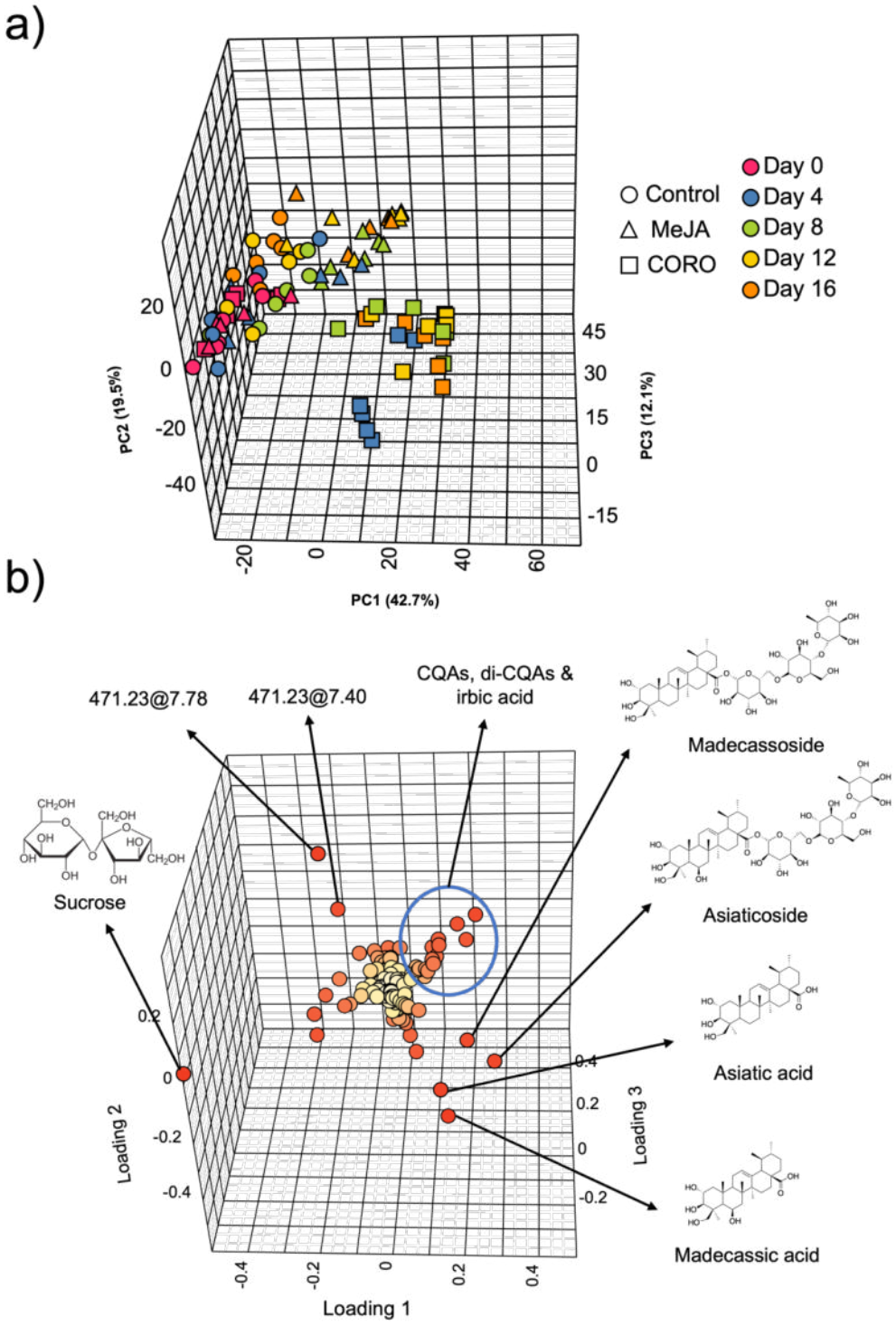

Figure 54. PCA of the *C. asiatica* HRs non treated, treated with MeJA or CORO and harvested 0, 4, 8, 12 or 16 after elicitation on complete data set (Pareto scaling): **a)** 3D-score plot for PC1 vs. PC2 vs. PC3 and **b)** PCA loading plot

A heat map was constructed through an HCA (Figure 55) to improve the visualization of the elicitation phenomena. For its better comprehension, the major observed clusters were named as (a) and (b). They were subdivided into the clusters (a1) and (a2). Cluster (a) showed a group of ions that were mostly expressed in the same manner under both elicitors treatment from day 8 onwards. At the same time, these metabolites appeared not to be produced in control conditions. Cluster (a2) revealed a group of ions induced from day 8 beyond only under CORO elicitation. On the other hand, cluster (b) showed metabolites induced only by CORO in a similar way to (a2) but with a peak of production from day 4. Cluster (b) also exhibited features that were constitutively produced by untreated roots, but whose production were repressed by the effect of elicitors from day 4 after the two elicitations, especially by CORO.

In a global way, CORO seemed to have a greater effect on the activation of silenced metabolites than MeJA. The HCA also revealed the counterpart of the overactivation of specialised pathways by the means of a faster consumption of many metabolites that may be primary energy sources and/or carbon skeletons. These hypotheses are consistent with those generated after the NMR metabolomics study. There seem to be a transformation of primary metabolites into intermediates and end products that are likely to belong to the specialised metabolism. This general analysis demonstrated the strength of the two elicitors and their usefulness as possible regulators of metabolism towards the enhancement and/or activation of the specialised metabolism.

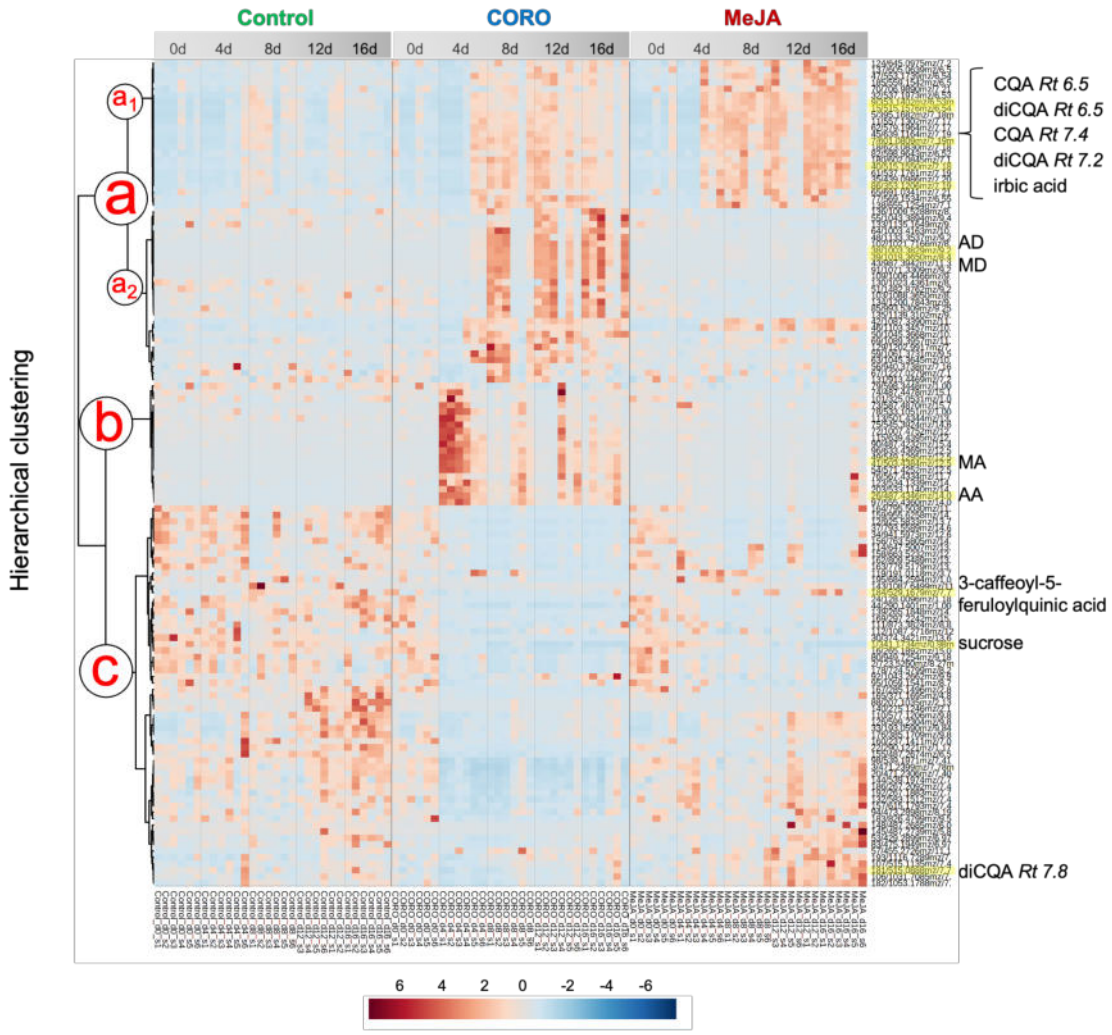

Figure 55. Hierarchical Clustering Analysis (HCA) of the most significantly variable (*p*-value < 0.005) 128 features (figured by their *m/z* ratio and their retention time Rt) among the samples corresponding to the three different treatments and represented on a heatmap (ranging from red colour for high AUC (area under the curve) to blue for low abundance). Highlithed features correspond to identified and annotaded ions.

4.2.3.1. Further untargeted metabolomics study assisted by UHPLC-HRMS/MS-derived MN

The main biomarkers contributing variability to the model turned out to be

the same as expected: CQAs and centellosides. However, there were other minor variables affecting to the variance between groups. ANOVA revealed 99 significant variables (p-value < 0.005) (data not shown). Moreover, the PCA loading plot (Figure 54b) showed two variables of importance at *m/z* 471 that have not yet been described in *C. asiatica*. The annotation of all minor variables affecting the models results difficult and time-consuming. Unsupervised statistical analysis such as PCA are exploratory methods that seek to understand the relationship of the data and its structure. By contrast, supervised statistical analyses allow the use of predictive methods to obtain a relatively short list of variables that affect the groups previously defined (here elicitation and time of harvesting). It is possible to focus on the annotation of these lists containing a smaller number of variables (features). Then, the shorter the lists the more simplicity to work on the dereplication of the variables of importance. Nevertheless, annotation becomes complex when working with low resolution UHPLC-MS/MS data. Therefore, one representative replicate of each treatment and time of harvesting was analysed by UPLC-HRMS/MS with the aim of constructing Molecular Networks (MNs). This chemoinformatic approach allows to visualize the structural relationship of the detected ions based on their MS/MS spectra. MNs facilitates the dereplication of ions of interest or, at least, their classification within a family of compounds. (246). All MS/MS data is organised and visualised through a spectral similarity map in which structurally close molecules sharing similar fragmentation patterns are assembled into clusters. This allows simultaneous visual explorations of analogous molecules in single or multiple datasets and from a wide variety of biological sources. After importing

MS/MS spectra, the network is generated based in trigonometry and cosine score to measure the structural relationships between ions based on their fragmentation. The network is visualised using a tool integrating networks of interactions such as Cytoscape. In the networks, nodes correspond to ions, generally labelled by the mass of the precursor. Nodes are connected by edges if they have similar fragmentations. The thickness of the edges can be used to visualize the strength of the relationships; the thicker the lines, the closer the nodes are structurally (247). In addition, MNs are complemented by quantification data of the areas under the peaks. Nodes can be tailored to graphically represent the relative production of a given ion depending on the elicitor and/or sample collection time (Figure 56). Thus, the MNs become an excellent approach for metabolomic exploration but also for dereplication by comparison of nodes. The following MN was generated using the open-access GNPS and visualised with Cytoscape 3.9.1. GNPS contains a mass spectral database that is convenient for direct dereplication. However, supervision of the putative annotations is recommended to avoid mismatching.

Thus, we constructed a global molecular network of *C. asiatica* HRs in order to investigate the effect of treatment conditions not on individual compounds but on biosynthetic pathways. This should also allow for improved annotation of compounds of interest. For this purpose, a representative sample of each of the six replicates samples for the three groups control, MeJA and CORO, at the 5 days of sampling, was analysed by UHPLC-HRMS/MS, and the data set was collected and processed by GNPS.

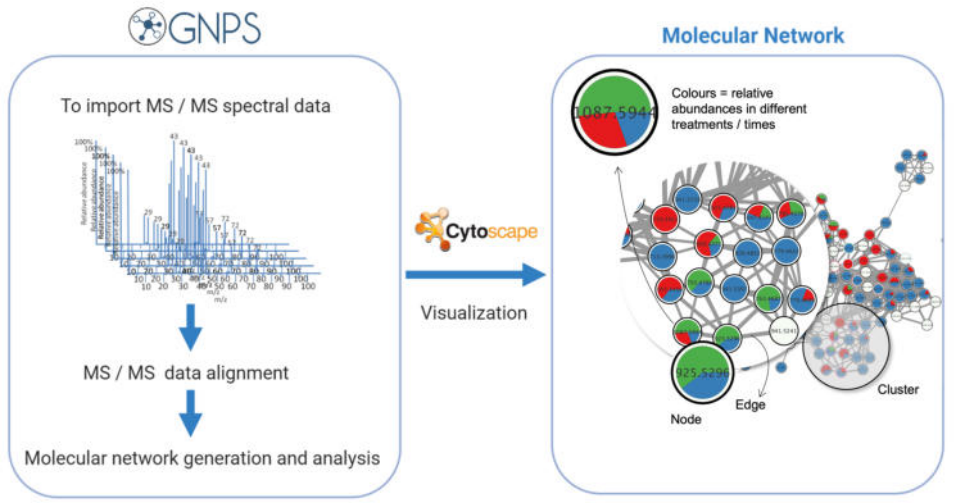

Figure 56. Procedure for the generation of MNs using GNPS

4.2.3.1.1. MNs overview

The MN obtained from the ion list of the UPLC-HRMS/MS (-)ESI is shown in Figure 57. It was composed of 386 nodes of which 281 were grouped with at least one other node for a total of 24 networks (N-1 to 24). Most of the ions could not be regrouped due to the absence of fragmentation spectra or because their non-informative spectra. Some of the nodes could be annotated by comparison with the to the spectral data and Rt of the targeted ions annotated (chapter 4.2.3.1). Some others were annotated automatically by the internal GNPS database or manually via the Dictionary of Natural Products (DNP). The annotations were characterized according to the levels of confirmation as proposed by Schymanski *et al*. (2014) (248) (Table 14).

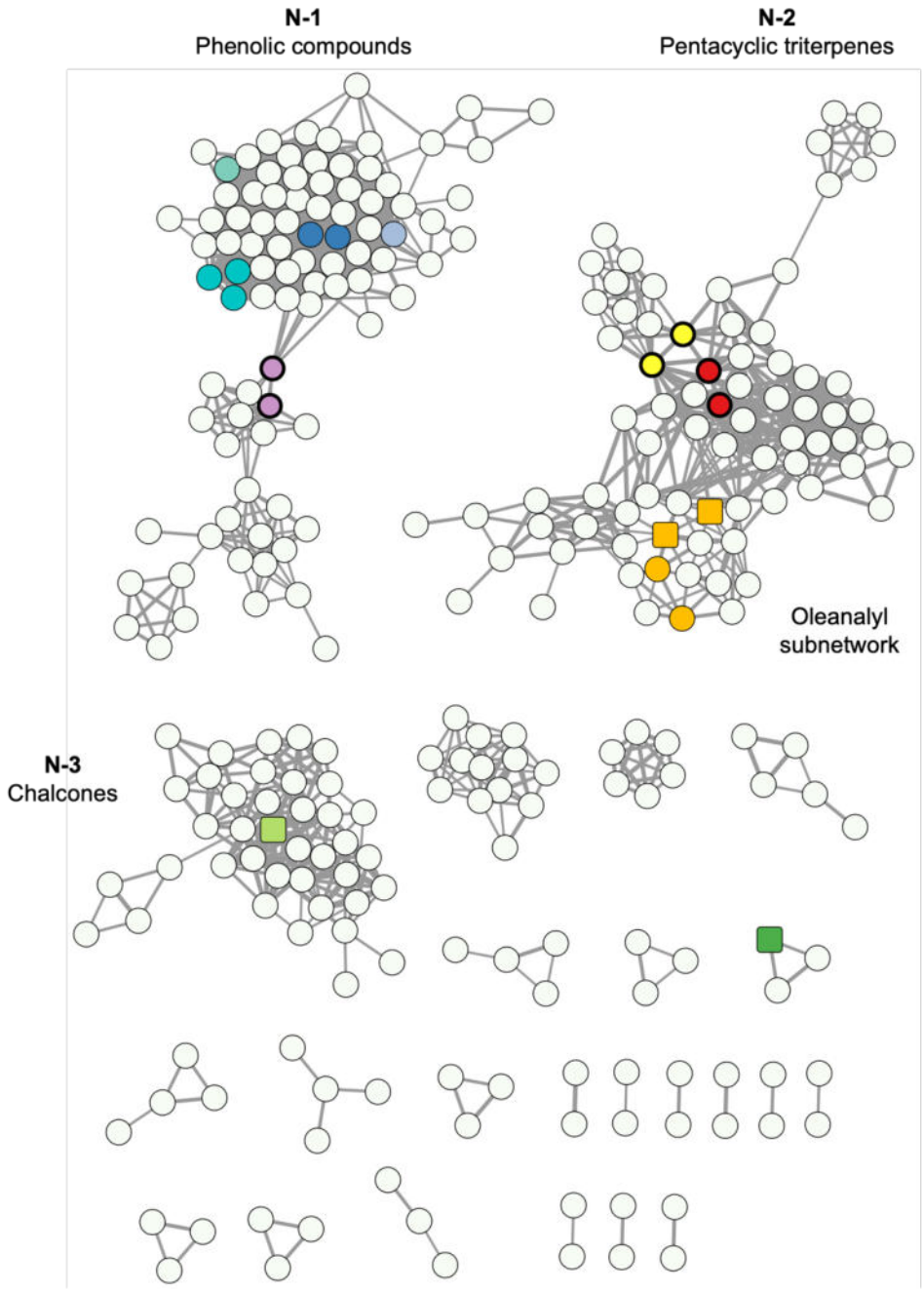

Figure 57. Overview of the of global *C. asiatica* HRs MN. Identified metabolites (see Table 14) are indicated in colours. Different levels of identification are signalied as: **bold-rounded nodes** are compounds identified by comparision with standard compounds; **rounded** nodes were identified by structure prediction based on their high-resolution mass and fragmentation spectrum; and **squared nodes** were prediceted by GNPS.

Table 14. Newly dereplicated metabolites from the MN

Measured *m/z*	adduct	Rt (min)	Calculated *m/z*	Molecular Formula	Δppm	Annotations	Sub-Network	Confidence level of annotation (248)	Ref.
471.2473	[M-H]-	7.40	472.2541	$C_{31}H_{36}O_4$	-15.21	Panduratin E	N-1 Phenols	L2a	GNPS
925.5296	[M-H]-	13.77	926.5368	$C_{47}H_{74}O_{18}$	53.19	3-*O*-Pentose-Hexose-oleanolic acid-28-*O*-Hexose	N-2 Oleanalyl subcluster (Pentacyclic tritepenes)	L3	(249)
793.4788	[M-H]-	14.71	794.4860	$C_{42}H_{66}O_{14}$	51.29	3-*O*-Hexose-oleanolic acid-28-*O*-Hexose	N-2 Oleanalyl subcluster (Pentacyclic tritepenes)	L3	(249)
371.1159	[M-H]-	4.71	372.1231	$C_{16}H_{20}O_{10}$	46.90	3-(Benzoyloxy)-2-hydroxypropyl beta-D-glucopyranosiduronic acid	N-4	L2a	GNPS
809.4771	[M-H]-	10.68	810.4843	$C_{42}H_{66}O_{15}$	54.54	Maslinic acid-3-hexopyranuronic acid-28-glucose	N-2 Oleanalyl subcluster (Pentacyclic tritepenes)	L2a	GNPS (250)
647.4141	[M-H]-	13.61	648.4213	$C_{36}H_{56}O_{10}$	52.48	Oleanolic acid-3-hexopyranuronic acid	N-2 Oleanalyl subcluster (Pentacyclic tritepenes)	L2a	GNPS (250)
341.1282	$[M-H]^-$	1.11	342.1355	$C_{12}H_{22}O_{11}$	56.38	Sucrose (targeted ion 1)	Unclustered	L2b	(240)
353.1056	$[M-H]^-$	6.38	354.1129	$C_{16}H_{18}O_9$	56.53	3-CQA isomer (targeted ion 2)	N-1 Phenols	L2b	(102,237,241)
353.1078	$[M-H]^-$	7.26	354.1151	$C_{16}H_{18}O_9$	56.53	4-CQA isomer (targeted ion 3)	N-1 Phenols	L2b	(102,237,241)
515.1448	$[M-H]^-$	6.42	516.1521	$C_{25}H_{24}O_{12}$	49.07	di-CQA isomer 1 (targeted ion 4)	N-1 Phenols	L2b	(102,237,241)
515.1583	$[M-H]^-$	7.26	516.1656	$C_{25}H_{24}O_{12}$	75.22	di-CQA isomer 2 (targeted ion 5)	N-1 Phenols	L2b	(102,237,241)
515.1466	$[M-H]^-$	7.61	516.1539	$C_{25}H_{24}O_{12}$	52.55	di-CQA isomer 3 (targeted ion 6)	N-1 Phenols	L2b	(102,237,241)
601.1508	$[M-H]^-$	7.26	602.1581	$C_{28}H_{26}O_{15}$	51.37	3,5-O-di-Caffeoyl-4-O-malonylquinic acid isomer a (targeted ion 7)	N-1 Phenols	L2b	(102,237,241)
529.1627	$[M-H]^-$	7.59	530.1700	$C_{26}H_{26}O_{12}$	52.01	3- caffeoyl-5-feruloylquinic acid (targeted ion 8)	N-1 Phenols	L2b	(221)
973.5601	$[M-H]^-$	8.49	974.5674	$C_{48}H_{78}O_{20}$	60.29	MD (targeted ion 9)	N-2 Pentacyclic tritepenes	L1	standard

Table 14. (*continued*)

Measured *m/z*	adduct	Rt (min)	Calculated *m/z*	Molecular Formula	Δppm	Annotations	Sub-Network	Confidence level of annotation (248)	Ref.
957.5552	$[M-H]^-$	9.27	958.5625	$C_{48}H_{78}O_{19}$	50.88	AD (targeted ion 10)	N-2 Pentacyclic tritepenes	L1	standard
549.3761	$[M+FA-H]^-$	12.95	504.3779	$C_{30}H_{48}O_6$	65.06	MA (targeted ion 11)	N-2 Pentacyclic tritepenes	L1	standard
533.3802	$[M+FA-H]^-$	14.22	488.3820	$C_{30}H_{48}O_5$	65.17	AA (targeted ion 12)	N-2 Pentacyclic tritepenes	L1	standard
193.0581	$[M-H]^-$	5.57	194.0654	$C_{10}H_{10}O_4$	38.60	Ferulic acid	N-1 Phenols	L1	standard
179.0451	$[M-H]^-$	3.60	180.0524	$C_9H_8O_4$	56.33	Caffeic acid	N-1 Phenols	L1	standard

L1: Confirmed structure by reference standard
L2a: Confirmed structure by library spectrum match
L2b: Confirmed structure by diagnostic evidence
L3: Tentative candidate(s) (structure, substituent or class of molecule)

The main cluster N-1 concerned mostly molecules belonging to CQAs and their derivatives (Figure 58). It should be noted that most of the non-annotated nodes concern compounds of higher molecular weight than the identified molecules.

Cluster N-2 was the second in term of number of nodes: it was found to contain AD, MD, AA and MA (Figure 59). In a very interesting manner, it can shown that many compounds belonging to this series can be observed, showing a high chemical diversity of triterpenes produced. Some of the nodes corresponded to isobaric compounds to the saponins AD and MD; or methylated analogues of the sapogenins AA and MA. The internal data base of GNPS also revealed the annotation of two oleanane-type pentacyclic triterpene saponins: the molecular ions $[M-H]^-$ at *m/z* 809.4771 and *m/z* 647.4141. They were placed in a subcluster within the N-2 together with other nodes as shown in Figure 60. To the best of our knowledge, this is the first time that these two oleanane-type saponins have been described in *C. asiatica*.

In cluster N-3 (Figure 61) only one metabolite could be annotated, which showed a $[M-H]^-$ peak at *m/z* 471.2469. After obtaining the calculated molecular mass, the DNP database revealed that it could be the molecule Panduratin E with raw molecular formula $C_{30}H_{48}O_5$ (Table 14). This compound is a prenylated cyclohexenyl chalcone which, to the best of our knowledge, has only been described in the plant *Boesenbergia pandurata* (230). These types of molecules have not been described in *C. asiatica* to date.

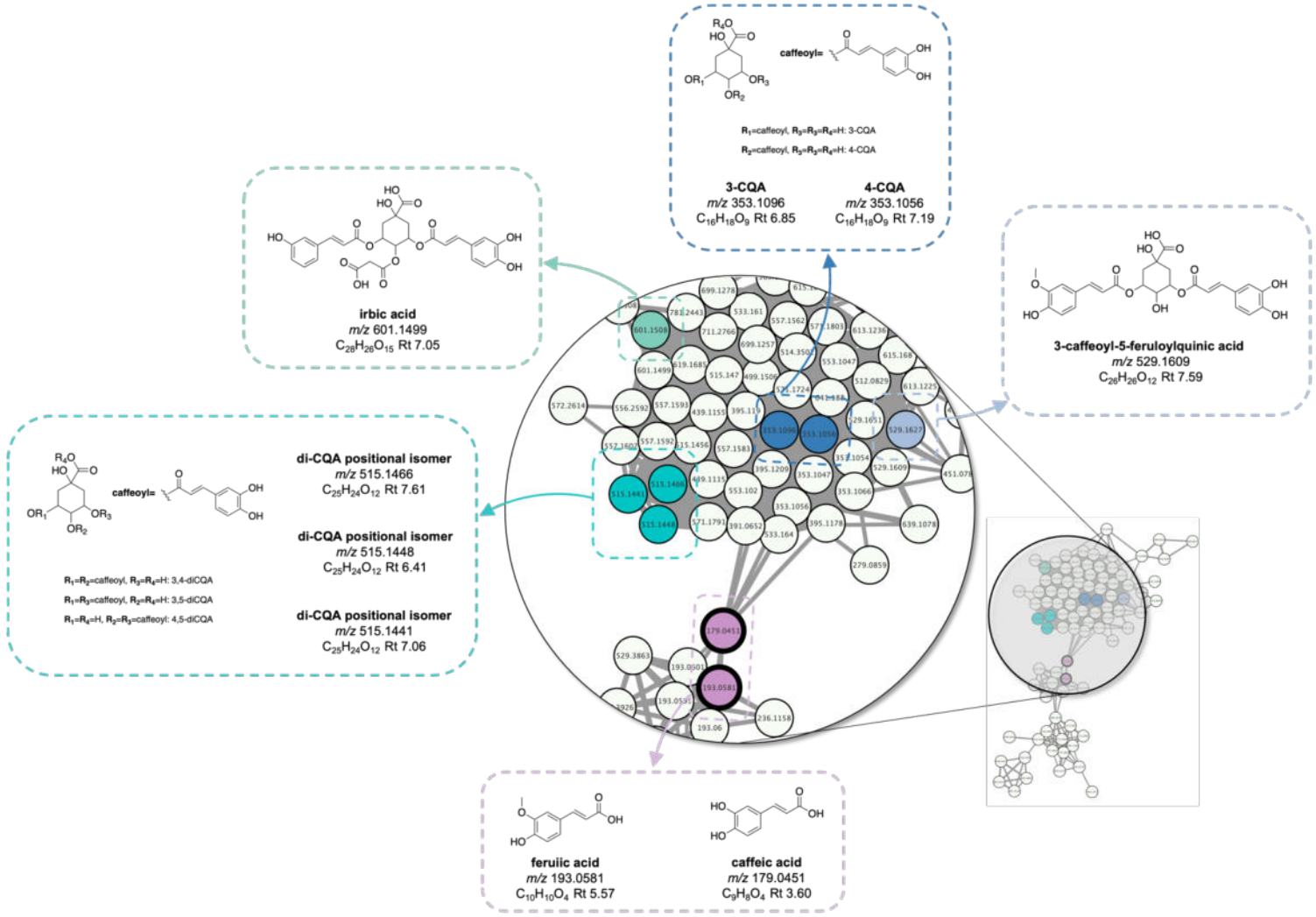

Figure 58. Overview of N-1 (CQAs-like molecules). Identified metabolites by comparison of their high-resolution mass and fragmentation spectrum with either with the literature or authentical standards are coloured.

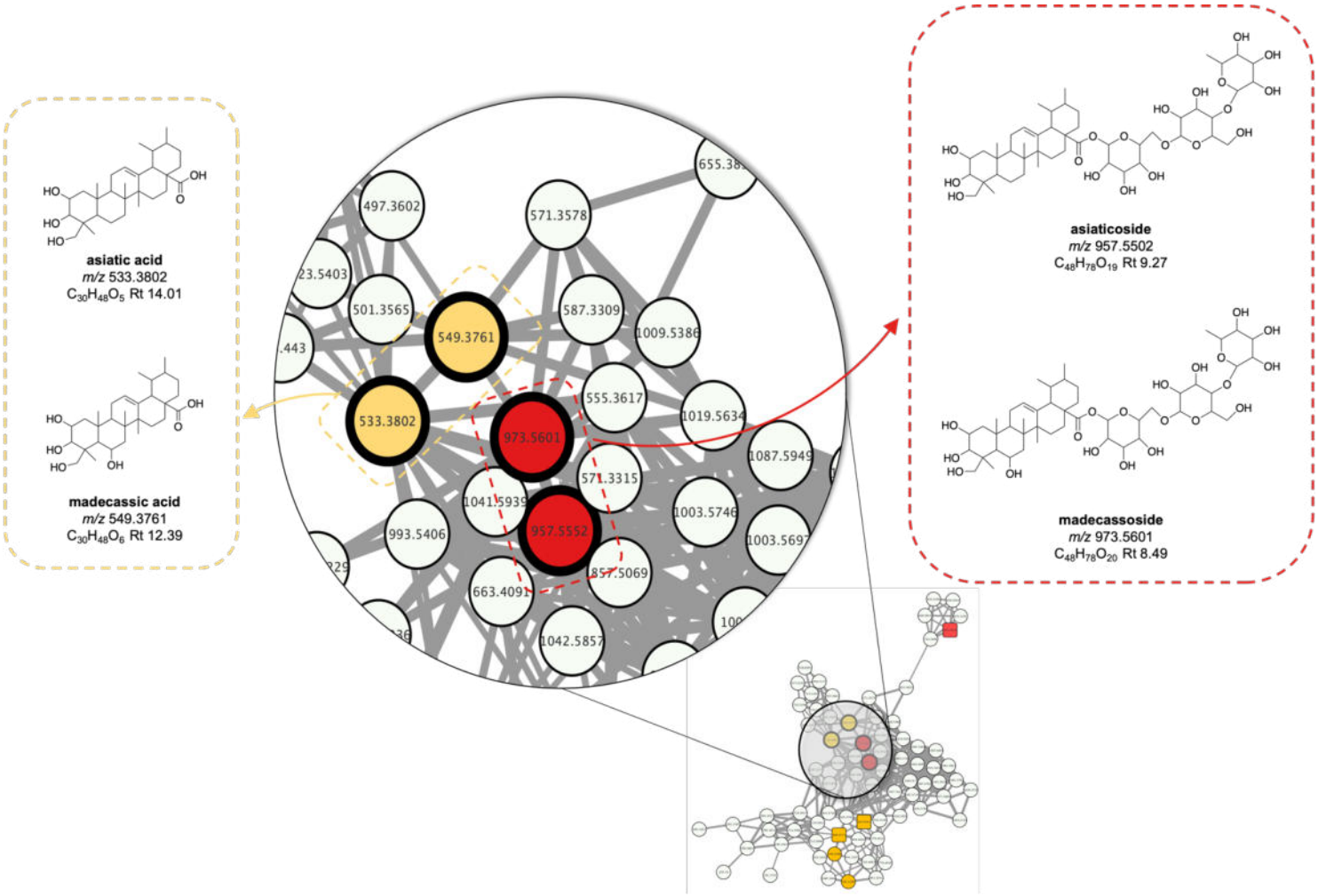

Figure 59. Overview of N-2 (centellosides-like molecules). Identified metabolites by comparison of their high-resolution mass and fragmentation spectrum with authentical standards are coloured.

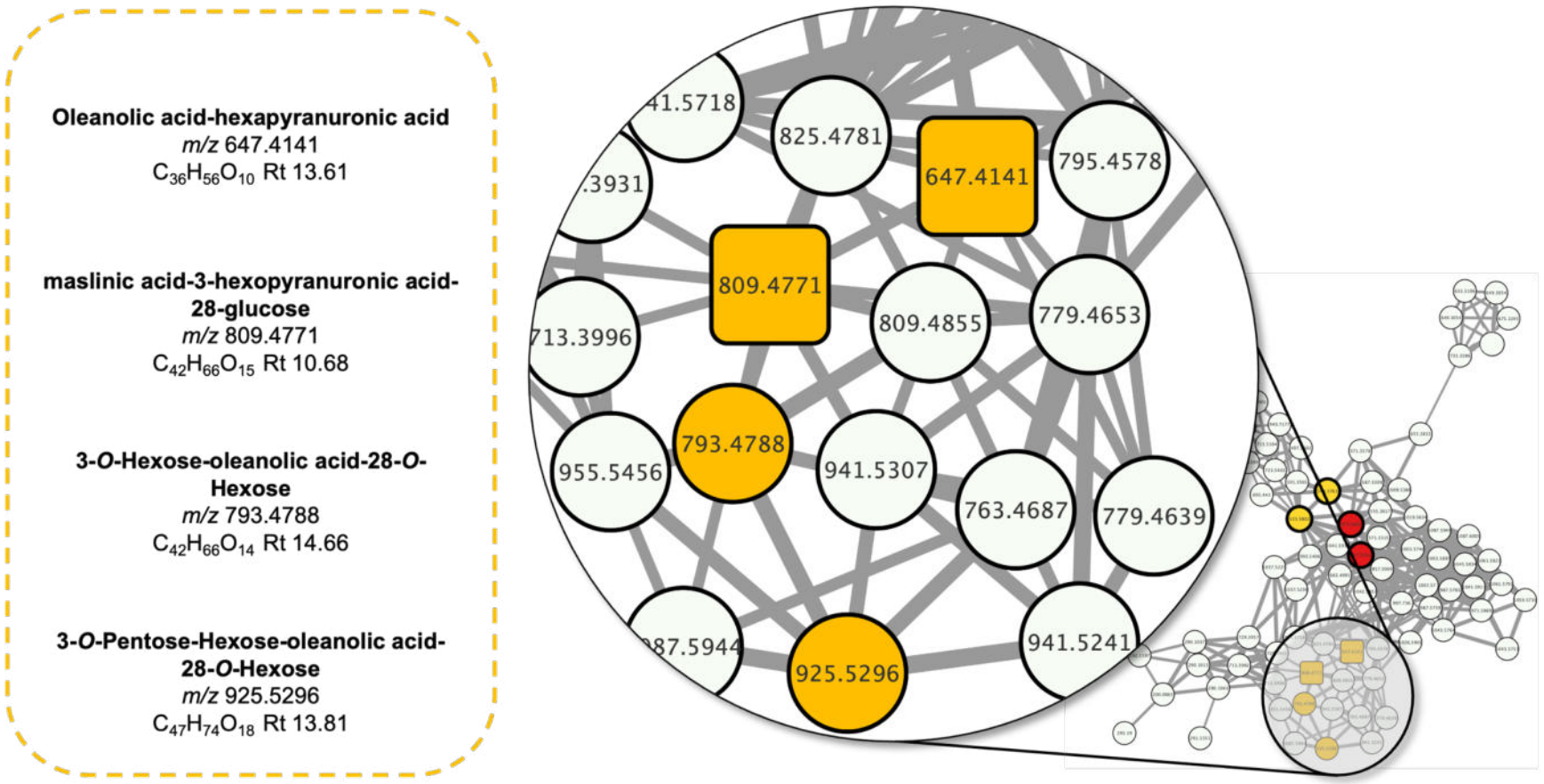

Figure 60. Overview of N-2 subnetwork (oleanane centellosides-like molecules). Identified metabolites by structure prediction based on their high-resolution mass and fragmentation spectrum are coloured.

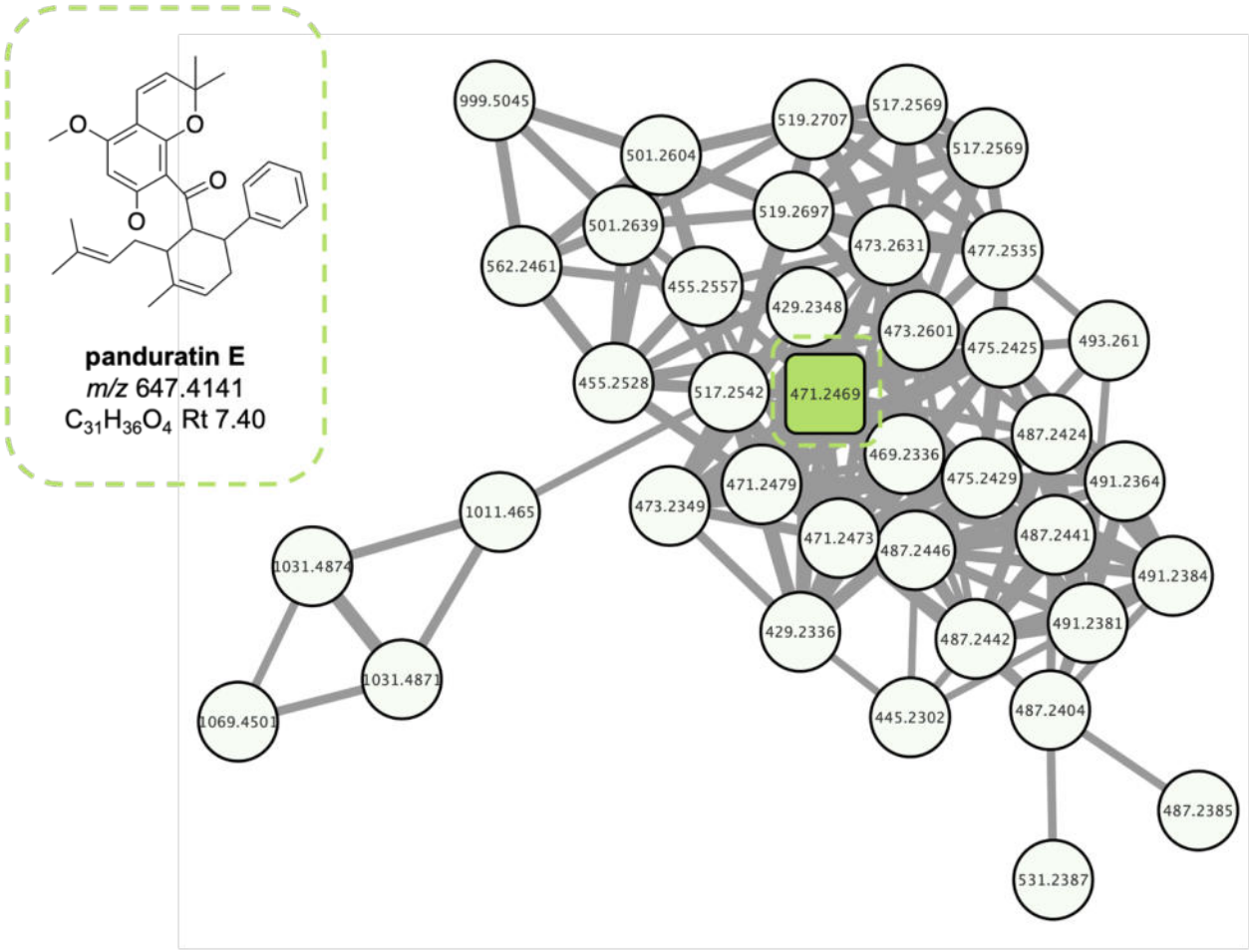

Figure 61. Overview of N-3 subnetwork (chalcones). Identified metabolites by structure prediction based on their high-resolution mass and fragmentation spectrum are coloured.

Cytoscape allows the attachment of the quantification data from the different samples and to project them onto the nodes as pie charts. The relative amount of each of the peaks corresponding to the nodes in the 4 annotated clusters is then presented in Figures 62-64. Moreover, for each figure, 4 subfigures were constructed representing the state of the production from day 4 to 16 after the elicitation. Thus, the relative production of each node can be analysed following the time-course of the experimental design. Overall, some nodes are only coloured with the relative production of the ion under elicitation conditions as the amount of the peak under Control conditions was as low that it cannot be observed in the pie chart. This shows that some compounds are only (or mainly) produced under elicitation conditions.

In cluster N-1, MeJA induces the production of phenolics in a very early manner. And clearly, elicitors enhance the diversity of compounds produced (Figure 62).

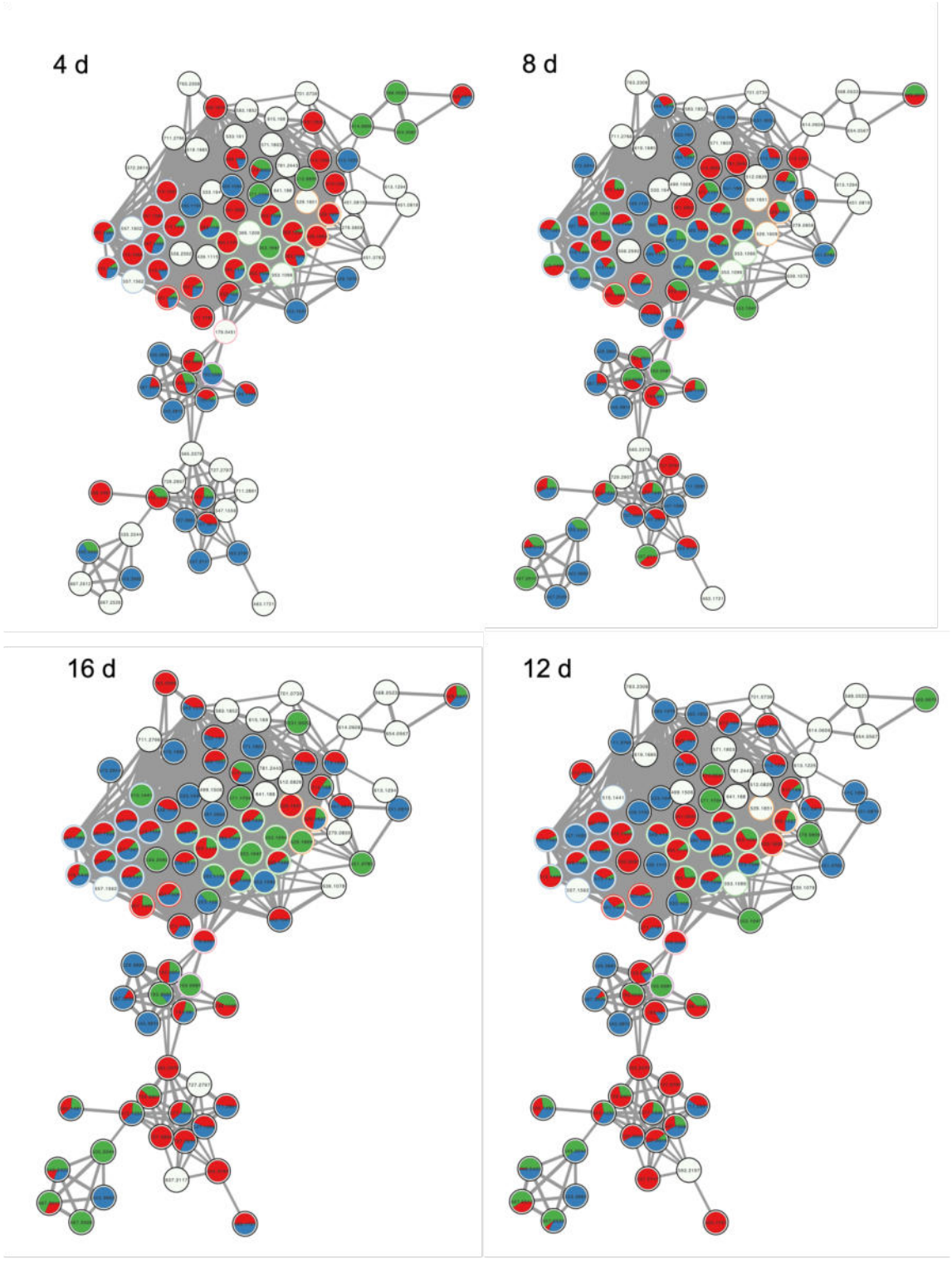

Figure 62. Molecular networking of N-1 (CQA-like molecules) relative production each day of harvesting in control (green) conditions or elicited with MeJA (red) or CORO (blue)

As shown un cluster N-2, most of the triterpenes are exclusively produced under CORO treatment: it is the case for all the non-annotated saponins (high masses on the right of the cluster). Also, it is clear that for those compounds produced in all conditions, CORO accelerates the expression of their biosynthesis. However, MeJA is also interesting for the production of some compounds not found in other conditions (left side).

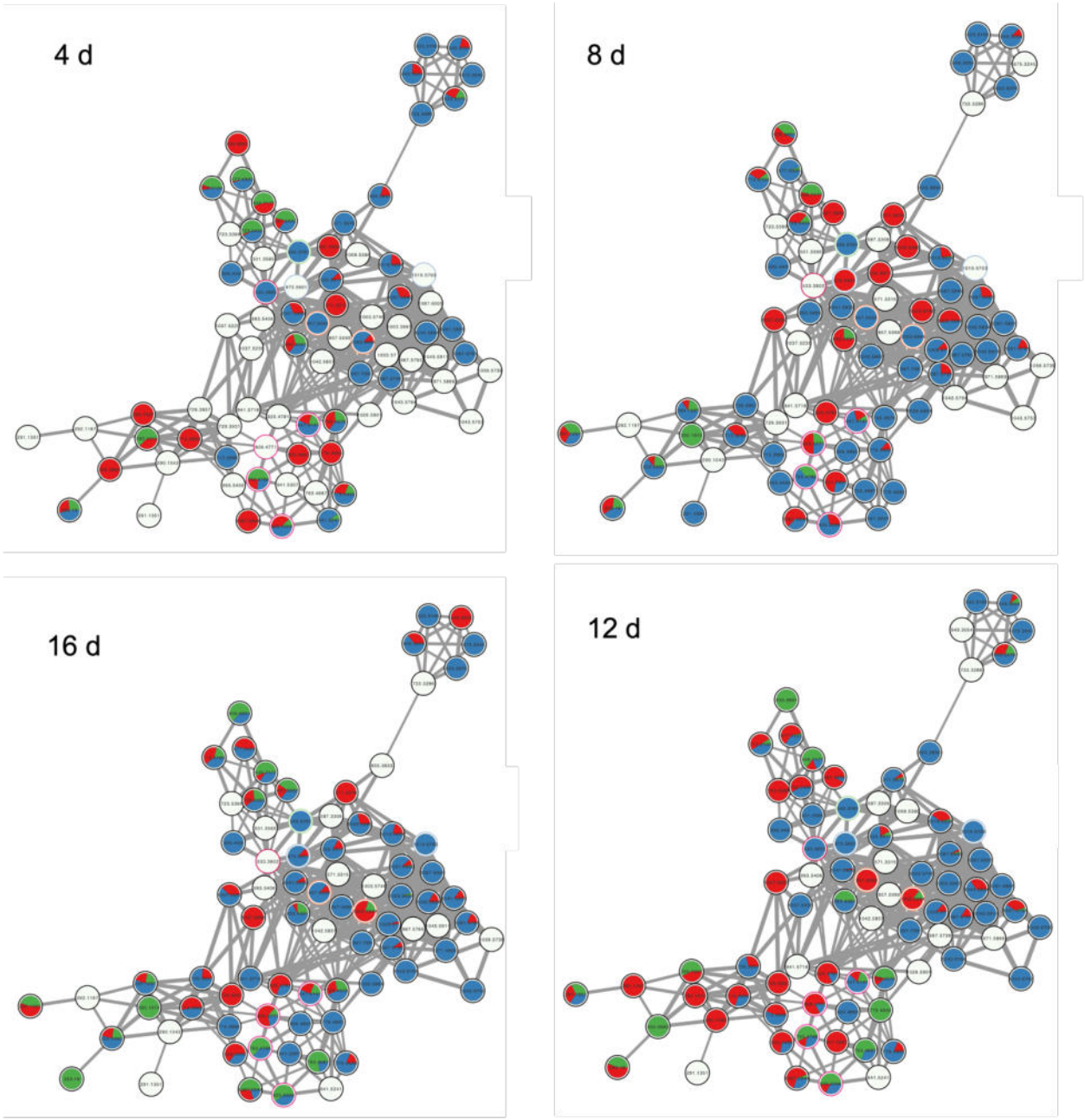

Figure 63. Molecular networking of N-2 (centellosides-like molecules) relative production each day of harvesting in control (green) conditions or elicited with MeJA (red) or CORO (blue)

In N-3 (Figure 64), it is observed that compounds produced at early stages of the culture. There is not clear distinction between the treatment. Most of the compounds can be found under the 3 conditions, at a moment or another, even if we could say that CORO is not favourable for the production of these compounds. Then, it is quite surprising that none of these putative chalcones has been previously described in *C. asiatica*, as there is a high chemical diversity. It can be hypothetisez that these family of compounds are produced only in HRs and not in cell cultures or *in planta*.

These MNs heralds the potential for further exploration of the metabolism of CORO and MeJA-elicited HRs of *C. asiatica*.

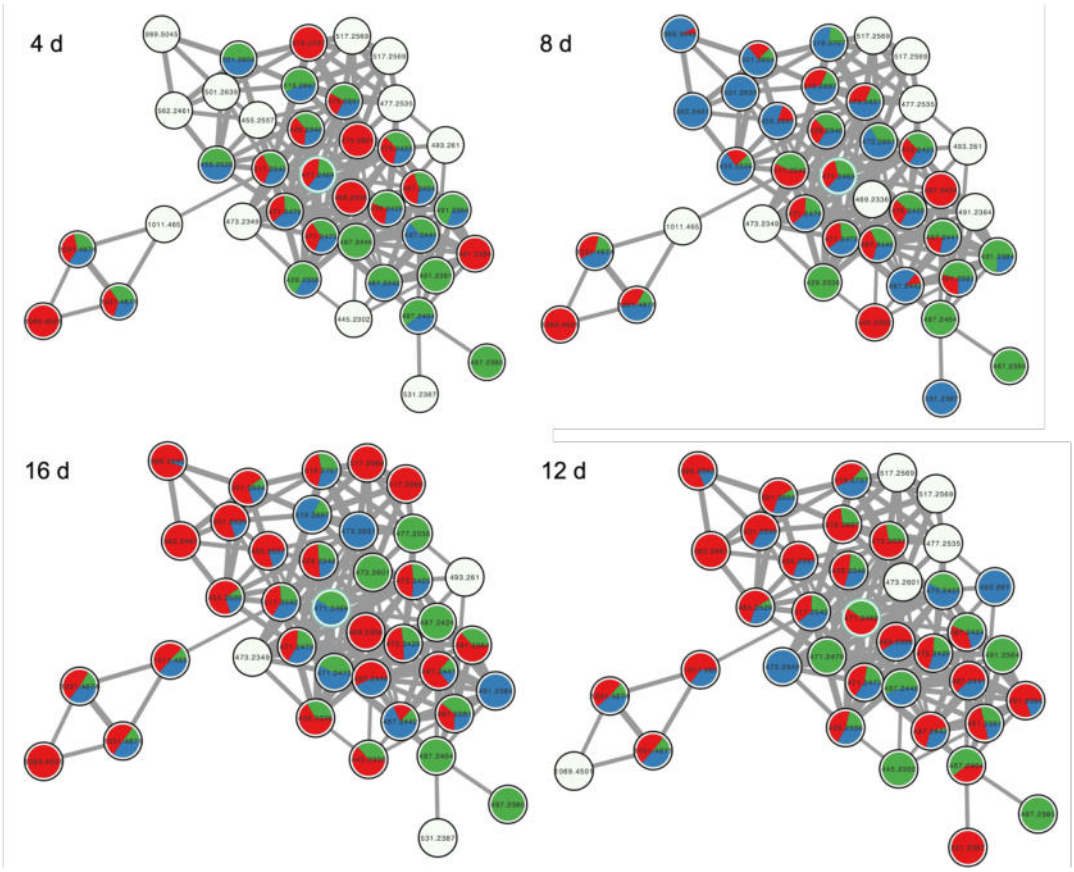

Figure 64. Molecular networking of N-3 (chalcones-like molecules) relative production each day of harvesting in control (green) conditions or elicited with MeJA (red) or CORO (blue)

4.2.3.1.2. Study of the reprogramming effect of CORO on the metabolism

One of the most remarkable hypotheses derived from the PCA was the separation of samples collected 4 days after elicitation with CORO from the rest. Moreover, the HCA indicated that at 4 days after elicitation with CORO there is a strong and unique reprogramming effect on the metabolism. This phenomenon was also observed but in a lower manner with MeJA and the MN quantitative

analysis showed that it seemed to be focused on phenolics. To simplify the study of this phenomenon, an OPLS-DA was performed with the aim of extracting the VIPs which significantly discriminated the treated samples from the control at that time (Figure 65). The OPLS-DA analyses were performed with the samples treated with each elicitor separately on the Pareto-scaled data matrix. Both 2D graphs showed the separation between the control samples and each elicitor-treated sample. This shows that at day 4 the elicitors were able to produce differential changes with respect to the Control. Figure 66 shows the 15 TOP VIPs for each analysis, including their annotation and/or their membership in each cluster of the global MN.

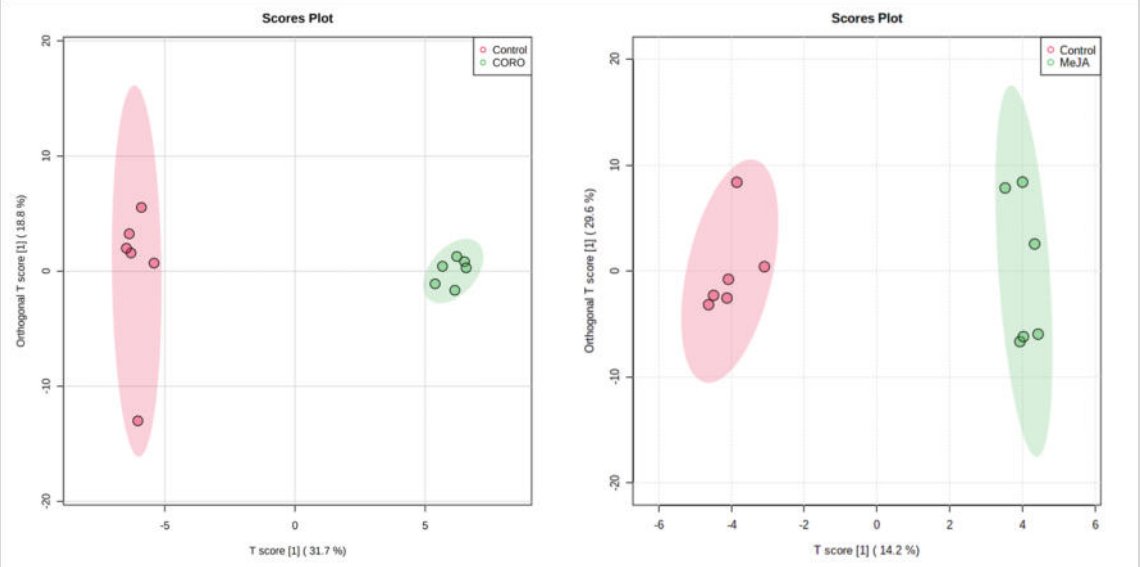

Figure 65. Score plot of OPLS-DA analyses of the UHPLC-MS/MS-derived data of the HRs samples harvested after 4 days of elicitation with CORO (left) and MeJA (right)

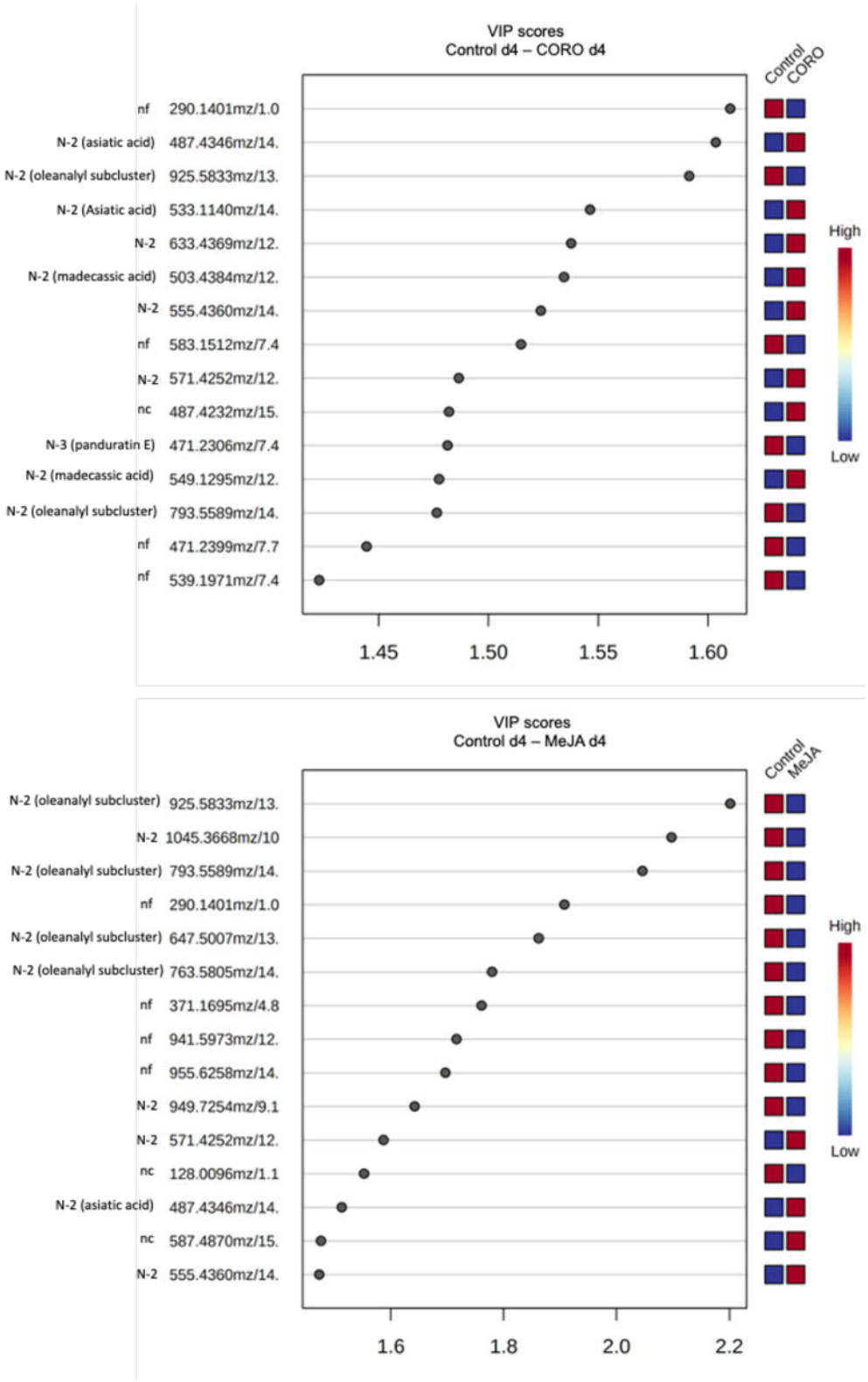

Figure 66. Top 15 VIPs of the OPLS-DA models Control d4 vs. CORO d4 (above) and Control d4 vs. MeJA d4 (below). Features are identified with either their network annotation, annotation, nc = not networked, nf = not fragmented

Among the 15 VIPs form the Control vs CORO OPLS-DA, 9 metabolites belonged to the N-2 cluster, including AD, MD, AA (both $[M-H]^-$ and $[M+FA-H]^-$ molecular ions), MA (both $[M-H]^-$ and $[M+FA-H]^-$ molecular ions), and two ions from the oleanane subnetwork and two other unclustered metabolites. As the two putative oleanane-like centelloside ions were automatedly annotated by GNPS, we performed a more in-depth analysis of these ions: they showed a $[M-H]^-$ peak at *m/z* 925.5833 and *m/z* 793.5589 respectively. Their MS/MS spectra were similar both producing a base peak ion at *m/z* 455 (Figure 67).

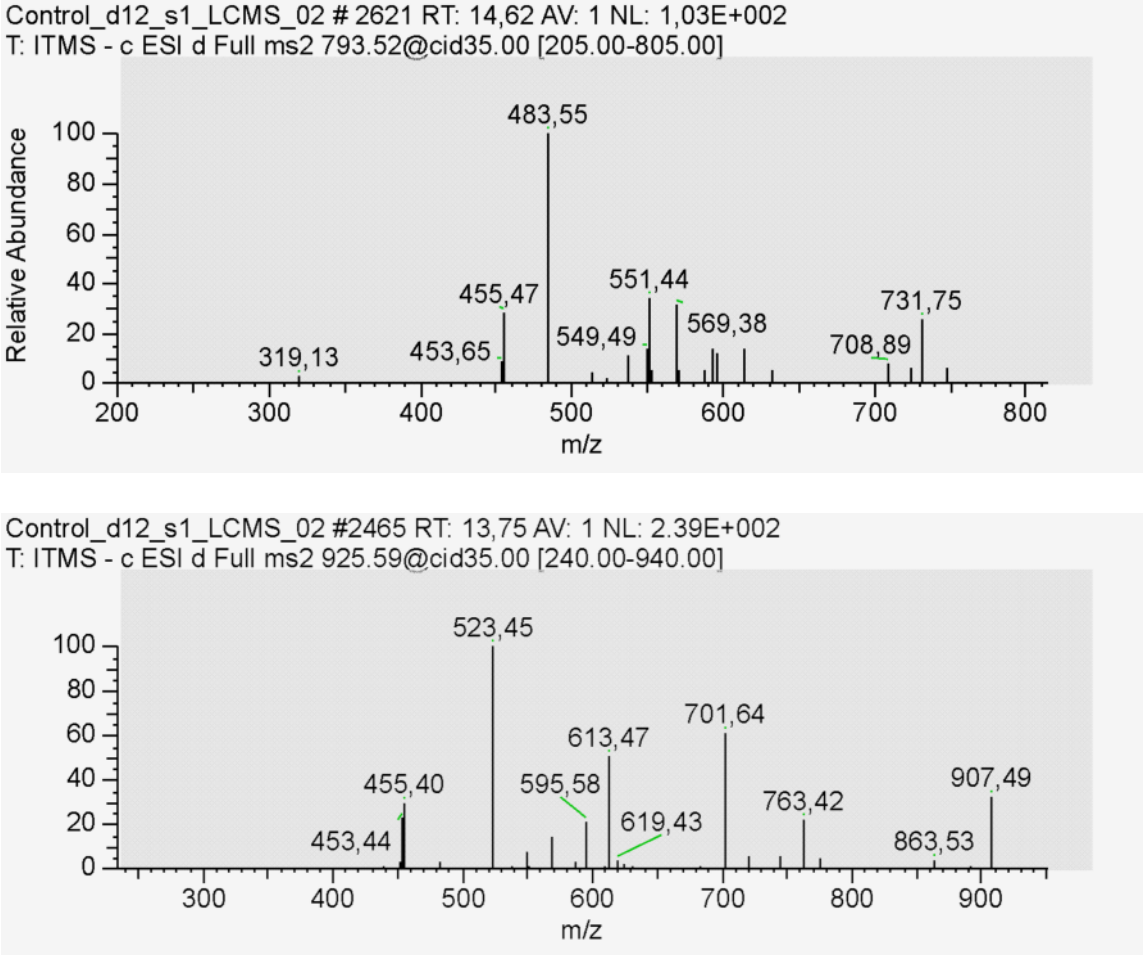

Figure 67. MS/MS spectra of ions at *m/z* 793 (above) and 925 (below)

The hypothesis that they are oleanane-like centellosides was confirmed by similar MS/MS spectrum data with the ion at *m/z* 925 described in the phytochemical study of *Chenopodium quinoa* (249). Then, features at *m/z* 925 and 793 were definitively annotated as oleanane-like saponins (Table 14). Other compounds of interest were also further analysed. Overall, the VIPs were mostly centelloside-like molecules. Their production was up-regulated by CORO except for the oleanane-type saponins ions at *m/z* 925 and *m/z* 793, for which the production was clearly repressed by the elicitor treatment (Figure 68). The same was observed for panduratin E, with a lower production in CORO samples. Chalcones, like panduratin E, are phenolic compunds derived from a mixed biosynthesis between polyketides (derived from the acetate-malonate pathway) together with cinnamic acids. They are intermediates products of the biosynthesis of flavonoids (251). The NMR analysis showed that CORO caused a significant increase in malonate, the early precursor of polyketides. It could be hypothesised that CORO activates the flavonoid pathway causing panduratin E to be consumed, since. It is an intermediate metabolite in the biosynthesis of flavonoids. In the present work, flavonoids were not detected in the analysis. Thereby, CORO could be redirecting mevalonate to other pathways or HRs are unable to produce the flavonoids. The redirection could be the mevalonate pathway towards the biosynthesis of triterpenes. As described in Table 2, several flavonoids have been found in various tissues of *C. asiatica*. However, most of them have been found *in planta*. While there are no data on the phytochemical profile in HRs, in MeJA-treated suspension cell cultures it has been observed that the production of flavonoids is decreased (198).

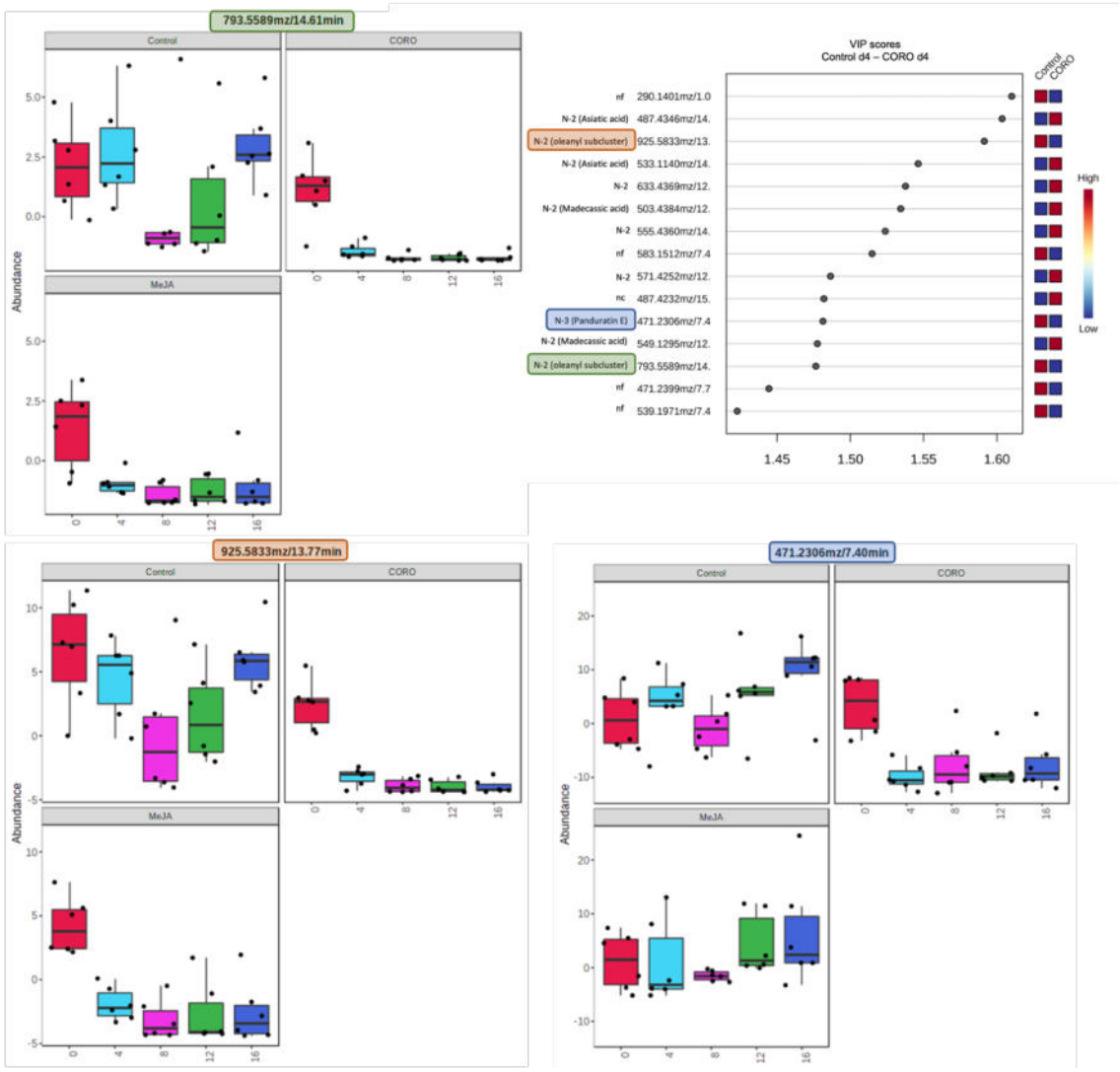

Figure 68. Bloxplot of the time course normalised relative abundance of the ions at *m/z* 925.5833, 793.5589 and 471.2306 (panduratin E).

The VIPs obtained from OPLS-DA with the MeJA-treated samples at day 4 showed 4 down-regulated oleanane-like centellosides, 3 up-regulated centellosides ions (one being AA), 1 down-regulated non-clustered ion and 4 non-fragmented ions. The fact that only AA appeared in the list of top VIPs suggests that CORO is able to more rapidly activate the production of the 4 major

centellosides than MeJA does. Similarly to CORO, oleanane-like centellosides appeared as VIPs showing that MeJA may also downregulate this branch of the pathway in favour of ursane-like centellosides. However, the ability of CORO to induce ursane-like molecules would be greater. This is consistent with data from the targeted metabolomics approach in which CORO elicited significantly higher production of the 4 major centellosides than MeJA.

It seems then that CORO and MeJA drive the synthesis flux to the ursane pathway rather than the oleanane pathway through a very precise regulation within the triterpene pathway.

4.2.3.1.3. Correlation analysis of the elicitors

To go further on the confirmation of this hypothesis, an elicitor correlation analysis was performed. The MetaboAnalyst module of Correlation Analysis allowed the obtention of the 25 most elicitor-sensitive features either up- or down-regulated for both elicitation treatments (Figure 69).

The elicitor correlation study of the MeJA samples revealed di-CQAs as the main metabolites positively correlated. Among the enlisted correlated features were not MD, AD, but two ions from the N-2. On the other hand, the down-regulated features were 3 ions found in the oleanane-type saponin subnetwork. On the other hand, CORO positively correlated features were MD, AD and its respective sapogenins, 4 ions of the N-2 and 1 di-caffeoylquinic acid. The most down-regulated ions were 5 ions belonging to the oleanane-type centellosides

subnetwork, 4 ions from N-3 including panduratin E, and an ion from N-4 annotated as 3-benzoyloxy-2-hydroxypropyl-β-D-glucopyranosiduronic acid. Generally, it was observed again that both elicitors could downregulate the oleanane pathway, especially CORO.

Correlation analyses were then performed on specific metabolites. The features correlated with AA (Figure 70a) and MA (Figure 70b) in the CORO-treated samples were features from the N-2. On the other hand, all the inversely correlated ions were oleanane-type centelloside subnetwork ions. The latter fact reinforces the idea of the movement of carbon flux towards the ursane and not the oleanane pathway. In the case of the positively correlated ions with the AD (Figure 70c) and MD (Figure 70d) in CORO treatment, almost all were from the N-2 with *m/z* above 900. It could indicate a positive correlation with saponins since they usually offer higher *m/z*. The same analysis was performed on the MeJA-treated samples and yielded results very similar to those of CORO (Figure 71a-d).

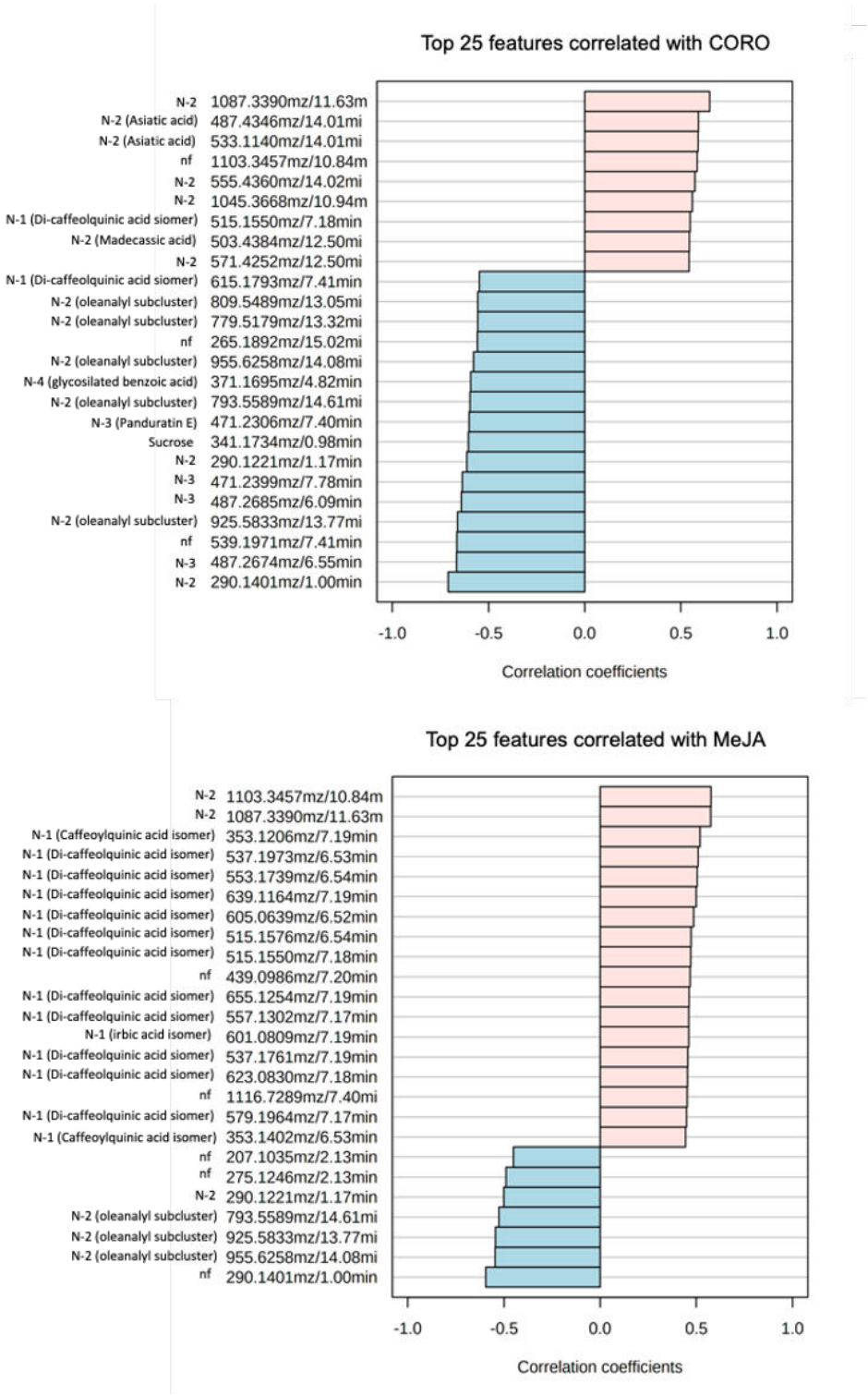

Figure 69. Features positively or negatively correlated with the elicitation with CORO (above) or MeJA (below). Features are identified with either their network annotation, annotation, nc = no networked, nf = no fragmented

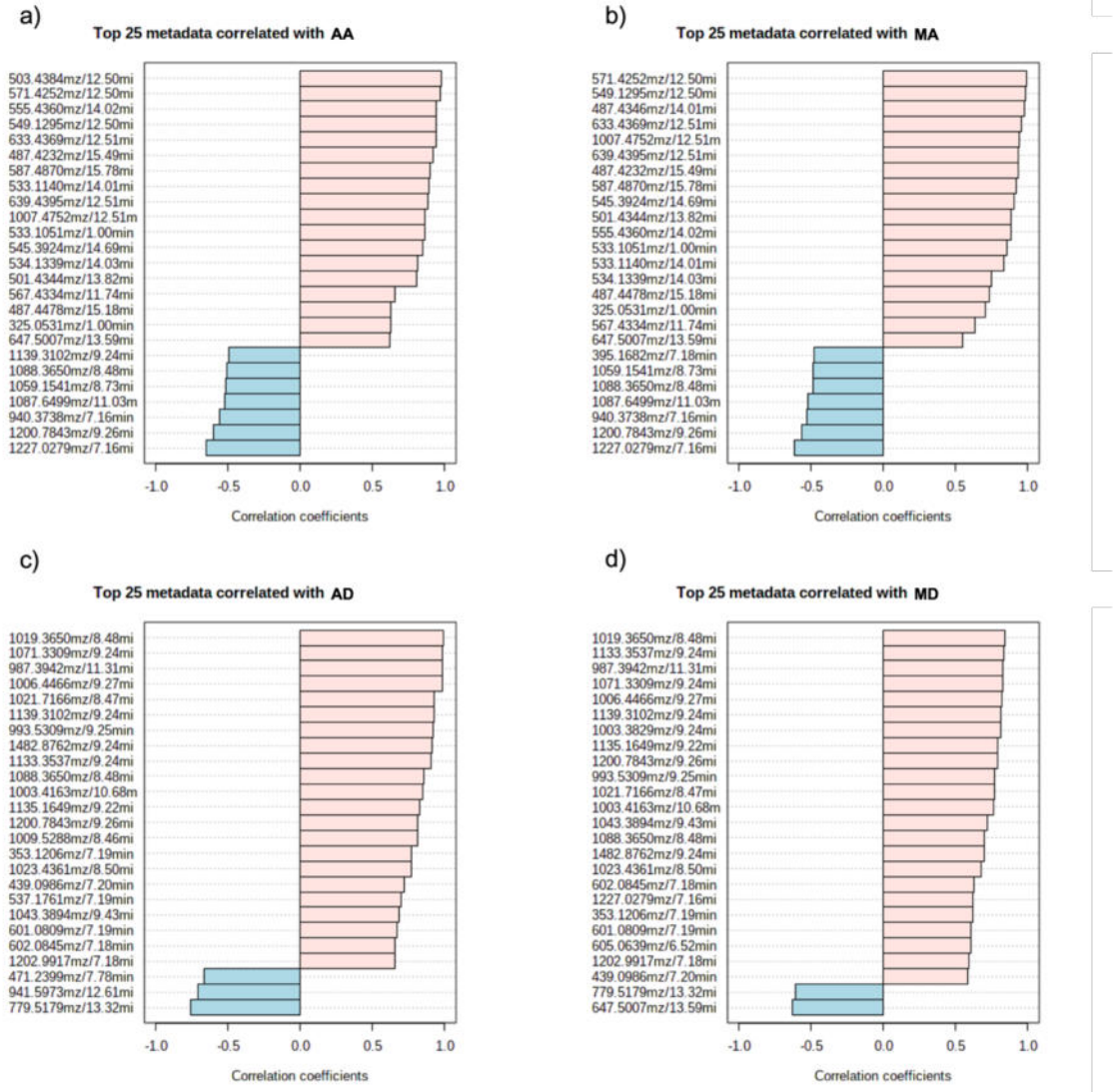

Figure 70. Features positively or negatively correlated with the production of AA (a) MA (b) AD (c) and MD (d) under CORO elicitation during all the experiment.

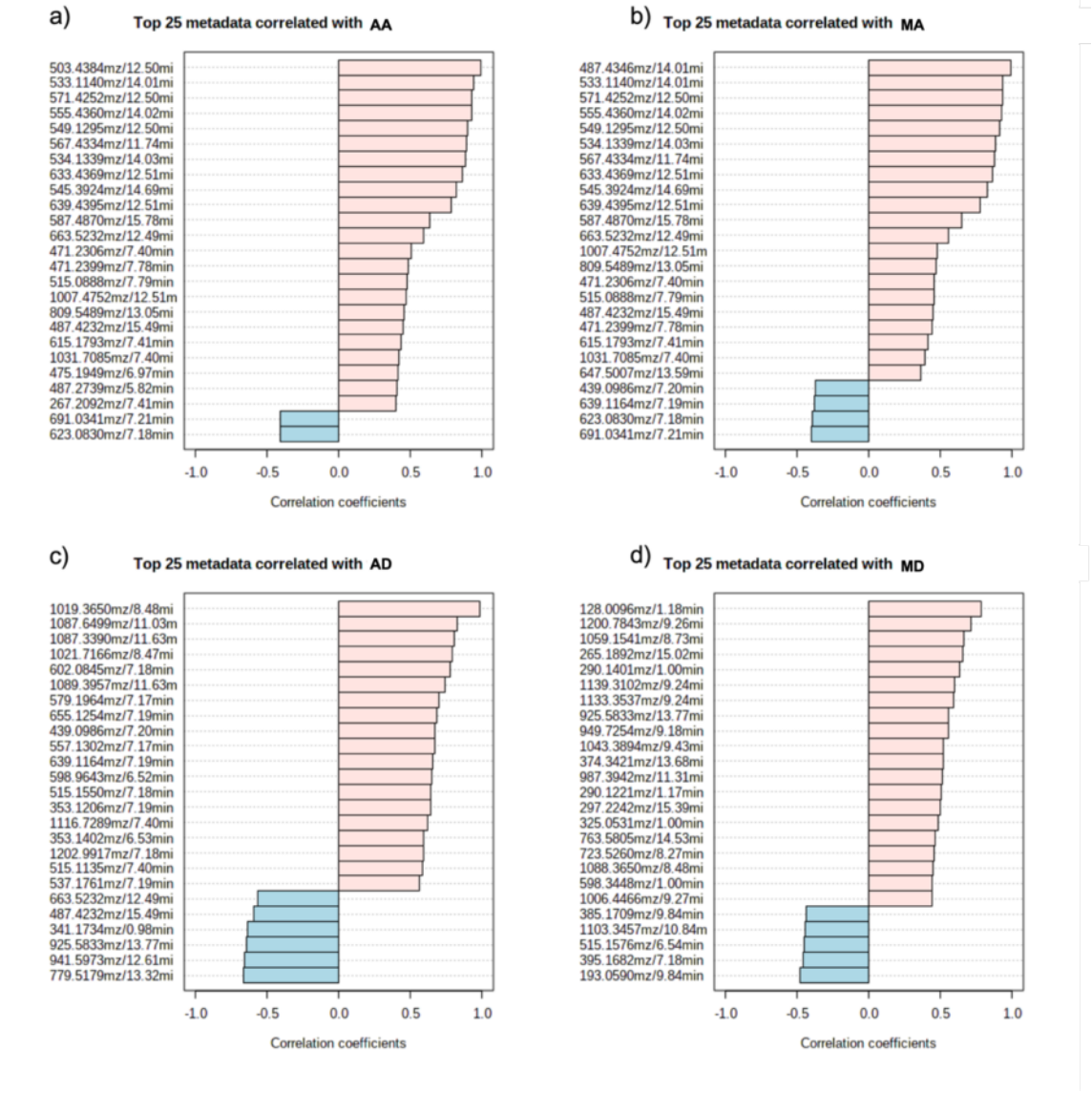

Figure 71. Features positively or negatively correlated with the production of AA (a) MA (b) AD (c) and MD (d) under MeJA elicitation during all the experiment.

4.2.3.1.4. Correlation analysis of the time of harvesting

It results difficult to explain the inhibition of the putatively annotated oleanane-type centelloside ions. In *C. asiatica*, the OxidoSqualene Cyclase

(OSC) named as α/βAS has been described as responsible for cyclising the 2,3-oxidosqualene into α-amyrin (ursane skeleton) and β-amyrin (oleanane skeleton) at the same time (197,252,253). The regulation of this enzyme remains unknown. There is only evidence regarding the expression of the gene encoding α/βAS, investigated in two studies. The use of MeJA in a different HR line (142), and the use of MeJA and CORO in the same root line as used in this study (157) increased the expression of the gene. Plants typically contain a dozen of OSCs that catalyse the cyclisation reaction to triterpenes reaching different products (254). CORO and/or MeJA could then regulate some others OSCs not yet found in *C. asiatica*. After the formation of the triterpene products, these are tailored by oxidations and glycosylations. The oleanane-like ions dereplicated in this study were putatively annotated as saponins. Therefore, it is suggested that elicitation may inhibit one of these enzymes downstream of the pathway. To explore this hypothesis, we looked for ions in the chromatograms that might belong to non-glycosylated oleanane-like aglycones. For this purpose, it was considered that the ursane-oleanane pathway is symmetrical and that structural isomers can be found with the only difference being the methyl substitution positions on C-19 and C-20. Isobaric ions of AA and MA were effectively found in LC-HRMS/MS profiles with different Rt: *m/z* 487.3691 with Rt 15.47 and *m/z* 503.3640 with Rt 12.96. These ions were found as unpaired nodes in none of the molecular networks, and only the relative abundance data for the ion at *m/z* 487.3691 with an Rt of 15.47 could be retrieved. Its fragmentation spectrum showed no similarities with AA suggesting that it could not be an analogue of it with an oleanane skeleton (data

not shown). Therefore, these data do not allow us to consider the possibility that CORO inhibits the glycotransferase that form the saponins on this side of the branch. In contrast, these results suggested that CORO could inhibit the entire oleanane pathway. However, it is worth considering that plants produce different glycotransferases (254) and in *C. asiatica* only one has been described. Transcriptomic study of this pathway and identification of new enzymes of the centelloside pathway is imperative. This could shed light on the regulation of the centelloside pathway.

HCA revealed time-course production patterns for CORO samples (Figure 72). CQAs and di-CQAs seemed to be produced from day 8 until day 16. The inhibition of oleanane-type centellosides after 4 days of elicitation was observed. Moreover, CORO inhibited the production of features belonging to cluster N-3 since the beginning of the experiment.

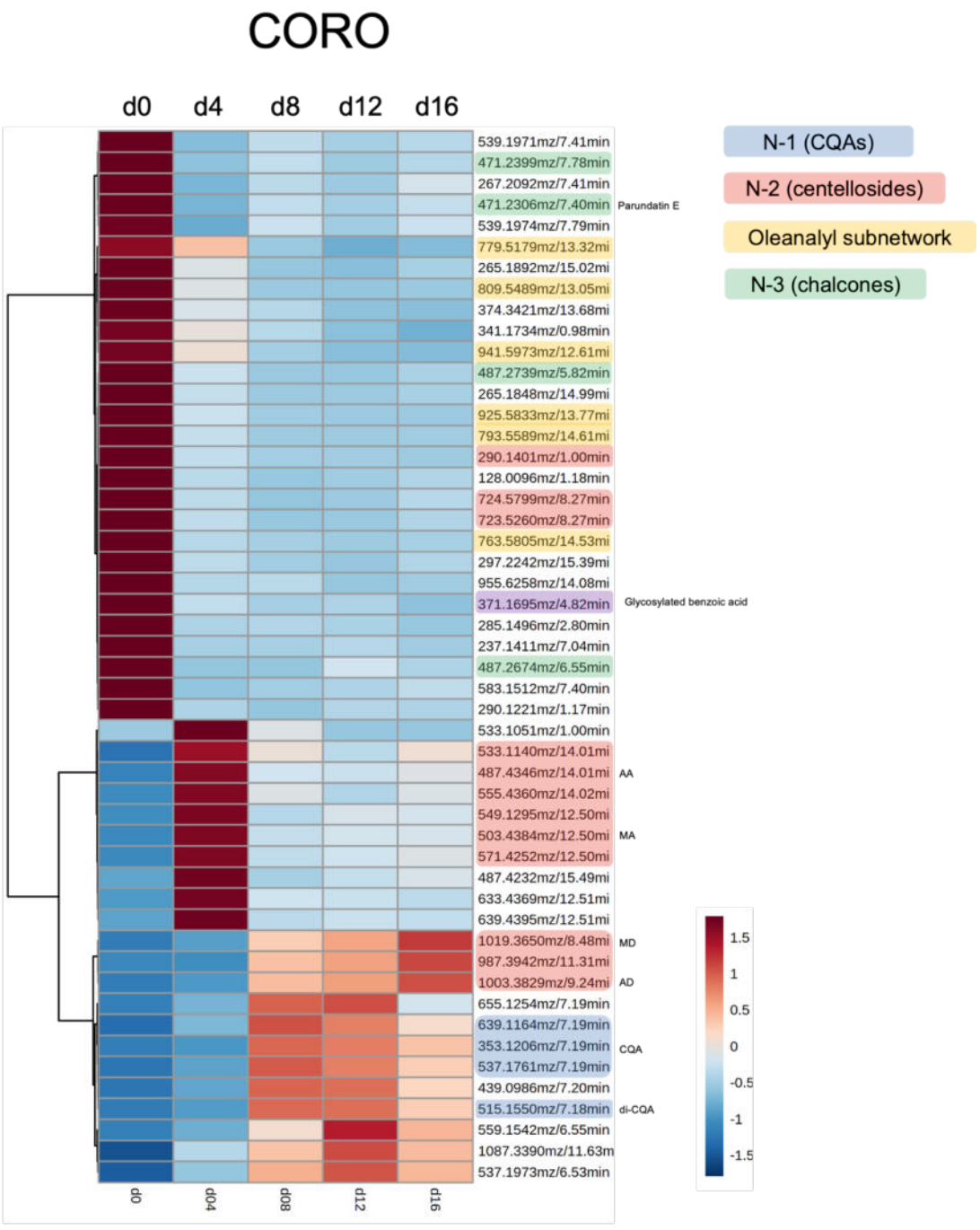

Figure 72. Hierarchical Clustering Analysis (HCA) of the most significantly (*p*-value < 0.005) features (figured by their *m/z* ratio and their retention time Rt) for CORO and represented on a heatmap (ranging from red colour for high AUC (area under the curve) to blue for low abundance).

CHAPTER 5

5. CONCLUSIONS

1. The primary metabolism is affected by both elicitors, but CORO triggered an earlier and superior reprogramming effect than MeJA.

2. The analysis of the NMR signals allowed the identification of 40 compounds including 4 specialised metabolites: 3 CQAs and ferulic acid.

3. CORO and MeJA caused a significant consumption of carbohydrates and some amino acids compared to control. At the same time, the concentration of CQAs and ferulic acid were significatively higher under both elicitations.

4. CORO triggered significant higher concentration of total CQAs only at day 12 after elicitation.

5. The concentration of certain primary metabolites such as GABA or succinate, were significatively affected by elicitation as a possible response to ameliorate the stress provoked by elicitation.

6. The UHPLC-MS/MS method was optimised obtaining proper resolution between the peaks corresponding to centellosides.

7. The signal intensity of standard compounds was better in the ESI negative mode then in the ESI positive mode.

8. The UHPLC-MS/MS-based targeted metabolomics analysis permitted the annotation of 12 metabolites including sucrose, different CQAs, AA, MA, AD, and MD.

9. As observed in the NMR analysis, CORO and MeJA significatively increased the levels of CQAs at day 8 after elicitation compared to the control samples.

10. Between the elicitors, the relative abundance of most of CQAs detected was only significatively higher after 12 days of CORO elicitation then MeJA.

11. CORO significatively increased levels of AA, MA, AD and, MD during the complete time-course compared to MeJA and control samples.

12. UHPLC-MS/MS untargeted metabolomics suggested an elicitation-derived reprogramming effect on the specialised metabolism. However, CORO caused major changes in the specialised metabolism after 4 days.

13. CORO and MeJA stimulated the activation of the specialised metabolism in a different manner.

14. Molecular Networks derived from the UPLC-HRMS/MS data showed that,

under the experimental conditions, the HRs of *C. asiatica* produce mostly CQAs, centellosides, chalcones and their derivatives. Most of the modelled ions in the MN have never been described in *C. asiatica*. Chemical diversity is far away more important than that is found in the databases.

15. Oleanane-type centellosides were annotated for the first time in *C. asiatica*.

16. Both elicitors could inhibit the oleanane-branch of the centelloside pathway. CORO could inhibit the production of chalcones.

17. The production of ursane-type centellosides seems to be superior and earlier under CORO elicitation. However, MeJA could activate the production of CQAs earlier than CORO.

18. The methanolic extraction was sufficient to detect the most relevant metabolites found in the HR of *C. asiatica*.

CHAPTER 6

6. PERSPECTIVES

1. The use of standard compounds corresponding to both ursane- and oleanane-type centellosides will contribute to better explore the regulation between these two branches of the centelloside pathway.

2. To perform MS-guided isolation of centellosides analogues detected in the N-2 cluster; to determine their structure using MS/MS and NMR spectroscopy; and to test them for biological activities.

3. To go deeper in the annotation of the N-3 cluster nodes (here putatively annotated as “chalcone network”) by MS^n fractionation, annotation propagation, or by the subsequent isolation and structure determination of the molecules.

4. To analyse the extracts by Gas Chromatography Mass Spectrometry to detect sesquiterpenes and sterols and to study their regulation under elicitation.

5. To perform a time-course transcriptomics approach using CORO and MeJA to explore the expression of key genes and their role in the regulation of the centellosides and other triterpenes pathway.

REFERENCES

1. Long HS, Stander MA, Van Wyk BE. Notes on the occurrence and significance of triterpenoids (asiaticoside and related compounds) and caffeoylquinic acids in *Centella* species. South African J. Bot. 2012;82:53–9.
2. Brinkhaus B, Lindner M, Schuppan D, Hahn EG. Chemical, pharmacological and clinical profile of the East Asian medical plant *Centella asiatica*. Phytomedicine. 2000;7(5):427–48.
3. Biswas D, Mandal S, Chatterjee Saha S, Tudu CK, Nandy S, Batiha GES, *et al*. Ethnobotany, phytochemistry, pharmacology, and toxicity of *Centella asiatica* (L.) Urban: A comprehensive review. Phyther. Res. 2021;35(12):6624–54.
4. Singh S, Gautam A, Sharma A, Batra A. *Centella asiatica* (L.): A plant with immense medicinal potential but threatened. Int. J. Pharm. Sci. Rev. Res. 2010;4(2):9–17.
5. European Medicines Agency. Assessment report on *Centella asiatica* (L.) Urban, herba [Internet]. London; 2010.
6. Gallego A, Ramirez-Estrada K, Vidal-Limon HR, Hidalgo D, Lalaleo L, Khan Kayani W, *et al*. Biotechnological production of centellosides in cell cultures of *Centella asiatica* (L) Urban. Eng. Life Sci. 2014;14(6):633–42.
7. Jamil S, Nizami Q, Salam M. *Centella asiatica* (Linn.) Urban. A Review. Nat. Prod. Radiance. 2007;6(2):158–70.
8. Bylka W, Znajdek-Awizeń P, Studzińska-Sroka E, Brzezińska M. *Centella asiatica* in cosmetology. Postep Derm Alergol. 2013;30(1):46–9.
9. Farnsworth NR, Fong HHS, Mahady GB, editors. Herba Centellae. In: WHO monographs on selected medicinal plants - Vol 1. Geneva: WHO Graphics; 1999. p. 77–86.
10. James J, Dubery I. Identification and quantification of triterpenoid centelloids in *Centella asiatica* (L.) Urban by densitometric TLC. J. Planar Chromatogr. - Mod. TLC. 2011;24(1):82–7.
11. Arpaia MR, Ferrone R, Amitrano M, Nappo C, Leonardo G, Del Guercio R. Effects of *Centella asiatica* extract on mucopolysaccharide metabolism in subjects with varicose veins. Int. J. Clin. Pharmacol. Res. 1990;10(4):229–33.
12. Wu F, Bian D, Xia Y, Gong Z, Tan Q, Chen J, *et al*. Identification of major active ingredients responsible for burn wound healing of *Centella asiatica* herbs. Evidence-based Complement. Altern. Med. 2012;2012(848093).
13. Pan Y, Abd-Rashid BA, Ismail Z, Ismail R, Mak JW, Pook PCK, *et al*. In vitro modulatory effects on three major human cytochrome P450 enzymes by multiple active constituents and extracts of *Centella asiatica*. J. Ethnopharmacol. 2010;130(2):275–83.
14. Coldren CD, Hashim P, Ali JM, Oh S-K, Sinskey AJ, Rha C. Gene expression changes in the human fibroblast induced by *Centella asiatica* triterpenoids. Planta Med. 2003;69(8):725–32.

15. Maquart FX, Bellon G, Gillery P, Wegrowski Y, Borel JP. Stimulation of collagen synthesis in fibroblast cultures by a triterpene extracted from *Centella asiatica*. Connect. Tissue Res. 1990;24(2):107–20.
16. Luo Y, Yang Y-P, Liu J, Li W-H, Yang J, Sui X, *et al*. Neuroprotective effects of madecassoside against focal cerebral ischemia reperfusion injury in rats. Brain Res. 2014;1565:37–47.
17. Nataraj J, Manivasagam T, Justin Thenmozhi A, Essa MM. Neuroprotective effect of asiatic acid on rotenone-induced mitochondrial dysfunction and oxidative stress-mediated apoptosis in differentiated SH-SYS5Y cells. Nutr. Neurosci. 2017;20(6):351–9.
18. Sharifi-Rad M, Lankatillake C, Dias DA, Docea AO, Mahomoodally MF, Lobine D, *et al*. Impact of Natural Compounds on Neurodegenerative Disorders: From Preclinical to Pharmacotherapeutics. J. Clin. Med. 2020;9(4):1061.
19. Shinomol GK, Muralidhara. Effect of *Centella asiatica* leaf powder on oxidative markers in brain regions of prepubertal mice in vivo and its in vitro efficacy to ameliorate 3-NPA-induced oxidative stress in mitochondria. Phytomedicine. 2008;15(11):971–84.
20. Viswanathan G, Dan VM, Radhakrishnan N, Nair AS, Rajendran Nair AP, Baby S. Protection of mouse brain from paracetamol-induced stress by *Centella asiatica* methanol extract. J. Ethnopharmacol. 2019;236:474–83.
21. Jiang W, Li M, He F, Bian Z, He Q, Wang X, *et al*. Neuroprotective effect of asiatic acid against spinal cord injury in rats. Life Sci. 2016;157:45–51.
22. Arora R, Kumar R, Agarwal A, Reeta KH, Gupta YK. Comparison of three different extracts of *Centella asiatica* for anti-amnesic, antioxidant and anticholinergic activities: in vitro and in vivo study. Biomed. Pharmacother. 2018;105:1344–52.
23. Shinomol GK, Muralidhara. Prophylactic neuroprotective property of *Centella asiatica* against 3-nitropropionic acid induced oxidative stress and mitochondrial dysfunctions in brain regions of prepubertal mice. Neurotoxicology. 2008;29(6):948–57.
24. Gray NE, Zweig JA, Murchison C, Caruso M, Matthews DG, Kawamoto C, *et al*. *Centella asiatica* attenuates A-induced neurodegenerative spine loss and dendritic simplification. Neurosci. Lett. 2017;646:24–9.
25. Gray NE, Alcazar Magana A, Lak P, Wright KM, Quinn J, Stevens JF, *et al*. *Centella asiatica*: phytochemistry and mechanisms of neuroprotection and cognitive enhancement. Phytochem. Rev. 2018;17(1):161–94.
26. Zhang X, Wu J, Dou Y, Xia B, Rong W, Rimbach G, *et al*. Asiatic acid protects primary neurons against C 2-ceramide- induced apoptosis. Eur. J. Pharmacol. 2012;679(1–3):51–9.
27. Xu CL, Wang QZ, Sun LM, Li XM, Deng JM, Li LF, *et al*. Asiaticoside: Attenuation of neurotoxicity induced by MPTP in a rat model of Parkinsonism via maintaining redox balance and up-regulating the ratio of Bcl-2/Bax. Pharmacol. Biochem. Behav. 2012;100(3):413–8.
28. Murakami T, Yamane H, Tomonaga S, Furuse M. Forced swimming and imipramine modify plasma and brain amino acid concentrations in mice. Eur. J. Pharmacol. 2009;602(1):73–7.

29. Gray NE, Morré J, Kelley J, Maier CS, Stevens JF, Quinn JF, *et al*. Caffeoylquinic acids in *Centella asiatica* protect against amyloid-β toxicity. J. Alzheimer's Dis. 2014;40(2):359–73.
30. Xu MF, Xiong YY, Liu JK, Qian JJ, Zhu L, Gao J. Asiatic acid, a pentacyclic triterpene in *Centella asiatica*, attenuates glutamate-induced cognitive deficits in mice and apoptosis in SH-SY5Y cells. Acta Pharmacol. Sin. 2012;33(5):578–87.
31. Bobade V, Bodhankar SL, Aswar U, Vishwaraman M, Thakurdesai P. Prophylactic effects of asiaticoside-based standardized extract of *Centella asiatica* (L.) Urban leaves on experimental migraine: Involvement of 5HT1A/1B receptors. Chin. J. Nat. Med. 2015;13(4):274–82.
32. Chen S, Yin ZJ, Jiang C, Ma ZQ, Fu Q, Qu R, *et al*. Asiaticoside attenuates memory impairment induced by transient cerebral ischemia-reperfusion in mice through anti-inflammatory mechanism. Pharmacol. Biochem. Behav. 2014;122:7–15.
33. Chen Y, Han T, Qin L, Rui Y, Zheng H. Effect of total triterpenes from Centella asiatica on the depression behavior and concentration of amino acid in forced swimming mice. Zhong Yao Cai. 2003;26(12):870–3.
34. Gray NE, Zweig JA, Caruso M, Martin MD, Zhu JY, Quinn JF, *et al*. *Centella asiatica* increases hippocampal synaptic density and improves memory and executive function in aged mice. Brain Behav. 2018;8(7).
35. Ceremuga TE, Valdivieso D, Kenner C, Lucia A, Lathrop K, Stailey O, *et al*. Evaluation of the anxiolytic and antidepressant effects of asiatic acid, a compound from Gotu kola or *Centella asiatica*, in the male Sprague Dawley rat. AANA J. 2015;83(2):91–8.
36. Lokanathan Y, Omar N, Ahmad Puz NN, Saim A, Hj Idrus R. Recent updates in neuroprotective and neuroregenerative potential of *Centella asiatica*. Malaysian J. Med. Sci. 2016;23(1):4–14.
37. Muralidhara MS, Bharath M. Exploring the Role of "Brahmi" (*Bacopa monnieri* and *Centella asiatica*) in Brain Function and Therapy. Recent Pat. Endocr. Metab. Immune Drug Discov. 2011;5(1):33–49.
38. Sarris J, McIntyre E, Camfield DA. Plant-based medicines for anxiety disorders, part 2: A review of clinical studies with supporting preclinical evidence. CNS Drugs. 2013;27(4):301–19.
39. Tiwari S, Singh S, Patwardhan K, Gehlot S, Gambhir IS. Effect of *Centella asiatica* on Mild Cognitive Impairment (Mci) and Other Common Age-Related Clinical Problems. Dig. J. Nanomater. Biostructures. 2008;3(4):215–20.
40. Gohil KJ, Patel JA, Gajjar AK. Pharmacological review on *Centella asiatica*: A potential herbal cure-all. Indian J. Pharm. Sci. 2010;72(5):546–56.
41. Wanasuntronwong A, Tantisira MH, Tantisira B, Watanabe H. Anxiolytic effects of standardized extract of *Centella asiatica* (ECa 233) after chronic immobilization stress in mice. J. Ethnopharmacol. 2012;143(2):579–85.
42. Chanana P, Kumar A. Possible Involvement of Nitric Oxide Modulatory Mechanisms in the Neuroprotective Effect of *Centella asiatica* Against Sleep Deprivation Induced Anxiety Like Behaviour, Oxidative Damage and Neuroinflammation. Phyther. Res. 2016;30(4):671–80.

43. Hamid K, Ng I, Tallapragada VJ, Váradi L, Hibbs DE, Hanrahan J, *et al*. An Investigation of the Differential Effects of Ursane Triterpenoids from *Centella asiatica*, and Their Semisynthetic Analogues, on GABAA Receptors. Chem. Biol. Drug Des. 2016;(13):386–97.
44. Wanasuntronwong A, Wanakhachornkrai O, Phongphanphanee P, Isa T, Tantisira B, Tantisira MH. Modulation of Neuronal Activity on Intercalated Neurons of Amygdala Might Underlie Anxiolytic Activity of a Standardized Extract of *Centella asiatica* ECa233. Evidence-based Complement. Altern. Med. 2018;2018.
45. Awad R, Levac D, Cybulska P, Merali Z, Trudeau VL, Arnason JT. Effects of traditionally used anxiolytic botanicals on enzymes of the γ-aminobutyric acid (GABA) system. Can. J. Physiol. Pharmacol. 2007;85(9):933–42.
46. Mitha K V., Yadav S, Ganaraja B. Improvement in Cognitive Parameters Among Offsprings Born to Alcohol Fed Female Wistar Rats Following Long Term Treatment with *Centella Asiatica*. Indian J. Physiol. Pharmacol. 2016;60(2):167–73.
47. Wijeweera P, Arnason JT, Koszycki D, Merali Z. Evaluation of anxiolytic properties of Gotukola - (*Centella asiatica*) extracts and asiaticoside in rat behavioral models. Phytomedicine. 2006;13(9–10):668–76.
48. Siddique YH, Ara G, Beg T, Faisal M, Ahmad M, Afzal M. Antigenotoxic role of *Centella asiatica* L. extract against cyproterone acetate induced genotoxic damage in cultured human lymphocytes. Toxicol. Vitr. 2008;22(1):10–7.
49. Laszczyk MN. Pentacyclic triterpenes of the lupane, oleanane and ursane group as tools in cancer therapy. Planta Med. 2009;75(15):1549–60.
50. Wu T, Geng J, Guo W, Gao J, Zhu X. Asiatic acid inhibits lung cancer cell growth in vitro and in vivo by destroying mitochondria. Acta Pharm. Sin. B. 2017;7(1):65–72.
51. Nhiem NX, Tai BH, Quang TH, Kiem P Van, Minh C Van, Nam NH, *et al*. A new ursane-type triterpenoid glycoside from *Centella asiatica* leaves modulates the production of nitric oxide and secretion of TNF-α in activated RAW 264.7 cells. Bioorganic Med. Chem. Lett. 2011;21(6):1777–81.
52. Lin KH, Yang YY, Yang CM, Huang MY, Lo HF, Liu KC, *et al*. Antioxidant activity of herbaceous plant extracts protect against hydrogen peroxide-induced DNA damage in human lymphocytes. BMC Res. Notes. 2013;6(490):1–10.
53. Meng XM, Zhang Y, Huang XR, Ren GL, Li J, Lan HY. Treatment of renal fibrosis by rebalancing TGF-β/Smad signaling with the combination of asiatic acid and naringenin. Oncotarget. 2015;6(35):36984–97.
54. Qiu J, Yu L, Zhang X, Wu Q, Wang D, Wang X, *et al*. Asiaticoside attenuates lipopolysaccharide-induced acute lung injury via down-regulation of NF-κB signaling pathway. Int. Immunopharmacol. 2015;26(1):181–7.
55. Infante-Garcia C, Garcia-Alloza M. Review of the effect of natural compounds and extracts on neurodegeneration in animal models of diabetes mellitus. Int. J. Mol. Sci. 2019;20(10):2533.
56. Sharma H, Kumar P, Deshmukh RR, Bishayee A, Kumar S. Pentacyclic triterpenes: New tools to fight metabolic syndrome. Phytomedicine.

2018;50:166–77.
57. Sun B, Wu L, Wu Y, Zhang C, Qin L, Hayashi M, *et al*. Therapeutic Potential of *Centella asiatica* and Its Triterpenes: A Review. Front. Pharmacol. 2020;11(568032):1–24.
58. Rosenberg H, Stohs SJ. The utilization of tyrosine for mescaline and protein biosynthesis in *Lophophora Williamsii*. Phytochemistry. 1974;13:1861–3.
59. Bergfeld FACP;, Donald V, Belsito RA, Hill CD, Klaassen DC, Liebler JG, *et al*. Safety Assessment of *Centella asiatica*-derived Ingredients as Used in Cosmetics. Cosmet. Ingred. Rev. 2015.
60. EMA. European Union herbal monograph *Centella asiatica*. Eur. Med. Agency - Sci. Med. Heal. 2022;31(March):0–5.
61. James JT, Dubery IA. Pentacyclic triterpenoids from the medicinal herb, *Centella asiatica* (L.) Urban. Molecules. 2009;14(10):3922–41.
62. Cohen BE, Edmondson D, Kronish IM. State of the art review: Depression, stress, anxiety, and cardiovascular disease. Am. J. Hypertens. 2015;28(11):1295–302.
63. Alvarez-Monjaras M, Gonzalez D. MEXICO Depression: Stigma and its Policy Implications. Yale Glob. Heal. Rev. 2016;4(1):13–6.
64. Cerel J, Brown MM, Maple M, Singleton M, Venne J, Moore M, *et al*. How Many People Are Exposed to Suicide? Not Six. Suicide Life-Threatening Behav. 2019;49(2):529–34.
65. Risk Factors and Warning Signs — AFSP [Internet]. American Foundation for Suicide Prevention.
66. Cooperman S. State of the art. Forbes. 2007;180(12 SUPPL.):94.
67. Patriquin MA, Mathew SJ. The Neurobiological Mechanisms of Generalized Anxiety Disorder and Chronic Stress. Chronic Stress. 2017;1:1–10.
68. Fajemiroye JO, da Silva DM, de Oliveira DR, Costa EA. Treatment of anxiety and depression: Medicinal plants in retrospect. Fundam. Clin. Pharmacol. 2016;30(3):198–215.
69. Newman DJ, Cragg GM. Natural Products as Sources of New Drugs over the Nearly Four Decades from 01/1981 to 09/2019. J. Nat. Prod. 2020;83(3):770–803.
70. EMA. European Medicines Agency [Internet]. Search for Herbal Medicines for Mental stress and mood disorders. 2021.
71. Bradwejn J, Zhou Y, Koszycki D, Shlik J. A Double-Blind, Placebo-Controlled Study on the Effects of Gotu Kola (*Centella asiatica*) on Acoustic Startle Response in Healthy Subjects. J. Clin. Psychopharmacol. 2000;20(6):680–4.
72. Jana U, Bhattacharyya D, Sur TK, Lyle N, Debnath PK. A clinical study on the management of generalized anxiety disorder with *Centella asiatica*. Nepal Med. Collect. J. 2010;12:8–12.
73. Martin EI, Ressler KJ, Binder E, Nemeroff CB. The Neurobiology of Anxiety Disorders: Brain Imaging, Genetics, and Psychoneuroendocrinology. Psychiatr. Clin. North Am. 2009;32:549–75.
74. Kunjumon R, Johnson AJ, Baby S. *Centella asiatica*: Secondary metabolites, biological activities and biomass sources. Phytomedicine Plus. 2022;2(1):100176.

75. Kadam P, Bhalerao S. Sample size calculation. Int. J. Ayurveda Res. 2010;1(1):55–7.
76. Chen Y, Han T, Rui Y, Yin M, Qin L, Zheng H. Effects of total triterpenes of *Centella asiatica* on the corticosterone levels in serum and contents of monoamine in depression rat brain. J. Chinese Med. Mater. 2005;28(6):492–6.
77. Wong JH, Barron AM, Abdullah JM. Mitoprotective Effects of *Centella asiatica* (L.) Urb.: Anti-Inflammatory and Neuroprotective Opportunities in Neurodegenerative Disease. Front. Pharmacol. 2021;12(June):1–9.
78. Ashour AS, El Aziz MMA, Gomha Melad AS. A review on saponins from medicinal plants: chemistry, isolation, and determination. J. Nanomedicine Res. 2019;7(4):282–8.
79. Weng A, Thakur, Melzig, Fuchs. Chemistry and pharmacology of saponins: special focus on cytotoxic properties. Bot. Targets Ther. 2011;1:19–29.
80. Moses T, Pollier J, Almagro L, Buyst D, Van Montagu M, Pedreño MA, *et al*. Combinatorial biosynthesis of sapogenins and saponins in Saccharomyces cerevisiae using a C-16α hydroxylase from *Bupleurum falcatum*. Proc. Natl. Acad. Sci. U. S. A. 2014;111(4):1634–9.
81. Thimmappa R, Geisler K, Louveau T, O'Maille P, Osbourn A. Triterpene Biosynthesis in Plants. Annu. Rev. Plant Biol. 2014;65(1):225–57.
82. Böttger A, Vothknecht U, Bolle C, Wolf A. Lessons on Caffeine, Cannabis & Co. Cham: Springer International Publishing; 2018. 217 p. (Learning Materials in Biosciences).
83. Kalita R, Patar L, Shasany AK, Modi MK, Sen P. Molecular cloning, characterization, and expression analysis of 3-hydroxy-3-methylglutaryl coenzyme A reductase gene from *Centella asiatica* L. Mol. Biol. Rep. 2015;42(9):1431–9.
84. Kim OT, Ahn JC, Hwang SJ, Hwang B. Cloning and expression of a farnesyl diphosphate synthase in *Centella asiatica* (L.) urban. Mol. Cells. 2005;19(2):294–9.
85. Kim O-T, Seong N-S, Kim M-Y, Hwang B. Isolation and Characterization of Squalene Synthase cDNA from *Centella asiatica* (L.) Urban. J. Plant Biol. 2005;48(3):263–9.
86. Kim OT, Kim MY, Huh SM, Bai DG, Ahn JC, Hwang B. Cloning of a cDNA probably encoding oxidosqualene cyclase associated with asiaticoside biosynthesis from *Centella asiatica* (L.) Urban. Plant Cell Rep. 2005;24(5):304–11.
87. Kim OT, Lee JW, Bang KH, Chang Kim Y, Yun Hyun D, Cha SW, *et al*. Characterization of a dammarenediol synthase in *Centella asiatica* (L.) Urban. Plant Physiol. Biochem. 2009;47(11–12):998–1002.
88. Prasad A, Mathur AK, Mathur A. Advances and emerging research trends for modulation of centelloside biosynthesis in *Centella asiatica* (L.) Urban-A review. Ind. Crops Prod. 2019;141(September):111768.
89. Wu S, Zhang F, Xiong W, Molnár I, Liang J, Ji A, *et al*. An Unexpected Oxidosqualene Cyclase Active Site Architecture in the *Iris tectorum* Multifunctional α-Amyrin Synthase. ACS Catal. 2020;10(16):9515–20.
90. Kim OT, Um Y, Jin ML, Kim JU, Hegebarth D, Busta L, *et al*. A novel

multifunctional C-23 Oxidase, CYP714E19, is involved in asiaticoside biosynthesis. Plant Cell Physiol. 2018;59(6):1200–13.
91. James JT, Dubery IA. Pentacyclic triterpenoids from the medicinal herb, *Centella asiatica* (L.) Urban. Molecules. 2009;14(10):3922–41.
92. Azerad R. Chemical structures, production and enzymatic transformations of sapogenins and saponins from *Centella asiatica* (L.) Urban. Fitoterapia. 2016;114:168–87.
93. Miettinen K, Pollier J, Buyst D, Arendt P, Csuk R, Sommerwerk S, *et al*. The ancient CYP716 family is a major contributor to the diversification of eudicot triterpenoid biosynthesis. Nat. Commun. 2017;8.
94. Clifford MN, Jaganath IB, Ludwig IA, Crozier A. Chlorogenic acids and the acyl-quinic acids: Discovery, biosynthesis, bioavailability and bioactivity. Nat. Prod. Rep. 2017;34(12):1391–421.
95. Gil M, Wianowska D. Chlorogenic acids – their properties, occurrence and analysis. Ann. Univ. Mariae Curie-Sklodowska, Sect. AA – Chem. 2017;72(1):61.
96. Ncube EN, Steenkamp PA, Madala NE, Dubery IA. Stimulatory effects of acibenzolar-S-methyl on chlorogenic acids biosynthesis in centella asiatica cells. Front. Plant Sci. 2016;7(September2016):1–15.
97. Ncube EN, Steenkamp PA, Madala NE, Dubery IA. Chlorogenic Acids Biosynthesis in *Centella asiatica* Cells Is not Stimulated by Salicylic Acid Manipulation. Appl. Biochem. Biotechnol. 2016;179(5):685–96.
98. Identification and determination of naturally occurring folates in grains of rice (*Oryza sativa* L.) by UPLC-MS/MS analysis. Nat. Prod. Res. 2017;1–5.
99. Buranasudja V, Rani D, Malla A, Kobtrakul K, Vimolmangkang S. Insights into antioxidant activities and anti-skin-aging potential of callus extract from *Centella asiatica* (L.). Sci. Rep. 2021;11(1):1–16.
100. Oyedeji OA, Afolayan AJ. Chemical Composition and Antibacterial Activity of the Essential Oil of *Centella asiatica*. Growing in South Africa. Pharm. Biol. 2005;43(3):249–52.
101. James JT, Tugizimana F, Steenkamp PA, Dubery IA. Metabolomic analysis of methyl jasmonate-induced triterpenoid production in the medicinal herb *Centella asiatica* (L.) urban. Molecules. 2013;18(4):4267–81.
102. Tugizimana F, Ncube EN, Steenkamp PA, Dubery IA. Metabolomics-derived insights into the manipulation of terpenoid synthesis in *Centella asiatica* cells by methyl jasmonate. Plant Biotechnol. Rep. 2015;9(3):125–36.
103. Ncube EN, Steenkamp PA, Madala NE, Dubery IA. Metabolite profiling of the undifferentiated cultured cells and differentiated leaf tissues of *Centella asiatica*. Plant Cell, Tissue Organ Cult. 2017;129(3):431–43.
104. Subban R, Veerakumar A, Manimaran R, Hashim KM, Balachandran I. Two new flavonoids from *Centella asiatica* (Linn.). J. Nat. Med. 2008;62(3):369–73.
105. Maulidiani, Abas F, Khatib A, Shaari K, Lajis NH. Chemical characterization and antioxidant activity of three medicinal Apiaceae species. Ind. Crops Prod. 2014;55:238–47.
106. Suntornsuk L, Anurukvorakun O. Precision improvement for the analysis of

flavonoids in selected Thai plants by capillary zone electrophoresis. Electrophoresis. 2005;26(3):648–60.
107. Satake T, Kamiya K, An Y, Oishi T, Yamamoto J. The anti-thrombotic active constituents from *Centella asiatica*. Biol. Pharm. Bull. 2007;30(5):935–40.
108. Antognoni F, Perellino NC, Crippa S, Dal Toso R, Danieli B, Minghetti A, *et al*. Irbic acid, a dicaffeoylquinic acid derivative from *Centella asiatica* cell cultures. Fitoterapia. 2011;82(7):950–4.
109. Govindan G, Sambandan TG, Govindan M, Sinskey A, Vanessendelft J, Adenan I, *et al*. A bioactive polyacetylene compound isolated from *Centella asiatica*. Planta Med. 2007;73(6):597–9.
110. Rajkumar S, Jebanesan. Repellent activity of selected plant essential oils against the malarial fever mosquito *Anopheles stephensi*. Trop. Biomed. 2007;24(2):71–5.
111. Cañigueral S, Tschopp R, Ambrosetti L, Vignutelli A, Scaglione F, Petrini O. The development of herbal medicinal products: Quality, safety and efficacy as key factors. Pharmaceut. Med. 2008;22(2):107–18.
112. Prasad A, Mathur AK, Mathur A. Advances and emerging research trends for modulation of centelloside biosynthesis in *Centella asiatica* (L.) Urban-A review. Ind. Crops Prod. 2019;141:111768.
113. Verpoorte R. Chemodiversity and the Biological Role of Secondary Metabolites, Some Thoughts for Selecting Plant Material for Drug Development. In: Bioassay Methods in Natural Product Research and Drug Development. Springer Netherlands; 1999. p. 11–23.
114. Brinkhaus B, Lindner M, Schuppan D, Hahn EG. Chemical, pharmacological and clinical profile of the East Asian medical plant *Centella asiatica*. Phytomedicine. 2000;7(5):427–48.
115. CONABIO. Centella asiatica (L.) Urb. In: Método de Evaluación Rápida de Invasividad (MERI) para especies exóticas en México. 2016. p. 1–7.
116. Sugiyama M. Historical review of research on plant cell dedifferentiation. J. Plant Res. 2015;
117. Marchev AS, Yordanova ZP, Georgiev MI. Green (cell) factories for advanced production of plant secondary metabolites. Crit. Rev. Biotechnol. 2020;40(4):443–58.
118. Mustafa NR, De Winter W, Van Iren F, Verpoorte R. Initiation, growth and cryopreservation of plant cell suspension cultures. Nat. Protoc. 2011;6(6):715–42.
119. Shakya P, Marslin G, Siram K, Beerhues L, Franklin G. Elicitation as a tool to improve the profiles of high-value secondary metabolites and pharmacological properties of *Hypericum perforatum*. J. Pharm. Pharmacol. 2019;71(1):70–82.
120. Singh J, Sabir F, Sangwan RS, Narnoliya LK, Saxena S, Sangwan NS. Enhanced secondary metabolite production and pathway gene expression by leaf explants-induced direct root morphotypes are regulated by combination of growth regulators and culture conditions in *Centella asiatica* (L.) urban. Plant Growth Regul. 2014;75(1):55–66.
121. Sangwan RS, Tripathi S, Singh J, Narnoliya LK, Sangwan NS. *De novo* sequencing and assembly of *Centella asiatica* leaf transcriptome for

mapping of structural, functional and regulatory genes with special reference to secondary metabolism. Gene. 2013;525(1):58–76.
122. Aziz ZA, Davey MR, Power JB, Anthony P, Smith RM, Lowe KC. Production of asiaticoside and madecassoside in *Centella asiatica in vitro* and *in vivo*. Biol. Plant. 2007;51(1):34–42.
123. Kim OT, Kim MY, Hong MH, Ahn JC, Hwang B. Stimulation of asiaticoside accumulation in the whole plant cultures of *Centella asiatica* (L.) urban by elicitors. Plant Cell Rep. 2004;23(5):339–44.
124. Mangas S, Bonfill M, Osuna L, Moyano E, Tortoriello J, Cusido RM, *et al*. The effect of methyl jasmonate on triterpene and sterol metabolisms of *Centella asiatica*, *Ruscus aculeatus* and *Galphimia glauca* cultured plants. Phytochemistry. 2006;67(18):2041–9.
125. Wang SQ, Lim HW. Principles and practice of photoprotection. Principles and Practice of Photoprotection. Springer International Publishing; 2016. 1–487 p.
126. Mangas S, Moyano E, Bonfill M. *Centella asiatica* (L) Urban: An updated approach. In: Palazón J, Cusidó RM, editors. Plant Secondary Terpenoids. Kerala: Research Singpost; 2009. p. 55–74.
127. Kabera JN, Semana E, Mussa AR, He X. Plant Secondary Metabolites: Biosynthesis, Classification, Function and Pharmacological Properties. J. Pharm. Pharmacol. 2014;2(July 2014):377–92.
128. Thakur M, Sohal BS. Role of Elicitors in Inducing Resistance in Plants against Pathogen Infection: A Review. ISRN Biochem. 2013;2013:762412.
129. Ramirez-Estrada K, Vidal-Limon H, Hidalgo D, Moyano E, Golenioswki M, Cusidó RM, *et al*. Elicitation, an effective strategy for the biotechnological production of bioactive high-added value compounds in plant cell factories. Molecules. 2016;21(2).
130. Naik PM, Al-Khayri JM. Abiotic and Biotic Elicitors–Role in Secondary Metabolites Production through *In Vitro* Culture of Medicinal Plants. In: Shanker AK, Shanker C, editors. Abiotic and Biotic Stress in Plants - Recent Advances and Future Perspectives. London: InTechOpen; 2016. p. 247–77.
131. Luthra R, Satija G, Roy A. Centellosides: pharmaceutical applications and production enhancement strategies. Plant Cell. Tissue Organ Cult. 2021
132. Yan C, Fan M, Yang M, Zhao J, Zhang W, Su Y, *et al*. Injury Activates Ca2+/Calmodulin-Dependent Phosphorylation of JAV1-JAZ8-WRKY51 Complex for Jasmonate Biosynthesis. Mol. Cell. 2018;70(1):136-149.e7.
133. Dar TA, Uddin M, Khan MMA, Hakeem KR, Jaleel H. Jasmonates counter plant stress: A review. Environ. Exp. Bot. 2015;115:49–57.
134. De Geyter N, Gholami A, Goormachtig S, Goossens A. Transcriptional machineries in jasmonate-elicited plant secondary metabolism. Trends Plant Sci. 2012;17(6):349–59.
135. Jiang D, Yan S. MeJA is more effective than JA in inducing defense responses in *Larix olgensis*. Arthropod. Plant. Interact. 2018;12(1):49–56.
136. Kim OT, Kim SH, Ohyama K, Muranaka T, Choi YE, Lee HY, *et al*. Upregulation of phytosterol and triterpene biosynthesis in *Centella asiatica* hairy roots overexpressed ginseng farnesyl diphosphate synthase. Plant

Cell Rep. 2010;29(4):403–11.
137. Hernandez-Vazquez L, Bonfill M, Moyano E, Cusido RM, Navarro-Ocaña A, Palazon J. Conversion of α-amyrin into centellosides by plant cell cultures of *Centella asiatica*. Biotechnol. Lett. 2010;32(2):315–9.
138. Hidalgo D, Steinmetz V, Brossat M, Tournier-Couturier L, Cusido RM, Corchete P, *et al*. An optimized biotechnological system for the production of centellosides based on elicitation and bioconversion of *Centella asiatica* cell cultures. Eng. Life Sci. 2017;17(4):413–9.
139. Krishnan ML, Roy A, Bharadvaja N. Elicitation effect on the production of asiaticoside and asiatic acid in shoot, callus, and cell suspension culture of *Centella asiatica.* J. Appl. Pharm. Sci. 2019;9(6):67–74.
140. Kim OT, Bang KH, Shin YS, Lee MJ, Jung SJ, Hyun DY, *et al*. Enhanced production of asiaticoside from hairy root cultures of *Centella asiatica* (L.) Urban elicited by methyl jasmonate. Plant Cell Rep. 2007;26(11):1941–9.
141. Kim OT, Um Y, Jin ML, Kim YC, Bang KH, Hyun DY, *et al*. Analysis of expressed sequence tags from *Centella asiatica* (L.) Urban hairy roots elicited by methyl jasmonate to discover genes related to cytochrome P450s and glucosyltransferases. Plant Biotechnol. Rep. 2014;8(2):211–20.
142. Kim OT, Um Y, Jin ML, Kim JU, Hegebarth D, Busta L, *et al*. A novel multifunctional C-23 Oxidase, CYP714E19, is involved in asiaticoside biosynthesis. Plant Cell Physiol. 2018;59(6):1200–13.
143. Sharma P, Padh H, Shrivastava N. Hairy root cultures: A suitable biological system for studying secondary metabolic pathways in plants. Eng. Life Sci. 2013;13(1):62–75.
144. Shi M, Liao P, Nile SH, Georgiev MI, Kai G. Biotechnological Exploration of Transformed Root Culture for Value-Added Products. Trends Biotechnol. 2021;39(2):137–49.
145. Gutierrez-Valdes N, Häkkinen ST, Lemasson C, Guillet M, Oksman-Caldentey KM, Ritala A, *et al*. Hairy Root Cultures—A Versatile Tool With Multiple Applications. Front. Plant Sci. 2020;11(33).
146. Sevón N, Oksman-Caldentey KM. *Agrobacterium rhizogenes*-mediated transformation: Root cultures as a source of alkaloids. Planta Med. 2002;68(10):859–68.
147. Bahramnejad B, Naji M, Bose R, Jha S. A critical review on use of *Agrobacterium rhizogenes* and their associated binary vectors for plant transformation. Biotechnol. Adv. 2019;37(7):107405.
148. Häkkinen ST, Oksman-Caldentey KM. Progress and prospects of hairy root research. Hairy Roots: An Effective Tool of Plant Biotechnology. 2018. 3–19 p.
149. Kim OT, Bang KH, Shin YS, Lee MJ, Jung SJ, Hyun DY, *et al*. Enhanced production of asiaticoside from hairy root cultures of *Centella asiatica* (L.) Urban elicited by methyl jasmonate. Plant Cell Rep. 2007;26(11):1941–9.
150. Zahanis. The Effect of Squalene Addition *In-Vitro* to Increase Asiatiaticoside Hairy Root Culture of *Centella Asiatica* (L.) Urban. IOP Conf. Ser. Earth Environ. Sci. 2019;347(1).
151. Nguyen K Van, Pongkitwitoon B, Pathomwichaiwat T, Viboonjun U, Prathanturarug S. Effects of methyl jasmonate on the growth and

triterpenoid production of diploid and tetraploid *Centella asiatica* (L.) Urb. hairy root cultures. Sci. Rep. 2019;9(1).
152. Baek S, Ho TT, Lee H, Jung G, Kim YE, Jeong CS, *et al*. Enhanced biosynthesis of triterpenoids in *Centella asiatica* hairy root culture by precursor feeding and elicitation. Plant Biotechnol. Rep. 2020;14(1):45–53.
153. Ruslan K, Selfitri AD, Bulan SA, Rukayadi Y, Elfahmi. Effect of *Agrobacterium rhizogenes* and elicitation on the asiaticoside production in cell cultures of *Centella asiatica*. Pharmacogn. Mag. 2012;8(30):111–5.
154. Alcalde MA, Cusido RM, Moyano E, Palazon J, Bonfill M. Metabolic gene expression and centelloside production in elicited *Centella asiatica* hairy root cultures. Ind. Crops Prod. 2022;184(April):114988.
155. Zhang W, Franco C, Curtin C, Simon C. To Stretch the Boundary of Secondary Metabolite Production in Plant Cell-Based Bioprocessing: Anthocyanin as a Case Study. J. Biomed. Biotechnol. 2004;2004(5):264–71.
156. Gandhi SG, Mahajan V, Bedi YS. Changing trends in biotechnology of secondary metabolism in medicinal and aromatic plants. Planta. 2015;241(2):303–17.
157. Narayani M, Srivastava S. Elicitation: a stimulation of stress in in vitro plant cell/tissue cultures for enhancement of secondary metabolite production. Phytochem. Rev. 2017;16(6):1227–52.
158. Cusido RM, Onrubia M, Sabater-Jara AB, Moyano E, Bonfill M, Goossens A, *et al*. A rational approach to improving the biotechnological production of taxanes in plant cell cultures of Taxus spp. Biotechnol. Adv. 2014;32(6):1157–67.
159. Ramirez-Estrada K, Osuna L, Moyano E, Bonfill M, Tapia N, Cusido RM, *et al*. Changes in gene transcription and taxane production in elicited cell cultures of *Taxus* × *media* and *Taxus globosa*. Phytochemistry. 2015;117:174–84.
160. James JT, Tugizimana F, Steenkamp PA, Dubery IA. Metabolomic analysis of methyl jasmonate-induced triterpenoid production in the medicinal herb *Centella asiatica* (L.) urban. Molecules. 2013;18(4):4267–81.
161. Murashige T, Skoog F. A Revised Medium for Rapid Growth and Bio Assays with Tobacco Tissue Cultures. Physiol. Plant. 1962;15(3):473–97.
162. Hohmann M, Christoph N, Wachter H, Holzgrabe U. 1H NMR profiling as an approach to differentiate conventionally and organically grown tomatoes. J. Agric. Food Chem. 2014;62(33):8530–40.
163. Becerra-Martínez E, Florentino-Ramos E, Pérez-Hernández N, Gerardo Zepeda-Vallejo L, Villa-Ruano N, Velázquez-Ponce M, *et al*. 1H NMR-based metabolomic fingerprinting to determine metabolite levels in serrano peppers (*Capsicum annum* L.) grown in two different regions. Food Res. Int. 2017;102(September):163–70.
164. Verpoorte R, Choi YH, Kim HK. NMR-based metabolomics at work in phytochemistry. Phytochem. Rev. 2007;6(1):3–14.
165. Sánchez-Sampedro A, Kim HK, Choi YH, Verpoorte R, Corchete P. Metabolomic alterations in elicitor treated *Silybum marianum* suspension cultures monitored by nuclear magnetic resonance spectroscopy. J.

Biotechnol. 2007;130(2):133–42.
166. Almagro L, Belchí-Navarro S, Martínez-Márquez A, Bru R, Pedreño MA. Enhanced extracellular production of trans-resveratrol in *Vitis vinifera* suspension cultured cells by using cyclodextrins and coronatine. Plant Physiol. Biochem. 2015;97:361–7.
167. Gigliarelli G, Becerra JX, Curini M, Marcotullio MC, Forti L. Chemical composition and biological activities of fragrant mexican copal (*Bursera spp*.). Molecules. 2015;20(12):22383–94.
168. Florentino-Ramos E, Villa-Ruano N, Hidalgo-Martínez D, Ramírez-Meraz M, Méndez-Aguilar R, Velásquez-Valle R, *et al*. 1 H NMR-based fingerprinting of eleven Mexican *Capsicum annuum* cultivars. Food Res. Int. 2019;121(December 2018):12–9.
169. Gabotti D, Locatelli F, Cusano E, Baldoni E, Genga A, Pucci L, *et al*. Cell suspensions of *Cannabis sativa* (var. futura): Effect of elicitation on metabolite content and antioxidant activity. Molecules. 2019;24(22).
170. Ramírez-Meraz M, Méndez-Aguilar R, Hidalgo-Martínez D, Villa-Ruano N, Zepeda-Vallejo LG, Vallejo-Contreras F, *et al*. Experimental races of *Capsicum annuum* cv. jalapeño: Chemical characterization and classification by 1H NMR/machine learning. Food Res. Int. 2020;138(July).
171. Villa-Ruano N, Rosas-Bautista A, Rico-Arzate E, Cruz-Narvaez Y, Zepeda-Vallejo LG, Lalaleo L, *et al*. Study of nutritional quality of pomegranate (*Punica granatum* L.) juice using 1H NMR-based metabolomic approach: A comparison between conventionally and organically grown fruits. Lwt. 2020;134(110222).
172. Chenomx. Chenomx Inc | Metabolite Discovery and Measurement [Internet]. 2020.
173. Kim HK, Choi YH, Verpoorte R. NMR-based metabolomic analysis of plants. Nat. Protoc. 2010;5(3):536–49.
174. Chambers MC, Maclean B, Burke R, Amodei D, Ruderman DL, Neumann S, *et al*. A cross-platform toolkit for mass spectrometry and proteomics. Nat. Biotechnol. 2012;30(10):918–20.
175. Olivon F, Grelier G, Roussi F, Litaudon M, Touboul D. MZmine 2 Data-Preprocessing To Enhance Molecular Networking Reliability. Anal. Chem. 2017;89:7840.
176. Zhao X, Zeng Z, Chen A, Lu X, Zhao C, Hu C, *et al*. Comprehensive Strategy to Construct In-House Database for Accurate and Batch Identification of Small Molecular Metabolites. Anal. Chem. 2018;90:19.
177. Alseekh S, Fernie AR. Metabolomics 20 years on: what have we learned and what hurdles remain? Plant J. 2018;94(6):933–42.
178. Pluskal T, Castillo S, Villar-Briones A, Orešič M. MZmine 2: Modular framework for processing, visualizing, and analyzing mass spectrometry-based molecular profile data. BMC Bioinformatics. 2010;11(1):395.
179. Katajamaa M, Miettinen J, Orešič M. MZmine: toolbox for processing and visualization of mass spectrometry based molecular profile data. Bioinformatics. 2006;22(5):634–6.
180. Nothias L-F, Petras D, Schmid R, Dührkop K, Rainer J, Sarvepalli A, *et al*. Feature-based molecular networking in the GNPS analysis environment.

Nat. Methods. 2020;17(9):905–8.
181. Mohimani H, Gurevich A, Shlemov A, Mikheenko A, Korobeynikov A, Cao L, *et al*. Dereplication of microbial metabolites through database search of mass spectra. Nat. Commun. 2018;9(1):4035.
182. Ono K, Demchak B, Ideker T. Cytoscape tools for the web age: D3.js and Cytoscape.js exporters. F1000Research. 2014;3(143).
183. Voll LM, Zhang W, Hesse H, Marcellin E, Hill CB, Beate Hill C, *et al*. Metabolomics, standards, and metabolic modeling for synthetic biology in plants. 2015;3.
184. Kim OT, Um Y, Jin ML, Kim JU, Hegebarth D, Busta L, *et al*. A novel multifunctional C-23 Oxidase, CYP714E19, is involved in asiaticoside biosynthesis. Plant Cell Physiol. 2018;59(6):1200–13.
185. Kim HK, Choi YH, Verpoorte R. NMR-based plant metabolomics: Where do we stand, where do we go? Trends Biotechnol. 2011;29(6):267–75.
186. Salem MA, De Souza LP, Serag A, Fernie AR, Farag MA, Ezzat SM, *et al*. Metabolomics in the context of plant natural products research: From sample preparation to metabolite analysis. Metabolites. 2020;10(1):1–30.
187. Patel MK, Pandey S, Kumar M, Haque MI, Pal S, Yadav NS. Plants metabolome study: Emerging tools and techniques. Plants. 2021;10(11):1–24.
188. Caesar LK, Montaser R, Keller NP, Kelleher NL. Metabolomics and genomics in natural products research: complementary tools for targeting new chemical entities. Nat. Prod. Rep. 2021.
189. Ono NN, Tian L. The multiplicity of hairy root cultures: Prolific possibilities. Vol. 180, Plant Science. 2011. p. 439–46.
190. Halder M, Sarkar S, Jha S. Elicitation: A biotechnological tool for enhanced production of secondary metabolites in hairy root cultures. Eng. Life Sci. 2019;19(12):880–95.
191. Onrubia M, Moyano E, Bonfill M, Cusidó RM, Goossens A, Palazón J. Coronatine, a more powerful elicitor for inducing taxane biosynthesis in *Taxus media* cell cultures than methyl jasmonate. J. Plant Physiol. 2013;170(2):211–9.
192. Ahmad I, Hussain T, Ashraf I, Nafees M, Rafay M, Iqbal M. Lethal Effects of Secondary Metabolites on Plant Tissue Culture. Environ. Sci. 2013;13(4):539–47.
193. Erb M, Kliebenstein DJ. Plant Secondary Metabolites as Defenses, Regulators, and Primary Metabolites: The Blurred Functional Trichotomy. Plant Physiol. 2020;184(1):39–52.
194. Caretto S, Linsalata V, Colella G, Mita G, Lattanzio V. Carbon fluxes between primary metabolism and phenolic pathway in plant tissues under stress. Int. J. Mol. Sci. 2015;16(11):26378–94.
195. Roullier C, Bertrand S, Blanchet E, Peigné M, Pont TR Du, Guitton Y, *et al*. Time dependency of chemodiversity and biosynthetic pathways: AnLC-MS metabolomic study of Marine-Sourced Penicillium. Mar. Drugs. 2016;14(5).
196. Gabotti D, Locatelli F, Cusano E, Baldoni E, Genga A, Pucci L, *et al*. Cell suspensions of *Cannabis sativa* (var. futura): Effect of elicitation on metabolite content and antioxidant activity. Molecules. 2019;24(22).

197. Caesar LK, Kellogg JJ, Kvalheim OM, Cech NB. Opportunities and Limitations for Untargeted Mass Spectrometry Metabolomics to Identify Biologically Active Constituents in Complex Natural Product Mixtures. J. Nat. Prod. 2019;82(3):469–84.
198. Tugizimana F, Ncube EN, Steenkamp PA, Dubery IA. Metabolomics-derived insights into the manipulation of terpenoid synthesis in *Centella asiatica* cells by methyl jasmonate. Plant Biotechnol. Rep. 2015;9(3):125–36.
199. Zulak KG, Weljie AM, Vogel HJ, Facchini PJ. Quantitative 1H NMR metabolomics reveals extensive metabolic reprogramming of primary and secondary metabolism in elicitor-treated opium poppy cell cultures. BMC Plant Biol. 2008;8:1–19.
200. Mendoza D, Arias JP, Cuaspud O, Esturau-Escofet N, Hernández-Espino CC, de San Miguel ER, *et al*. 1H-NMR-based metabolomic of plant cell suspension cultures of *Thevetia peruviana* treated with salicylic acid and methyl jasmonate. Ind. Crops Prod. 2019;135:217–29.
201. Akhgari A, Laakso I, Maaheimo H, Choi YH, Seppänen-Laakso T, Oksman-Caldentey KM, *et al*. Methyljasmonate elicitation increases terpenoid indole alkaloid accumulation in *Rhazya stricta* hairy root cultures. Plants. 2019;8(12).
202. Vasconsuelo A, Boland R. Molecular aspects of the early stages of elicitation of secondary metabolites in plants. Plant Sci. 2007;172(5):861–75.
203. Ramos-Ruiz R, Martinez F, Knauf-Beiter G. The effects of GABA in plants. Vol. 5, Cogent Food and Agriculture. Informa Healthcare; 2019.
204. Li L, Dou N, Zhang H, Wu C. The versatile GABA in plants. Plant Signal. Behav. 2021;16(3).
205. Igamberdiev AU, Eprintsev AT. Organic acids: The pools of fixed carbon involved in redox regulation and energy balance in higher plants. Front. Plant Sci. 2016;7(1042):1–15.
206. Flores-Sanchez IJ, Verpoorte R. Plant Polyketide Synthases: A fascinating group of enzymes. Plant Physiol. Biochem. 2009;47(3):167–74.
207. Gao H, Zhou Q, Yang L, Zhang K, Ma Y, Xu ZQ. Metabolomics analysis identifies metabolites associated with systemic acquired resistance in Arabidopsis. PeerJ. 2020;8.
208. Kan CC, Chung TY, Juo YA, Hsieh MH. Glutamine rapidly induces the expression of key transcription factor genes involved in nitrogen and stress responses in rice roots. BMC Genomics. 2015;16(1):1–15.
209. Gaufichon L, Reisdorf-Cren M, Rothstein SJ, Chardon F, Suzuki A. Biological functions of asparagine synthetase in plants. Plant Sci. 2010;179(3):141–53.
210. Winter G, Todd CD, Trovato M, Forlani G, Funck D. Physiological implications of arginine metabolism in plants. Front. Plant Sci. 2015;6(534):1–14.
211. Rehman AU, Bashir F, Ayaydin F, Kóta Z, Páli T, Vass I. Proline is a quencher of singlet oxygen and superoxide both in *in vitro* systems and isolated thylakoids. Physiol. Plant. 2021;172(1):7–18.

212. Chen Z, Fang X, Yuan X, Zhang Y, Li H, Zhou Y, *et al*. Overexpression of transcription factor gmtga15 enhances drought tolerance in transgenic soybean hairy roots and arabidopsis plants. Agronomy. 2021;11(1).
213. Liu X, Jin M, Zhang M, Li T, Sun S, Zhang J, *et al*. The application of combined 1 H NMR-based metabolomics and transcriptomics techniques to explore phenolic acid biosynthesis in *Salvia miltiorrhiza* Bunge. J. Pharm. Biomed. Anal. 2019;172:126–38.
214. Sykłowska-Baranek K, Pilarek M, Bonfill M, Kafel K, Pietrosiuk A. Perfluorodecalin-supported system enhances taxane production in hairy root cultures of *Taxus x media* var. Hicksii carrying a taxadiene synthase transgene. Plant Cell. Tissue Organ Cult. 2015;120(3):1051–9.
215. Vaccaro MC, Mariaevelina A, Malafronte N, De Tommasi N, Leone A. Increasing the synthesis of bioactive abietane diterpenes in *Salvia sclarea* hairy roots by elicited transcriptional reprogramming. Plant Cell Rep. 2017;36(2):375–86.
216. Fattahi F, Shojaeiyan A, Palazon J, Moyano E, Torras-Claveria L. Methyl-β-cyclodextrin and coronatine as new elicitors of tropane alkaloid biosynthesis in *Atropa acuminata* and *Atropa belladonna* hairy root cultures. Physiol. Plant. 2021;172(4):2098–111.
217. Wang LY, Zhang Q, Wang ZQ, Li YC. Effect of coronatine on synthesis of cephalotaxine in suspension cells of *Cephalotaxus mannii* and its transcriptome analysis. Plant Cell. Tissue Organ Cult. 2021;147(2):209–20.
218. Yokoyama R, de Oliveira MVV, Kleven B, Maeda HA. The entry reaction of the plant shikimate pathway is subjected to highly complex metabolite-mediated regulation. Plant Cell. 2021;33(3):671–96.
219. Kosmacz M, Sokołowska EM, Bouzaa S, Skirycz A. Towards a functional understanding of the plant metabolome. Curr. Opin. Plant Biol. 2020;55:47–51.
220. Yuan H, Zeng X, Shi J, Xu Q, Wang Y, Jabu D, *et al*. Time-course comparative metabolite profiling under osmotic stress in tolerant and sensitive tibetan hulless barley. Biomed Res. Int. 2018;2018.
221. Chong J, Wishart DS, Xia J. Using MetaboAnalyst 4.0 for Comprehensive and Integrative Metabolomics Data Analysis. Curr. Protoc. Bioinforma. 2019;68(1):1–128.
222. Tugizimana F, Piater L, Dubery I. Plant metabolomics: A new frontier in phytochemical analysis. S. Afr. J. Sci. 2013;109(5–6):18–20.
223. Tugizimana F, Steenkamp PA, Piater LA, Dubery IA. Mass spectrometry in untargeted liquid chromatography/mass spectrometry metabolomics: Electrospray ionisation parameters and global coverage of the metabolome. Rapid Commun. Mass Spectrom. 2018;32(2):121–32.
224. Courant F, Antignac JP, Dervilly-Pinel G, Le Bizec B. Basics of mass spectrometry based metabolomics. Proteomics. 2014;14(21–22):2369–88.
225. Xia B, Bai L, Li X, Xiong J, Xu P, Xue M. Structural analysis of metabolites of asiatic acid and its analogue madecassic acid in zebrafish using LC/IT-MSn. Molecules. 2015;20(2):3001–19.
226. Du Q, Jerz G, Chen P, Winterhalter P. Preparation of ursane triterpenoids from Centella asiatica using high speed countercurrent chromatography

with step-gradient elution. J. Liq. Chromatogr. Relat. Technol. 2004;27(14):2201–15.
227. Shen Y, Liu A, Ye M, Wang L, Chen J, Wang XR, *et al*. Analysis of biologically active constituents in *Centella asiatica* by microwave-assisted extraction combined with LC-MS. Chromatographia. 2009;70(3–4):431–8.
228. Bouhafsoun A, Yilmaz MA, Boukeloua A, Temel H, Kaid Harche M. Simultaneous quantification of phenolic acids and flavonoids in Chamaerops humilis L. using LC-ESI-MS/MS. Food Sci. Technol. 2018;38:242–7.
229. Choi WG, Kim JH, Kim DK, Lee Y, Yoo JS, Shin DH, *et al*. Simultaneous determination of chlorogenic acid isomers and metabolites in rat plasma using LC-MS/MS and its application to a pharmacokinetic study following oral administration of *Stauntonia hexaphylla* leaf extract (YRA-1909) to rats. Pharmaceutics. 2018;10(3).
230. Ferreira-Lima N, Vallverdú-Queralt A, Meudec E, Pinasseau L, Verbaere A, Bordignon-Luiz MT, *et al*. Quantification of hydroxycinnamic derivatives in wines by UHPLC-MRM-MS. Anal. Bioanal. Chem. 2018;410(15):3483–90.
231. Basu S, Patel VB, Jana S, Patel H. Liquid chromatography tandem mass spectrometry method (LC-MS/MS) for simultaneous determination of piperine, cinnamic acid and gallic acid in rat plasma using a polarity switch technique. Anal. Methods. 2013;5(4):967–76.
232. Tani H, Hikami S, Takahashi S, Kimura Y, Matsuura N, Nakamura T, *et al*. Isolation, Identification, and Synthesis of a New Prenylated Cinnamic Acid Derivative from Brazilian Green Propolis and Simultaneous Quantification of Bioactive Components by LC-MS/MS. J. Agric. Food Chem. 2019;67(44):12303–12.
233. Chen Y, Yu H, Wu H, Pan Y, Wang K, Jin Y, *et al*. Characterization and quantification by LC-MS/MS of the chemical components of the heating products of the flavonoids extract in Pollen typhae for transformation rule exploration. Molecules. 2015;20(10):18352–66.
234. Kumar S, Singh A, Kumar B. Identification and characterization of phenolics and terpenoids from ethanolic extracts of *Phyllanthus* species by HPLC-ESI-QTOF-MS/MS. J. Pharm. Anal. 2017;7(4):214–22.
235. March RE, Miao XS. A fragmentation study of kaempferol using electrospray quadrupole time-of-flight mass spectrometry at high mass resolution. Int. J. Mass Spectrom. 2004;231(2–3):157–67.
236. Valgimigli L, Gabbanini S, Matera R. Analysis of Maltose and Lactose by U-HPLC-ESI-MS/MS. In: Preedy VR, editor. Dietary Sugars - Chemistry, Analysis, Function and Effects. Cambridge: Royal Society of Chemistry; 2012. p. 443–63.
237. Antognoni F, Perellino NC, Crippa S, Dal Toso R, Danieli B, Minghetti A, *et al*. Irbic acid, a dicaffeoylquinic acid derivative from *Centella asiatica* cell cultures. Fitoterapia. 2011;82(7):950–4.
238. Clifford MN, Kirkpatrick J, Kuhnert N, Roozendaal H, Salgado PR. LC-MSn analysis of the cis isomers of chlorogenic acids. Food Chem. 2008;106(1):379–85.
239. Maulidiani, Abas F, Khatib A, Shaari K, Lajis NH. Chemical characterization

and antioxidant activity of three medicinal Apiaceae species. Ind. Crops Prod. 2014;55:238–47.
240. Ağalar HG, Çiftçi GA, Göger F, Kırımer N. Activity guided fractionation of Arum italicum miller tubers and the LC/MS-MS profiles. Rec. Nat. Prod. 2018;12(1):64–75.
241. Ramabulana AT, Steenkamp P, Madala N, Dubery IA. Profiling of chlorogenic acids from bidens pilosa and differentiation of closely related positional isomers with the aid of UHPLC-QTOF-MS/MS-based in-source collision-induced dissociation. Metabolites. 2020;10(5).
242. Tao X, Wu Q, Li J, Cai L, Mao L, Luo Z, *et al*. Exogenous methyl jasmonate regulates sucrose metabolism in tomato during postharvest ripening. Postharvest Biol. Technol. 2021;181
243. Li J, Min D, Li Z, Fu X, Zhao X, Wang J, *et al*. Regulation of Sugar Metabolism by Methyl Jasmonate to Improve the Postharvest Quality of Tomato Fruit. J. Plant Growth Regul. 2022;41(4):1615–26.
244. Roy MA, Krishnan L, Roy Roy A. Qualitative and Quantitative Phytochemical Analysis of *Centella asiatica*. Nat. Prod. Chem. Res. 2018;06(04):4–7.
245. Ncube EN, Steenkamp PA, Madala NE, Dubery IA. Metabolite profiling of the undifferentiated cultured cells and differentiated leaf tissues of *Centella asiatica*. Plant Cell. Tissue Organ Cult. 2017;129(3):431–43.
246. Yang JY, Sanchez LM, Rath CM, Liu X, Boudreau PD, Bruns N, *et al*. Molecular networking as a dereplication strategy. J. Nat. Prod. 2013;76(9):1686–99.
247. Wang M, Carver JJ, Phelan V V., Sanchez LM, Garg N, Peng Y, *et al*. Sharing and community curation of mass spectrometry data with Global Natural Products Social Molecular Networking. Nat. Biotechnol. 2016;34(8):828–37.
248. Schymanski EL, Jeon J, Gulde R, Fenner K, Ruff M, Singer HP, *et al*. Identifying small molecules via high resolution mass spectrometry: Communicating confidence. Environ. Sci. Technol. 2014;48(4):2097–8.
249. Pandya A, Thiele B, Zurita-Silva A, Usadel B, Fiorani F. Determination and metabolite profiling of mixtures of triterpenoid saponins from seeds of chilean quinoa (*Chenopodium quinoa*) germplasm. Agronomy. 2021;11(9).
250. Duyen Vu TP, Quan Khong T, Nguyet Nguyen TM, Kim YH, Kang JS. Phytochemical profile of Syzygium formosum (Wall.) Masam leaves using HPLC–PDA–MS/MS and a simple HPLC–ELSD method for quality control. J. Pharm. Biomed. Anal. 2019;168:1–12.
251. Dao TTH, Linthorst HJM, Verpoorte R. Chalcone synthase and its functions in plant resistance. Phytochem. Rev. 2011;10(3):397–412.
252. Brendolise C, Yauk YK, Eberhard ED, Wang M, Chagne D, Andre C, *et al*. An unusual plant triterpene synthase with predominant α-amyrin- producing activity identified by characterizing oxidosqualene cyclases from Malus × domestica. FEBS J. 2011;278(14):2485–99.
253. Hoshino T. β-Amyrin biosynthesis: catalytic mechanism and substrate recognition. Org. Biomol. Chem. 2017;15(14):2869–91.
254. Srivastava G, Sandeep, Garg A, Misra RC, Chanotiya CS, Ghosh S.

Transcriptome analysis and functional characterization of oxidosqualene cyclases of the arjuna triterpene saponin pathway. Plant Sci. 2020;292:110382.

APPENDIXES

LIST OF FIGURES

Appendix A. 2D NMR corroboration experiments for metabolites identified in elicited hairy roots culture of *C. asiatica*

(A)

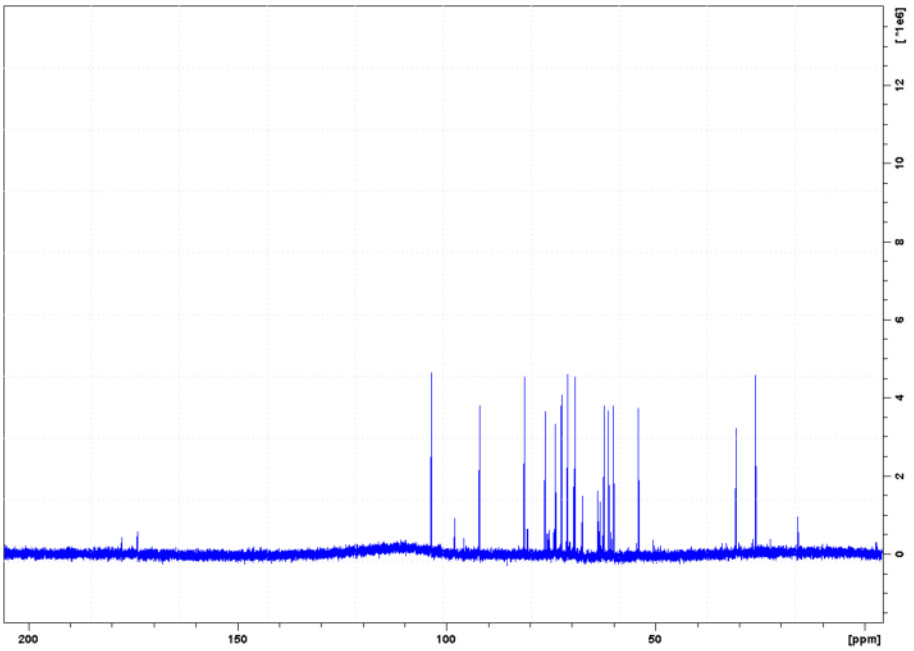

(B)

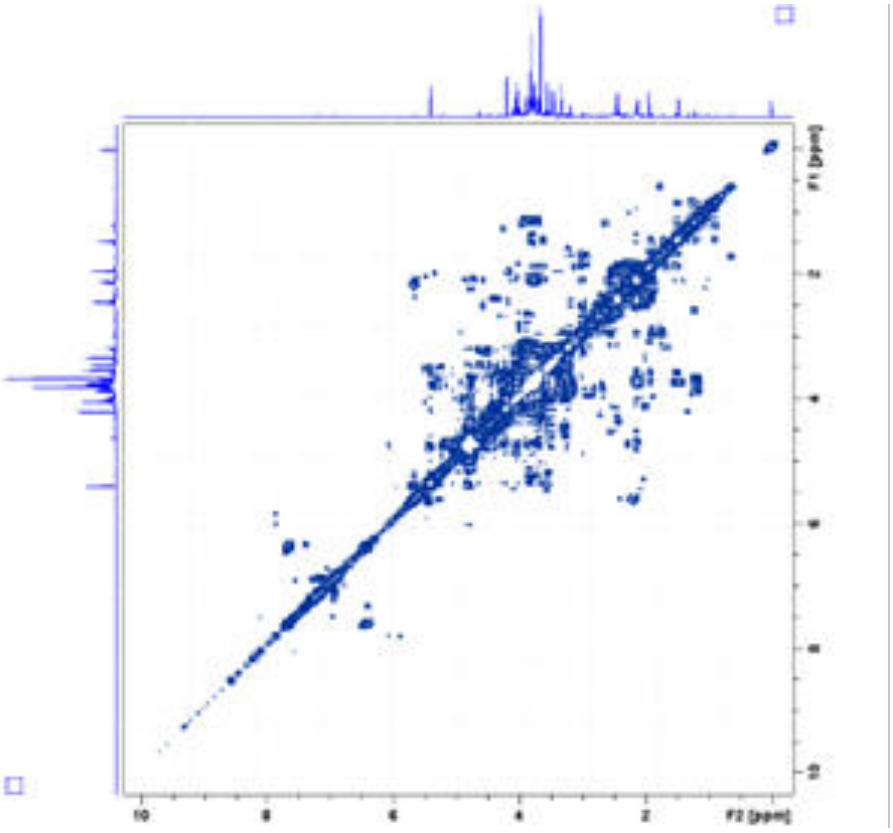

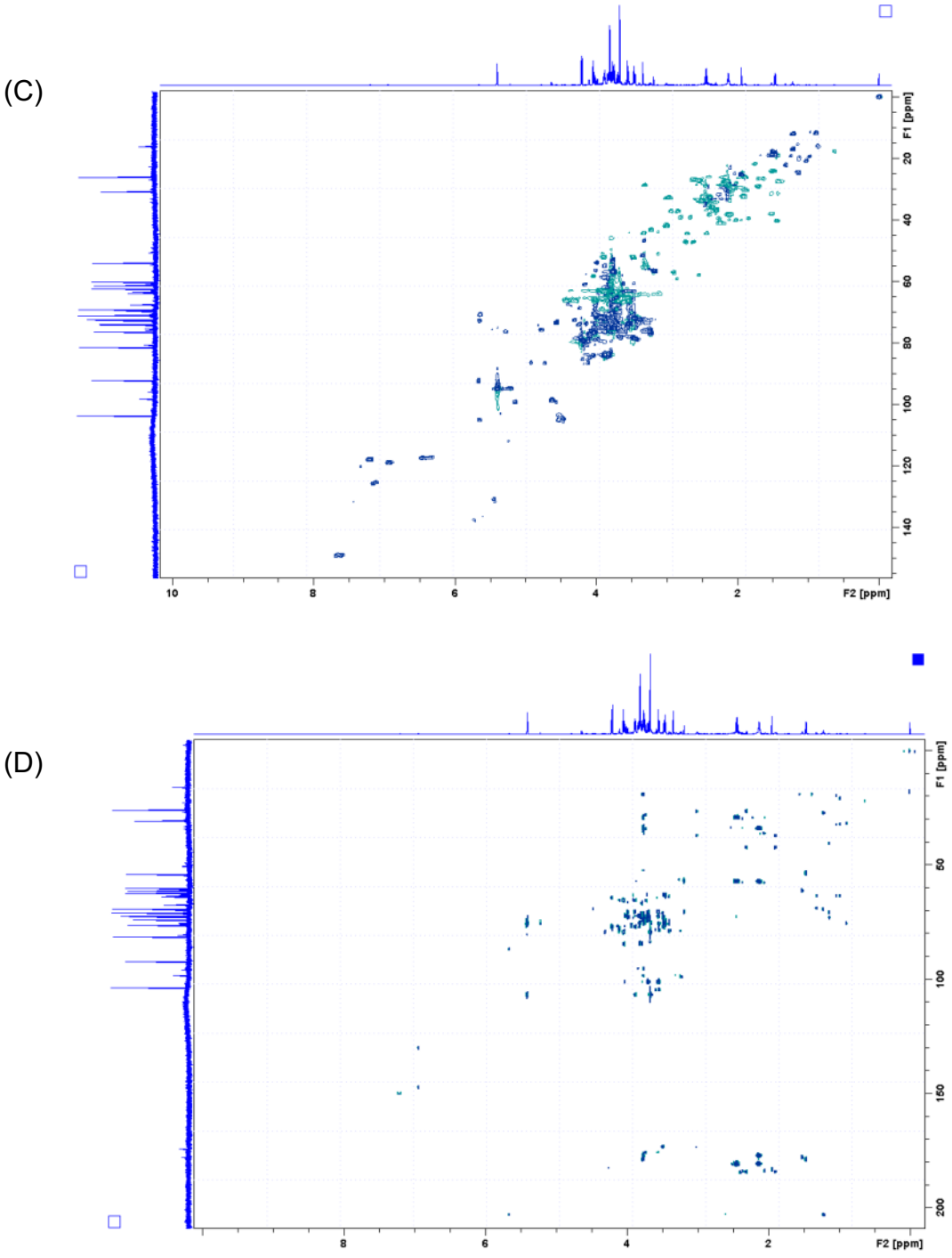

Fig. A.1. 2D NMR corroboration experiments for metabolites identified in elicited hairy roots culture of *C. asiatica*. (A) ^{13}C RMN approach. (B) Homonuclear correlation spectroscopy (2D ^{1}H-^{1}H COSY). (C) Heteronuclear Multiple Bond Correlation (2D ^{1}H-^{13}C HMBC) results. (D) heteronuclear single quantum correlations (2D ^{1}H-^{13}C HSQC). The ^{13}C NMR spectra were collected at a frequency of 188.6 MHz. A total of 5120 scans were collected by setting the

acquisition time to 0.72 s, the relaxation delay to 2 s. The FIDs were collected using a spectral width of 45,454.54 Hz, and the FID size was 64 K. For COSY, the spectral width was 7500.00 Hz in both dimension; 2 k x 128 were acquired with 64 scans per increment and a 2 s relaxation delay. For gHSQC, there parameters were set to obtain a total of 64 scans with 256 increments. The acquisition time and the relaxation delay were set to 0.042 s and1.5 s, respectively. For the ^{1}H dimension, the spectral width was 7,500.00 with $^{1}J_{CH}$ = 145 Hz. On the other hand, the spectral width was 45,454.54 Hz for ^{13}C dimension with $^{1}J_{CH}$ = 145 Hz. gHMBC measurements consisted in 32 scans and 256 increments. The acquisition time and the relaxation delay were set to 0.18 s and 2 s, respectively. The spectral widths of the ^{1}H and ^{13}C dimension were identical to the gHSQC measurement.

Appendix B. MS/MS spectra of targeted ions in the analysis UHPLC-MS/MS in ESI (-)

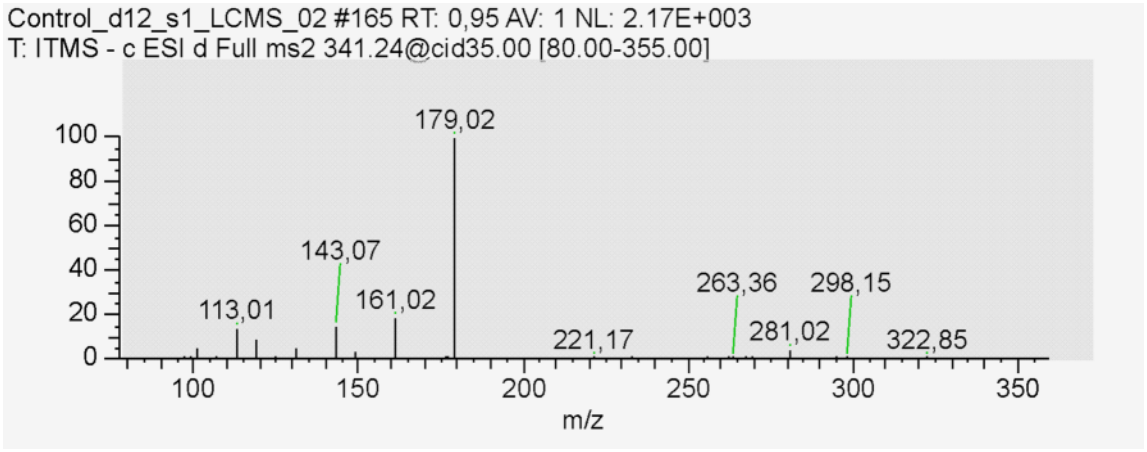

Figure B.2. UHPLC-MS/MS fragmentation spectra of targeted ion 1 (sucrose)

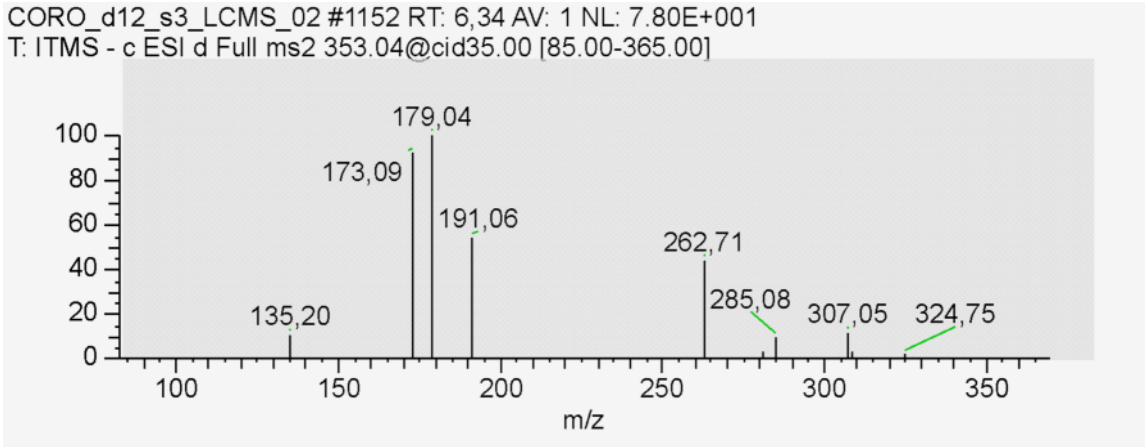

Figure B.3. UHPLC-MS/MS fragmentation spectra of targeted ion 2 (3-CQA)

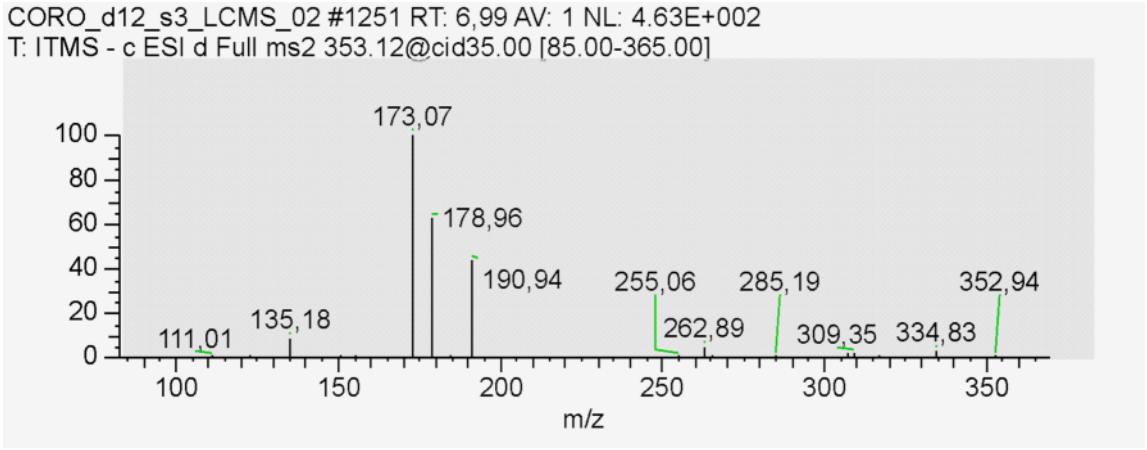

Figure B.4. UHPLC-MS/MS fragmentation spectra of targeted ion 3 (4-CQA)

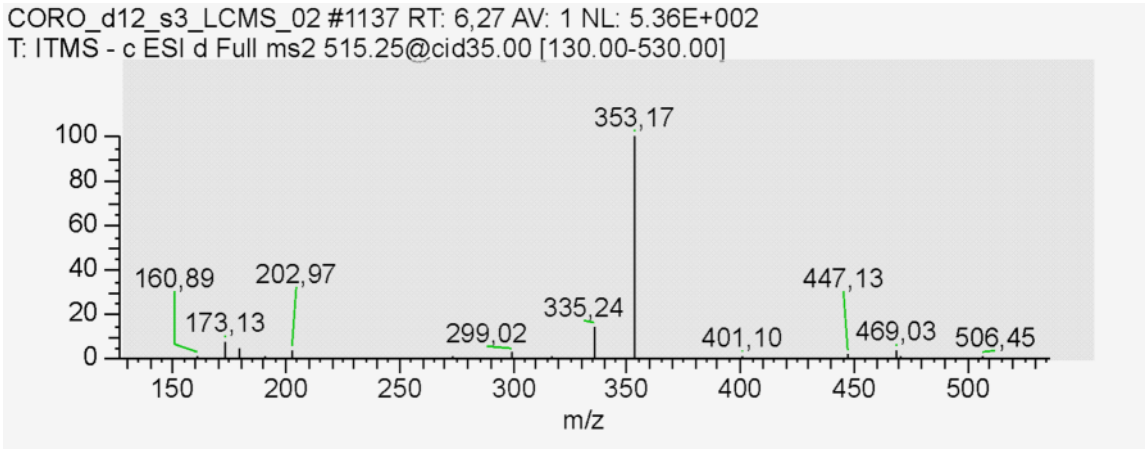

Figure B.5. UHPLC-MS/MS fragmentation spectra of targeted ion 4 (di-CQA isomer 1)

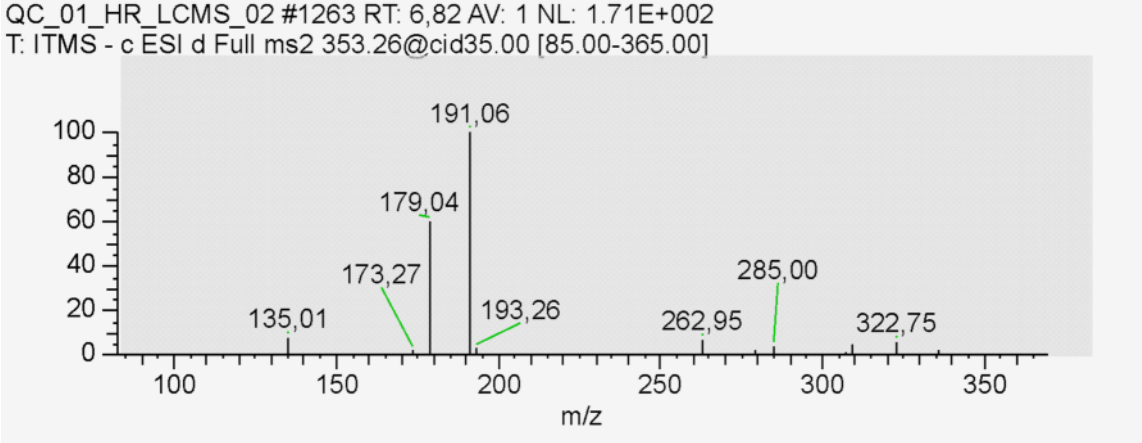

Figure B.6. UHPLC-MS/MS fragmentation spectra of targeted ion 5 (di-CQA isomer 2)

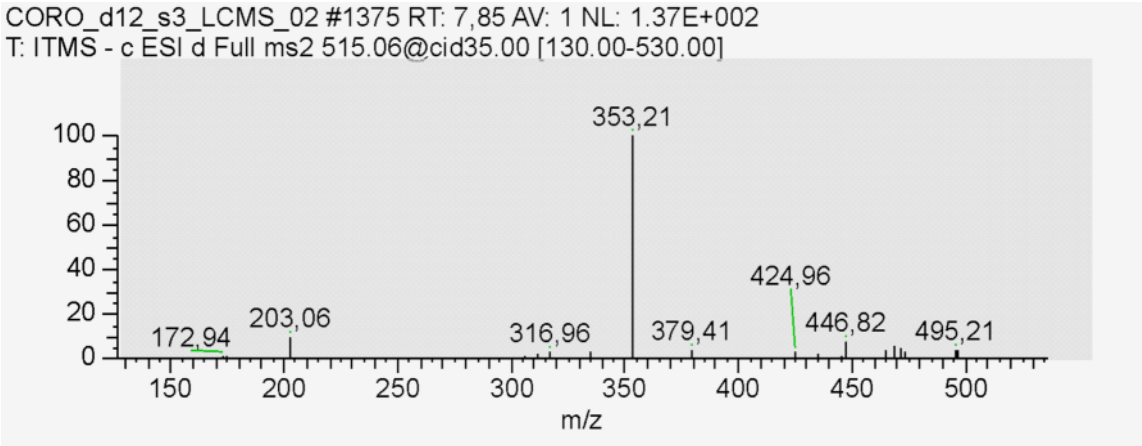

Figure B.7. UHPLC-MS/MS fragmentation spectra of targeted ion 6 (di-CQA isomer 3)

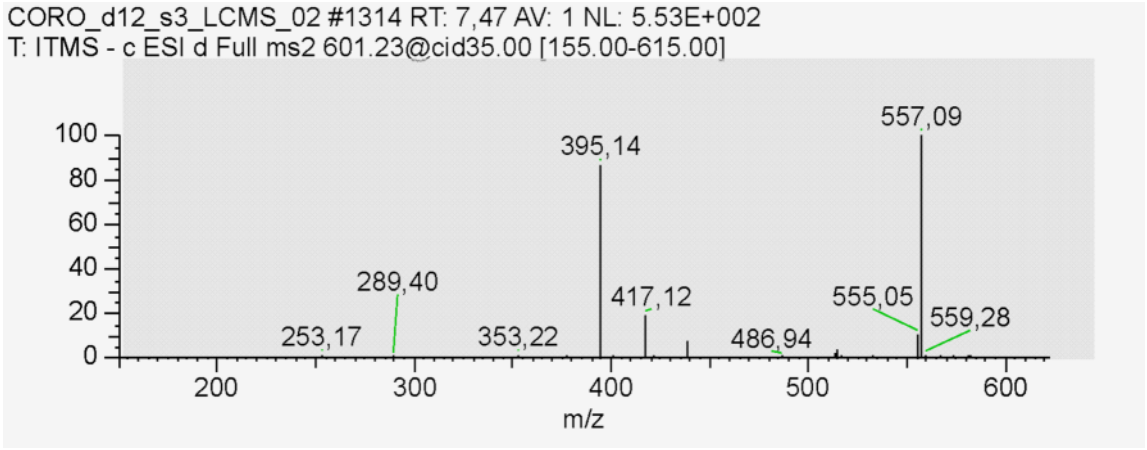

Figure B.8. UHPLC-MS/MS fragmentation spectra of targeted ion 7 (irbic acid)

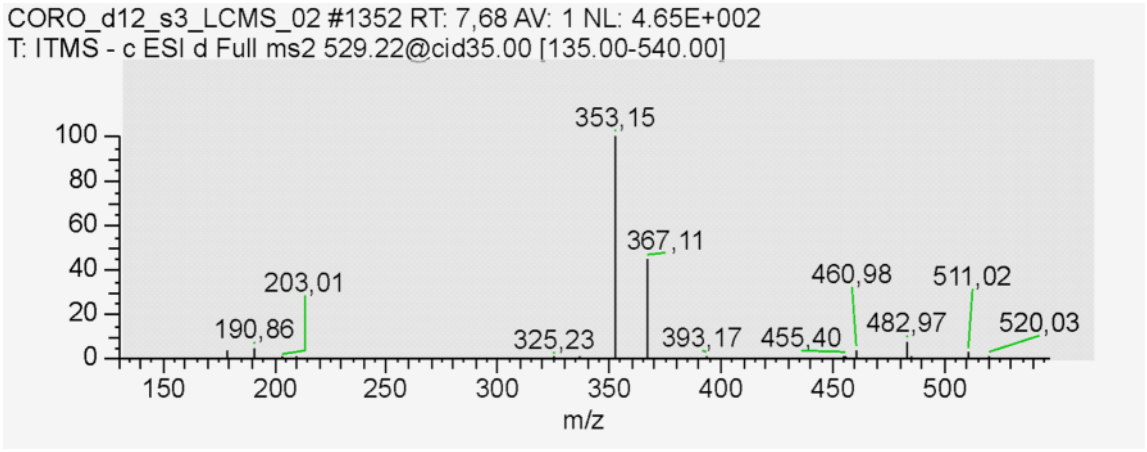

Figure B.9. UHPLC-MS/MS fragmentation spectra of targeted ion 8 (3- caffeoyl,5-feruloylquinic acid)

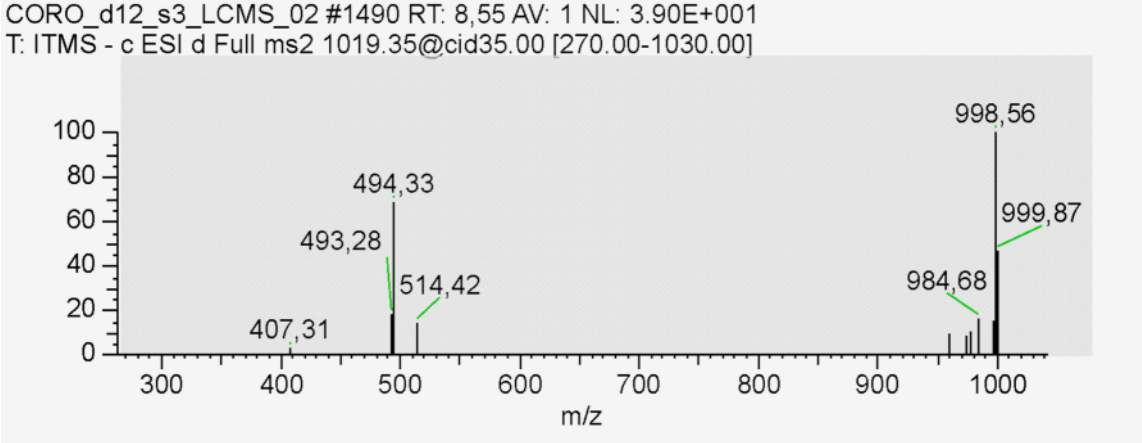

Figure B.10. UHPLC-MS/MS fragmentation spectra of targeted ion 9 (MD)

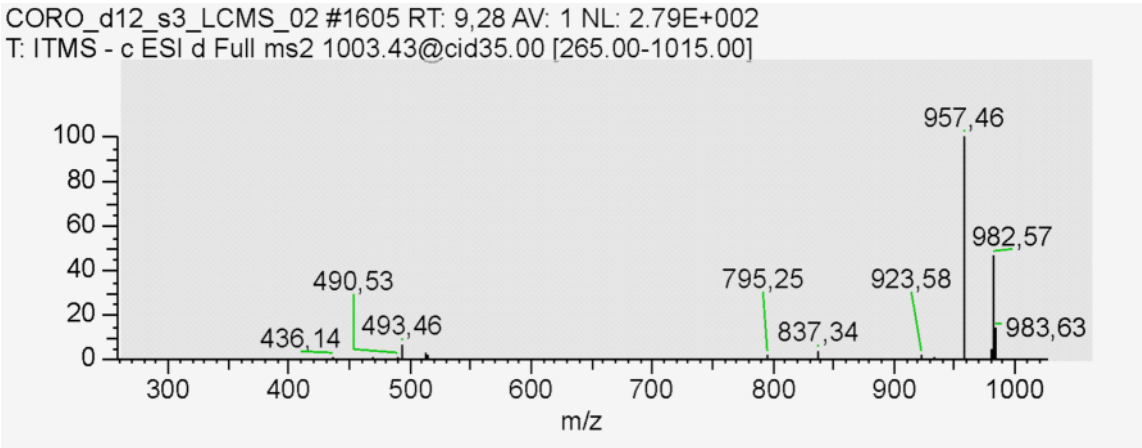

Figure B.11. UHPLC-MS/MS fragmentation spectra of targeted ion 10 (AD)

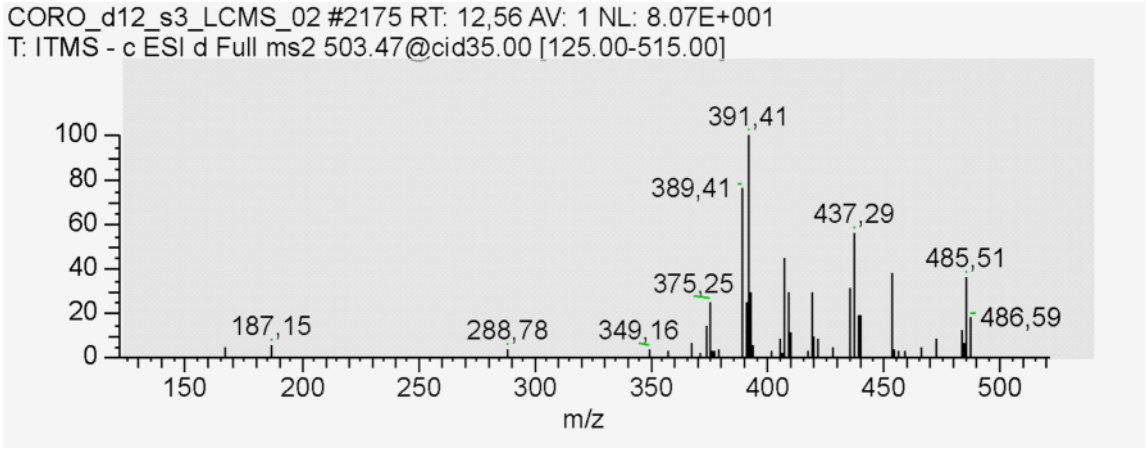

Figure B.12. UHPLC-MS/MS fragmentation spectra of targeted ion 11 (MA)

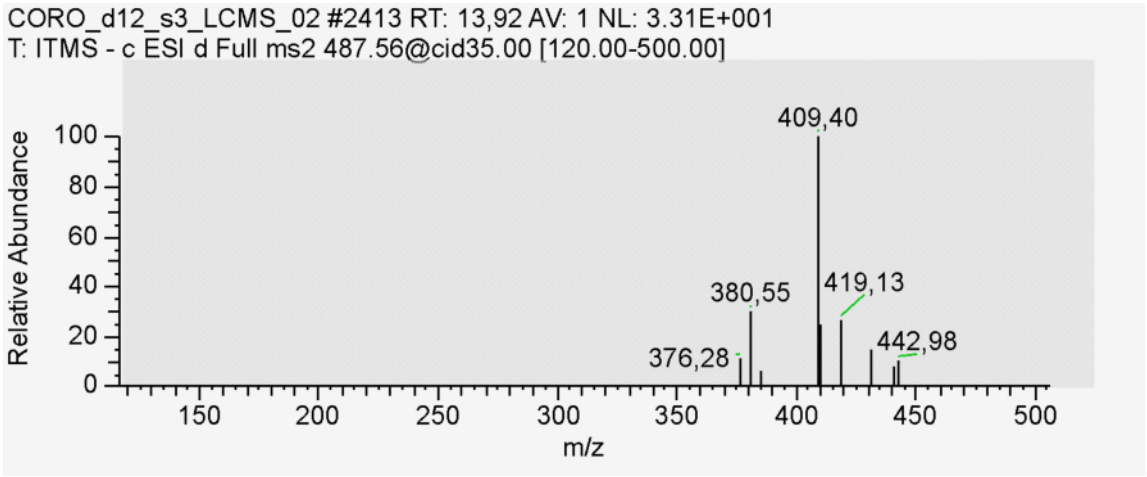

Figure B.13. UHPLC-MS/MS fragmentation spectra of targeted ion 12 (AA)

Appendix C. List of publications

Garcia-Baeza, A., Alcalde, M. A., Grovel, O., Balderas-Renteria, I., Villa-Ruano, N., Velázquez-Ponce, M., Becerra-Martínez, E., & Ramirez-Estrada, K. (2023). Metabolic changes in hairy root cultures of *Centella asiatica* treated with methyl-jasmonate and coronatine: a ^{1}H-NMR-based metabolomics approach. In Vitro Cellular and Developmental Biology - Plant, 59, 2, 179-196. https://doi.org/10.1007/s11627-023-10350-8

Torres-Contreras, A.M.; Garcia-Baeza, A.; Vidal-Limon, H.R.; Balderas-Renteria, I.; Ramírez-Cabrera, M.A.; Ramirez-Estrada, K. Plant Secondary Metabolites against Skin Photodamage: Mexican Plants, a Potential Source of UV-Radiation Protectant Molecules. Plants 2022, 11, 220. https://doi.org/10.3390/ plants11020220

Valdez-Arellanes A.L.; Alcaraz-Madrigal K.X.; Garcia-Baeza A.; Ramirez-Estrada K. Efectos neuroprotectores de moléculas provinientes de *Solanum licopersicum* y su potencial uso en la prevención y tratamiento de las enfermedades neurodegenrativas. RCFB 2020, 3, 24.

Appendix D. Certificate of formations

Nantes Université

ATTESTATION DES FORMATIONS SUIVIES

Mardi 06 septembre 2022

Garcia baeza Antoni

Doctorant(e) à

- **Etablissement** : Université de Nantes
- **Ecole Doctorale** : École doctorale Sciences de La Mer et du Littoral

Total du nombre d'heures comptabilisées : 108:00

Total autres modes de comptabilisations éventuels :

a suivi les formations ci-dessous :

Catégorie : Éthique et intégrité scientifique

Nombre d'heures comptabilisées dans la catégorie : 15:00

Autres mode de comptabilisation éventuel :

Sous-catégorie de formation	Intitulé de la formation ou équivalence	Intitulé Session ou demande d'équivalence	Année civile	Comptabilisation (heures et autres)	Type
	Lyon ou Bordeaux ou autre	Research Integrity in Scientific Professions	2021	15:00	Equivalence

Catégorie : Expertise et méthodes scientifique et technique

Nombre d'heures comptabilisées dans la catégorie : 41:00

Autres mode de comptabilisation éventuel :

Sous-catégorie de formation	Intitulé de la formation ou équivalence	Intitulé Session ou demande d'équivalence	Année civile	Comptabilisation (heures et autres)	Type
	sur décision ED	Técnicas para la mejora de la Investigación. Programa de formación para jóvenes Investigadores de la Universidad de Barcelona . Institut de Desenvolupament Profesional de la Universitat de Barcelona	2021	16:00	Equivalence
	sur décision ED	¿Qué hacer después del doctorado? Técnicas	2021	05:00	Equivalence

DOCTORAT BRETAGNE LOIRE
École des Docteurs Bretagne Loire
1 PLACE PAUL-RICOEUR
35044 Rennes
ecole-des-docteurs@doctorat-bretagneloire.fr

Appendix F. Certificate of attendance as oral communicator in the 2nd Congreso Internacional de NanoBioIngeniería at the Centro de Investigación en Biotecnología y Nanotecnología at the UANL.

2do Congreso Internacional de NanoBioIngeniería
Virtual Congress

Universidad Autónoma de Nuevo León
Facultad de Ciencias Químicas

Otorgan el presente reconocimiento a:

Antoni Garcia-Baeza, Miguel Angel Alcalde-Alvites, Javier Palazon-Barandela, Karla Ramirez-Estrada

Por su participación como expositor del trabajo científico "Induction of hairy roots in Centella asiatica (L.) Urban: a preliminary outcome towards the biotechnological production of anxiolytic natural compounds" en modalidad de **Oral** en el 2do Congreso Internacional de NanoBioIngeniería, realizado en el Foro Virtual del Centro de Investigación en Biotecnología y Nanotecnología del 24 al 30 de Octubre 2020.

Dr. José Rubén Morones Ramírez
Coordinador Centro de Investigación en Biotecnología y Nanotecnología

Dra. Argelia Vargas Moreno
Directora Facultad de Ciencias Químicas

Centro de Investigación en Biotecnología y Nanotecnología a 30 de Octubre, 2020

UANL
FCQ
FACULTAD DE CIENCIAS QUÍMICAS
CIBYN IFCQ
CONACYT

Appendix G. Front page of the thesis-derived publication as first author

In Vitro Cellular & Developmental Biology - Plant (2023) 59:179–196
https://doi.org/10.1007/s11627-023-10350-8

BIOTECHNOLOGY

Metabolic changes in hairy root cultures of *Centella asiatica* treated with methyl-jasmonate and coronatine: a ^{1}H-NMR-based metabolomics approach

Antoni Garcia-Baeza[1,2] · Miguel Angel Alcalde[3,4] · Olivier Grovel[2] · Isaias Balderas-Renteria[1] · Nemesio Villa-Ruano[5] · Manuel Velázquez-Ponce[6] · Elvia Becerra-Martínez[7] · Karla Ramirez-Estrada[1]

Received: 16 February 2023 / Accepted: 18 April 2023 / Published online: 16 May 2023 / Editor: Yong Eui Choi

Abstract
Hairy root cultures of *Centella asiatica*–based coupled with exogenous application of methyl-jasmonate and coronatine are suitable bioproduction platforms to overproduce this plant-occurring high-valuable metabolite. These two molecules orchestrate cellular responses in metabolism that have not been yet deeply explored in hairy roots of this plant. The exploration of metabolic changes is crucial since the biotechnological system productivity depends on the knowledge of the biosynthetic machinery of the culture. To understand how methyl-jasmonate and coronatine cause changes in the metabolism of hairy roots of *C. asiatica*, the metabolic responses to these molecules were monitored through a nuclear magnetic resonance time-series metabolomics approach. The acquired data was analyzed to perform untargeted and targeted metabolomics approaches. Multivariate data analysis statistical models revealed that coronatine caused an early and superior reprogramming effect on the metabolome compared to methyl-jasmonate. We identified 40 compounds from primary and specialized metabolism. The relative production kinetics of these metabolites in the two treatments and their possible links in the metabolic pathways of the plant were discussed. We were able to observe that in coronatine-treated cultures, phenolic specialized pathways were activated 8 d after treatment exposure while the pool of carbohydrates and nitrogen-carrier amino acids were consumed at early stages. This evidenced the clear and high reprogramming effect in the metabolism of *C. asiatica* hairy roots in response to coronatine. These findings provide important insights on the metabolic alterations caused by methyl-jasmonate and coronatine and on the possibility to redirect the metabolism of hairy root cultures of *C. asiatica*.

Keywords *C. asiatica* · Hairy roots · ^{1}H-NMR metabolomics · Coronatine · Metabolism regulation

✉ Elvia Becerra-Martínez
elmartinezb@ipn.mx

✉ Karla Ramirez-Estrada
karla.ramirezst@uanl.edu.mx

[1] Laboratorio de Metabolismo Celular, Facultad de Ciencias Químicas, Universidad Autónoma de Nuevo León, Ciudad Universitaria, Pedro de Alba S/N, 66451 San Nicolás de los Garza, Mexico

[2] Nantes Université, Institut Des Substances Et Organismes de La Mer, ISOMER, UR 2160, F-44000 Nantes, France

[3] Laboratori de Fisiologia Vegetal, Facultat de Farmacia, Universitat de Barcelona, Av. Joan XXIII 27-31, 08028 Barcelona, Spain

[4] Escuela de Posgrado, Universidad Cesar Vallejo, Av. Larco 1770, 13001 Trujillo, Perú

[5] CONACyT-Centro Universitario de Vinculación Y Transferencia de Tecnología, Benemérita Universidad Autónoma de Puebla, Prolongación de La 24 Sur Y Av. San Claudio, Ciudad Universitaria, Col. San Manuel, 72570 Puebla, México

[6] Unidad Profesional Interdisciplinaria de Ingeniería Campus Guanajuato, Instituto Politécnico Nacional, 36275 Guanajuato, México

[7] Centro de Nanociencias Y Micro Y Nanotecnologías, Instituto Politécnico Nacional, Unidad Profesional Adolfo López Mateos, Zacatenco, Av. Luis Enrique Erro S/N, Delegación Gustavo A. Madero, 07738 Ciudad de Mexico, Mexico

Springer

Appendix H. Scientific communications

Garcia-Baeza A. 1H-NMR-based metabolomics of hairy roots suspension cultures of Centella asiatica treated with methyl jasmonate and coronatine. **Poster**. Gen2Bio 2022. La Baulle, France, 2022.

Garcia-Baeza A. Green biofactories for the production of centellosides. **Oral presentation**. PRISMA Conference 2021. Valencia, Spain, 2021.

Garcia-Baeza A., Alcalde-Alvites M.A., Palazon-Barandela J., Ramirez-Estrada R. Metabolomics derived insights into the regulation and control of centellosides in hairy roots of Centella asiatica. **Oral presentation**. 19th International Congress Mexican Society of Biotechnology. Ciudad de Mexico, Mexico. 2021.
1st place award

Garcia-Baeza A., Alcalde-Alvites M.A., Palazon-Barandela J., Ramirez-Estrada R. Metabolomics derived insights into the regulation and control of centellosides in hairy roots of Centella asiatica. **Poster presentation**. 2nd Virtual Conference LatinXChem. Ciudad de Mexico, Mexico. 2021
3rd place award

Garcia-Baeza A., Alcalde-Alvites M.A., Palazon-Barandela J., Ramirez-Estrada R. Induction of a biomass producer hairy root suspension culture of Centella asiatica. **Poster presentation**. VII National Symposium of Pharma. And Biomed. Sciences, Universidad Autónoma de Nuevo León, Monterrey (Mexico). 2020
2nd place award

Garcia-Baeza A., Alcalde-Alvites M.A., Palazon-Barandela J., Ramirez-Estrada R. Induction of a biomass producer hairy root suspension culture of Centella asiatica. Poster presentation. **Oral presentation**. International Congress of Nanobioengineering. Monterrey (Mexico). 2020

AUTOBIOGRAPHY

Antoni Garcia Baeza

Candidate for the Grade of

Doctor of Science with orientation in Pharmacy (UANL)
Doctor of Natural Products Chemistry (Nantes Université)

Thesis: METABOLOMICS-DERIVED INSIGHTS INTO THE REGULATION AND CONTROL OF CENTELLOSIDES IN HAIRY ROOTS OF *Centella asiatica*

Field of study: Pharmacy

Biography: Born in Barcelona, Spain the 21st of April of 1995, son of Antonio Garcia and Gabriela Baeza

Education: Bachelor's degree in Biotechnology at the University of Barcelona in 2017. Master's degree in Research, Development and Control of Drugs at the University of Barcelona in 2018.

Professional Experience: Junior Scientific Researcher at Alkion Bioinnovations SAS (Versailles, France) since January 2023.